Interaction between the failure mechanisms backward erosion piping and slope instability

Identification and quantification of interactions between failure mechanisms of a levee

L. van der Doef

Interaction between the failure mechanisms backward erosion piping and slope instability

Identification and quantification of interactions between failure mechanisms of a levee

by

L. van der Doef

in partial fulfilment of the requirements for the degree of

Master of Science

in Civil Engineering

at the Delft University of Technology,
to be defended publicly on Wednesday July 17, 2019 at 11:00 AM

Student number:	4222210	
Project duration:	2018 – 2019	
Thesis committee:	Prof. dr. ir. M. Kok,	TU Delft, Chairman
	V. K. Duvvuru Mohan, Msc,	TU Delft, PhD
	Dr. ir. W. Kanning,	TU Delft, supervisor
	Ir. M. M. de Visser,	RWS-WVL, supervisor
	J. C. Pol, Msc,	TU Delft, PhD

Cover image is obtained from: `https://beeldbank.rws.nl/MediaObject/Details/349447`.

A scene of the breach of the Grebbedijk in 1855.

TUDelft
Delft
University of
Technology

Ministerie van Infrastructuur
en Waterstaat

Preface

This thesis finalises my MSc study Hydraulic Engineering at Delft University of Technology within the specialisation Hydraulic Structures and Flood Risk. This research has been performed with the support of Delft University of Technology and Rijkswaterstaat- WVL.

I would like to thank all members of my graduation committee, Prof. dr. ir. M. Kok, Dr. ir. W. Kanning, Ir. M. M. de Visser, J. C. Pol, Msc and V. K. Duvvuru Mohan, Msc, for their expertise, feedback and support during the project. Special thanks to Matthijs Kok for his guidance, enthusiasm, and directing the committee meetings as the chair of my thesis committee. I wish to express my appreciation to Wim Kanning for his support and feedback throughout my graduation period. Thank you for always taking the time to answer any questions I may have. I would like to thank Marieke de Visser for always asking the right critical questions, this has helped me to come up with answers. I would also like to thank Joost Pol for the brainstorm sessions, for allowing me to participate in your experiment and for your constructive feedback. Lastly, I would like to express my thanks to Varenya Duvvuru Mohan for his thorough feedback on my report.

Special thanks to my colleagues at Rijkswaterstaat, for their interest, advice and the enjoyable time during the lunch and coffee breaks. Especially, Hoite and Alex, who introduced me to Rijkswaterstaat and the subject of my thesis. Thank you for your infinite cheerfulness and support.

I must express my gratitude to Tom, who supported and encouraged me throughout the entire process of writing this thesis. Thank you for reading the report so often. I couldn't have done it without you.

I want to thank my family for always supporting me and last of all, my friends for making my study time a great time.

L. van der Doef
Delft, 2019

Summary

With the shift of the safety standards for levees from exceedance probability (standard 1996) to flooding probability (new standard), the part of the levee failure process after the initial occurrence of a failure mechanism becomes more important for the calculation of the strength and thus, reliability of the levee cross-section. Interactions between failure mechanisms can take place in this part of the levee failure process. An interaction refers to one failure mechanism influencing the probability of another failure mechanism, where positive interaction is defined as a reduction and a negative interaction as an increase of the failure probability. The main problem is a lack of knowledge about the interactions of failure mechanisms and their influence on the failure probabilities of levees. Several studies (Calle, 2002; 't Hart et al., 2016; Kok et al., 2017) suggest that there is an interaction between different failure mechanisms. However, only the effects of overtopping on slope instability (de Visser et al., 2018) and a reduction of the shear strength in slope instability due to uplift (Kanning and van der Krogt, 2016) is currently included in the statutory assessments of levees (Rijkswaterstaat WVL, 2017a,d). This research aims to quantify the influence of the interaction between the failure mechanisms backward erosion piping (BEP) and slope instability (SI) on the safety of a levee.

The parametric study of this research assesses whether the occurrence of a failure mechanism (BEP or SI) affects the parameters' present states in the limit state functions of the other failure mechanism. This qualitative study is executed for both interactions (BEP to SI and SI to BEP). Subsequently, a quantitative study is carried out on the influence of SI on BEP. For this purpose, a model was created to calculate this interaction between SI with BEP. After a slope instability, the remaining profile is assumed to contain a berm. This change in levee profile, does not result in the immediate breaching of the levee, it can however influence the probability of BEP. The model sequentially executes a stability analysis, a displacement analysis of the sliding plane and a BEP analysis. The degree of interaction is defined as the difference between the safety factor of BEP of the original profile (prior to sliding) and the safety factor of BEP of the remaining profile (after sliding).

The parametric study identified multiple interaction points of BEP on SI. The first main driver for the interaction is the lack of shear strength in pipes or hollow spaces due to the presence of water or fluidised sand in these pipes or spaces. The second driver is the reduction of the head in the sand layer due to the presence of seepage to the pipe, increasing the shear strength in the sand layer. Lastly, the rupture of the blanket layer causes a reduction of shear strength in the soil surrounding the rupture point at the interface between the clay and sand layer. The shear strength can reach zero landward of the rupture point. The interaction from BEP to SI is governed by the 3D-effect, as different locations in and adjacent to the location of a pipe have contradictory effects on slope instability.

The parametric study also identified interaction points of SI on BEP. Due to the formation of a berm after sliding, the exit point of the BEP is relocated. If this exit point is located at the end of the berm, the occurrence of BEP depends on the valve effect due to sliding, the thickness of the blanket layer and the seepage length. These parameters lead to a decrease in the occurrence of BEP. When the exit point is located in the berm, the occurrence of BEP is affected by the properties of the berm. The modelling study shows that the degree of interaction from SI to BEP is significantly affected by the presence of cracks in the berm. A consequence of these cracks is that the exit point moves and is now located in the berm. The degree of interaction also depends on the shape and size of the sliding plane, because it determines the size of the berm of the remaining profile.

Based on the modelling study, a vast majority (50% to over 75%) of the considered scenarios of the seven considered levee profile cases result in a positive interaction. However, in all the considered cases, negative interactions were found that give a reduction of 50% to 2% on the original safety factor, which could lead to an overestimation of the safety in the assessment of the levee. All of these negative interactions result from the assumption that large cracks can form in the soil after sliding.

It is recommended to continue the research into the interaction between SI and BEP, as significant interactions have been found. Future studies should focus on determining the effect of different sizes of cracks in the remoulded soil, especially on the weight of the blanket, the aquifer head and the critical heave gradient. These cracks have a large effect on the interaction through these parameters and are still unknown. The parametric study shows that there is also a possible interaction from BEP to SI. It is essential to directly account for 3D-effects in this interaction.

Finally, it is recommended to omit the quantitative interaction from SI to BEP from this study in the assessment and design of levees for the foreseeable future, since more research is needed before this interaction is ready for implementation.

Contents

1

Introduction

Flooding is an age-old problem. It occurs all over the world and can have different causes, such as a flood wave in a river and a storm surge at sea. Especially in the Netherlands, which lies beneath mean sea level, flooding forms a threat. Since the North Sea flood of 1953, the Netherlands has been actively working against flooding. It launched the Delta programme, which resulted in the construction of the Delta works. The Netherlands is renowned for its knowledge of flood defences and strives to keep itself safe from the threat of flooding. This is achieved by the on-going development of the knowledge of flood defences, a proper assessment plan, and up-to-date maintenance strategies. To understand how to protect the land from flooding, it is essential to know how flood defences can fail and in which steps the failure process takes place. This research will focus on a flood defence type known as levees, which are earthen embankments. In particular Dutch river levees will be addressed.

Since 1996, levees in the Netherlands have been required to comply with the first standard defined in the Flood Defence Act (1996). This standard specifies the annual allowed exceedance probability of water levels, indicating how much the flood defence must withstand. As of 1 January 2017, a modification of the water act has been effective in the Netherlands. This law prescribes a new standard that is based on the probability of flooding but differs from the previously used probability of exceedance (Helpdesk Water and Rijkswaterstaat, 2018). With the probability of exceedance, the water level against the flood defence indicates if the flood defence is expected to fail. The strength of the flood defence can no longer be guaranteed when this water level is reached. However, this does not mean that the flood defence has been breached; it merely shows that there is no guarantee that the flood defence will not be breached. With the probability of flooding approach, flood defences are deemed to fail, when they lose the water retaining capacity through which the area protected by the flood defences is flooded in such a way as to result in loss of life or substantial economic damage (Art. 1.1 Water Act (1 July, 2018)). The Flood Defence Act (1996) introduced a periodic assessment of all Dutch primary flood defences. In each round of assessment, all primary flood defences are marked by a pass, fail, or no judgement. For the assessment round in 2017, a Statutory Assessment Instrument (WBI2017) was developed.

In WBI2017, the WBI failure definitions of some of the failure paths do not correspond with the actual flooding of the hinterland as defined in the new standard. The time or the mechanisms it needs to get from the failure definition to the actual flooding of the hinterland is called the residual strength. Within this residual strength, failure mechanisms can start to interact. By shifting the failure definitions closer to actual flooding and by including these interactions, the assessment method could better comply with the new standard.

1.1. Interactions between failure mechanisms of levees

With the shift of the standard for levees from exceedance probability (standard 1996) to flooding probability (new standard), the part of the failure process after the initial occurrence of a failure mechanism becomes more important for the calculation of the strength and thus reliability of the levee cross-section. In literature,

this part is called residual strength of the levee. Interactions between failure mechanisms can take place in this part of the failure process. *Interactions* are defined as one failure mechanism influencing the probability of another failure mechanism in a positive or negative sense, where positive interaction is defined as a reduction and a negative interaction as an increase of the failure probability. *Failure mechanism* describes the different ways a levee can lose its primary function, which is preventing flooding of the hinterland.

Figure 1.1 gives an overview of the possible failure mechanisms known in the literature. These failure mechanisms are currently used to describe the strength of the levee.
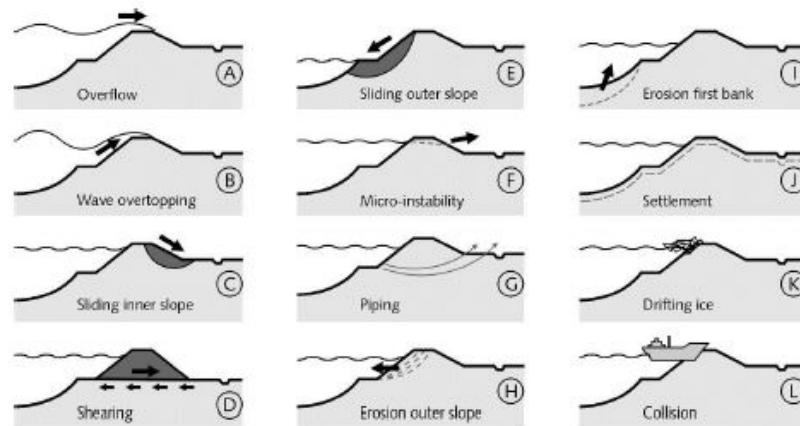
Figure 1.1: Schematic overview of the most relevant failure mechanisms of flood defences (Jonkman et al., 2017, p. 20)

Calle (2002) and 't Hart et al. (2016) suggest that there can be interactions between the different failure mechanisms. For example, between the mechanism of overtopping and the mechanism of slope instability with overtopping water flows over the inner slope of the levee. This water partially infiltrates into the levee, which increases the phreatic surface that causes the slope to become unstable. Here, one failure mechanism influences the other failure mechanism to occur.

Knoeff et al. (2018) mentions another interaction, which is the interaction between the failure mechanisms of slope instability and backward erosion piping. Not much is known about these possible interactions and how these affect the probability of flooding. The main focus of this report will be on the failure mechanisms slope instability (C) and Backward erosion piping (G), as depicted in Figure 1.1, and the interactions between these mechanisms. These failure mechanisms are shortly described below. Note, as mentioned above these failure mechanisms do not necessarily lead to flooding of the hinterland. Only the assessment uses the failure definitions of these mechanisms.

Slope instability
Slope instability (SI) is the sliding of the slope of the levee. Instability can occur at the inner slope when there is a rise in outside water level or excessive rainfall or an additional traffic load. It can also occur at the outer slope when there is a sudden drop in outside water level. This thesis only considers the slope instability of the inner slope, when the term 'slope instability' is used, it refers to inner slope instability. Inner slope instability is often caused by a high water level which has a long duration, for example, a flood wave in a river. The high water gives an increase in pore pressure, which reduces the effective stress. This reduction leads to a reduction of shear strength in the soil, that can cause the sliding planes to develop (Jonkman et al., 2017).
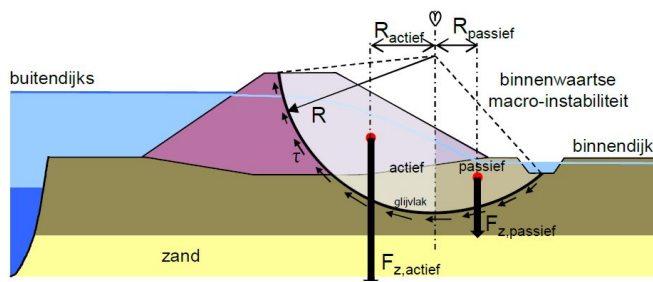
Figure 1.2: Schematic overview of the failure mechanism slope instability, ('t Hart et al., 2016, p. 8)

Figure 1.3: Slope instability of a inner slope levee (Evers, 2018, p. 26)

In Figure 1.2, a schematic drawing of slope instability is shown. Slope instability considers an equilibrium of the soil, where the momentum balance between the active soil part of the levee and passive soil part of the levee plus the shear strength along the sliding plane is taken.

Backward erosion piping
Backward erosion piping is a form of internal erosion, where hollow spaces are formed underneath the levee or flood defence by the erosion of the soil particles due to the present hydraulic gradient. When a cohesive layer (hereafter referred to as 'blanket layer') on top of the erodible subsoil is present, pipes can form at the interface between the soil layers. These pipes start at the land-side growing to the water-side (Jonkman et al., 2017). Piping is the Dutch term for backward erosion piping (BEP). BEP consist of three sub-mechanisms uplift, heave and piping that need to occur in sequences in order to have backward erosion piping failure.

Figure 1.4: A pipe under a levee, (Evers, 2018, p. 29)

1.2. Problem statement

Several studies (Calle, 2002; 't Hart et al., 2016; Kok et al., 2017) suggest that there are interactions between different failure mechanisms. However, not all of the suggested interactions have yet been researched. The interaction between the failure mechanisms overtopping/overflow and slope instability was researched to quantify this contribution (e.g. Hoven et al., 2011; de Visser et al., 2018). This research shows that this interaction can negatively affect the erosion resistance of a levee, which is detrimental to the reliability of a levee. This interaction has, therefore, also been included in the assessment and design of levees.

Currently, there is a lack of knowledge about the other possible interactions of failure mechanisms and their influence on the failure probability of levees. This study focuses on the interaction between the failure mechanisms of backward erosion piping and slope instability as it has been identified by the studies mentioned

above as potentially significant. However, the contribution of interactions between the failure mechanisms of backward erosion piping and slope instability to the reliability of a levee remains unknown. The reliability of levees could currently be overestimated for not including this potentially relevant interaction in the assessment and design of levees.

1.3. Objective

The purpose of this study is to assess the possible existence of interactions between the failure mechanisms induced by backward erosion piping and slope instability. This research seeks to discover what contribution these interactions have on the safety of a levee. In particular, whether these interactions have a positive or negative effect on the failure probability and what factors govern their occurrence.

Research question
The following questions will support this research:

> *How do interactions between backward erosion piping and slope instability affect the safety of a levee?*

Sub-questions

1. How are interactions between failure mechanisms currently assessed?
2. How do interactions between backward erosion piping and slope instability occur?
3. How can the interaction from slope instability to backward erosion piping be quantified?
4. What is the range of the degree of interaction from slope instability to backward erosion piping and which conditions and assumptions govern this range?
5. Which (environmental) circumstances affect the degree of interaction?

1.4. Relevance

The predictions are that many levees will not pass the assessment of the levee assessment round of 2017 for various reasons. According to Maaskant and Knoeff (2016), there are three main changes in the assessment that may cause this:

1. The new standard;
2. Different hydraulic loads and a new approach to hydraulic loads;
3. New insights on strength calculations.

The interaction researched in this thesis (which is part of the residual strength) is present in the third cause: the strength calculations. It is expected that in addition to possible negative interactions, positive interactions can also occur that are beneficial for the strength of a levee. When levees do not pass the assessment, they need to be improved. The cost of improvements is high. In the case that many improvements are needed, it might be more cost-efficient to refine the assessment and make more detailed calculations. This may enable more levees to pass the assessment. This will depend on which way the interaction takes place.

Another reason to research interactions is practical: if an initial failure has occurred due to a failure mechanism, should we be concerned about the continuation of this failure mechanism or another failure mechanism in which the interaction is essential? This affects the location where the necessary emergency measure must be taken to prevent flooding of the hinterland. This location will differ if there is an interaction and if there is another continuation of the failure process because of this interaction.

1.5. Thesis outline and approach

In order to answer the research questions and to fulfil the objectives presented before, the study is divided into four parts, namely:

1. Introduction and theoretical background
   An introduction to the problem statement, the goal and the relevance is provided. The theoretical background includes a description of the past literature on the interaction between failure mechanisms in general. It further focusses on the knowledge of the failure mechanisms BEP and SI, which is used in the next part of this study.
2. Identifying possible interactions
   Identifying the possible interaction between the failure mechanisms BEP and SI is done through a parametric study. Based on the currently used limit state models, possible interactions are described.
3. Quantifying the possible interactions
   In the quantification of the interaction, a model is developed to calculate the degree of interaction from SI to BEP. The Grebbedijk is used as a case study (described in Appendix B). After this, a sensitivity analysis is conducted to determine the case dependency of this interaction.
4. Discussion, conclusions and recommendations
   The results of the research, as well as the limitations and assumptions that were required or made, are discussed. The conclusion of this study and answers the research questions, based on the results of qualitative and quantitative analysis are given, as well as, recommendations on further research.

In Figure 1.5, the corresponding thesis outline is illustrated.
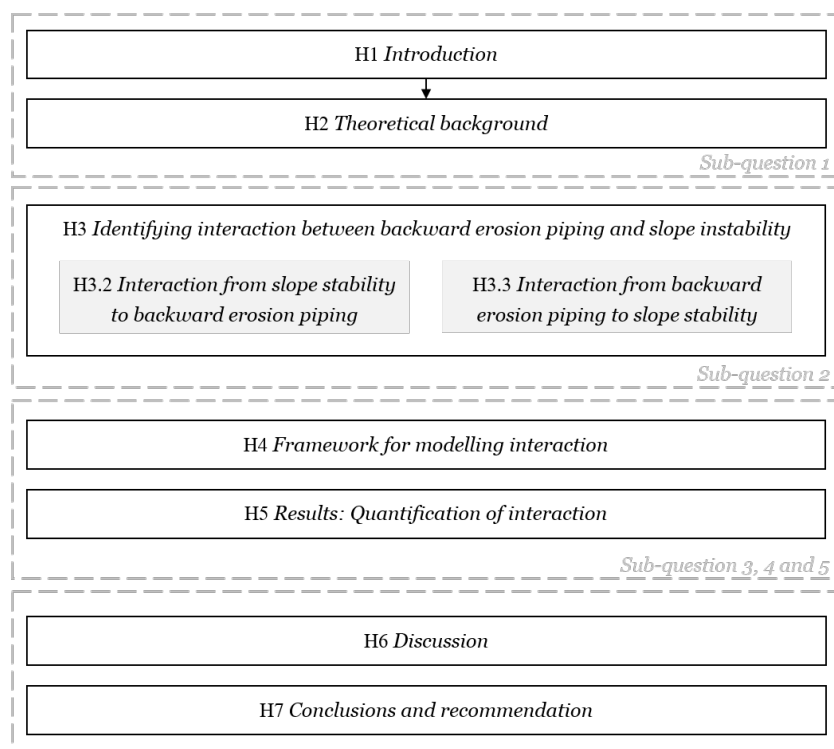
Figure 1.5: Thesis outline

2

Theoretical background

The interaction between failure mechanisms, in particular between backward erosion piping (from here on called 'BEP') and slope instability (from here on called 'SI') , is relatively unknown among hydraulic engineers. Therefore, this Chapter begins by describing the definitions that relate to interactions and are used in this study. Next, the previous study on interactions and some examples of suspected interaction cases are presented, followed by a detailed description of BEP and SI.

2.1. Definitions

2.1.1. Definition of "Levee failure" and "Initial failure"

Since the definition of failure varies among researchers, it is important to clarify how the term is used in this study.

This study will use the definition as (Rijkswaterstaat WVL, 2017b) defines it. A levee has failed when there is loss of primary function, which is retaining water and preventing flooding of the hinterlands (Rijkswaterstaat WVL, 2017b, p. 41). There does not have to be a full breach to get flooding of the hinterlands (for example when there is a lot of overflow), but in most cases a breach is present. Throughout this study, the term levee failure will refer to a loss of primary function.

The failure mechanisms of a levee, as shown in Figure 1.1 can be calculated until the defined failure definition. This failure definition does not always coincide with levee failure. The failure definition of the failure mechanism is often called a failure of a levee or is used as the failure point in the assessment and design of a levee. Throughout this study, the failure mechanisms defined failure point will be referred to as the initial failure of a failure mechanism.

The initial failure definition for SI failure as it is used in the assessment is described as: "A levee has failed due to slope instability when the sliding of a soil plane results in lowering of the crest level and loss of its water retaining function"(Rijkswaterstaat WVL, 2017d, p. 30). The initial failure definition for BEP failure as it is used in the assessment is described as: "A levee has failed due to the backward erosion piping mechanism when the critical hydraulic gradient, where the progressive erosion can come to an equilibrium, is exceeded"(Rijkswaterstaat WVL, 2017d, p. 41).

2.1.2. Definition of "Limit state function and Factor of safety (FoS)"

In this thesis the limit state functions are used to identify and quantify possible interactions. Limit state functions (Z) describe the relation between resistance(R) and load (S), see equation 2.1. The limit state function

represents the line between failure ($Z < 0$) and non-failure ($Z > 0$). The probability of failure is the probability that the $Z < 0$ (Jonkman et al., 2015).

$$Z = R - S \tag{2.1}$$

This can also be expressed in factor of safety (FoS) equation 2.2, if the FoS is smaller than 1 the mechanism is "not safe" and it can lead to initial failure.

$$FoS_z = \frac{R}{S} \tag{2.2}$$

2.1.3. Definition of "Remaining profile'

The remaining profile is defined as the profile that remains after a failure mechanism has occurred. This can be a profile after sliding or a profile after partial occurrence of a sub-mechanism like when there is a boil present. Not to be confused with residual strength, which is used to define the strength that remains in the levee after initial failure has occurred.

2.1.4. Definition of "Interaction"

Murthy and Nguyen (1985) mentions the first failure interaction between components in reliability. He defines three types of failure interactions, wherein his type I failure interaction is conform with the definition used in this thesis. "*A failure of item 1 can induce a failure of item 2 with probability p an a failure of item 2 can induce a failure of item 1 with probability q.*" (Murthy and Nguyen, 1985, p. 8)

In this thesis *Interactions* refers to one failure mechanism influencing the probability of another failure mechanism in a positive or negative sense. If failure mechanism X has occurred, it changes the characteristics of the levee. If this new situation changes the failure probability of failure mechanism Y, it is an interaction. This interaction can be found at a parameter level, where a slight change in a parameter can be the interaction. This study does not consider correlations between different failure mechanisms and does not quantify dependencies between parameters. Correlation is a mathematical relationship between one or more variables that is reciprocal and reflects a dependency. This differs from interaction, as an interaction does not have to be cross-contributory and can show a new effect.

2.2. Interaction between failure mechanisms

2.2.1. Previous research on interactions between failure mechanisms

There is not much known about the interaction between failure mechanisms of flood defences. From the current approach, which focusses on the individual failure mechanisms listed above, new insights were gained to look at the residual strength after the occurrence of the initial failure as defined in WBI 2017. This has led to the discussion of follow-up mechanisms.

The options on different follow-up mechanisms are defined in Calle (2002), after initiation of one failure mechanism another could take over to continue the failure process. This follow-up mechanism can be considered an interaction following the definition in the previous Section 2.1.4. Calle (2002) does not include this. Calle (2002) mentions the the following interactions/follow-up mechanisms:

- Overtopping combined with inner SI, erosion of core material or backward erosion.
- Inner SI combined with overtopping, second sliding or micro instability.
- BEP combined with crest lowering followed by overtopping or overflow.

Breteler et al. (2010) describes the residual strength of a levee after initial failure. They focus on the follow-up mechanisms: erosion of the core material, micro instability and instability of the cover material. They quantified residual strength in hours until failure. Breteler et al. (2010) states that further research is needed on the topic of residual strength regarding BEP, which needs to follow from the IJkdijk experiments (Sellmeijer et al., 2011).

In Knoeff et al. (2018) different failure paths of levee are discussed by means of fault trees. The fault tree in Figure 5.1 from Knoeff et al. (2018) suggests a possible interaction between SI and the forming of (sand) boils, in the form of one arrow in the fault tree. This arrow suggests an interaction between SI and BEP, where the SI causes a rupture in the blanket (relocation of the exit point) and gives BEP a better opportunity. It states that this is never observed. The examples in Knoeff et al. (2018) are mostly descriptions of the possible interactions. However, these examples are not quantified yet. The mention interactions are:

- Overtopping and overflow combined with erosion of cover material, slope instability of cover material, inner SI.
- Inner SI combined with micro instability, second sliding, BEP and overtopping or overflow.
- BEP combined with crest lowering.

In Kok et al. (2017), the influence of SI on the erosion resistance of the levee is mentioned as an interaction, and they recommend more research on the topic of interactions between failure mechanisms in general and on correlation of failure mechanisms due to the same initiation mechanism.

The interaction between overtopping/overflow and inner SI (or cover layer stability) is researched by Hoven et al. (2011). Hoven et al. (2011) examined this influence of the infiltration of water into the inner slope due to wave overtopping, on the stability of the inner slope. In the test, sliding did not occur, probably due to the higher horizontal permeability than vertical permeability of the soil. The phreatic line did rise due to overtopping which can influence the stability. This interaction between overtopping and SI is introduced in the design method for levees OI2014v4 (Rijkswaterstaat WVL, 2017a) by de Visser et al. (2018). The interaction between SI and overtopping is defined as; the phreatic line in the levee rises due to overtopping. This leads to a (small) sliding plane, which causes the erosion resistance of the inner slope to decrease. The interaction is taken into account in the design by analysing a second load condition, which is based on a higher saturation of the levee by infiltration.

Margo (2018) states that the USACE does not model interactions in event trees via correlations in event trees. They do include interactions in failure mechanisms descriptions, the building of event trees and when eliciting probabilities for event trees. Margo (2018) gives the following example: 'If internal erosion might lead to slope instability, we would typically call it a slope instability failure mechanism and include the internal erosion contribution as steps in a slope instability event tree.'.

The current assessment and design method of levees in the Netherlands (Rijkswaterstaat WVL, 2017a,d) does not include the interactions between failure mechanisms for all possible combinations. Currently, it only includes the effects of overtopping on SI (de Visser et al., 2018) and a reduction of the shear strength in SI due to uplift (Kanning and van der Krogt, 2016).

2.2.2. Examples of interactions

Breach by Hohenwisch (Germany)
Nine levees located in Hamburg, Germany breached during the 1962 storm surge. Kolb et al. (1962) describe these breaches in detail. The breach at Hohenwisch shows a possible interaction between BEP and SI. "At Hohenwisch, a full sliding of the levee occurred over a distance of 80 meters. Five days before the full breach, the soil at the inner side of the levee swelled. The day of the breach a eye witness states water was flowing out of the underground. A little while later, the levee over-topped and simultaneously horizontal sliding occurred (Kolb et al., 1962)". The swollen inner side of the levee is an indication of the sub- mechanism uplift for SI and for BEP. If the soil ruptures, the water that was trapped will start to flow out of the underground, this is called a boil. Kolb et al. (1962) does not describe if the boil was carrying sand or how long it was transporting water with perhaps sand particles. Thus, it is unknown whether the sub-mechanism of Heave occurred or if a network of pipes had already been created. Eventually, horizontal instability lead to levee failure. The high water pressure that caused uplift or the presences of pipes might also have influenced a reduction in shear strength of the soil, which is known to cause instability.

Hondsbroeksche Pleij DP 220-223
In Koopmans (2011), a case is re-evaluated. During high water, sand boils appeared at a location where it was

not expected for this water level. The levee considered has a berm and a seepage screen (kwelscherm) in the berm. They calculated what could happen if below the berm hollow spaces are formed like small pipes and if they could lead to SI of the berm due to the reduced shear strength of the soil. Koopmans (2011) concluded that the safety factor of the SI of the berm reduces due to these hollow spaces. This reduction indicates an interaction between the failure mechanisms BEP and SI.

2.3. Backward erosion piping

2.3.1. Backward erosion piping process

Backward erosion piping is erosion underneath a levee due to seepage, causing the formation of hollow spaces called pipes (Van Beek, 2015). Other terms which refer to the same process are under seepage and piping. The backwater erosion piping process is set in motion by an increase in water level with a long duration. This increase in water level gives an hydraulic gradient over the levee, which results in groundwater flow beneath the levee. This flow leads to an increase in pore water pressures in the aquifer. The permeability difference causes an overpressure in the aquifer compared with the blanket layer. At the toe of the levee, the blanket layer gets in contact with this over-pressures. When this pressure exceeds the weight of the blanket, the blanket is lifted and deformed. If the pressure is high enough, it can lead to rupture of the blanket. At the point of the rupture, water will flow through the blanket layer to the surface (Förster et al., 2012). In BEP calculations this process is called 'Uplift' this includes uplift, and it includes the assumption that rupture has also taken place. When there is no blanket present uplift and rupture is not needed to get to seepage.

When groundwater flows through the blanket to the surface, this is called a water boil. The seepage through the sand layer that supplies water for the boil can transport sand particles into the boil. This sand is fluidised, and it increases the resistance of flow through the boil channel. This resistance lowers the flow velocity at the bottom of the boil in the sand layer, and there is a head loss over the boil. The decrease in flow velocity can stop the sand particles from eroding. When the flow velocity remains strong enough to supply sand out of the boil channel, the transport will create a hollow space in the sand layer near the blanket layer. The vertical transport of sand particles to the surface making the water boil a sand boil is called 'Heave'. In the calculation of BEP, the critical heave gradient may not be exceeded. Else heave can occur (Förster et al., 2012).
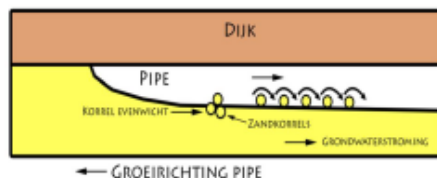
Figure 2.1: Sand particle transport in a pipe ('t Hart et al., 2016, p. 39)
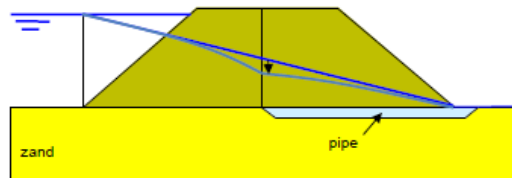
Figure 2.2: Change in hydraulic head in aquifer due to a pipe (Förster et al., 2012, p. 39)

If the transport of grain particles continues, it initiates the pipe formation. At first, small channels will develop in all directions and eventually it will develop in one main direction. The pipe will start to progress towards the entry point, against the groundwater flow direction (see Figure2.1). This process is called 'backward erosion' or 'piping'. The erosion of the front of the pipe and erosion of the walls causes this progression of the pipe. The pipe acts as a drain which leads to an increase in the hydraulic gradient at the tip of the pipe which fuels the groundwater flow which in turn influences the erosion (see Figure 2.2). At a specific critical gradient, the pipe can no longer stop growing.

If the pipe has reached the entry point at the river side of the levee, the pipe will start to widen (lateral pipe development). If there is a continuous pipe with sufficient width, two things can happen: the levee can settle closing the pipe with or without crest lowering, or there can be slope instabilities with or without eventual crest lowering. When there is crest lowering, an overflow will follow with erosion and breach growth leading to flooding. In the current assessment, the failure mechanism BEP includes the sub-mechanisms Uplift,

Heave and piping. The initial failure definition of BEP is if there is progressive pipe development, which is approximately when the pipe reaches half of the levees' width. The rest of the failure process passed this point is not include the assessment. The possible interaction can take place in the part of the process which is excluded from the assessment.

Uplift, Heave and Piping all need to occur in sequence to get backward erosion piping (BEP). When one of the three does not occur, initial failure due to BEP will not occur.

The driving force of BEP is the hydraulic gradient over the levee and the pressure difference between the blanket layer and aquifer. These are described in detail in appendix A.

2.3.2. Uplift

To check for uplift problems, the weight of the blanket is compared with the uplift pressure under the blanket. Note, as mentioned in 2.3.1, uplift check is only necessary when there is a blanket layer present. The weight of the blanket is the resistance in the limit state function (Z_u, see Equation (2.3)), which is defined as the critical head difference at which uplift can occur. The occurring head difference is the load parameter in the limit state function.

$$Z_u = \Delta\phi_{c,u} - \Delta\phi \tag{2.3}$$

$$FoS_u = \frac{\Delta\phi_{c,u}}{\Delta\phi} \tag{2.4}$$

Where	Z_u	Limit state function of Uplift	[-]
	$\Delta\phi_{c,u}$	Critical head difference at the exit point	[m]
	$\Delta\phi$	Head difference at the exit point	[m]

In which the critical head difference at the exit point is described in Equation (2.5).

$$\Delta\phi_{c,u} = \frac{d(\gamma_{sat} - \gamma_w)}{\gamma_w} \tag{2.5}$$

Where	γ_{sat}	Volumetric weight of the saturated blanket	[kN/m^3]
	γ_w	Volumetric weight of water	[kN/m^3]

The head difference at the exit point is shown in Equation (2.6).

$$\Delta\phi = \phi_{exit} - h_p \tag{2.6}$$

Where	ϕ_{exit}	Head at the exit point	[m+NAP]
	h_p	Phreatic level at the exit point	[m+NAP]

Rupture of the blanket layer occurs when the occurring head difference ($\Delta\phi$) is higher than the critical head difference ($\Delta\phi_{c,u}$). After rupture, the head in the aquifer at the rupture point can not exceed the weight of the blanket and is therefore limited by the so-called limit potential, see equation 2.7 (Zwanenburg et al., 2013). This limit potential is the head in the aquifer where an equilibrium is present with the weight of the blanket layer, is also referred to as head limit (Förster et al., 2012).

$$\phi_{limit} = h_p + d\frac{\gamma_{sat} - \gamma_w}{\gamma_w} \tag{2.7}$$

Where	ϕ_{limit}	Head in the aquifer (sand layer) at interface with the blanket	[-]
	h_p	Hinterland phreatic level	[-]
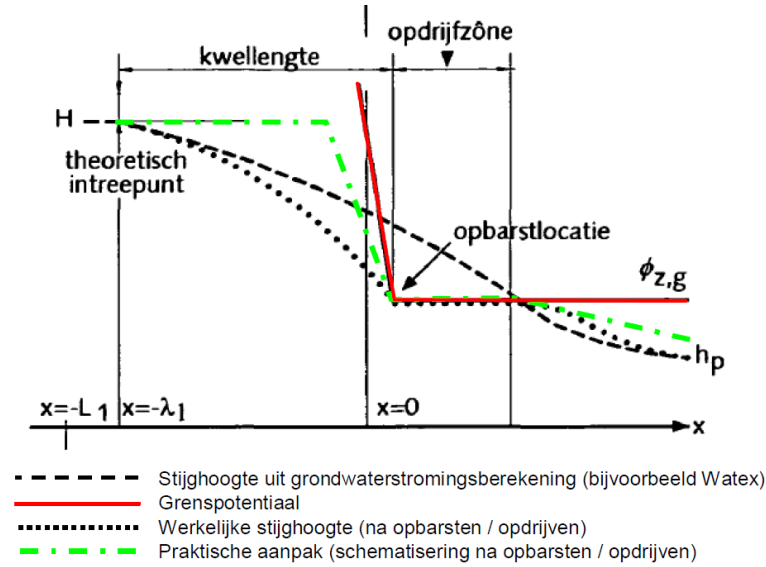
Figure 2.3: Limit potential in sand layer (Zwanenburg et al., 2013)

2.3.3. Heave

When the blanket is ruptured or when there is no blanket, the water in the aquifer can flow upwards through the exit point. When the upwards flow velocity is high enough, sand grains will start to move up to the surface. Heave occurs when the occurring gradient exceeds the critical heave gradientFörster et al. (2012). The following limit state function (Jonkman et al., 2017) describes this heave process:

$$Z_h = i_{c,h} - i \tag{2.8}$$

$$FoS_h = \frac{i_{c,h}}{i} \tag{2.9}$$

Where Z_h Limit state function for heave   [-]

                         $i_{c,h}$ Critical heave gradient   [-]

                         i Exit gradient   [-]

The occurring hydraulic gradient at the exit can be calculated analytically as Equation (2.10) (Jonkman et al., 2017).

$$i = \frac{\phi_{exit} - h_p}{d} \tag{2.10}$$

Where d Thickness of the blanket   [m]

The head at the exit ϕ_{exit} for heave is lower than for Uplift, it will go back to the limit potential after rupture.

Critical Heave gradient

Terzaghi first introduced the critical heave gradient in 1922 in the form of equation 2.11 (Van Beek et al., 2014). It is based on the vertical equilibrium of a soil particle, where fluidisation is the loss of equilibrium (uplift of one particle). To cause erosion of the soil, a group of particles need to move. The vertical movement of a particle depends on the porosity n, because water in porous material can more easily carry a particle between other soil particles.

$$i_{c,h} = -(1-n)\left(\frac{\rho_s - \rho_w}{\rho_w}\right) \tag{2.11}$$

Where n Soil porosity   [-]

                         ρ_w Water density   [kg/m^3]

                         ρ_s Soil density   [kg/m^3]

Van Rhee and Beezuijn include cohesion of the soil particles to account for a group of particles eroding (Van Beek et al., 2014).

$$i_{c,h} = -(1-n)\left(\frac{\rho_s - \rho_w}{\rho_w}\right)\frac{\sin(\phi - \beta)}{\sin(\phi)} \qquad (2.12)$$

Where ϕ Friction angle   [deg]
               β Angle of the sloping surface   [kg/m^3]

Figure 2.4 shows the observation of the USACE at the Mississippi river of under seepage and sand boils during the 1950 flood. This observations show that for a vertical gradient between the 0.5-0.8, sand boils occur. The theory is called the blanket theory (USACE, 1956; Van Beek, 2015).
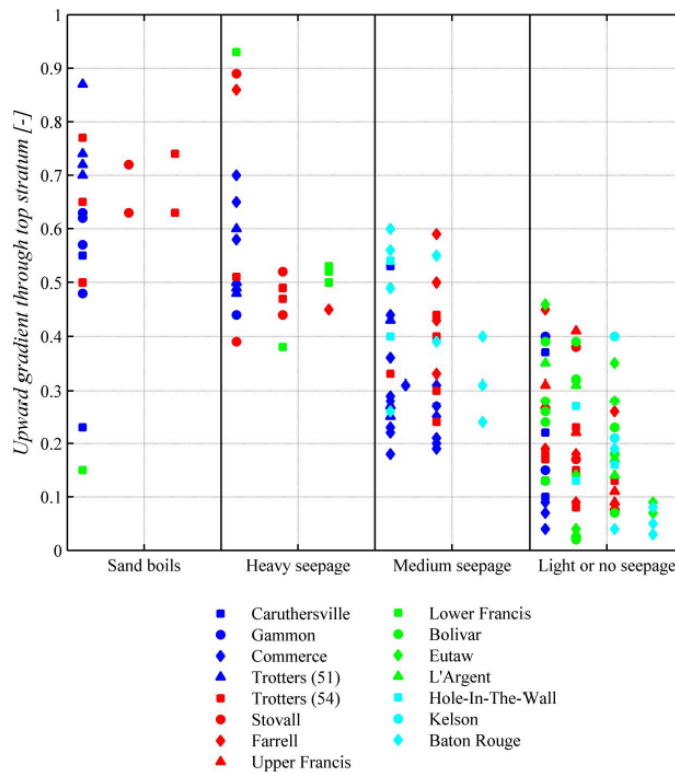
Figure 2.4: Vertical exit gradient against the amount of seepage and sand boils (Van Beek, 2015, p. 33) based on USACE (1956)

However, a critical heave gradient of 0.3 is used by Rijkswaterstaat WVL (2017d), as a part of the backward erosion process. These conservative assumptions were reconsidered for the new assessment by Koelewijn (2009). His study concluded that although the current substantiation is weak, there are not enough field observation and reasons to reject it.

2.3.4. Piping

After heave has created the hollow space and initiated the pipe, the pipe can start to progress in the direction of the outer water. Bligh (1910) found that piping was dependent on the head difference, the seepage length and grain size. Lane (1935) added the importance of the distinction between horizontal flow and vertical flow, where the vertical distance has more influence (Van Beek, 2015). The currently used model in the Netherlands is the newly fitted piping rule of Sellmeijer et al. (2011). The equation 2.14 shows the limit state at which the pipe cannot stop progressing (Jonkman et al., 2017). The 0.3d accounts for the head loss in the boil due to the presence of fluidised sand (Rosenbrand, 2017). Initiation of the pipe is a different process than the

progression. The Sellmeijer rule only counts for the progression.

$$\Delta H_c = l_{pipe}/L_{seepage} = 0.5 \tag{2.13}$$

Sellmeijer describes pipe progression via the balance between the maximum hydraulic gradient over the levee and the sediment balance of the sand particles in the pipe. The maximum hydraulic gradient where there is no movement of the sand particles at the bottom of the pipe, is called the critical hydraulic gradient for piping (ΔH_c). Förster et al. (2012) states that this maximum occurs at the ratio of a 0.5 between the pipe length and the total seepage length (see equation 2.13).
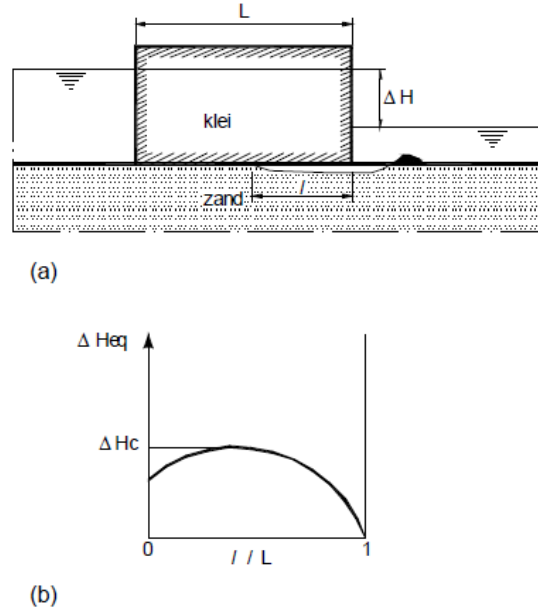
Figure 2.5: The critical hydraulic gradient as function of the pipe length and the total seepage length (Förster et al., 2012, p. 86)

When the hydraulic gradient increases over the levee, the pipe will increase in length until it reaches equilibrium again, and it stops progressing. This will continue until the hydraulic gradient ranges above the critical hydraulic gradient when the pipe does not stop progressing.

$$Z_p = H_{c,p} - H, \quad H = h - h_p - 0.3d \tag{2.14}$$

$$FoS_p = \frac{H_{c,p}}{h - h_p - 0.3d} \tag{2.15}$$

Where	Z_p	Limit state function for piping	[-]
	$H_{c,p}$	Critical head difference piping	[m]

The critical head difference for piping is calculated by Rijkswaterstaat (2017) following the rule of Sellmeijer with formula :

$$H_c = L F_{resistance} F_{scale} F_{geometry} \tag{2.16}$$

with:

$$F_{resistance} = \eta \frac{\gamma_p}{\gamma_w} \tan(\Theta) \tag{2.17}$$

$$F_{scale} = \frac{d_{70m}}{\sqrt[3]{\kappa L}} \left(\frac{d_{70}}{d_{70m}} \right)^{0.4}, \quad \kappa = \frac{\upsilon_{water}}{g} k \tag{2.18}$$

$$F_{geometry} = 0.91 \left(\frac{D}{L} \right)^{\frac{0.28}{\left(\frac{D}{L} \right)^{2.8} - 1} + 0.04} \tag{2.19}$$

Where			
	L	Seepage length	[m]
	d_{70m}	Reference value for d_{70}	[m]
	d_{70}	70%-fractile of the grain size distribution	[m]
	κ	Intrinsic permeability coefficient	[m^2]
	k	Darcy permeability	[m/s]
	ν	Kinematic viscosity	[m^2/s]
	γ'_p	Submerged specific weight sand	[kN/m^3]
	θ	Bedding angle (=37 deg)	[deg]

Equation 2.16 has a slightly different formulation than the original correction by Sellmeijer et al. (2011). The factors for relative density, uniformity and angularity of the grains are excluded.

2.4. Slope instability

2.4.1. Slope instability process

Slope instability is lost when the soil-body slides along a sliding plane, which is often schematized as a circle, as shown in Figure 2.6. When there is high water for a significant duration, the water will seep into the levee and the subsoil. This increase in water level will increase the pore water pressures in the levee and subsoil, which leads to a decrease in effective stress, which in turn causes a decrease in shear strength of the soil. The high water will also increase the saturation of the levee, which influences the weight of the soil body.

In the initial situation before high water, the soil is in equilibrium. When the hydraulic load on the levee increases, this causes a disturbance of the soil equilibrium, which consists of a balance between a driving moment M_d and a resisting moment M_r. The driving moment consists of external forces, like hydraulic load or traffic loads etc. and internal forces like the weight of the soil body. The resisting moment is internal, the resistance at the sliding plane formed by the shear strength of the soil. The shear capacity of the soil can be determined in an undrained and drained analysis as mentioned in Section 2.4.3.

The increase in water level (hydraulic load), gives an increase in the driving moment and a decrease in the resisting moment can cause sliding of the inner slope (TAW, 1985).
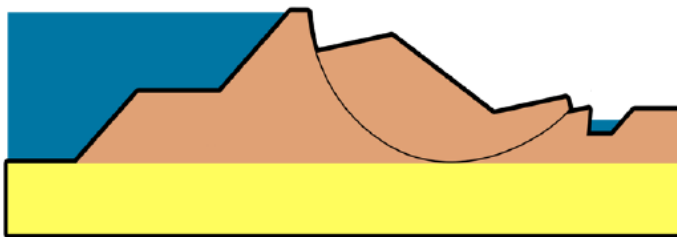
$$FoS_s = \frac{M_r}{M_d} \tag{2.20}$$

Figure 2.6: Inner slope failure for typical Dutch river levee, from (Jonkman et al., 2017, p. 114)

There are different sliding planes that can lead to initial failure due to SI. To determine which of these sliding planes is critical a factor of safety (FoS) is used. In which the FoS is calculated by dividing the resisting moment by the driving moment, as shown in equation 2.20. Each sliding plane has a different FoS. The critical sliding plane is the sliding plane which has the least resistance against sliding, hence the lowest FoS.

There are different methods of calculating SI, which uses different assumptions on the shape of the sliding plane and the shear strength calculation. These models are described in Section 2.4.2.

2.4.2. Models

As mentioned in Section 2.4.1, SI is caused by a disturbance in the soil equilibrium. The equilibrium can be modelled by limit equilibrium methods (LEM). These models calculate the different possible sliding planes and determine which one is the critical sliding plane. These sliding planes are divided into slices. The critical sliding plane is determined by an iteration of the moment equilibrium, the vertical force equilibrium of a slice, and the horizontal force equilibrium of a slice(Rijkswaterstaat, 2016).

The moment equilibrium is the equilibrium between the driving moment and the resisting moment. Where driving moment (M_s) is the weight of the soil at the active side (side closest to the water) and the resisting moment (M_r) is the weight of the soil at the passive side plus the shear capacity of the soil in the sliding plane. (Jonkman et al., 2017).
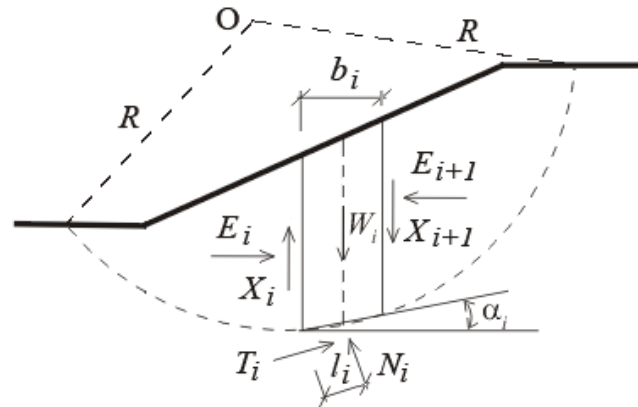
Figure 2.7: Sliding plane with slice and forces acting on slice (Wikipedia, the free encyclopedia, 2009)

Most commonly used limit equilibrium methods (LEM) for SI are Bishop, Uplift-Van (used in WBI 2017) and Spencer, which are all 2D models. They can only work with static pore water pressure. They are not able to include strain-hardening and deformation dependent pore water pressure generation. To include these traits finite element modelling (FEM) can be used, e.g. PLAXIS. A disadvantage of FEM is the computational time.

Bishop method
Bishop (1955) started with the Fellenius method, which considers the equilibrium of slices where the interaction between slices is neglected. In Bishop's method, these interactions are not neglected in the calculation. Bishop (1955) assume that the resultant of the inter-slice forces is horizontal. Bishop (1955) only considers the vertical equilibrium of the slice and the total moment equilibrium, see Figure 2.8. He worked with drained shear strength (Mohr-Coulomb).

To calculate the FoS of the SI with Bishop's method the equation 2.21 and 2.22 need to be iteratively calculated. This iteration needs to be done for different sliding planes, to get to the critical sliding plane. If the slice is partially saturated, this can be implemented in the formula.
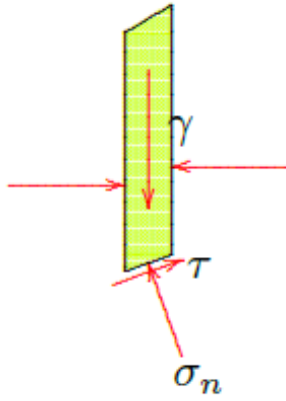
$$FoS_{bishop} = \frac{\sum_j \frac{[c'l_j + (W_j - u_j l_j)\tan(\phi')]}{\psi_j}}{\sum_j W_j \sin(\alpha_j)} \quad (2.21)$$

$$\psi_j = \cos(\alpha_j) + \frac{\sin(\alpha_j)\tan(\phi')}{F} \quad (2.22)$$

Where

j	Slice index	[-]
l	Width of each slice	[m]
W	Weight of each slice	[kg/m^3]
α	Angle of slice	[Deg]

Figure 2.8: Slice with forces from Bishop
(Verruijt, 2001)

Uplift-Van

The big difference between Bishop and Uplift Van is the sliding plane shown in Figure 2.9. Here, a pressure bar which can experience uplift connects the two circles. Due to this bar, the horizontal equilibrium must be taken into account (Van et al., 2005). This results in the equation 2.23 for the FoS.
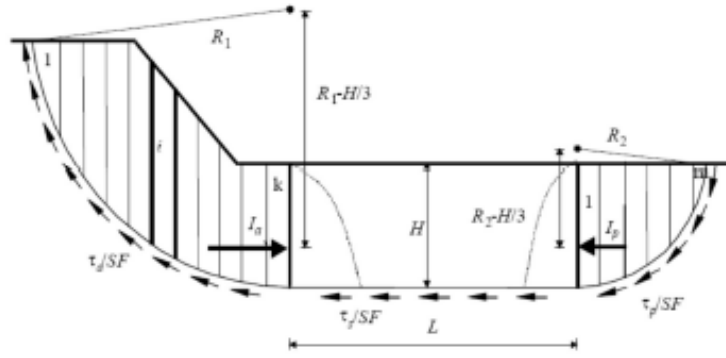
Figure 2.9: Sliding plane Uplift-Van (Zwanenburg et al., 2013)

$$FoS_{Uplift-Van} = \frac{\left[\frac{\sum_{i=1}^{k}\left(\frac{c_i + (\gamma_i h_i - u_i)\tan(\phi_i)}{1 + \frac{\tan(\alpha_i)\tan(\phi_i)}{F}} * \frac{b_i}{\cos(\alpha_i)} \right)}{1 - \frac{H}{3R_1}} + \frac{\sum_{j=1}^{m}\left(\frac{c_j + (\gamma_j h_j - u_j)\tan(\phi_j)}{1 + \frac{\tan(\alpha_j)\tan(\phi_j)}{F}} * \frac{b_j}{\cos(\alpha_j)} \right)}{1 - \frac{H}{3R_2}} + \tau_s L \right]}{\left[\frac{\sum_{i=1}^{k}(\gamma_i h_i b_i \sin(\alpha_i))}{1 - \frac{H}{3R_1}} + \frac{\sum_{j=1}^{m}(\gamma_j h_j b_j \sin(\alpha_j))}{1 - \frac{H}{3R_2}} \right]} \quad (2.23)$$

Important to the uplift situation is the difference between uplift and rupture. Rupture occurs if the head in the sand layer exceeds the weight of the blanket, as is the case with Uplift from BEP. This 'limit potential' is calculated in equation 2.7 and visualized in Figure 2.3 (Zwanenburg et al., 2013). If the outside water level increases, the area where the limit potential is present will expand further land-inward. This area, the uplift zone, is important for stability analysis at uplift (Förster et al., 2012).

If this limit potential is not reached, the safety against uplift is calculated with equation 2.24.

$$F_{SI-uplift} = \frac{(h_g - h_p) * \gamma + (h_p - h_s)\gamma_{sat}}{(\phi_s - h_s)\gamma_w}$$ (2.24)

Where	h_g	Ground level polder	[m]
	h_s	Ground level start sand layer	[m]

If the blanket layer is lifted, it starts to floats on top of the sand layer. There is a reduction of the shear strength. If at some places the limit potential is reached there is no shear strength at the interface. With rupture, the limit potential is reached, and the shear strength is assumed to be zero.

All three LEMs calculate the moment equilibrium and vertical equilibrium, Uplift-Van and Spencer also calculate the horizontal equilibrium. The difference lies in the schematization of the slide surface in which Bishop uses the most straightforward surface, a circle. Uplift Van uses two circles connected by a line, and with Spencer, the slide plane can be custom defined. Bishop does not take into account the possibility of Uplift, which in the case of interaction might be important. So, the Uplift-Van method is the most suited to use.

The FEM and LEM are built into the models like PLAXIS and D-Geo stability. PLAXIS is a more complex finite element model, and D-Geo stability uses the LEM. For the aim of this thesis, the LEM and thus D-Geo stability is used. D-Geo stability gives as output a factor of safety, where the LSF can be defined as Equation (2.25).

$$Z_s = FoS_s - 1$$ (2.25)

The levee is assessed for SI in WBI 2017 (Rijkswaterstaat WVL, 2017d) through the D-Geo stability program. This program uses the Uplift-Van method to calculate the stability factor for SI.

2.4.3. Shear strength model

The shear strength of a soil can be described in a drained or undrained condition. These conditions dictate the way to calculate the shear strength.

Which of the two conditions should be used depends on the soil type/grain size, saturation, consolidation and the rate of loading. In drained condition, the pore water can drain out quickly. In the undrained condition, the soil is unable to drain. This condition of the soil influences the reaction of the soil equilibrium to a particular load. If the effective stress is reduced due to this reaction, there is a loss in shear capacity.

For example with slow loading in comparison to consolidation time, saturated soil consisting of sand or gravel is considered in the drained condition. Clays and silts saturated soils with the same load are considered undrained. When there is fast loading in comparison to the consolidation time, sand can act undrained. (Zwanenburg et al., 2013)

Drained shear strength model
In earlier assessments the shear strength of the soil was modelled as drained only. To calculate the shear capacity the Mohr- Coulomb model (see Equation (2.26)) was used (Verruijt, 2001).

$$\tau = c' + \sigma'_n \tan(\phi')$$ (2.26)

Where	τ	Shear stress	[kN/m^2]
	c'	Cohesion	[kN/m^2]
	σ'	Effective normal stress	[kN/m^2]
	ϕ'	Effective friction angle	[°]

In WBI 2017 the Critical State Soil Mechanics (CSSM) model (Schofield and Wroth, 1968) is used to assess levee on SI as cited by Rijkswaterstaat (2016). In CSSM model distinction is made between the peak strength, the critical shear strength and consolidated and over-consolidated soil behaviours. The critical shear strength is defined as:

$$t_{max} = s' \sin(\phi'_{cz})$$ (2.27)

Where	t_{max}	Maximum mobilizable shear stress $(\frac{\sigma'_v - \sigma'_h}{2})$	[kN/m^2]
	s'	Mean effective principal stress $(\frac{\sigma'_v + \sigma'_h}{2})$	[kN/m^2]
	ϕ'_{cz}	Angle of internal friction	[°]

The critical state line (CSL) is described by the t/s'. The cohesion is considered to be a part of the over-consolidation and is not directly taken into account in the CSL.

Undrained shear strength model

In WBI 2017 undrained shear strength is defined based on the SHANSEP model (Rijkswaterstaat, 2016):

$$s_u = \sigma'_{v,i} SOCR^m \tag{2.28}$$

$$OCR = \frac{\sigma'_{vy}}{\sigma'_{v,i}} \tag{2.29}$$

$$\sigma'_{vy} = \sigma'_{v,i} + POP \tag{2.30}$$

Where	s_u	Undrained shear strength	[kN/m^2]
	$\sigma'_{v,i}$	In situ effective vertical stress	[kN/m^2]
	S	Undrained shear strength ratio	[-]
	OCR	Over-consolidation ratio	[-]
	m	stress increase exponent	[-]
	σ'_{vy}	Vertical yield stress	[kN/m^2]
	POP	Pre-overburden pressure	[kN/m^2]

The important difference between drained and undrained is in an undrained analysis, the groundwater pressures which develops when the ground starts to deform are included in the calculation. These pressures have an unfavourable effect on the shear strength. In a drained analysis, these are not taken into account. Which of the two methods should be used depends on the soil properties. Rijkswaterstaat (2016) makes a distinction between lightly over-consolidated clay and peat, sandy-clay, sand and heavy over-consolidated soil. The first two are assumed to behave like undrained soil because they are less permeable and the others are assumed to behave like drained soil.

2.4.4. Remaining profile

Rijkswaterstaat (2016) defines that the calculated critical sliding circle needs to result in loss of primary function. If this is not the case, they advise to take residual strength into account by optimizing the zoning. van der Krogt et al. (2019) states that not all sliding planes will lead to immediate levee failure. Zwanenburg et al. (2013) states that different approaches for residual strength are used in the past based on the Technical Report Current Strength of levees[1] (ENW et al., 2009) and HCO (TAW, 1994). These reports also provide a schematic representation of the remaining profile as seen in for example Figure 2.10.
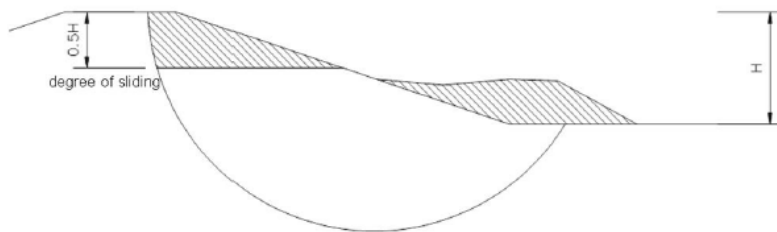
Figure 2.10: Remaining profile after first sliding from TAW 1994 as cited by (Den Haan et al., 2014, p. 13)

---

[1]'Technisch Rapport Actuele Sterkte van dijken' in Dutch, hereafter referred to as TRAS

The amount of sliding is important for the formation of the remaining profile. Zwanenburg et al. (2013) determines from observations that a sliding plane often lowers 1 meter. On the other hand, Den Haan et al. (2014) states that this lowering depends on the height of your sliding plane and that it slides down 0.35-0.5 times that height. Whereas ENW et al. (2009) assumes 0.5 times the height of the sliding plane as a conservative assumption based on observations of sliding planes. ENW et al. (2009) states that the method is not suited for uplift sliding planes because the location of the entry point is too uncertain. The more recent study of Zwanenburg et al. (2013) refutes the arguments from TRAS and states that the method can also be used for uplift situations because the entry locations for both shapes are equally uncertain.

After this first sliding, a second sliding can take place if the remaining slope is too steep. In which TRAS defines a new slope as described in Table 2.1. This slope has an angle which depends on the soil type, shear strength of the soil and the retaining water height (H).

Figure 2.11: Remaining profile after first sliding in Schipluiden (South Holland) (Den Haan et al., 2014, p. 24).

Soil type	Precondition	Slope
Clay	Su >3,5 H	slope 1:2
Peat	Su >3,5 H	slope 1:4
Sand	ϕ >22 degrees	slope 1:4

Table 2.1: Slope second sliding translate from (ENW et al., 2009, p. 31)

3

Identifying interaction between backward erosion piping and slope instability

The purpose of this chapter is to identify the possible interaction between backward erosion piping (BEP) and slope instability (SI). First, a brief introduction to the interaction between BEP and SI is given, and the method of identification is discussed (section 3.1). After that, the interaction is split in two directions, where Section 3.2 examines the interaction from SI to BEP and Section 3.3 examines the interaction from BEP to SI. In the Chapters 4 and 5 that follow, only the interaction from SI to BEP will be quantified.

3.1. Introduction

Traditionally, the failure of a levee is described by the known failure mechanisms. However, the focus in this study lies on combinations of two failure mechanisms and its interaction as a cause for the failure of a levee. An interaction is defined as one failure mechanism influencing the probability of occurrence of another failure mechanism in a positive or negative sense. The interaction is an alternating process, where the dominant failure mechanism continuously switches during the failure process. For example, a pipe in the subsurface causes sliding of a part of the levee. This sliding may lead to clogging of the pipe, but at the same time this sliding also causes a new exit point for piping and thus, restarts the BEP process (repeated cycle in Figure 3.1 over time and space). Such an alternating process is complex. Therefore, a first step is made in the approximation of this alternating process by looking at the interaction in a linear way (only one direction at a time) by looking to BEP after the occurrence of SI and vice versa.
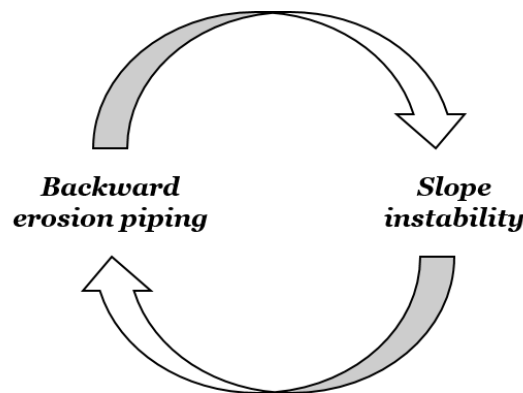
Figure 3.1: Interaction cycle

21

The interaction between BEP and SI is considered in both directions, see Sections 3.2 and 3.3. Intermediate switches between the failure mechanisms (alternating process) are not considered in this study. BEP consists of three sub-mechanisms (uplift, heave and piping) that need to occur in sequence to get BEP. Both Sections are therefore divided into multiple subsections, one for each sub-mechanism of BEP and one for combined BEP.

This chapter consists of a parametric study, in which the limit state functions (for uplift, heave, piping and SI) act as a guide to determine the effects of changes in the parameters' present states in these limit state functions, see equations 2.3, 2.8, 2.14 and 2.25. The effects of these changes determine the occurrence of the mechanisms described by the limit state function. The leading failure mechanism determines the changes in the parameters. This failure mechanism influences the surroundings and transforms the levee into a remaining profile, which alters the parameters present in the limit state functions of the other failure (sub-)mechanisms.

Within an interaction, the 3D-effect, the spatial scale and the time dependence are important to keep in mind.

- *3D effect*
  The location of the considered cross-section can lead to a different result of the interaction. For example, when looking at the cross-section where a pipe filled with water is present, there is no shear strength in this pipe. This might cause SI in this cross-section. In the cross-section next to the pipe, the effect on the shear strength is different. This effect can only be described by taking the 3D effect into account.
- *Spatial scale*
  BEP and SI influence the surroundings on a different scale. A pipe can have a diameter of approximately one to two meter, and SI can occur in a levee Section of approximately 30-100 meters. The effect that a pipe has on the surrounding is of a different scale than SI.
- *Time dependence*
  The load condition which causes the failure mechanisms of BEP and SI is a flood wave in the river, which has a duration of several weeks and is time-dependent. Especially for BEP initial failure, an increase in load can make a difference in the continuation to the next sub-mechanism. In the description of the interaction, only an extreme high water level is considered.

In this chapter, a simple standard Dutch river levee is used to describe the interaction, as shown in Figure 3.2. Next to this Figure is the legend for the Figures in this chapter.

(a) Original BEP parameters and the original phreatic lines and aquifer head

(b) Legend of the figures in this chapter
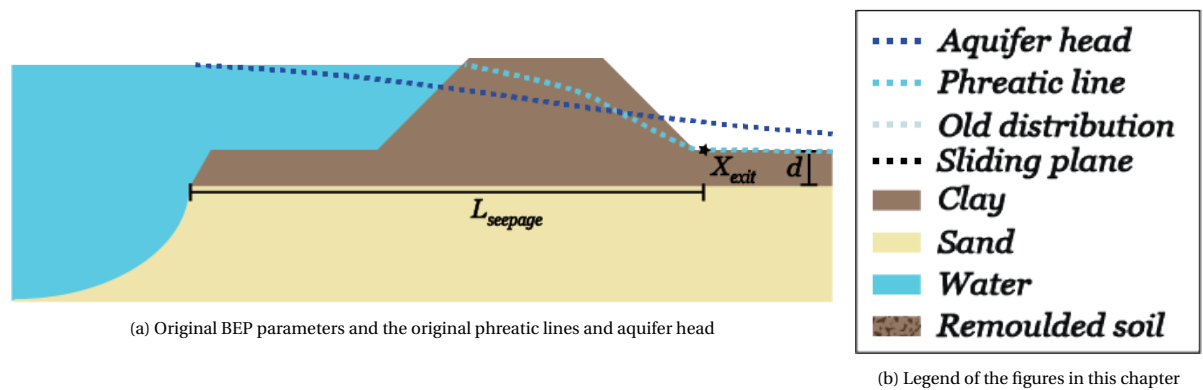
Figure 3.2: Original BEP situation

Section 3.2 elaborates on the interaction from SI to BEP and Section 3.3 on the interaction from BEP to SI. The conclusions that follow from these Sections can be found in Section 3.4.

3.2. Interaction from slope instability to backward erosion piping

This Section is divided into multiple subsections. Subsection 3.2.1 elaborates upon the formation of the remaining profile after SI. The next subsections qualify the effect of SI on one of the sub-mechanisms of BEP (uplift (Subsection 3.2.2), heave (Subsection 3.2.3) and piping (Subsection 3.2.4). Subsection 3.2.5 shows the effect of SI on the occurrence of BEP. The final subsection contains alternative situations for the interaction from SI to combined BEP.

3.2.1. Mechanism slope instability

The interaction where SI influences BEP is based on the assumption that SI has occurred, but did not cause immediate levee failure. This interaction starts when the pore water pressures in the aquifer at the toe of the levee increase. The increase causes the effective stresses at the toe to decrease around the interface of the blanket and the sand layer, which in turn decreases the shear strength of the soil at the interface of the blanket and the sand layer at the toe of the levee. Simultaneously, the phreatic level in the levee will also increase, increasing the driving moment of the soil equilibrium. Together, these processes lead to SI.

There are different shapes and sizes of sliding planes, as a result of SI. The first requirement for the interaction is about the size of the sliding plane; this sliding plane may not cause immediate flooding. The second requirement for the interaction is that a second sliding also does not cause loss of the primary function of the levee.

In this section, four different kinds of sliding planes are defined and shown in Figure 3.3.

1. *Sliding through the **crest** into the **blanket** layer*
2. *Sliding through the **crest** into the **sand** layer*
3. *Sliding through the **slope** into the **blanket** layer*
4. *Sliding through the **slope** into the **sand** layer*

There are different approaches to schematize real sliding planes. In this chapter, the Bishop shaped sliding planes are considered in the drawings and text.

(a) Option 1: Crest - Sand layer

(c) Option 3: Slope - Sand layer

(b) Option 2: Crest - blanket layer

(d) Option 4: Slope - Blanket layer
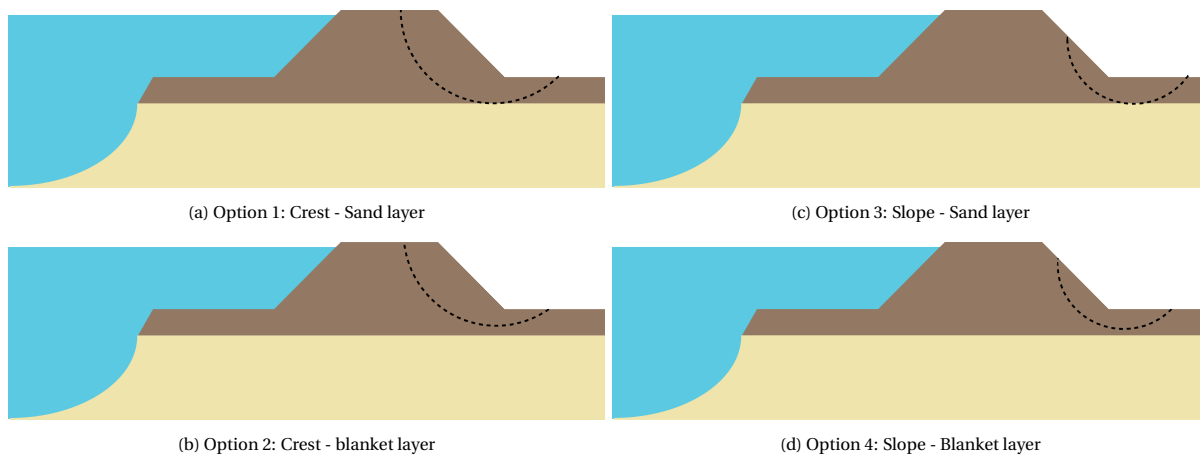
Figure 3.3: Sliding plane locations

Each of these sliding plane options will deform into a so-called remaining profile. The shape of this remaining profile is highly simplified to fit this exploratory research. The shape of the remaining profile is based on the video of levee failure of the IJkdijk experiments of 2008 (ICTdijk, 2009) and the pictures of slope instabilities in Den Haan et al. (2014).

First, the sliding plane is rotated to come to a remaining profile (see Figure 3.4a). A second sliding or insta-

bility will cause a layer of remoulded soil to accumulate at the toe of the levee and steepening of the inner slope (dotted line in Figure 3.4a). This remoulded soil will form a berm at the toe of the levee, see Figure 3.4b. The size and shape of the sliding plane influence the size of the displaced volume of soil and thus the height of the berm. Depending on the different sliding planes, the remaining profiles have a steeper inner slope, a narrower crest width and a bigger berm of remoulded soil.

(a) Sliding along the sliding plane of option 3 (Figure 3.3 (c)) (b) Remaining profile of option 3 (Figure 3.3 (c))
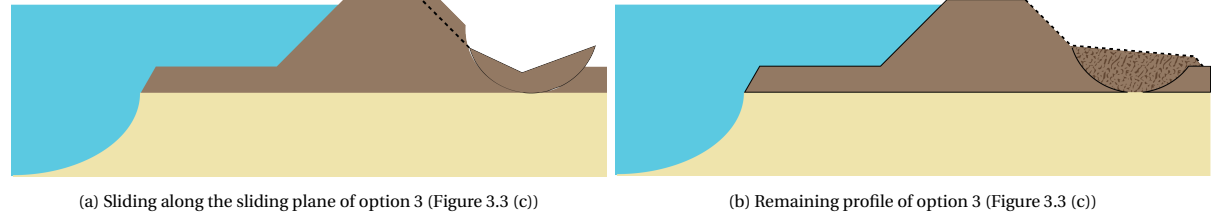
Figure 3.4: Creation of the remaining profile

The characteristics of the remoulded soil in the berm are different from the characteristic of the original soil. As stated by Van Montfoort (2018), more research is needed to know the properties of the remoulded soil. He made assumptions on the remaining strength of the soil. However, these assumptions are not suited to use for the interaction because here, the effect on BEP is identified. Only reasonable assumptions on the parameter changes that affect BEP need to be analysed.

When comparing the remaining profile (Figure 3.4b) with the original profile (Figure 3.2), several parameters have changed. The following subsections elaborate upon the exact relation between these parameters and (the sub-mechanisms of) BEP.

- The blanket layer thickness (d) is increased at the location of the berm.
- The location of the phreatic line (h_p) stays the same or increases due to the saturation of the berm material.
- The head in the aquifer (ϕ) may decrease if the sliding plane ruptures the blanket layer.
- The porosity (n) and permeability (k) of the remoulded soil can differ from the original soil.
- The exit point location for BEP (X_{exit}) may change, depending on all parameters mentioned above. The exit point location determines the seepage length ($L_{seepage}$).

These changed parameters influence the sub-mechanisms of BEP in different ways. The used limit state functions are equation (2.3), (2.8) and (2.14).

3.2.2. Sub-mechanism uplift and rupture

This interaction starts at the remaining profile after the first and second sliding, which resulted in a steeper inner slope, a narrower crest width and a berm of remoulded soil. The first sub-mechanism of focus is uplift and rupture, wherein rupture is always assumed to occur after uplift. In this interaction, the SI may cause immediate rupture or a change the uplift resistance at the original exit point location. This is dependent on the size and shape of the sliding plane. There are two remaining profiles of interest, one where the sliding plane perforates the entire blanket layer (can have immediate rupture) and one it does not. Whether the sliding plane starts at the crest or the inner slope does not influence the different interaction options. It is assumed that the SI has a bigger spatial scale than the described BEP, and thus only one 2D cross-section per remaining profile is considered.

The effect of the interaction in remaining profile 1, where the blanket layer is perforated by the sliding plane, is described in the five parts below.

1. *Rupture*
   The occurrence of uplift is not required to get rupture of the blanket, because the blanket can already be perforated by the sliding plane. The occurrence of SI can create new weak spots in the blanket layer in the berm, via large cracks in the remoulded soil. When the blanket layer is perforated by the

sliding plane, it cannot be guaranteed that rupture did not occur. Therefore, it is assumed that rupture occurs, due to these cracks, at the locations where the sliding plane perforates the blanket layer (see Figure 3.5a). If a rupture is assumed to occur, the occurrence of uplift is not required in the total BEP calculation. The exit point location can be assumed at the rupture location (see Figure 3.5b), and the sub-mechanisms heave and piping need to be calculated at this location. However, even if this rupture created a new exit point location, it might be the case that combined BEP is more likely to occur at another possible exit point location. These other exit point locations follow from an uplift analysis with the assumed reduced head in the aquifer due to the rupture, but not the exit point location of the rupture.

(a) Rupture by crack in remoulded soil

(b) Exit location with rupture
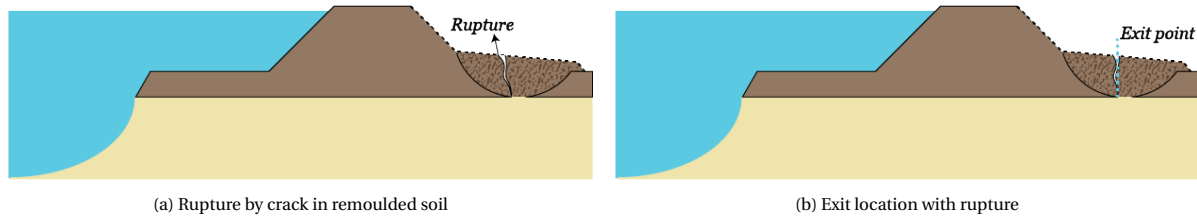
Figure 3.5: Effect of rupture of the blanket layer due to SI

2. *Head difference over the berm*
   If the blanket layer is perforated, there is a pressure relief of the head in the aquifer. The head in the aquifer reduces to the limit potential at this location. When the rupture is located in the berm, the limit potential is higher than the original limit potential due to the increased blanket layer thickness (d) at this location. The aquifer head drop is often schematized to be two times the blanket layer in width, in the land-inward direction. A reduction of the head in the aquifer (Φ) leads to a reduction of the head difference over the berm and at the rupture point ($\Delta\phi$) describe in the previous part.
   The phreatic line in the berm (h_p) depends on the saturation of the soil prior to the displacement and the weather conditions during the displacement. It can be on polder level if the water is drained out during sliding or it can be higher than polder level if the remoulded soil remains to contain some water from its original position. In the extreme case, the phreatic line can be at the top of the berm when it rains, or overtopping occurs during the sliding of the berm. This further reduces the head difference over the berm and at the rupture point.

(a) Head drop in aquifer due to perforation of the blanket layer

(b) Possible phreatic line locations
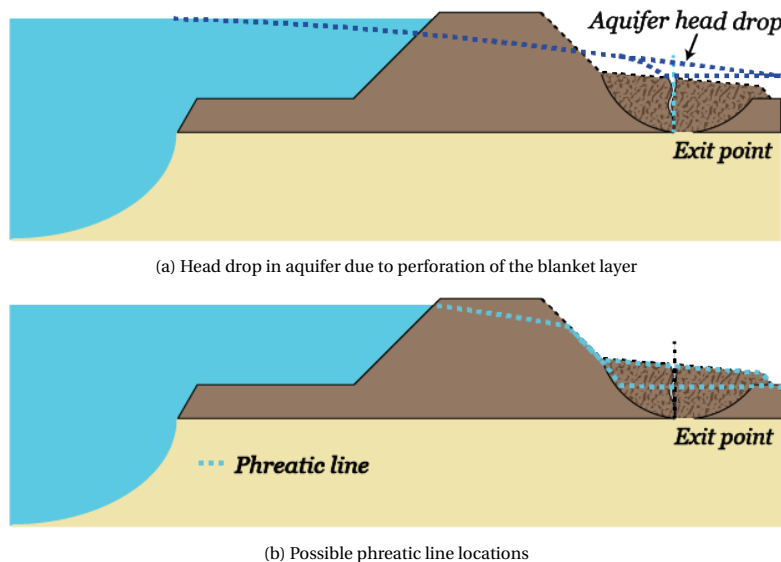
Figure 3.6: Effect of the change in phreatic line and aquifer head

3. *Porosity and permeability*
   There can be an increase in porosity due to an increase in the air in the pores caused by the chunks and cracks in the remoulded soil due to the SI. Alternatively, there can be a decrease in porosity due

to compaction of the soil due to the SI. The increase in porosity leads to a reduction of the specific volumetric weight of the remoulded soil (γ_{sat}) but at the same time an increase in berm volume (and thus an increase in blanket layer thickness). The opposite applies to a decrease in porosity here. It leads to an increase in specific volumetric weight and a decrease of berm volume. Both, the volumetric specific weight and the blanket layer thickness, influence the critical head difference of uplift ($\Delta\phi_{c,u}$) if the critical head difference increases or decreases depends on the combined effect of the two.

The permeability might change due to the change in porosity and cracks. The remoulded soil might have a lower resistance against vertical seepage. As a consequence, less pore water pressure can build up in the aquifer. The permeability influences the damping factor of the aquifer and thus its head distribution. The opposite is true for compaction of the remoulded soil. This effect needs more time compared to the time it takes to get a drop in the aquifer head (ϕ) as described in the previous part 2: head difference over the berm.

The clay blanket layer forming into chunks with cracks is seen as a more logical consequence of deformation than making the clay layer even more compact because clay is already very compact.
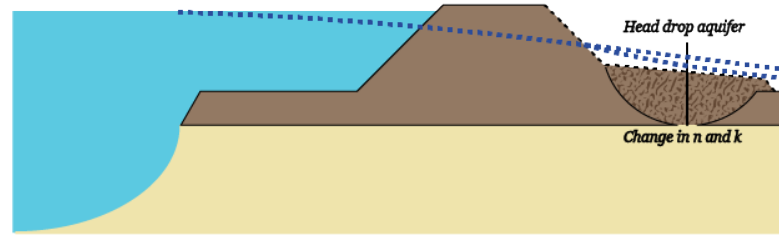
Figure 3.7: The long term effect of this change on the aquifer head

4. *Blanket layer thickness*

   The blanket layer thickness (d) is an important parameter for determining the critical head difference of the blanket layer. The berm locally increases the thickness of the blanket layer. This increase might lead to a relocation of the exit point further from the river to the end of the berm. If the exit point will be relocated depends on the characteristic of the remoulded soil in the berm. Herein, the specific weight of the remoulded soil is an important factor. It is partly dependent on the increase or decrease of the volume of remoulded soil via the porosity as described in the previous part 3: Porosity and permeability.
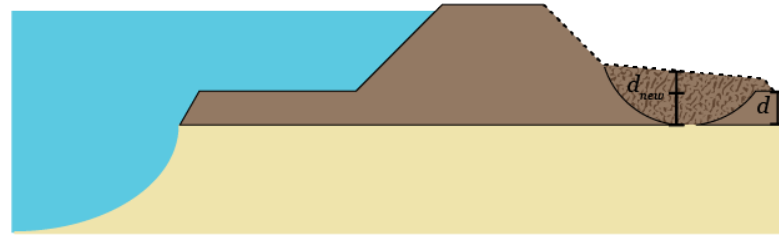
Figure 3.8: Change in blanket thickness

5. *Exit point location*

   There are three options for the possible exit point location. The location depends on the effect of the change in the head difference at the possible exit point (head aquifer and phreatic line) and the critical head difference at the possible exit point (blanket layer thickness and the porosity and permeability). The first location follows from part 1: Rupture, where the exit point is located at the point where the sliding plane fully perforated the blanket layer, and a large crack occurred. Even with this rupture causing a drop in the head of the aquifer, uplift and rupture can still occur at other locations depending on the extent of this head drop.

   The other two possible exit point locations are more traditional locations; at the toe of the levee or the end of the berm. An uplift calculation determines which of these two locations is most likely to be the exit point location, taking into account the effects mentioned in step 1, 2, 3 and 4. The exit point at the

new toe of the levee is assumed to be less likely to occur because the blanket layer thickness is still thick and has only reduced a smaller amount, and the head in the aquifer has not changed for this location. Both locations (at the rupture point and the exit point at the end of the berm) can be dominant for the complete BEP calculation, and therefore both locations need to be considered in the Heave and Piping calculations.
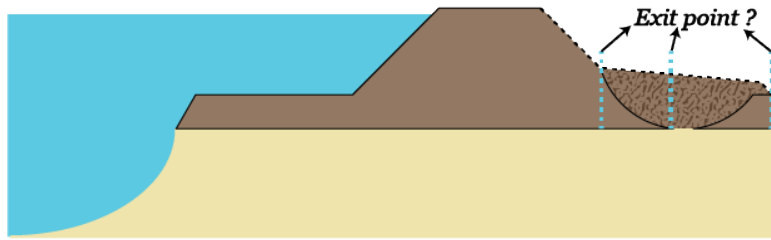
Figure 3.9: Possible exit locations

The effect of the interaction in remaining profile 2, where the blanket layer is *not* perforated by the sliding plane, is described in the five parts below. Only the differences with the remaining profile one are explicitly stated.

1. *Rupture*
   If the blanket layer is not perforated by the sliding plane, there is a small intact blanket layer which is not remoulded (see Figure 3.10). There is no immediate rupture due to the SI, and thus no aquifer head drop. However, when there are still possible large cracks in the remoulded soil, only the intact layer would need to uplift and rupture. Whether this is a possibility depends on the characteristics of the remoulded soil and the thickness of this intact layer.
   However, even if this rupture created a new exit point location, it might be the case that combined BEP is more likely to occur at another possible exit point location. These other exit point locations follow from an uplift analysis where there is no head drop in the aquifer.
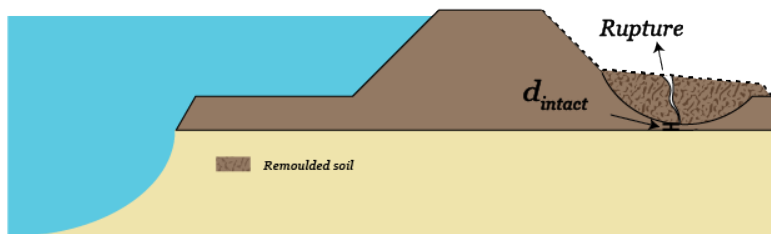
Figure 3.10: Intact part of the blanket layer

2. *Head difference over the berm*
   There is no drop in aquifer head (ϕ) and the original head distribution is still valid. The phreatic line in the berm can again be on polder level or higher as described in the part 2: Head difference over the berm of the remaining profile 1.

3. *Blanket layer thickness*
   The blanket layer thickness is locally increased due to the berm formation. The berm now consists of a remoulded part and an intact part (see Figure 3.11). In which the remoulded part has a different characteristic than the intact layer part.
   There are different possible starting assumptions. For instance, the remoulded part of the blanket layer has already ruptured and will give no resistance against uplift, so only the intact weight is taken into account in the critical head difference. This may forces the exit point to the smallest intact layer part because the complete blanket layer is ruptured if this small intact blanket layer ruptures provided that the soil above it has already ruptured.
   Another option is that the remoulded soil in the berm does offer resistance due to its weight (γ) and

height (d). This extra resistance results in a relocation of the exit point to a location with a smaller thickness, at the end of the berm.
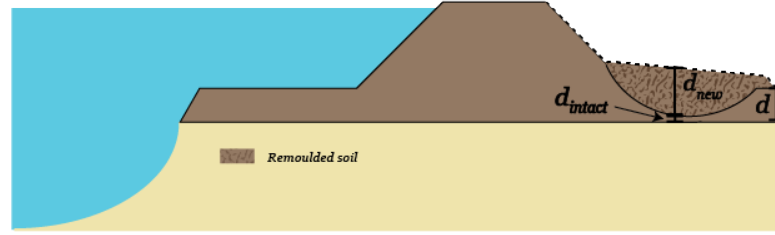
Figure 3.11: The difference between the old and the new blanket layer thickness

4. *Porosity and permeability*
   Again, the porosity of the remoulded soil might increase or decrease which influences the specific weight of the blanket layer (γ_{sat}) and the thickness of the blanket layer (d). These parameters both influence the critical head difference of uplift ($\Delta\phi_{c,u}$). The effect of change in specific volumetric weight and change in volume and thus thickness depends on the ratio of the two in the uplift equation.
5. *Exit point location*
   The exit point location has again three possible locations; At the new toe of the levee, at smallest intact layer point closest to the river and at the end of the berm (see Figure 3.9). Which of these three is normative will follow from an uplift calculation.

The two most likely exit point locations are at the end of the berm, and in the berm at the first point, the sliding plane perforates the blanket layer, or in the berm at the thinnest intact layer.

Exit point location at the end of the berm
When comparing the original situation before sliding and the remaining profile assuming that the exit point is indeed located at the end of the formed berm, the occurrence of uplift will reduce because the thickness of the blanket layer is the same, there is no remoulded soil and the phreatic line remains unchanged, for this exit point location. There is only a change in aquifer head compared with the original situation. Namely, the exit point is located further away from the river and therefore the head in the aquifer is already lower, in case the blanket layer has not ruptured due to sliding. Leading to a lower head difference and the same critical head difference as the original situation reducing the occurrence of uplift. When there is rupture due to sliding, the head in the aquifer goes to the limit potential, which is lower than the head in the aquifer in the original situation where there is no rupture — therefore reducing the occurrence of uplift as well.

Exit point location in the berm
If a rupture is assumed to occur in the berm due to the sliding plane perforating the blanket layer, the occurrence of uplift is not required in the total BEP calculation. When comparing the original situation before sliding and the remaining profile assuming that the exit point is located in the formed berm and that the blanket has not ruptured, there is only an intact layer that needs to be uplifted, which increases the occurrence for uplift at this location due to its small thickness.

3.2.3. Sub-mechanism heave

The interaction between SI and Heave is the next step after the occurrence of rupture due to SI or uplift. The rupture leads to an exit point location and a drop in head to the limit potential of the blanket layer. Two possible exit point locations are elaborated for this interaction; In the berm and at the end of the berm. Where these possible locations stem from is described in Section 3.2.2.

This interaction does not differ for the different sliding plane sizes, and it is still assumed that the SI has a bigger spatial scale than BEP and only one 2D cross-section is considered per exit point location.

The following statements describe the effect of SI on heave for an exit point location *at the end of the berm*:

1. *Blanket layer thickness*
   At the end of the berm, the thickness of the blanket is the same as the original thickness at this point and the original location at the toe of the levee (see Figure 3.8 compared to Figure 3.2).
2. *Porosity of the remoulded soil*
   There is no change in porosity (n) at this location because the soil is not remoulded; it has its original value. So, there is no change in critical heave gradient ($i_{c,h}$). The porosity of the remoulded soil (n) influences the critical heave gradient ($i_{c,h}$), see equation 2.11.
3. *Head difference at the exit point ($\phi_{exit} - h_p$)*
   The head in the aquifer (ϕ) drops to the limit potential of the blanket layer due to the rupture. This limit potential is the same as the original limit potential because the blanket layer thickness and specific volumetric weight did not change compared to the original exit point location at the toe of the original levee. It can be that the head in the aquifer at this location is already lower than the limit potential of the blanket layer, because of the extra distance from the river, and therefore remains the original value at this location which is lower than at the original exit point location. This can reduce the occurrence of heave because there is a smaller head difference.

The effect of SI on heave for the exit point location *in the berm*:

1. *Blanket layer thickness*
   The blanket layer is thicker than the original thickness at the exit location (see Figure 3.8). The increase in thickness reduces the exit gradient (i) at the exit point, see equation 2.10.
2. *Porosity of the remoulded soil*
   The displacement can lead to clumping into chunks of clay of the remoulded soil in the blanket layer. Water can flow through the cracks between the chunks. These cracks increase the permeability of the soil and thus the permeability of the blanket layer. The presence of chunks and cracks result in a non-uniform porosity of the blanket layer, although it on average increases. However, critical heave gradient ($i_{c,h}$) uses the porosity (n), instead of the permeability of the blanket layer, see equation 2.11. If the porosity is higher, there is less resistance against heave and the critical heave gradient is lower. With a lower critical heave gradient, heave is more likely to occur.
   Another option is that the soil compacts in the berm and decreases its permeability. This has the opposite effect on the heave gradient. However, this is assumed less likely than the first option, because the initial permeability of clay already is very low.
3. *Aquifer head at the exit point*
   The head in the aquifer (ϕ) at the exit point location again drops to the limit potential of the blanket layer, but because of the increase in blanket layer thickness due to the berm formation the limit potential is higher (depending on the change in specific weight (γ_{sat})). The aquifer head at the exit location is, therefore, higher than the original dropped head in the aquifer at the exit point. The exit gradient (i) increases if the difference between the head in the aquifer and the phreatic level in the blanket layer increases at the exit point, see equation 2.10. This increase in the difference is only true if there is no increase in the phreatic level and this depends on the saturation of the remoulded soil.
4. *Phreatic line at the exit point*
   As mentioned in Section 3.2.2 part 2, the phreatic line in the berm at the exit point location can either be on the polder level, which is the same in the original situations' exit point, or it can be higher due to the saturation of the soil prior to the sliding. The effect of the remaining profile on the head difference ($\phi_{exit} - h_p$) used for the calculation of the exit gradient (i) on the exit point location is unknown as it depends on the extent to which there is an increase in the phreatic line and an increase in the aquifer head.

Exit point location at the end of the berm
For the exit point location at the end of the berm, there is no change in the occurrence of heave due to the interaction because there is no change in blanket layer thickness, aquifer head, phreatic line and critical heave gradient. Except for when the head in the aquifer is already lower than the limit potential, this can cause a reduction of the occurrence of heave.

Exit point location in the berm
For this exit location, it is difficult to determine whether the occurrence of heave increases or decreases because there is a thicker blanket layer (*decrease occurrence*). However, from the porosity, there is a lower critical heave gradient, which in turn would lead to a *increase in occurrence*. With the head difference, the direction of the change is still unclear because and the phreatic line probably increases and as well the head in the aquifer (*decrease or increase*).

The effect of the interaction in the case of the exit point in the berm on heave depends on which of the above-described changes and the ratio between the changes has the most influence on heave.

3.2.4. Sub-mechanism piping

The occurrence of the SI changes the location of the exit point, as is stated in Section 3.2.2. Two situations are considered for the interaction between SI and piping; the exit point location in the berm and the exit point location at the end of the berm.

The effect of the interaction at the exit point location *at the end of the berm*:

1. *Blanket layer thickness*
   The thickness of the blanket layer at the end of the berm (d) does not increase compared to the original situation (see Figure 3.8 compared to Figure 3.2). The thickness of the blanket gives a reduction of the load over the vertical channel due to the presence of sand particles, see equation 2.14.
2. *Head difference over the levee*
   The water level in the river (h) does not change due to the interaction. The phreatic line at the exit location is the same as in the original situation. These are both important to determine the occurring head difference together with the blanket layer thickness ($H = h - h_p - 0.3d$). At this exit point location, the occurring head difference remains unchanged, and therefore, the occurrence of piping is unchanged.
3. *Seepage length*
   The seepage length increases due to the relocation of the exit point to the end of the berm (see Figure 3.12). This increase in seepage length increases the critical head difference (H_c) of piping, which reduces the occurrence of piping.
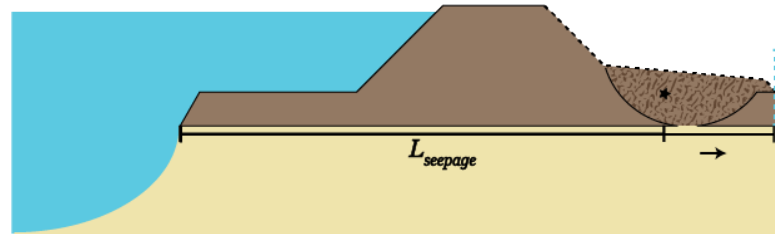
Figure 3.12: The seepage length for exit point at the end of the berm

The effect of the interaction at the exit point location *in the berm*.

1. *Blanket thickness*
   At the exit location in the berm, there is an increase in blanket layer thickness (d) due to the berm formation, which results in a reduction of the occurring head difference ($H = h - h_p - 0.3d$) (see Figure 3.8).
2. *Head difference over the levee*
   The phreatic level (h_p) in the berm is unknown, but it will probably be higher than the original phreatic level at the location of the exit point depending on the saturation of the berm as described in Section 3.2.2. This higher phreatic level reduces the occurring head difference. Again, the water level in the river (h) is not affected by the SI. The occurrence of piping is reduced due to the increase in blanket layer thickness and the possible increase in the phreatic line.
3. *Seepage length*
   If the exit point is located in the berm, it is around the original exit point. So, there is only a small

change in seepage length (see Figure 3.13) at this location. This change can be closer to the river or further from the river depending on the exact new location of the exit point and thus the sliding plane depth and shape.
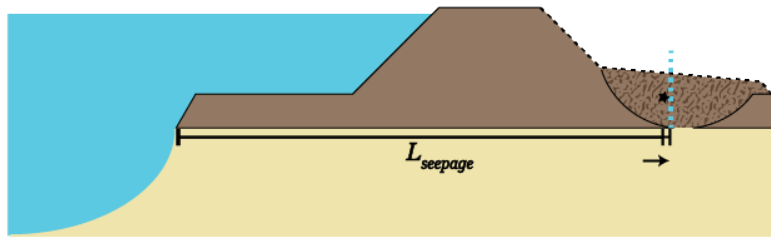
Figure 3.13: The seepage length for exit point in the berm

Exit point location at the end of the berm
If the exit point is located at the end of the berm, the critical head difference increases due to the increased seepage length, this decreases the occurrence of piping.

Exit point location in the berm
If the exit point is located in the berm, it is uncertain whether this has a positive or negative effect on the piping occurrence. The occurring head difference certainly reduces at the location in the berm, due to the thickness of the blanket layer and the location of the phreatic line in the berm. However, the seepage length can increase or decrease compared to the original situation and depends on the exact location of the exit point. The occurrence of piping probably decreases, and can only increase, if the seepage length decreases enough to compensate for the decrease in occurring head. This occurrence depends on the ratio in which parameters change relative to each other.

3.2.5. Influence of slope instability on backward erosion piping

The SI and remaining profile influence BEP as a whole. The combination of the three sub-mechanisms is essential for the outcome of the interaction. The sub-mechanism need to occur in sequence and the influence on the interaction depends on the relation between the sub-mechanisms. If one cannot occur, the entire failure mechanism will not be able to occur. Two different situations are of importance for the interaction, the location of the exit point in the berm and at the end of the berm. Which of the two locations is normative cannot be concluded from this parametric analysis.

Exit point location at the end of the berm
As elaborated in the subsections 3.2.2, 3.2.3 and 3.2.4, all three sub-mechanism decrease in occurrence when the exit point is located at the end of the berm. The combined effect of these interactions on the BEP is, therefore, also a reduction in the occurrence of BEP. *Exit point location in the berm*
When the exit point is located in the berm, it is more challenging to combine the effects of the sub-mechanisms interactions. Since in this case, the remoulded soil needs to be taken into account of which the properties are uncertain. If the blanket layer is ruptured due to sliding, uplift is not required in the total BEP calculation. When the blanket layer is not fully ruptured, only the remoulded soil, there is an increase in occurrence for uplift because only an intact layer with a small thickness needs to be uplifted. For the mechanism heave (see Section 3.2.3), several different parameters change: thicker blanket layer, lower critical heave gradient, aquifer head drops to a higher limit potential and an increase in the phreatic line. These all have different effects on the mechanism heave. However, it is the ratio between these effects that determines whether the interaction increases or decreases the occurrence of heave and because there are no known amounts at the moment, it is not possible to give a definite answer about the consequences for the heave. Something similar is also the case for the mechanism piping. Here, the occurring head difference reduces due to the blanket layer thickness in the berm and the location of the phreatic line. The seepage length can increase or decrease compared to the original situation and effect the critical head difference. It depends on the amount of change and the direction of this change in the seepage length compared to the occurring head difference. Therefore, it is not possible to give a definite answer on the consequences for piping.

3.2.6. Alternative situations

There is also a second option for the exit point in the berm situation, where the seepage path does not go straight through the blanket layer but follows the sliding plane (see Figure 3.14). The soil particles around the sliding plane can form a compacted layer, which might be more impermeable than the original soil. Although, this effect would be bigger in a sand levee than in a clay levee. The path of the least resistance might be to stay under this layer. This will form an alternative seepage path that can not be expressed with the currently used BEP models. The path through the blanket layer will increase in length. This does not increase the seepage length in the Sellmeijer formula but increases the reduction of the load by the blanket layer thickness. This can affect the occurrence of piping in a positive sense.
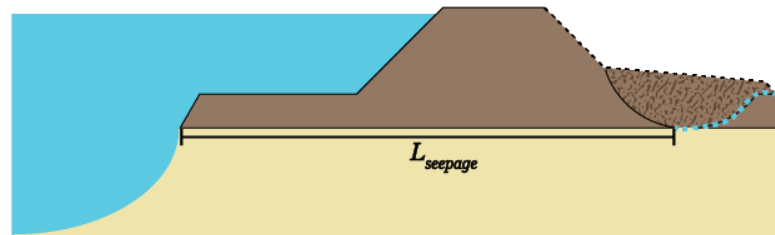
Figure 3.14: The seepage length for exit point in the berm with alternative path

Another alternative situation is when the original situation includes a toe ditch (see Figure 3.15a). If the original exit point is located in this ditch, the effect of the interaction can be different. The SI might press the toe ditch closed (see Figure 3.15c). The exit point can be relocated in the berm closer to the levee than the original exit point, or it might be relocated to the end of the berm (see Figures 3.15b and 3.15d). All three sub-mechanisms experience a change in this case.

If the exit point is located at the end of the berm, and this location is further away from the original location, the BEP occurrence will decrease because it experiences the same effect as in the non-alternative situation (see Section 3.2.5). Except for the fact that the thickness of the blanket layer is increasing, this also has only a reducing effect on the occurrence of BEP. When the exit point is in the berm, it is again difficult to give a definite answer about the effect of the interaction on the BEP. Here, too, the same thing happens as in the non-alternative situation described in Section 3.2.5, with the exception that it can be assumed here that the seepage length will be shorter.

(a) Start situation

(c) Slope instability

(b) Effect of closure ditch option 1

(d) Effect of closure ditch option 2
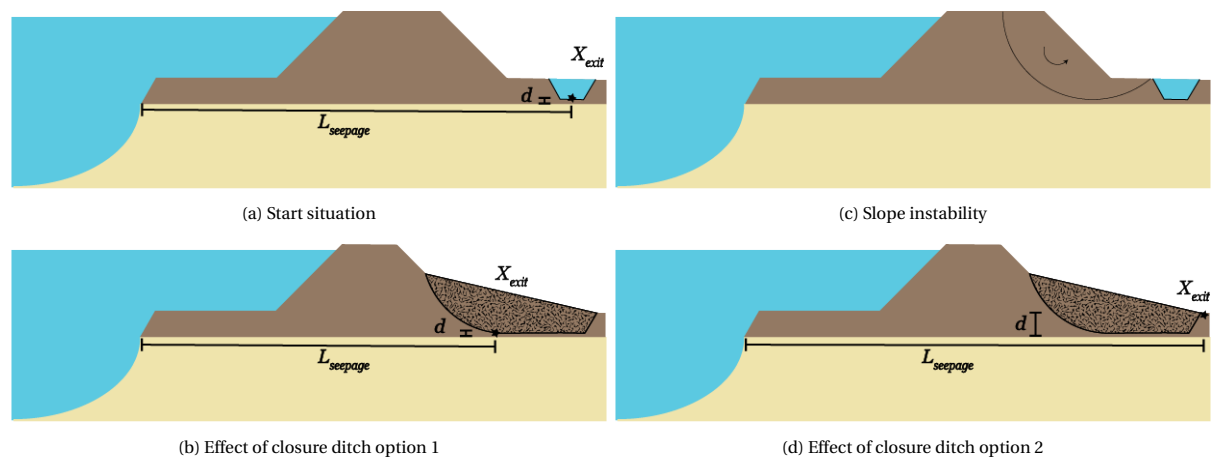
Figure 3.15: Situation levee with a toe ditch

3.3. Interaction from backward erosion piping to slope instability

The interaction from backward erosion piping (BEP) to slope instability (SI) is outlined in this section in four subsections. The first subsection elaborates on the flow patterns in the sand layer. The remaining subsections start at a sub-mechanism of BEP (the sub-mechanism uplift, heave and piping). First, the starting point of the interaction is pointed out, then the changes made to the surroundings due to the occurrence of the sub-mechanisms are elaborated. After that, the consequences of these changes to the failure mechanism SI is explained.

3.3.1. Flow patterns in sand layer

The interaction from BEP to SI is caused by changes in the water pressures (u) in the aquifer and levee. These water pressures changes are shown in a change of the head. Wherein there are two different heads; one in the aquifer and one in the levee (called phreatic line).

$$\phi = z + \frac{u}{\rho_w g} \tag{3.1}$$

The water pressures and the head in the aquifer and the phreatic line can change due to the presences of BEP.

$$\sigma' = \sigma_n - u \tag{3.2}$$

These changes have an influence on the shear strength of the soil (s_u/τ) at the interface between the blanket and the aquifer, via the effective stress (σ') that is present in the shear strength formulas for drained (2.26) and undrained (2.28) which is directly related to the groundwater pressures via equation A.1 and repeated 3.2. The shear strength, in turn, influences the occurrence of SI. Changes in the saturation of the levee affect the specific weight of the levee and therefore, the driving moment of the SI.

It is essential to look at how BEP affects the water pressure in and under the levee to determine possible interactions.

Figure 3.16: Top view of the levee, schematic drawing of flow patterns in the sand layer beneath the clay layer based on Vandenboer et al. (2014), (not to scale)

These changes in water pressures in the aquifer are depicted in Figure 3.16. The top left Figure (I) shows the flow pattern in the original situation. When the water level in the river increases, the head in the aquifer will increase. If there is a local weak spot in the blanket layer, for example, a thinner blanket layer part, the flow starts to focus towards this weak spot (II). The water pressure at the interface of the blanket layer and the aquifer increase, and push the blanket layer up (uplift). When the blanket layer ruptures due to the increase in water pressure an exit point is created at the weak spot (III), the head in the aquifer drops to the limit potential of the blanket layer. The vertical head difference over the blanket layer leads to vertical sediment transport through the blanket layer (Heave). The head difference over the levee can cause horizontal erosion beneath

the blanket layer at the interface, creating a pipe (IV) at the land-side of the levee. If the head difference over the levee passes the critical head difference, the pipe will continue to grow beneath the levee towards the river(V). In a typical Dutch levee this corresponds with the critical pipe length of half the seepage length (see Section 2.3.4). When the pipe reached the entry point, the pipe will start to widen and to undermine the levee (VI), eventually leading to a lowering of the crest and loss of primary function.

The steps described here are all points where something changes in the water pressures and each of these change may influence SI. Only, the situations II, III and IV from Figure 3.16 are further elaborated in the Sections 3.3.2, 3.3.3 and 3.3.4 to show the effect on the interaction. In situation V and VI, the pipe is past the critical gradient, and failure is inevitable when no flood wave is considered (lowering of the water level after some time).

This interaction might be observed once in the breach by Hohenwisch (Germany) described in Section 2.2.2.

When considering the effect of BEP on its surroundings, several parameters can change. The following sub-sections elaborate upon the exact relation between these parameters and SI.

- The specific weight of the soil in the levee (W) at the active and passive side may decrease due to drain effect
- The shear strength (s/τ) of the soil at the interface between the blanket layer and the sand layer can decrease surrounding the rupture point. It can go to zero land-inward of the rupture point at the interface.
- The shear strength (s/τ) of the soil in a pipe, that is located under the blanket layer at the interface with the sand layer can be zero due to the presence of fluidised sand or water in the pipe.
- The shear strength (s/τ) of the soil next to a pipe, that is located under the blanket layer at the interface with the sand layer, can increase due to drain effect of the pipe.

3.3.2. Sub-mechanism uplift and rupture

The starting point of the uplift and SI is the increase in the river water level. This water level increase leads to an increase in pore water pressure (u) in the aquifer and the levee. The increase of the pore water pressure is time-dependent, the pore water pressure increase travels faster through the aquifer (sand) than through the levee material (clay less permeable than sand). At the toe of the levee, the pore water pressure increases in the aquifer and stays the same in the blanket layer (see Figure 3.17). The pore water pressure increase relates to Uplift (BEP) as well as Uplift (SI).

<div align="center">(a) Low river water level   (b) Extreme high water level</div>
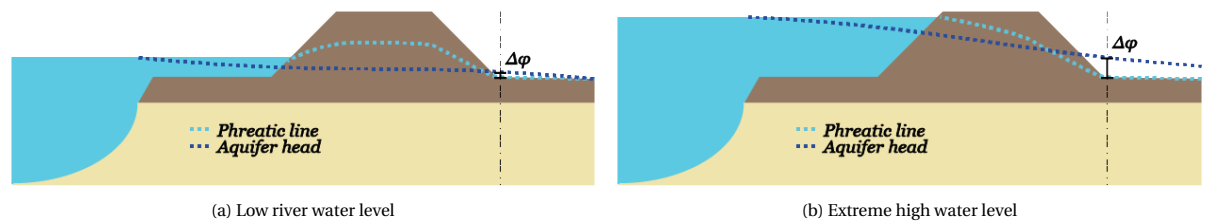
Figure 3.17: Change in aquifer head and phreatic line and in $\Delta\Phi$

In BEP, the increase in pore water pressure u in the aquifer increases the head in the aquifer (Φ) (see equation A.2 and repeated 3.1). When the head in the aquifer increases at the toe of the levee and the phreatic line/polder level at this location (h_p) stays the same, the head difference ($\Delta\Phi$) increases (see Figure 3.17b). The critical head difference ($\Delta\Phi_{c,u}$ equation 2.5) does not change in this situation, so the increase in occurring head difference leads to uplift (BEP). When uplift occurs, rupture is assumed to occur as well. The zone where uplift occurs is called the 'uplift zone'. A rule of thumb that is used in practice to estimate the size of the uplift zone is two times the thickness of the blanket layer (Förster et al., 2012). Only from the moment that rupture of the blanket layer occurs can the interaction between BEP and SI be considered. Otherwise, there is only an increase in water pressure that initiates both mechanisms (BEP and SI).
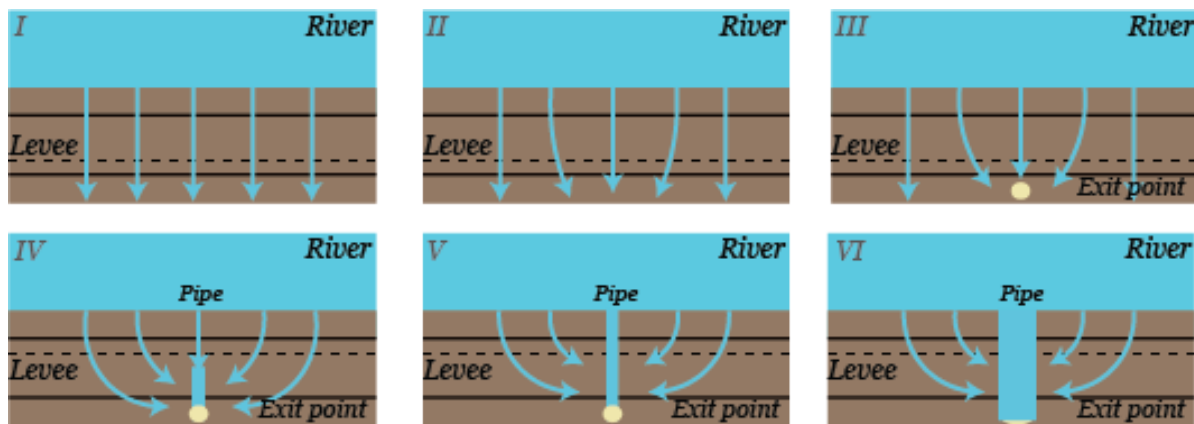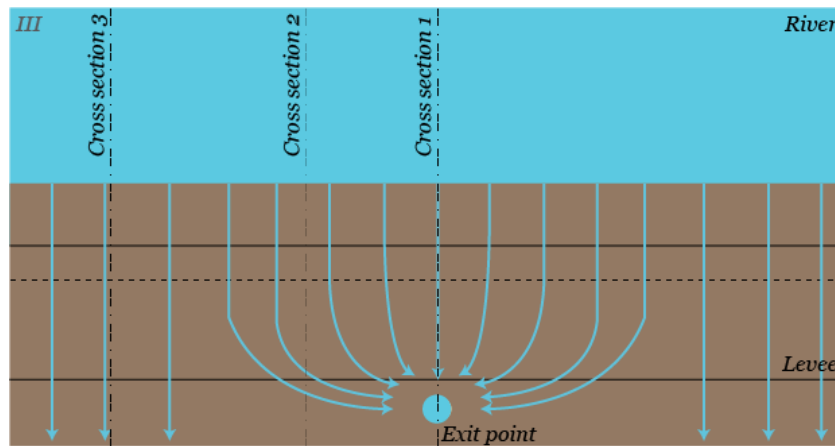
Figure 3.18: Top view of the levee, schematic drawing of flow patterns in the sand layer around a water boil based on Vandenboer et al. (2014), (not to scale) and the locations of the cross-sections labelled in the Figure

However, if uplift (BEP) causes rupture of the blanket layer, the head in the aquifer is reduced (due to the valve effect). The shear strength at the interface between the sand and clay layer below the exit point is still reduced due to the past occurrence of uplift (see Figure 3.19a in cross-section 1 of Figure 3.18), this increases the occurrence of SI. This interaction is implemented in WBI 2017 (Rijkswaterstaat, 2016), as discussed in Section 2.4.2. In this tool, the shear strength at the interface between the sand and clay layer land-inward of the exit point is reduced to zero if the FoS of uplift is smaller than 1.2 and the blanket layer is thinner than 4.0 m.

Kanning and van der Krogt (2016) define a difference in strength reduction between uplift and rupture. Where uplift causes a reduction of the local shear strength, the shear strength goes to zero at the interface between the blanket and the subsoil at the location where there is no effective stress. Rupture causes a reduction to zero shear strength in the whole uplift zone. Kanning and van der Krogt (2016) propose a gradual transition of the reduction used in WBI 2017.

(a) Uplift situration

(b) Rupture situation
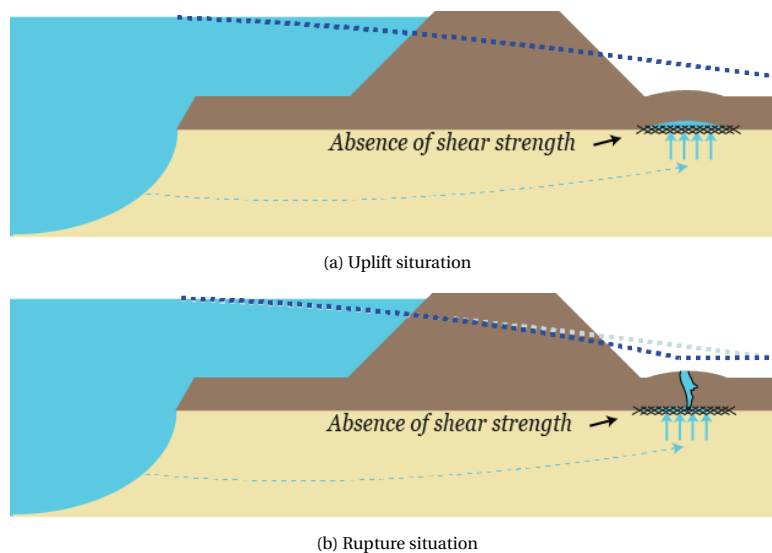
Figure 3.19: Cross-section 1: Change in aquifer head due to rupture

When uplift occurs, it cannot be guaranteed that the blanket layer has not ruptured due to uplift of the blanket layer. If the blanket layer is ruptured, this creates a vertical channel through the blanket layer, which is called an exit point (see Figure 3.19b). This channel acts as a valve; it relieves pore water pressures in the aquifer around the exit point. The magnitude of this decline in the aquifer head is decreased to the limit of the

potential of the aquifer layer, see Section 2.3.2. The range of the pressure drop due to rupture is small and in the order of centimetres (Vandenboer et al., 2014) especially in the beginning of the channel when the channel itself is small (in the order of a centimetre). At this time in the process, the channel will only be carrying water and is a so-called water boil. The aquifer head drop is schematized for the cross-section 1 (in Figure 3.19b, cross-section 1 of Figure 3.18) which is in the water boil. In cross-section 2 of Figure 3.18, the effect of the drop in the head in the aquifer at the location of the exit point can still be felt, however, the effect of the head drop is less at this location. The effect of the drop in the head on SI would be an increase in effective stress and thus an increase in shear strength.

To conclude, two effects can be identified:

1. Due to rupture, the soil at the interface of the blanket-sand layer land-inward from the exit point does not have any shear strength.
2. Due to valve effect (seepage through the blanket layer), a local reduction of the head in the aquifer surrounding the rupture point increases the shear strength in the surrounding soil.

Both effects are local and have a contradictory effect on shear strength. The valve effect probably has a greater range, as it could play in both cross-section 1 and 2, than the loss of shear strength at the exit point; however, this is not verified.

3.3.3. Sub-mechanism heave

This interaction starts when there is a sand boil at the toe of the levee. This sand boil transports the sand of the aquifer vertically up through the blanket layer. This only occurs if the vertical gradient over the blanket layer at this point exceeds the critical vertical heave gradient (i_c). A hollow space forms at the interface of the blanket layer and the sand layer, the size of the sand boil influences the size of the hollow space. The flow patterns in the aquifer start to concentrate towards the exit point (see Figure 3.20). This causes a spatial difference in the effect of SI. Therefore, two cross-sections are considered: cross-section one where the sand boil is located, and cross-section two where the effect of the sand boil is still present, but the sand boil itself is not.

Figure 3.20: Top view of the levee, schematic drawing of flow patterns based on Vandenboer et al. (2014), (not to scale) and the locations of the cross-sections

The effects of the interaction in cross-section 1 are as follows:

1. The hollow space is filled with fluidised sand when heave occurs. In this state, there is no effective stress present and thus also no shear strength (see Figure 3.21a). So in the hollow space, there is no shear resistance, which increases the occurrence of SI. This is similar to the effect identified with uplift, as the sand transport has started, there will be a slightly larger hollow space.
2. There is a drop in aquifer head over the sand boil as discussed in the section of uplift. In the sand boil

itself, this cannot lead to higher effective stress (σ'), due to the presence of the hollow space (see Figure 3.21b).

(a) Cross-section 1: Absence of shear strength in hollow space

(b) Cross-section 1: Drop of aquifer head over the sand boil
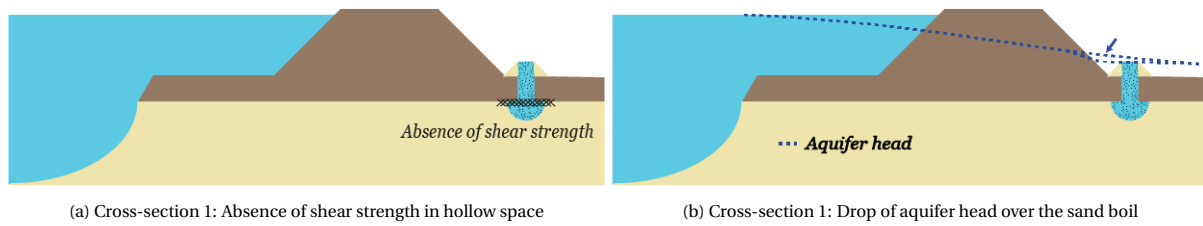
Figure 3.21: Cross-section 1: Schematic drawing of Heave at the exit point at the toe of the levee

The effects of the interaction in cross-section 2 are as follows:

1. There is a drop in aquifer head over the sand boil. This head drop is also present in the surrounding soil next to the sand boil (see Figure 3.22a). The drop in aquifer head is a reduction of the pore water pressures in the aquifer surrounding the boil. A reduction in pore water pressure (u) leads to an increase in effective stress (σ') and an increase in shear strength and thus an increase in SI.

2. The sand boil has a drainage effect on the cross-section just next to the sand boil (2) that reduces the pore water pressures (u) locally in the sand layer, increasing the effective stress (σ') and thus the shear strength (τ or s_u) at the interface between the sand and blanket layer around the sand boil, see Figure 3.22b. This increase reduces the occurrence of SI. However, due to the location and size, the effect of the drain will be smaller than for a full grown pipe.

(a) Cross-section 2: Drop of aquifer head over the sand boil

(b) Cross-section 2: Increase of shear strength due the drainage and drop in head next to hollow space
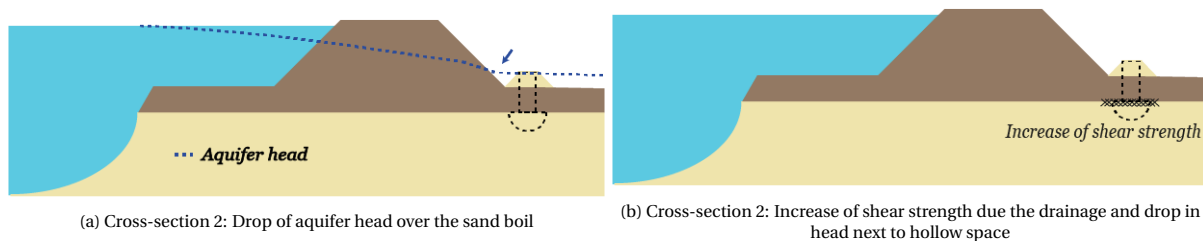
Figure 3.22: Cross-section 2: Schematic drawing of Heave next to the exit point at the toe of the levee

The influence of heave on SI is similar to the influence of uplift. There is no shear strength in the sand boil itself and the hollow space below the boil due to the increase in water pressure in the sand boil. There is a drop in the head in the aquifer around the exit point, which could increase the shear strength. Both effects are local, and both have an opposing effect on the shear strength. As a result, the effect on SI may be negligible.

3.3.4. Sub-mechanism piping

This interaction starts in the situation that a pipe is present in the sand layer at the interface with the blanket layer. When there is a pipe, the already present part of the pipe can act as a drain. The pore water pressures in the pipe and its surroundings decrease. Note, for this interaction the pipe is always drawn straight, in reality, the pipe can meander or form a network at the interface with the blanket.

In this interaction, there is a spatial difference in the draining effect of the pipe and the scale of the affected mechanism (SI). This can be illustrated using three cross-sections around the pipe, as seen in Figure 3.23. The exact area of influence of the pipe is case-dependent. The first levee cross-section includes a partial pipe. van Beek et al. (2015) computes that the width of the pipe is approximately 30 times the grain width, before widening of the pipe. The second cross-section is next to the pipe in the area that still feels the influence of the pipe. (Robbins et al., 2017) found that the pore water pressure changes in the sand layer due to the presence

of the pipe are felt at a distance of approximately 130 x D_{50} away from the pipe. Following the findings of Robbins et al. (2017), for example, the influence of approximately 2.5 cm, the pipe would be felt for fine sand ($D_{50} = 200\mu m$). However, in the IJkdijk experiments (Parekh et al., 2016), the piezometers that measured pore water pressures were spaced 1.15m and 1.5m apart and showed changes. In these IJkdijk experiments, a lot of small channels developed next to each other, forming a network that could be measured. These three studies indicate the possible scale of the area of influence of a pipe.

Within the scale of SI (30-100 m), there is a remaining zone in the levee that does not feel the presence of the pipe. The widening of the pipe or the development of extra piping channels near each other would change the width of the affected areas/zones and would give SI more opportunity to occur. So, depending on the size of the pipe and the size of the potential sliding plane, this interaction can be either have significant influence or almost none.
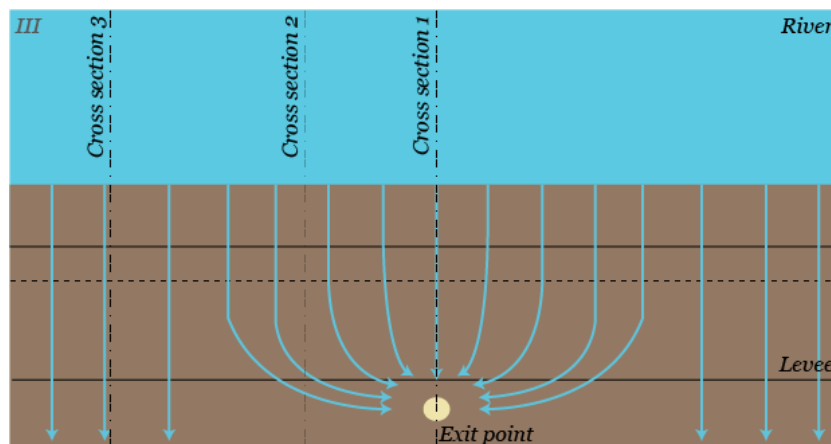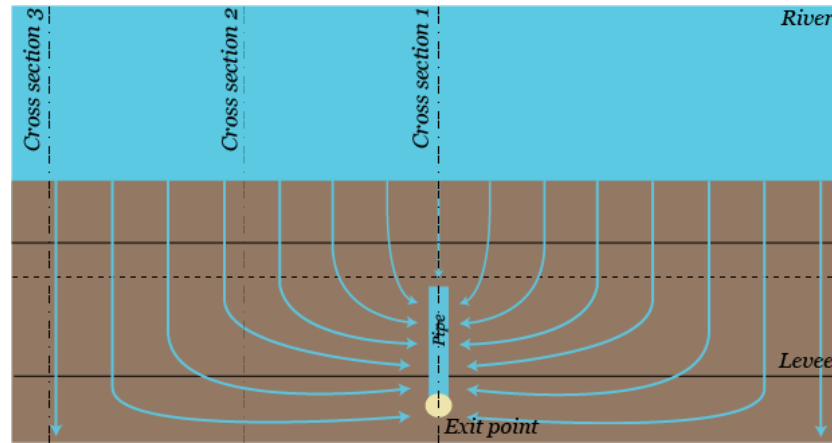

Figure 3.23: Interaction 6: Top view of the levee, a schematic drawing of flow patterns based on Vandenboer et al. (2014), (not to scale) and the locations of the cross-sections

The interaction is only relevant if the critical hydraulic gradient for piping is not yet reached. If the critical piping gradient is reached, it is assumed that levee failure is inevitable (Rijkswaterstaat WVL, 2017d), as no time-dependent erosion is considered. It is an unstable equilibrium past this critical point. For an average Dutch levee this corresponds with a critical pipe length that is approximately half the seepage length, see Section 2.3.4.

From equations 2.21, 2.26 and 2.28 can be seen that if the pore water pressure changes it influences three main parameters: the specific weight W_j, the drained shear strength $\tau_{drained}$ and the undrained shear strength $s_{undrained}$. The specific weight of the soil is of importance in the driving moment in the soil equilibrium. Both the shear strengths are essential for the resistance against sliding.

The effects of the interaction in the cross-section (1) of the levee with the pipe are as follows:

1. The water pressure (u) in the pipe decreases due to the direct contact with the atmosphere and due to the lower resistance in the pipe compared to the intact sand bed. The soil is fluidised or already removed in the pipe, so there is no effective stress present. If there is zero effective stress (σ') in the pipe, then there is no shear strength (s or τ) in the pipe-blanket interface. For this specific section, the absence of shear strength may trigger SI (see Figure 3.24a).
2. The pipe also has a draining effect for the soil on top of the pipe. This effect reduces the saturation of the soil on top of the pipe. Because the pipe is located under the levee, this reduction of saturation would reduce the specific weight of the soil at the active side of the slip circle. Depending on the location of the exit point, the reduction can also be partially at the passive side. If the ratio of the reduction is more to the active side, it reduces the driving moment of the soil equilibrium, which would decrease SI, see Figure 3.24b. How big the drain effect is, depends on the permeability of the soil and the duration of the presence of the "drain".

(a) Cross-section 1: Potential SI due to absence of shear strength due to pipe

(b) Cross-section 1: Less saturation above the pipe in the active part of the sliding plane, no SI due to pipe (pipe growth continues)
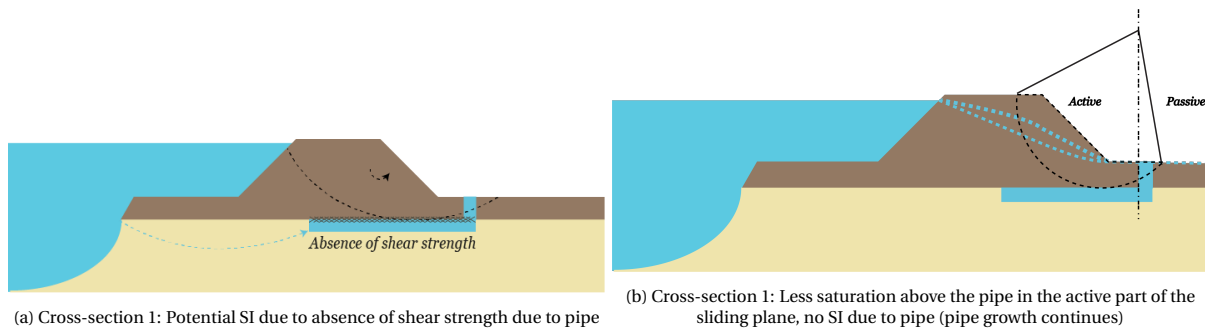
Figure 3.24: Cross-section 1 at axis of pipe

The effect of the interaction in the cross-section (2) of the levee near the pipe:

1. Near the pipe but not in the pipe at the interface between the blanket layer and the sand layer, the pore water pressures in the sand layer reduce as well (cross-section 2). This reduction of pore water pressure leads to an increase in effective stress, which in turn increases the shear strength of the soil. This effect would lead to a higher resistance against SI (see Figures 3.25a).
2. The pipe can act as a drain; hence, this reduces the saturation of the levee above the pipe and next to the pipe. As the pipe is located under the levee, this reduction of saturation would reduce the specific weight of the soil at the active side of the slip circle. This reduces the driving moment of the soil equilibrium, which, as previously stated, would increase SI (see Figures 3.25b). Again this highly depends on the permeability of the soil and the duration of the presence of the "drain".

(a) Cross-section 2: Drop in head in aquifer, increase shear strength. so, no SI

(b) Cross-section 2: Less saturation in the levee next to the pipe in the active part of the sliding plane, no SI due to pipe (pipe growth continues)
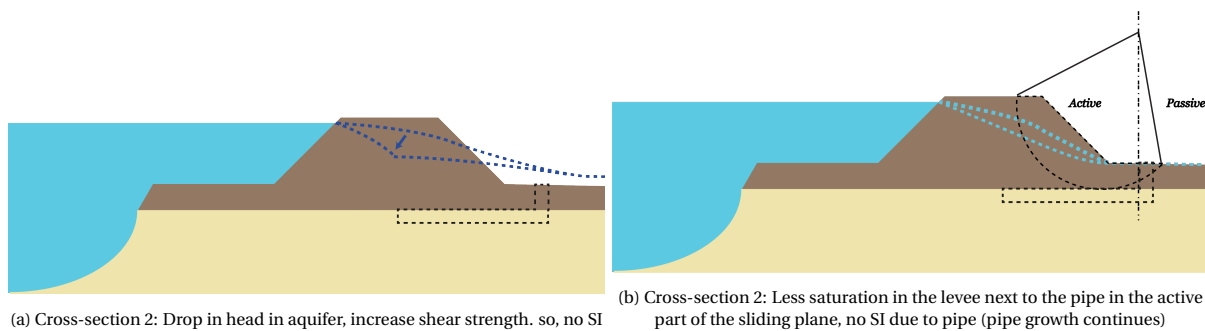
Figure 3.25: Cross-section 2 next to pipe

3.3.5. Influence of backward erosion piping on slope instability

All three sub-mechanisms of BEP have a similar influence on SI. There is an absence of shear strength in the uplift zone, in the hollow space and the pipe. The pipe presumably has the most influence on SI due to its size. Besides, all three sub-mechanisms lead to a local lowering of the aquifer head. This will also affect the cross-section next to the exit point, sand boil or the pipe. This drop in the head causes lower water pressures, higher effective stress and thus more shear strength below the exit point at the toe of the levee on the interface between clay and sand. For piping, the pressure drop follows the pipe towards the river. In the case of a pipe, there is a third effect, the drainage effect. In which the saturation of the levee reduces, mainly in the active part of the slip circle. This results in a reduction of the driving moment of the soil equilibrium through the reduction of the specific weight.

Most important for this interaction is the scale difference between SI and BEP. A large pipe or a network of pipes is probably not large enough to initiate a sliding plane in only the cross-section in which it is located. Let alone the 3D-effect, that next to this pipe, the effects of the interaction causes a reduction of the occurrence of SI instead of an increase in the pipe.

3.3.6. Alternative situations

Another possible interaction is when the SI occurs when there is a pipe present which is not yet past the critical piping gradient. This instability can close the pipe. Depending on how this closure takes place, for instance, the crest is lowered or not, and depending on the development of the water level, it can be a positive influence on the BEP development, but it can also cause the failure of the levee. This would be part of a more alternating process, where first BEP causes SI, and then the SI might prevent further BEP.

(a) Reduction of shear strength due to presence of the pipe cause SI   (b) Closure of the pipe due to SI
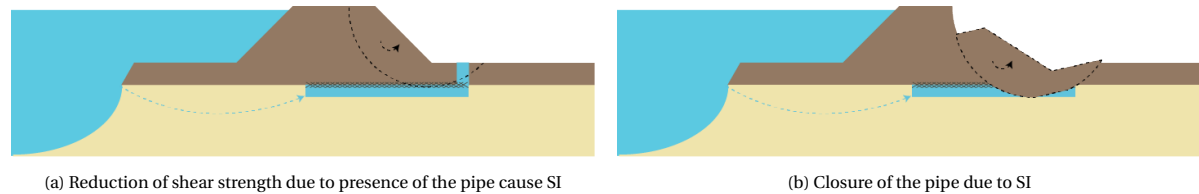
Figure 3.26: Alternating interaction at cross-section at axis of the pipe

3.4. Conclusions

There is an interaction possible between backward erosion piping (BEP) and slope instability (SI) in both directions.

The formation of a berm of remoulded soil that induces two possible exit point locations for BEP, namely, exit point location at the end of the berm and exit point location in the berm governs the interaction from SI to BEP. These two locations have a different effect on the outcome of the interaction, and these effects are:

- If the exit point is located at the end of the berm, the occurrence of BEP is not affected by the properties of the soil in the berm. It is only dependent on the valve effect due to sliding, the thickness of the blanket layer, including the berm height and the length of the berm, which determines the seepage length. These both lead to a decrease in the occurrence of BEP.
- When the exit point is located in the berm, the occurrence of BEP is affected by the properties of the berm. The effect of the thickness of the blanket layer including the berm height, the remoulded soil on the weight of the blanket layer, the change in aquifer head, the saturation of berm material and a change in critical heave gradient. However, these are uncertain, and therefore, the effect on the occurrence of BEP cannot be determined from only the parametric study.

The interaction from BEP to SI is governed by the 3D-effect, as different locations in and adjacent to the location of BEP have contradictory effects on SI.

- At the cross-section of the exit point, sand boil or pipe:
  There is a reduction of shear strength surrounding the soil below the exit point at the interface between sand and clay. There is no shear strength in the sand boil and pipe due to the presence of water and fluidised sand. In case of a pipe, the soil in the levee gets drained after a long period of time dependent on the permeability of the core material, reducing the driving moment of the soil equilibrium.
- Cross-section adjacent to the exit point, sand boil or pipe:
  There is a lowering in the aquifer head due to the presence of seepage towards the exit point, sand boil or pipe, which increases the shear strength of the soil experiencing the seepage. The drain effect affects both cross-sections. However, it reduces as the cross-section is further away from the pipe.

Only the interaction from SI to BEP is quantified in the next chapter, and it assesses the various possible effects of the remoulded soil on the interaction.

4

Framework for modelling interaction

This chapter describes the method of the quantification of the interaction, which focusses only on the interaction from slope instability (SI) to backward erosion piping (BEP).

4.1. Introduction

A 2D-model is developed to enable quantification of the interaction from SI to BEP. The main part of the model consists of three consecutive analyses: A stability analysis (section 4.3), displacement of the sliding plane (section 4.4) and a BEP analysis (section 4.5). The output of each of these analyses used as input for the next one, as seen in Figure 4.1. All three analyses use mean values for their input parameters. The model requires a representative cross-section of a river levee as input (section 4.2) for the quantification of the interaction. In this thesis, a cross-section of the Grebbedijk is used. This case study can be found in Appendix B. The model calculates the safety factor of the stability analysis, a remaining profile, and the three safety factors of the BEP analysis of the remaining profile. The difference between the original BEP safety factors and the BEP safety factors of the remaining profile relates to the interaction. This relation is further elaborated in Section 4.6.
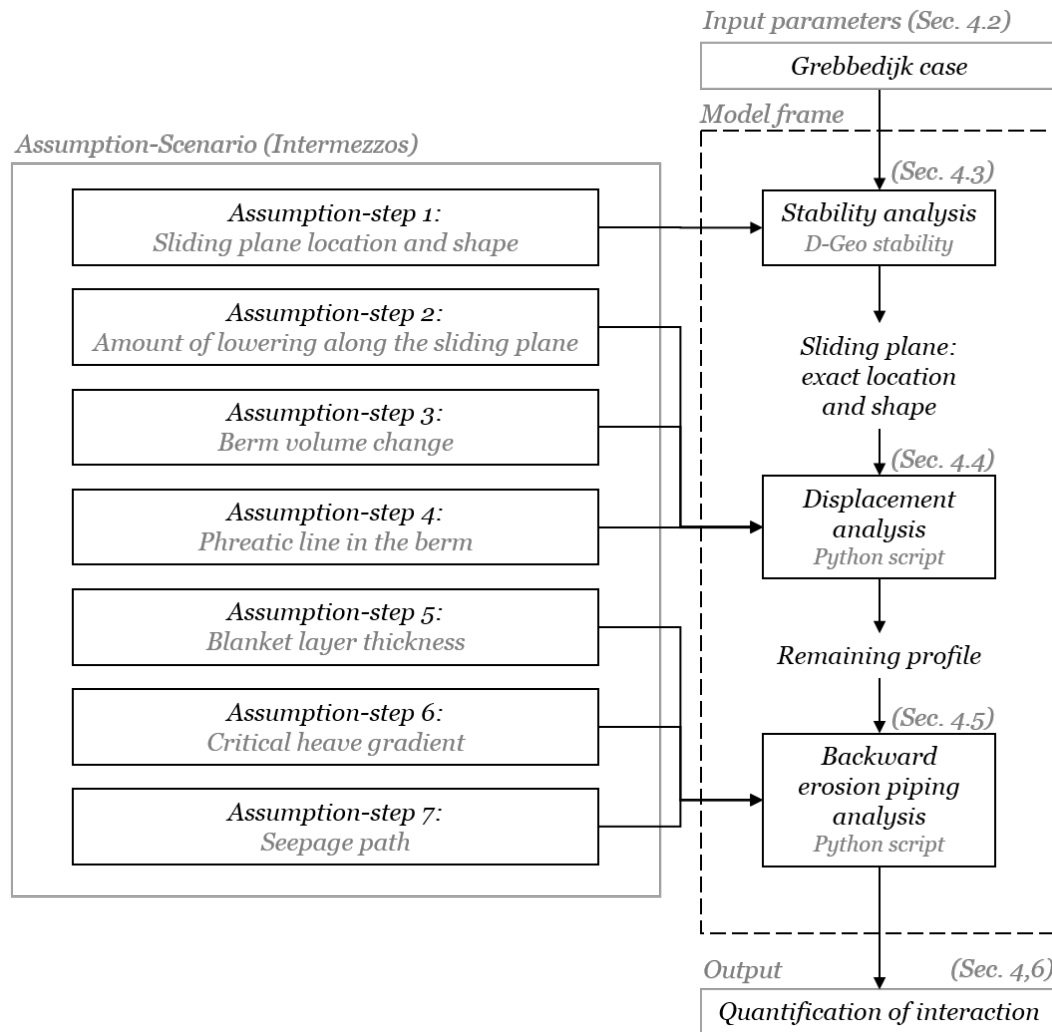
Figure 4.1: Model framework

In addition to the case, the model requires the input of an assumption-scenario, as shown in Figure 4.1. In this assumption-scenario, assumptions are made about the development of various aspects in the interaction failure process. One assumption-scenario consists of seven steps, which are referred to as assumption-steps. Each of these steps contains a limited number of options. These assumption-steps are of importance at a specific analysis in the model's calculation. Therefore, they are woven into the model framework at that specific analysis, in the form of an intermezzo. Every assumption-scenario (which is every possible combination of assumption-options) is run through the model. A base-case containing one assumption-scenario (with seven options) is introduced in Section 4.8. Variations on the base-case are used to assess the effect of the different assumption-scenarios on the interaction. In addition to the seven steps in the assumption-scenario, there are some fixed assumptions made in the model itself. These are also explained in the analyses.

At the start of the calculation, a case study and an assumption-scenario are selected. The model is then run for this case study and assumption-scenario. When the case study and input parameters have been determined, these are not changed in one run of the model.

A sensitivity analysis is conducted to get insight into the case-dependent sensitivity of the interaction. Thus, only the input parameters (see Figure 4.1) are varied in the sensitivity analysis. The methodology of the sensitivity analysis is described in Section 4.10. The failure of a levee by an interaction happens through a series of events. This chapter focuses on the path indicated in red in the event tree in Figure 4.2.
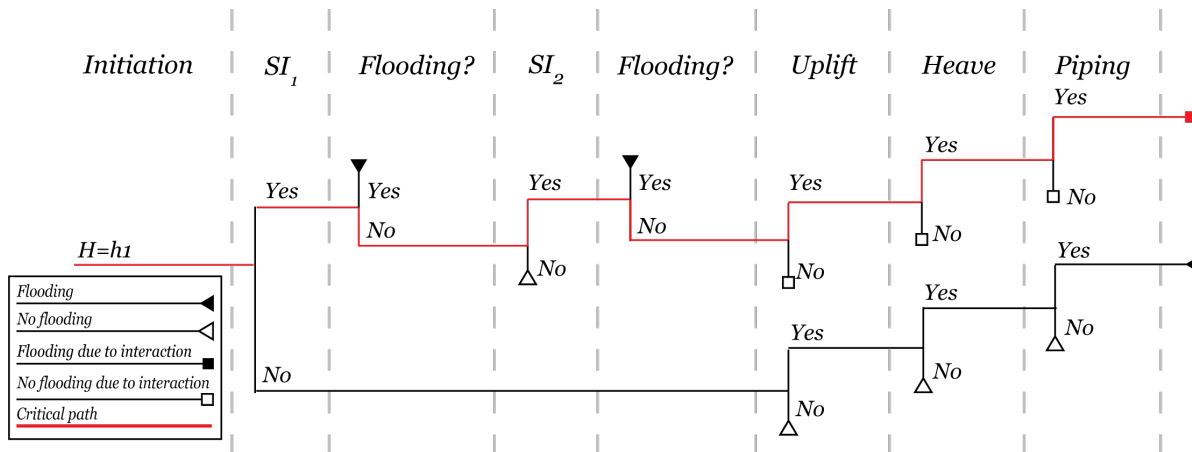
Figure 4.2: Event tree of the interaction from SI to BEP

4.2. Input parameters

Each of the three analyses in the model requires different parameters. All these parameters are called the input parameters of the model, and they are depicted in Table 4.1 in the second and third column. A mean value analysis was chosen to make a first quantification of the interaction. The interaction's sensitivity of the input parameters is illustrated by the sensitivity analysis (Section 4.10). A case is used to get realistic values for the input parameters. For this study, the case study of the Grebbedijk levee is chosen to evaluate the interaction. This levee did not pass the safety assessment round of 2017 on almost all failure mechanisms (Stuij et al., 2017a), including the failure mechanisms BEP and SI. This case is suitable for research on the interaction because these failure mechanisms may occur at the same levee Section, which allows for interaction. In Appendix B, a general description of the case and the input parameters values are given with there source in Table B.3, these values are also shown in Table 4.1. The head in the aquifer and the phreatic level are separately explained in Appendix B Sections B.3 and B.4, as well as the friction angle and cohesion of the different soil layers in Section B.5. The values of the parameters are the mean values unless otherwise indicated by *. Figure 4.3 shows the profile of the original Grebbedijk as it is used in the calculations. More information on the profile can be found in Appendix B, as well as the exact location of the characteristic points A, B, C, D, E and F (table B.1) and the exact locations of the phreatic line and aquifer head (Section B.3).
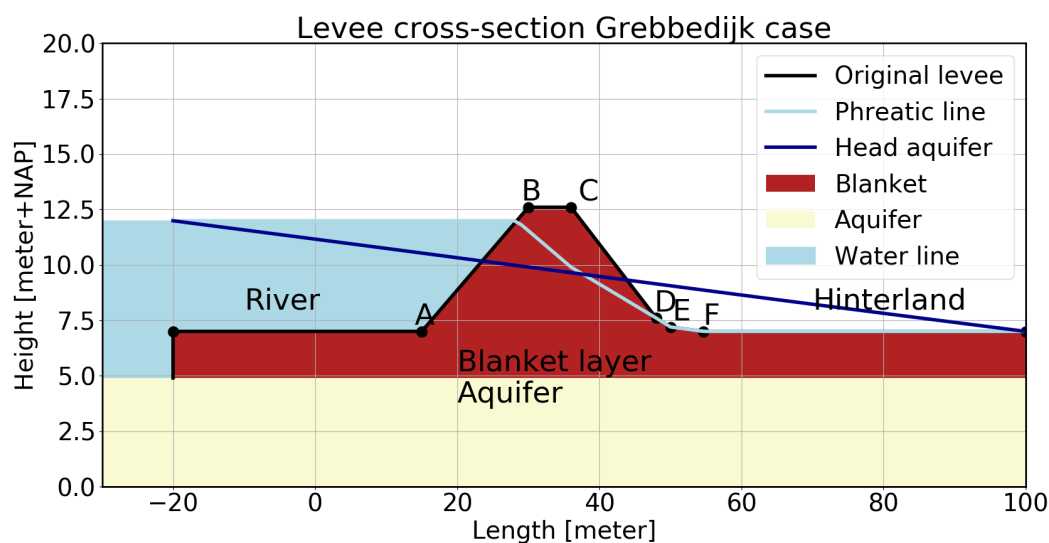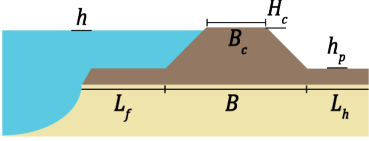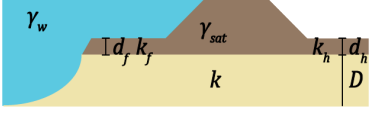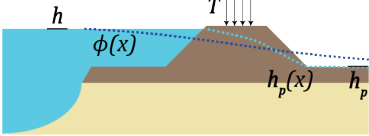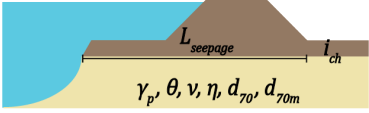
Figure 4.3: Levee profile of the Grebbedijk original input situation

Table 4.1: Input parameters for the model

Input parameters	Symbol	Description	Value	Unit
Geometry of the levee				
	H_c	Level of the levee	12.6	[m + NAP]
	B	Width of the levee	35.0	[m]
	B_c	Width of the crest of the levee	6.0	[m]
	h_p	Hinterland phreatic level	7.0	[m + NAP]
	L_h	Length of the hinterland	50.0	[m]
	L_f	Length (effective) foreshore	35.0	[m]
Soil characteristics and structure				
	-	Soil layer build up	Simple	[-]
	D	Aquifer thickness	22.0	[m]
	d_f	Thickness foreland blanket	2.3	[m]
	d_h	Thickness hinterland blanket	2.3	[m]
	k	Permeability aquifer	39	[m/s]
	k_h	Permeability blanket hinterland	0.05*	[m/s]
	k_f	Permeability blanket foreland	0.05*	[m/s]
	γ_{sat}	Saturated volumetric weight blanket	17.9	[kN/m^3]
	γ_{unsat}	Unsaturated volumetric weight blanket	17.4	[kN/m^3]
	γ_w	Volumetric weight water	9.81	[kN/m^3]
Load on the levee				
	h	Outside waterlevel	11.99	[m + NAP]
	$h_p(x)$	Phreatic line	[-]	[m + NAP]
	$\phi(x)$	Head in aquifer	[-]	[m + NAP]
	h_p	Hinterland phreatic level	7.0	[m + NAP]
	T	Traffic loads	13.3	[kN/m^2]
Specific for backward erosion piping				
	γ_p	Saturated volumetric sand grains	20	[kN/m^3]
	i_{ch}	Critical heave gradient	0.3	[-]
	θ	Bedding angle	37	[°]
	ν	Kinematic viscosity water	1.33 x 10^{-6}	[m^2/s]
	η	Constant of White	0.25	[-]
	g	Gravitational constant	9.81	[m^2/s]
	d_{70}	70% fractile of grain size distribution	0.208 x 10^{-3}*	[m]
	d_{70m}	Reference value for d70	0.307 x 10^{-3}*	[m]
Specific for slope instability analysis				
	-	Shear strength model	Critical state C-ϕ model	[-]
	-	Stability model	Uplift Van	[-]
	ϕ	Friction angle	28-31.8	[°]
	c	Cohesion	0	[kN/m^2]
	S	Undrained shear strength ratio	[-]	[-]
	POP	Pre-overburden pressure	[-]	[kN/m^2]
	m	Stress increase exponent	[-]	[-]
	σ'_{vy}	Vertical yield stress	[-]	[kN/m^2]

4.3. Stability analysis

The first step in the quantification of the interaction from SI to BEP is a stability analysis. This stability analysis is done on the levee in the program D-Geo stability (Deltares software). This program uses a chosen limit equilibrium method to calculate SI. It calculates all possible sliding planes and their corresponding safety factor. It shows the exact location and shape of the sliding plane with the lowest safety factor. This sliding plane is referred to as the critical sliding plane.

The calculated sliding plane itself may not lead to immediate levee failure due to SI, because this would make any interaction with BEP irrelevant. It is also assumed that a second sliding occurs. This sliding should not lead to failure of the levee either. It is important to consider a wide range of sliding plane sizes to interpret the effect of the size on the interaction. The different possible sizes are divided into six categories to limit the

number of calculations in assumption-step 1. These six categories maintain the distribution of the different sizes but do not require unnecessary computations.

Assumption-step 1: Sliding plane location and shape
The starting point of interaction is the sliding of the slope of the levee, which can occur in different shapes and sizes. The sliding plane locations and shapes are divided into three categories: The entry of the sliding plane, the depth of the sliding plane and the shape of the sliding plane, to limit the number of options of this assumption-step

The entry point of the sliding plane can be in the outer slope, the crest or the inner slope. Interaction can only occur if the initial sliding did not cause flooding. In this case, it is assumed that SI with the sliding plane entry at the outer slope always causes crest lowering and thus flooding. For this reason, only the crest and inner slope entry points are considered, in which the crest entry only suffices if the second sliding does not cause flooding.

The depth of the sliding plane can vary. There are three situations distinguished. In the first situation, the sliding plane partly disturbs the blanket layer. Secondly, the sliding plane reaches through the blanket and stays in the interface between the blanket layer and the aquifer. Thirdly, the sliding plane can go through the blanket layer and into the aquifer, disturbing both layers.

In reality, the shape of the sliding plane is difficult to predict. For the assumption-scenarios, only the Uplift Van shape is used. From these three categories, 6 assumption-options follow as shown in Figure 4.4.
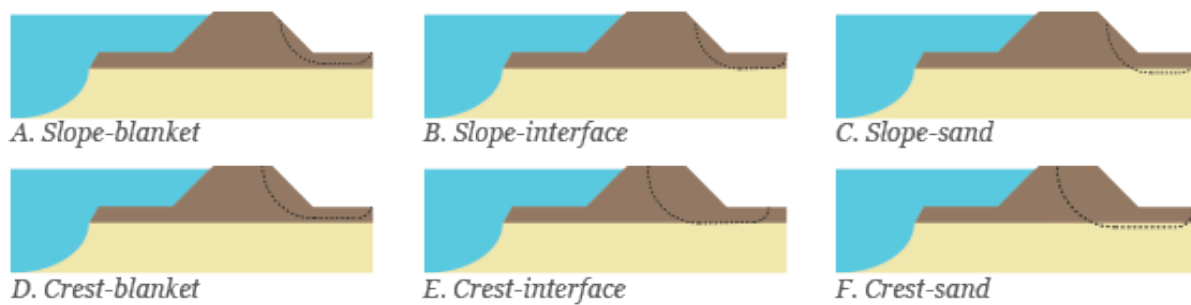
Figure 4.4: Location of the sliding planes and the shape of Uplift Van

---

Note that, for simplicity, the following Figures show a sliding plane with a Bishop shape.

In this study, only one case study is used. As a consequence, D-Geo stability gives only one critical sliding plane. However, for this research, different sizes of sliding planes are needed. Therefore, the functions to force D-Geo stability to show a sliding plane, which meets the conditions of the sizes categories, are used. The functions used to achieve this are forbidden lines or the minimum sliding plane depth, see Figure 4.5. For instance, to ensure that the levee does not fail due to the first or second sliding, a forbidden line is placed on the outer slope and a part of the crest. Each sliding plane that crosses this forbidden line is excluded from the results. A similar method can be used to force the entry point of the sliding plane into the slope or the crest. The minimum sliding plane depth is used to force the sliding plane into the blanket layer, interface or sand layer. Somewhere in the sliding plane, the vertical depth must be larger than the set minimum. Figure 4.5 shows an example of the above mentioned functions.
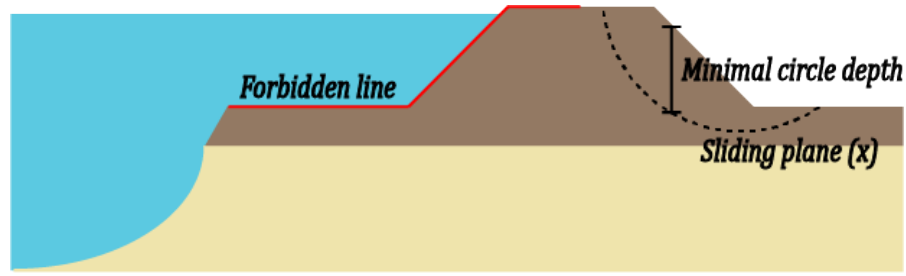
Figure 4.5: Example of D-Geo stability functions used to force a location of a sliding plane

As a consequence, the calculation does not generate the critical sliding plane and the corresponding safety factor, but a sliding plane with its corresponding safety factor. This safety factor of the calculated sliding plane still indicates the possible occurrence of the respective sliding plane. In this study, only sliding planes that have a safety factor lower than one are used, because they are more likely to occur than those with an FoS above 1.

The shape and location of this sliding plane are used to displace the soil in Section 4.4.

4.4. Displacement analysis of the sliding plane

The exact location of the sliding plane follows from the stability analysis in Section 4.3, and is required as input in this displacement analysis. It is assumed that the sliding takes place along this sliding plane. The next step is to determine the amount of displacement of the soil body along the sliding plane. The amount of lowering (A) depends on the height of the sliding plane (H_{sp}) and the value of lowering.

The height of the sliding plane is defined as the height of the sliding planes entry point ($Y_{sp,entry}$) minus the polder level (Y_{polder}), this definition is used in TRAS (ENW et al., 2009). A value is assumed for the lowering of this sliding plane. Three different values for this assumption are grouped in assumption-step 2.

Assumption-step 2: Amount of lowering along the sliding plane
Three possible options for the amount of lowering along the sliding plane follow from Section 2.4.4.

(a) Option A: sliding of 1 meter
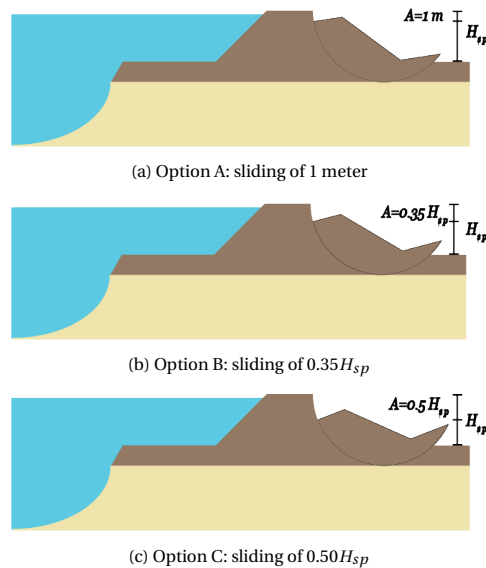
Option A: The sliding plane lowers approximately 1 meter based on observations (Zwanenburg et al., 2013).

(b) Option B: sliding of $0.35 H_{sp}$

Option B: The sliding plane lowers 0.35 times the height of the sliding plane; this assumption-option is based on the observations from different real-life sliding (Den Haan et al., 2014).

(c) Option C: sliding of $0.50 H_{sp}$

Option C: The sliding plane lowers 0.5 times the height of the sliding plane. This assumption is a part of the method for residual width (Restbreedtemethode bij overhoogte' in Dutch) of TRAS (ENW et al., 2009). This a conservative assumption based on observations.

Figure 4.6: Amount of lowering along the sliding plane

Each of the assumption-step 2 assumption-options give the amount of lowering of the sliding plane's entry point. The level of the new location of this entry point after displacement (Y_r) is the old location ($Y_{sp,entry}$) minus the amount of lowering (A) (i.e.: $Y_r = Y_{sp,entry} - A$). The corresponding new horizontal location (X_r) can be calculated with the sliding plane characteristics (circle radius (R) and centre point coordinates ((X_m, Y_m)) and the basic circle formula ($R^2 = X^2 + Y^2$). This calculation leads to two possible locations on the circle, where X_r is the smallest of the two intersections between the sliding circle and Y_r. Figure 4.7 provides an overview of these parameters.
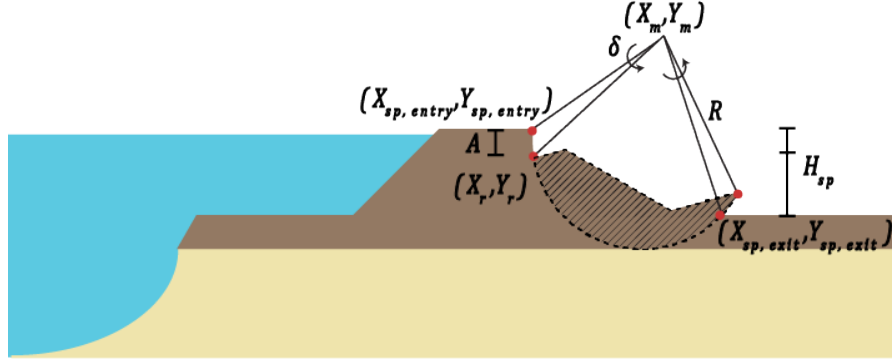
Figure 4.7: Rotation of the sliding plane and the rotation angle

It is assumed that all points in the sliding plane shift with the same rotation angle around the centre of the circle. This rotation angle is used to displace the characteristic points of the levee within the boundaries of the sliding plane (often points C, D, E, F (Figure 4.3) and the sliding plane's exit point ($X_{sp,exit}, Y_{sp,exit}$)). The rotation angle of a displaced point is calculated by determining the slope ($S1$) between the location of the entry point ($X_{sp,entry}, Y_{sp,entry}$) and the location of centre of the circle (X_m, Y_m) and the slope ($S2$) between the new location of the entry point (X_r, Y_r) and the location of centre of the circle. The angle between these two slopes follows from equation 4.3 and is called the rotation angle (δ).

$$S1 = \frac{Y_m - Y_{sp,entry}}{X_m - X_{sp,entry}} \tag{4.1}$$

$$S2 = \frac{Y_m - Y_r}{X_m - X_r} \tag{4.2}$$

$$\delta = \tan^{-1}\left(\left|\frac{S2 - S1}{1 + S2 * S1}\right|\right) \tag{4.3}$$

$$X_{r,exit} = \cos(\delta)(X_{sp,exit} - X_m) - \sin(\delta)(Y_{sp,exit} - Y_m) + X_m \tag{4.4}$$

$$Y_{r,exit} = \sin(\delta)(X_{sp,exit} - X_m) + \cos(\delta)(Y_{sp,exit} - Y_m) + Y_m \tag{4.5}$$

The location of the displaced point follows from equation 4.4.

Soil type	Precondition	Slope
Clay	Su >3,5 H	slope 1:2
Peat	Su >3,5 H	slope 1:4
Sand	ϕ >22 degrees	slope 1:4

Table 4.2: Slope second sliding translate from (ENW et al., 2009, p. 31)

Figure 4.8: Second sliding for clay levee

It is assumed that a second sliding takes place through the steep slope between the old entry point and the new entry point. For the schematization of this second sliding, no assumption-options are included in the

assumption-scenarios, this is a fixed assumption. The method described in TRAS (ENW et al., 2009) is used to estimate the new slope. Herein, it is assumed that from the location of the displaced sliding plane to the top of the levee, a new slope is formed (see Figure 4.8 dotted line). Depending on the soil type and shear strength of the soil and the retaining water height (H), the slope has an angle (see Table 4.2). The second sliding cannot cause lowering of the crest level and therefore limits the location of the entry point sliding plane. For this reason, a forbidden line was implemented at the outer slope and crest in the stability analysis as described in Section 4.3.

(a) Soil that displaces during failure process

(b) Displaced soil above dotted line forming a berm
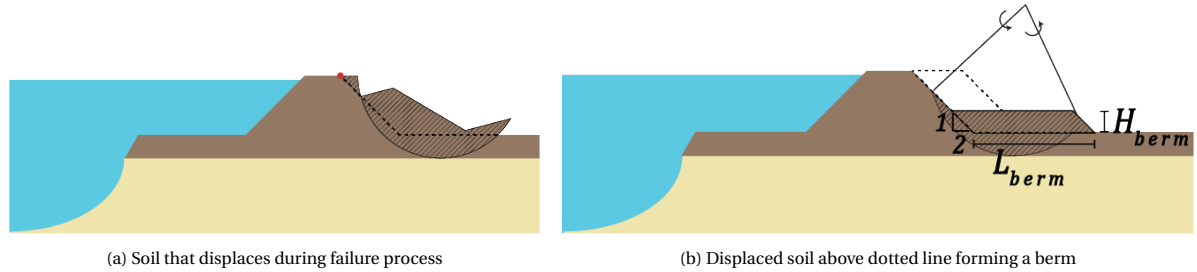
Figure 4.9: Displacement soil

All soil above the dotted line in Figure 4.9a is relocated. As seen in Chapter 3.2, the shape of the remaining profile is based on the video of levee failure of the IJkdijk experiments of 2008 (ICTdijk, 2009), the pictures of slope instabilities in Den Haan et al. (2014) and the schematization in Figure 2.10. From this example, one can say the soil accumulates at the original toe of the levee. The soil above the dotted line in Figure 4.9a is assumed to form a berm at the toe of the levee, as seen in Figure 4.9b. This accumulation of soil is schematized as a simple berm. The shape of the berm is assumed to be a parallelogram. This parallelogram is described by the length, the height and the slope angle (see Figure 4.9b). The length of the parallelogram has a set value which is determined by the x-coordinate of the displaced exit point of the sliding plane ($X_{r,exit}$). The slope angle of the berm is the same as the slope angle of the dotted line. The height of the berm follows from the volume, length and slope angle. It is assumed that the volume of the displaced soil can be approached as the area of the soil above the dotted line due to the 2D approach. However, there can be a change in the volume of the soil caused by the displacement, as explained in assumption-step 3.

Assumption-step 3: Remaining profile: Berm volume change
All soil that has moved during the displacement is assumed to be "remoulded soil". The characteristics of the remoulded soil are unknown. It is assumed that the composition of the remoulded soil can stay the same, contain more air and cracks, or the soil can compact due to the movement. The densening or loosening of the soil results in a volume change of the relocated soil. This assumed volume change affects the following parameters: The specific weight of the soil, the height of the berm and the porosity of the remoulded soil. The porosity change is important for assumption-step 6 and is discussed in assumption-step VI. The assumption-options for this assumption-step are shown in Figure 4.10.

(a) Option A: Berm volume same as the relocated volume

(b) Option B: Berm volume bigger than the relocated volume

(c) Option C: Berm volume smaller than the relocated volume

Option A: The berm volume is the same as the relocated soil volume. The ratio between the voids and the soil particles remains the same.

Option B: The berm volume is assumed to increase with 5 percent. However, the volume change is caused by the change in the amount of air in the soil, which is assumed to be massless. Therefore the specific weight decreases for an increase in volume.

Option C: The berm volume is assumed to decrease with 5 percent. However, the volume change is caused by the change in the amount of air in the soil which is assumed to be massless. Therefore the specific weight increases for a decrease in volume.

Figure 4.10: Berm formation

The height of the berm (H_{berm}) is calculated with the new volume (A_{berm}) and the length of the berm (L_{berm}), see equations 4.8, 4.6 and 4.7. The factor (f_A = 1.0, 1.05 or 0.95) used in equation 4.6 and 4.9 depends on which assumption-step 3 is chosen.

$$f_A = \frac{A_{berm}}{Area} \tag{4.6}$$

$$L_{berm} = X_{r,exit} - X_{newtoe} \tag{4.7}$$

$$H_{berm} = \frac{A_{berm}}{L_{berm}} \tag{4.8}$$

$$\gamma_{sat,remoulded} = \frac{\gamma_{sat}}{f_A} \tag{4.9}$$

Remaining profile (x)
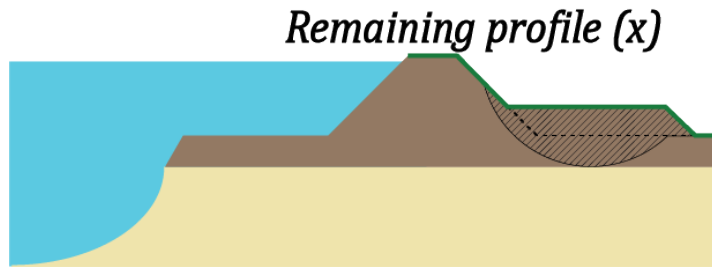
Figure 4.11: Schematization of remaining profile

The geometry and the soil characteristic of the remaining profile are now known, see Figure 4.11. The next step is to look at the new phreatic line ($h_{p,new}(x)$) and the aquifer head ($\phi_{new}(x)$). If an assumption-scenario is calculated where the blanket layer is perforated due to a large depth of the sliding plane, the head in the aquifer is changed to the limit potential of the blanket ($\phi_{limit}(x)$) at the location of the perforation. The value of the aquifer head remains equal to the limit potential until the original aquifer head is lower than this value.

$$\phi_{limit}(x) = h_p + \frac{d_i(x)(\gamma_{sat} - \gamma_w) + d_r(x)(\gamma_{sat,remoulded} - \gamma_w)}{\gamma_w} \tag{4.10}$$

When this is the case, the aquifer head returns to its original shape. This fixed assumption is based on an assumption made in the analysis of BEP: When the blanket layer has ruptured, the aquifer head approaches

the limit potential of the blanket layer. Figure 4.12a illustrates a drop at the rupture. After the drop, the aquifer head follows the limit potential of the blanket until the limit potential becomes lower than the original head. The head in the aquifer is not changed if an assumption-scenario is calculated where the sliding plane depth does not perforate the entire blanket layer.

(a) Schematization of a drop in aquifer head

(b) Note new phreatic line in orange square
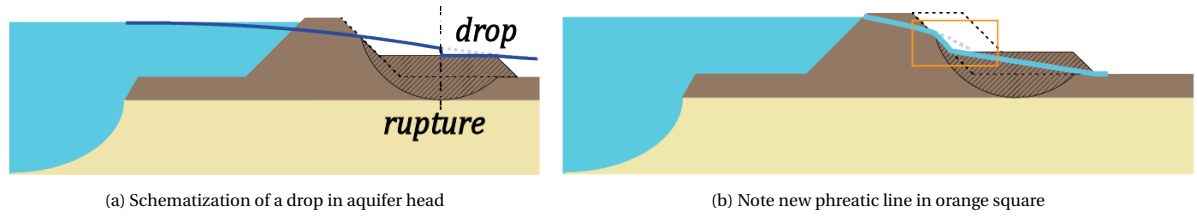
Figure 4.12: Aquifer head and phreatic line

The phreatic line in the undisturbed part of the levee is assumed to be the same as the original phreatic line. When the old phreatic line rises above the berm, the new phreatic line follows the profile of the new levee as depicted in Figure 4.12b. Assumption-step 4 is introduced to assume the phreatic line in the berm.

Assumption-step 4: Phreatic line in the berm

The saturation of berm and the location of the phreatic level in the berm are unknown and is highly dependent on the soil type of the remoulded soil. Part of the remoulded soil contains water, and the other part is dry. To get a good estimate of the influence of this saturation and the level three assumption-options are included in this assumption-step.

(a) Option A: Unsaturated berm

(b) Option B: Partly saturated berm

(c) Option C: Fully saturated berm
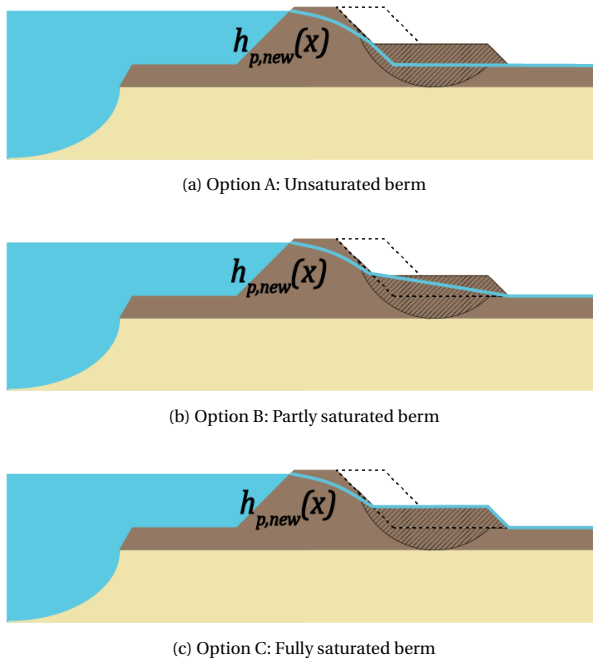
Figure 4.13: Phreatic line in the berm

Option A: The berm is completely drained
Option B: The berm is partly saturated
Option C: The berm is fully saturated. This assumption-option is unlikely because water must be added to the system. However this could occur from rain or overtopping and, therefore it is included to get a complete overview of the possibilities.

At this point in the model, a complete remaining profile is calculated in collaboration with the assumption-steps I, II, III and IV. This remaining profile includes the shape of the levee profile with the size of the berm of remoulded soil, the changed phreatic line and the head in the aquifer. A BEP calculation is done for this remaining profile in the next model step (section 4.5).

4.5. Backward erosion piping analysis

The factors of safety (FoS) of the sub-mechanisms of BEP (uplift, heave and piping) are calculated for the remaining profile with the berm. The used formulas for these FoS are defined in Chapter 2.3. The complete BEP analysis of the remaining profile results in three safety factors: A factor of safety of Uplift(FoS_u), a factor of safety of Heave(FoS_h) and a factor of safety of Piping(FoS_p). The combined effect of the three safety factors is defined in equation 4.11. The three mechanisms all need to occur in sequence. If one of the sub-mechanism passes the unity check (FoS-value above 1), this FoS-value is governing for the prevention of BEP. That is why the maximum of the three FoS is taken.

$$\Delta FoS_{BEP}(X_{exit}) = max\left(FoS_u(X_{exit}), FoS_h(X_{exit}), FoS_p(X_{exit})\right) \tag{4.11}$$

A Python script is built to enable the calculation for the different assumption-scenarios. If the FoS-value exceeds 1 at every location in the levee cross-section, it passes the unity check. For example, the unity check for uplift is passed if the critical value (limit potential of the blanket layer) is bigger than the occurring value (potential in the sand layer).

Uplift

The first step in the BEP analysis is the calculation of the FoS value of uplift along the entire remaining profile. In order to do this for each location, the difference between the head in the aquifer and the phreatic line ($\Delta\phi(x)$) and the weight of the blanket ($\Delta\phi_{c,u}(x)$) ts required. These two result in an uplift FoS-value for every location along the levee cross-section (a function of x).

$$FoS_u(x) = \frac{\Delta\phi_{c,u}(x)}{\Delta\phi(x)} \tag{4.12}$$

The head difference is calculated with equation 4.13, in which $\phi_{new}(x)$ is the value of the head in the aquifer at the location of the computation and $h_{p,new}(x)$ the value of the phreatic line at the location of the computation. Note, the locations of these lines are already determined in Section 4.4 and they are dependent on the assumption-steps I,II,III and IV.

$$\Delta\phi(x) = \phi_{new}(x) - h_{p,new}(x) \tag{4.13}$$

It is assumed that the soil in the berm is remoulded and all soil above the sliding plane location (see Figure 4.14). The thickness of the blanket is divided into an intact thickness (d_i) and a remoulded thickness (d_r). The ratio between these two depends on assumption-scenario, especially assumption-steps I (depth sliding plane), II and III (berm size). The weight of the blanket is determined with Equation 4.14. This equation differs from the equation in Section 2.5, an extra part is added to account for the presence of remoulded soil ($d_r(\gamma_{sat,remoulded} - \gamma_w)$).

$$\Delta\phi_{c,u}(x) = \frac{d_i(x)(\gamma_{sat} - \gamma_w) + d_r(x)(\gamma_{sat,remoulded} - \gamma_w)}{\gamma_w} \tag{4.14}$$

Figure 4.14: Intact and remoulded blanket layer thickness

There are different assumptions possible on how to account for this remoulded soil in the blanket weight calculation and thus uplift calculation. These assumption-options are implemented via assumption-step 5.

Assumption-step 5: Blanket layer thickness
The blanket layer thickness increases locally due to the berm, but what the effective thickness of the blanket is for uplift is unknown. There are three assumption-options to approach the blanket layer. In Figure 4.15, the three assumption-options for the blanket layer are illustrated. The parameters that are entered in equation 2.5 change due to the different assumption-options. A description of what changes per assumption-option is given below.

(a) Option A: The thickness of the blanket layer consist of only the intact part of the blanket

(b) Option B: The thickness of the blanket layer has partly or full remoulded soil properties

(c) Option C: The thickness of the blanket consist of the full thickness without remoulded soil properties
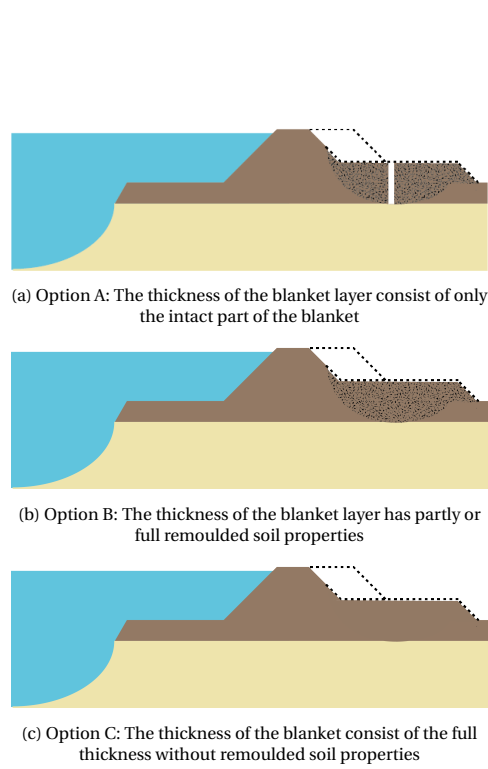
Figure 4.15: Blanket layer thickness

Option A is to only take the intact part of the blanket layer (d_i) into account ($d_r = 0$). It can not be guaranteed that there are no large cracks in the remoulded soil or that the soil has 'ruptured' in the remoulded part (Schematized in Figure 4.15a by white bar) Therefore, it can be assumed that there is no resistance left in the remoulded part against uplift at the exact location of a large crack. The remoulded soil still has a weight, but due to the assumption of rupture, this weight does not matter for the uplift FoS calculation. Note, even when the soil is assumed to compact in assumption-step 3 large cracks can still be present.

$$\Delta\phi_{c,u}(x) = \frac{d_i(\gamma_{sat} - \gamma_w)}{\gamma_w} \tag{4.15}$$

Option B is to take the total new thickness (d_i and d_r) and assume it may be partly or fully remoulded (depending on the depth of the sliding plane (assumption-step 1)). The remoulded soil has a different specific weight ($\gamma_{sat,remoulded}$) to take into account in the calculation FoS for uplift and is not assumed to have ruptured.

$$\Delta\phi_{c,u}(x) = \frac{d_i(x)(\gamma_{sat} - \gamma_w) + d_r(x)(\gamma_{sat,remoulded} - \gamma_w)}{\gamma_w} \tag{4.16}$$

Option C is the conservative assumption, which takes the full new thickness (d_i and d_r) into account with the soil properties of the original soil (γ_{sat}).

$$\Delta\phi_{c,u}(x) = \frac{(d_i(x) + d_r(x))(\gamma_{sat} - \gamma_w)}{\gamma_w} \tag{4.17}$$

The FoS of Uplift is now calculated with the head difference and the weight of the blanket, via equation 4.12. The location of the lowest uplift FoS-value is the most likely exit point location of BEP. It is therefore assumed and from here on used as the exit point location (X_{exit}). The calculations of the FoS-values of heave and piping are therefore done at this location. The location of the exit point varies depending on the assumption-scenario. The hypothesis is that this exit point can be located at three possible places in the remaining profile. Namely, at the beginning of the berm, at the end of the berm or in the berm at the level of the smallest intact layer. These locations are due to the bends in the remaining profile, and these give a sudden change in the value of the weight of the blanket, or due to the assumption of large cracks.

If the head in the aquifer is higher than the limit potential of the blanket at the exit point, it is assumed that it decreases to the limit potential of the blanket. This new location of the aquifer head is used in the subsequent calculations.

Heave

The FoS of heave is determined by the heave gradient (i_h) and the critical heave gradient ($i_{c,h}$) as described by equation 4.18.

$$FoS_h(X_{exit}) = \frac{i_{c,h}(X_{exit})}{i_h(X_{exit})} \tag{4.18}$$

The heave gradient follows from the head difference at the exit point divided by the blanket layer thickness, see equation 4.19.

$$i_h = \frac{\phi(X_{exit}) - h_p(X_{exit})}{d(X_{exit})} \tag{4.19}$$

In all assumption-scenarios, the heave gradient is defined as the vertical gradient of the blanket layer, so it requires the total blanket layer thickness at the exit location. Even when a large crack is assumed, the head difference must be sufficiently high to lift sediment to the highest level of the blanket layer.

$$i_{c,h} = -(1-n)\left(\frac{\rho_s - \rho_w}{\rho_w}\right) \tag{4.20}$$

There is an ongoing debate on the best approach to the critical heave gradient. Equation 4.20 gives an assumed definition of the critical heave gradient based on Terzaghi (Van Beek et al., 2014). Here the porosity (n) is defined by the volume of the voids (V_v) divided by the total volume of the soil (V_t) in which the total volume consists of the voids (V_v) and the solids (V_s),see Equation 4.21 and Equation 4.22.

The assumed volume changes in the assumption-step 3 are a (5%) change in total volume. It is also assumed that this volume change is translated into a change in the voids and not in the solids. This percentage volume change could be converted to a change in porosity if the original composition of the soil is known (V_v and V_v).

$$n = \frac{V_v}{V_T} \tag{4.21}$$

$$V_t = V_s + V_v \tag{4.22}$$

The initial porosity of the blanket layer for the Grebbedijk case is unknown. So, it is not possible to relate the assumed total volume change to a porosity change. Therefore, assumption-step 6 is introduced, which uses an entirely different approach. The exact characteristics of the critical heave gradient are highly uncertain, as described in Section 2.3.3. To prevent false security, it was decided to select three fixed values for the critical heave gradient: An extreme value, an average value and a conservative value. This different approach would not be necessary if the original ratio between the V_s and V_v is known: In that case, the percentage volume change can be translated into a percentage of change in porosity.

Assumption-step 6: Critical heave gradient
The soil's porosity may have changed due to the displacement of soil with the same, more, or less amount of air. The porosity of the soil influences the critical heave gradient relative to the original amount. The critical heave gradient is an uncertain parameter. For the assessment of levees, the critical heave gradient of 0.3 is used (Rijkswaterstaat WVL, 2017d). Another often used value is 0.5 for the critical gradient (The value of 0.3 is deducted from the value 0.5 with safety factors). For the assumption-options of this assumption-step, the critical heave gradient as it is used in the safety assessment is used, and two assumption-options are added to account for the lowering or rising.

The assumption-options which are used (in sequence) are $i_{c,h} = 0.1$, $i_{c,h} = 0.3$ and $i_{c,h} = 0.5$. Only the remoulded soil can experience the increase or decrease. Therefore only the critical heave gradient in the berm is changed due to the assumption-step changes. If the exit point location is outside the berm the value of 0.3 is used as is in the original situation.

(a) Option A: $i_{c,h} = 0.1$ (b) Option B: $i_{c,h} = 0.3$ (c) Option C: $i_{c,h} = 0.5$
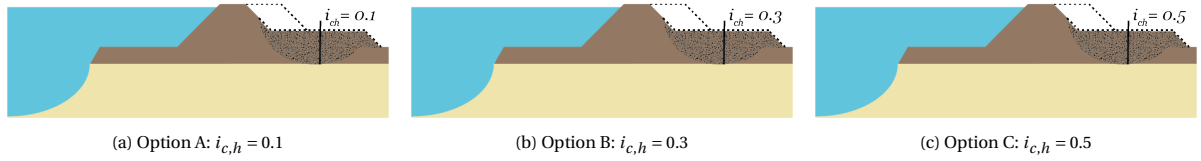
Figure 4.16: Critical heave gradient

Piping

The FoS of piping calculation is done by the use of equation 4.23 by Sellmeijer (Knoeff et al., 2009). The safety factor is calculated with the critical head difference over the levee ($H_{c,p}$) divided by the occurring head difference ($h - h_p - 0.3d$), see Equation 4.23.

$$FoS_p = \frac{H_{c,p}}{h - h_p(X_{exit}) - 0.3d(X_{exit})} \tag{4.23}$$

Herein is h_p the phreatic level at the exit location in the remaining profile and the h is the outside water level. The 0.3 times blanket layer thickness ($0.3d$) accounts for the head loss in the boil. The blanket layer thickness expresses the vertical distance of which the sand needs to be transported. Therefore the full blanket layer thickness at the exit point location (d_i and d_r) is typically used. This thickness accounts for the vertical part of the total seepage path. The horizontal part of the seepage path is accounted for by the seepage length (L) (horizontal distance in the aquifer). This seepage length is part of the resistance expressed by the critical head difference ($H_{c,p}$).

$$H_{c,p} = LF_{resistance}F_{scale}F_{geometry} \tag{4.24}$$
$$L = X_{exit} - X_f \tag{4.25}$$

$$F_{resistance} = \eta \frac{\gamma_p}{\gamma_w} \tan(\Theta) \tag{4.26}$$

$$F_{scale} = \frac{d_{70m}}{\sqrt[3]{\kappa L}} \left(\frac{d_{70}}{d_{70m}} \right)^{0.4}, \quad \kappa = \frac{v_{water}}{g} k \tag{4.27}$$

$$F_{geometry} = 0.91 \left(\frac{D}{L} \right)^{\frac{0.28}{\left(\frac{D}{L}\right)^{2.8} - 1} + 0.04} \tag{4.28}$$

However, this implies that the seepage path goes straight up through the blanket layer. The hypothesis is that the soil instability may have caused a compression of the soil along the boundary layer of the sliding plane, which prevents the seepage from going straight up through the blanket, regardless of the characteristics of the remoulded soil.

This hypothesis implies another seepage path that may follow the path with the least resistance along the sliding plane, instead of going through this thin compacted layer. To test this hypothesis correctly, a FEM of the groundwater flow would need to be developed, which included this layer. However, this study is exploratory research to find if this alternative seepage path would influence the amount of interaction and therefore, assumption-step 7 is introduced to show the possible effect of this assumption of a different seepage path.

To implement the assumption-step 7, where an alternative seepage path is examined, a different seepage path along the sliding plane is calculated. The currently used formula of FoS Piping is not able to calculate this path and, therefore, the following alternative approach is used for the second assumption-option of the assumption-step 7. The extra distance travelled through the blanket layer is calculated and implemented in the calculation as extra vertical distances (d in equation 4.23). This assumption-option 7B also affects the heave gradient (i_h) because the heave path (d in equation 4.19) is also elongated.

Assumption-step 7: Seepage path
The seepage path influences the horizontal seepage length used to express pipe progression in Sellmeijer for-
mula, and the vertical seepage is accounted for with the 0.3d-rule in the piping factor of safety. Two assumption-
options are defined for the seepage path. The first assumption-option A considers the normal seepage path in
which the water seeps along the interface between the sand layer and the blanket layer and goes up at the loca-
tion where the resistance is the least. This location is at the exit point location (X_{exit}) found by the FoS of uplift.
Figure 4.17a shows the first assumption-option.
The second assumption-option B is based on the hypothesis that the soil instability may have caused a compres-
sion of the soil along the sliding plane, which prevents the seepage from going straight up through the blanket.
This hypothesis implies it may follow another path with less resistance along the sliding plane. An example
of such a path is shown in Figure 4.17b. This assumption-step influences the FoS-values of Heave and Piping
in the model in Section 4.5. As a consequence, the horizontal distance travelled in the blanket layer is only
considered as extra damping of the load via the elongation of vertical distance.

(a) Option A: Seepage straigth thourgh the balnket layer   (b) Option B: Seepage along the sliding plane
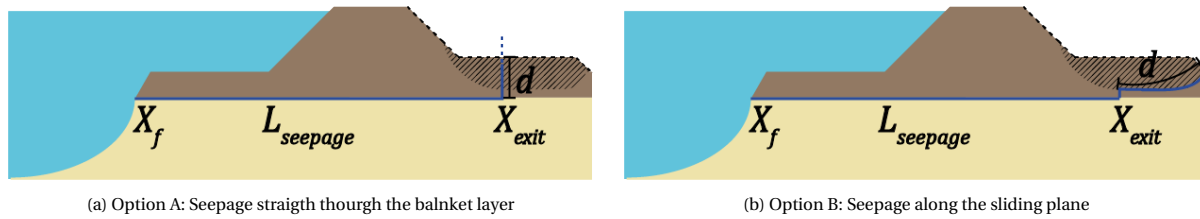
Figure 4.17: Location of the seepage path

4.6. Output

The safety factors FoS_u, FoS_h and FoS_p of the remaining profile can be compared with the three BEP safety
factors of the original levee cross-section that was used as input for the model ($FoS_{u,original}$, $FoS_{h,original}$,
$FoS_{p,original}$). The difference between the original FoS-values and the FoS-values of the remaining profile
indicate the effect of the interaction per sub-mechanism. The total safety of BEP is the combination of the
three sub-mechanisms. If one of the three passes the unity check (bigger than 1), it is assumed that the com-
plete BEP process is less likely to occur. It is important also to note if the interaction changes the combined
occurrence of three sub-mechanisms, see Equation 4.32. The maximum of the three sub-mechanism gives a
good indication of the combined effect. The difference between the maximum of the three FoS-values of the
remaining profile and the original profile indicates the combined effect of the interaction. The leading mech-
anism is the sub-mechanism with the highest safety factor of the three sub-mechanisms; this mechanism
determines the safety factor of combined BEP.

$$\Delta FoS_u = FoS_u - FoS_{u,original} \tag{4.29}$$
$$\Delta FoS_h = FoS_h - FoS_{h,original} \tag{4.30}$$
$$\Delta FoS_p = FoS_p - FoS_{p,original} \tag{4.31}$$
$$\Delta FoS_{BEP} = max\left(FoS_u, FoS_h, FoS_p\right) - max\left(FoS_{u,original}, FoS_{h,original}, FoS_{p,original}\right) \tag{4.32}$$

The model is run for the different possible assumption-options expressed in the assumption-steps. Each
assumption-scenario consists of seven assumption-steps. All possible combinations of assumption-steps
(2916 combinations when including all the assumption-options) are run through the model. This results in
2916 times three new FoS for the sub-mechanisms of BEP, which are compared in Equations 4.29, 4.30 and
4.31. These results are visualised in boxplots.

4.7. Dependencies of used parameters

Table 4.3 shows all dependencies implemented in the model. It can be seen that some parameters are used more than once in different parts of the model. For example, the exit point location (X_{exit}) is used in calculation of $i(X_{exit})$ and thus in FoS_h, as well as in the calculation of FoS_p via H_p and L in $H_{c,p}$. Parameters that are used more than once in a single model run maintain a fixed value within this run. Parameters are affected by the options from one or more assumption steps. These dependencies are also shown in the third column of Table 4.3.

Table 4.3 also illustrates which parameters change and which remain the same as the input. Table 4.3 shows a summery of the parameters used in Sections 4.3, 4.4 and 4.5. If the value of a parameter is location-dependent, this parameter is defined as a function of x. the D-Geo stability output and assumptions are not indicated on the left side of the table, but they are included by the color code. In the table the following color code is used:
Input parameter, Output parameter D-Geo stabilty, Assumption-step, Assumption.

Table 4.3: Overview of the dependencies of the parameters used

Parameter	Depends on parameters	Assumption-steps	Section	Equation
sliding plane (x)	$X_{sp,entry}, Y_{sp,entry}, X_{sp,exit}, Y_{sp,exit}, X_{m,circle1},$ $Y_{m,circle1}, R_{circle1}, X_{m,circle2}, Y_{m,circle2}, R_{circle2}$	1	4.3	-
H_{sp}	Y_{polder} , $Y_{sp,entry}$	1	4.4	-
A	H_{sp}, 2	1, 2	4.4	-
Y_r	$A, Y_{sp,entry}$	1, 2	4.4	-
X_r	$Y_r, R_{circle1}, X_{m,circle1}, Y_{m,circle1}$	1, 2	4.4	-
(X_{newtop}, Y_{newtop})	$Y_r, X_r, Y_{top},$ slope angle	1, 2	4.4	-
(X_{newtoe}, Y_{newtoe})	$X_{newtop}, Y_{newtop},$ slope angle	1, 2	4.4	-
S1	$X_{m,circle1}, Y_{m,circle1}, X_{sp,entry}, Y_{sp,entry}$	1, 2	4.4	4.1
S2	$X_r, Y_r, X_{m,circle1}, Y_{m,circle1}$	1, 2	4.4	4.2
δ	S1, S2	1, 2	4.4	4.3
($X_{r,exit}, Y_{r,exit}$)	$\delta, X_{sp,exit}, Y_{sp,exit}, X_{m,circle2}, Y_{m,circle2}$	1, 2	4.4	4.4
$Area$	$X_{newtop}, Y_{newtop}, X_{newtoe}, Y_{newtoe},$ $X_{top}, Y_{top}, X_{toe}, Y_{toe}$	1, 2	4.4	-
L_{berm}	$X_{r,exit}, X_{newtoe},$ parallelogram	1, 2	4.4	4.7
A_{berm}	$Area$, 3	1, 2, 3	4.4	4.6
H_{berm}	A_{berm}, L_{berm}	1, 2, 3	4.4	4.8
$\gamma_{sat,remoulded}$	γ_{sat}, 3	1, 2, 3	4.4	4.9
Remaining profile (x)	$H_{berm}, L_{berm},$ (X_{newtop}, Y_{newtop}), (X_{newtoe}, Y_{newtoe}), slope angle, Original profile(x)	1, 2, 3	4.4	-
$d_i(x), d_i(x), d(x)$	Remaining profile (x), sliding plane (x), $Y_{blanketlayer}$	1, 2, 3	4.4	-
$\phi_{new}(x)$	$\phi_{limit}(x), Y_{sp,depth}, Y_{blanketlayer}, \phi(x)$	1, 2, 3	4.4	-
$\phi_{limit}(x)$	$\gamma_{sat}, \gamma_w, \gamma_{sat,remoulded}, d_i(x), d_r(x)$	1, 2, 3	4.4	4.10
$h_{p,new}(x)$	$h_p(x),$ Remaining profile (x), 4, follow remaining profile	1, 2, 3, 4	4.4	-
$\Delta\phi(x)$	$\phi_{new}(x), h_{p,new}(x)$	1, 2, 3, 4	4.5	4.13
$\Delta\phi_{c,u}(x)$	$d_i(x), d_r(x), \gamma_{sat,remoulded}, \gamma_{sat}, \gamma_w$, 5	1, 2, 3, 5	4.5	2.5
$FoS_u(x)$	$\Delta\phi(x), \Delta\phi_{c,u}(x)$	1, 2, 3, 4, 5	4.5	4.12
X_{exit}	$min(FoS_u(x))$	1, 2, 3, 4, 5	4.5	-
$i_h(X_{exit})$	$\phi_{new}(X_{exit})$ or $\phi_{limit}(X_{exit}), h_{p,new}(X_{exit}), d(X_{exit})$	1, 2, 3, 4, 5	4.5	4.19
$i_{c,h}(x)$	$i_{c,h}$, 6	1, 2, 3, 4, 5, 6	4.5	4.20
FoS_h	$i_{c,h}(X_{exit}), i(X_{exit})$	1, 2, 3, 4, 5, 6	4.5	4.18
H_p	$h, h_{p,new}(X_{exit}), d(X_{exit})$, 7	1, 2, 3, 4, 5, 7	4.5	4.23
$H_{c,p}$	L, F_r, F_s, F_g	1, 2, 3, 4, 5	4.5	4.24
L	X_{exit}, L_f	1, 2, 3, 4, 5	4.5	4.25
F_r	$\eta, \gamma_p, \gamma_w, \Theta$	1, 2, 3, 4, 5	4.5	4.26
F_s	$L, d_{70m}, d_{70}, v_{water}, k, g$	1, 2, 3, 4, 5	4.5	4.26
F_g	L, D	1, 2, 3, 4, 5	4.5	4.26
FoS_p	$H_p, H_{c,p}$	1, 2, 3, 4, 5, 7	4.5	4.23

4.8. Base case

One assumption-scenario is appointed as the 'base case', which consist of seven assumption-steps where for each step a choice is made on the assumption-option used in this step. The base case choice is based on how realistic the assumption-options are to occur. This base case is thus subjective and is only used to elaborate on a probable interaction. In the summary sheet in Section 4.9, the grey-area represent the chosen base case.

Option per step	Rationale
1E.	A sliding plane in the crest and through the blanket layer is chosen because this is a common form of SI. A smaller sliding plane could also be caused by sliding of the levee cover or could be caused by micro instability.
2B.	The amount of lowering of the sliding plane is set at 0.35 times the sliding plane height. This value is deducted from observations in real life situations and is, therefore, a plausible assumption-option.
3B.	The change of volume of the berm is assumed to increase because no change after movement is more unlikely. Depending on the initial conditions of the soil (loose or dense) increase or decrease will be more likely however this is not known, for now, so increase is chosen.
4B.	A partly saturated berm is chosen because the original soil that displaced to create the berm was partly saturated. For an unsaturated berm, the water must drain away, and for a fully saturated berm water needs to be added, these are assumed to be less likely.
5B.	The blanket layer thickness is chosen as a partly remoulded blanket layer. A larger crack or no change is assumed to be less likely.
6B.	The value of 0.3 is chosen for the critical heave gradient because the exit point of the base case is at the end of the berm where the soil is not changed. In the original situation, a critical heave gradient of 0.3 was assumed based on the safety assessment criteria for the soil in the blanket layer.
7A.	The seepage path is set on standard assumptions for the seepage path straight up through the blanket layer because there are still doubts about whether the alternative path could occur.

4.9. Summary sheet assumption-steps

As described in Section 4.6, all combination of the assumption-steps are run through the model. The number of calculated assumption-scenarios is 2916 (6x3x3x3x3x3x2).

Assumption-step 1:
Sliding plane location and shape

A. Slope-blanket

B. Slope-interface

C. Slope-sand

D. Crest-blanket

E. Crest-interface

F. Crest-sand

Assumption-step 2:
Amount of lowering

$A=1\,m$ H_{sp}

A. 1m lowering

$A=0.35\,H_{sp}$ H_{sp}

B. 0.35 H lowering

$A=0.5\,H_{sp}$ H_{sp}

C. 0.5 H lowering

Assumption-step 3:
Berm volume change

$A_{berm}=Area \times 1.0$

A. Equal volume

$A_{berm}=Area \times 1.05$

B. Volume increase

$A_{berm}=Area \times 0.95$
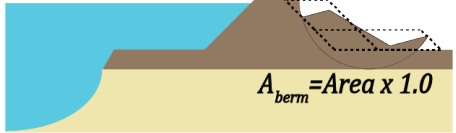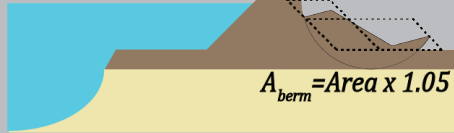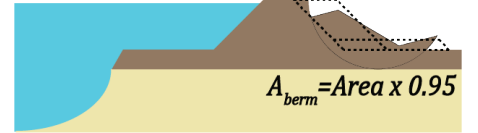
C. Volume decrease

Assumption-step 4:
Phreatic line in the berm

$h_{p,new}(x)$

A. Unsaturated

$h_{p,new}(x)$

B. Partly saturated

$h_{p,new}(x)$
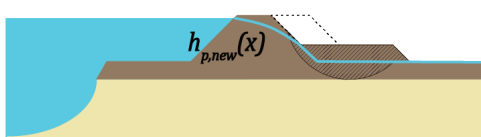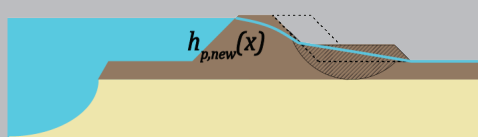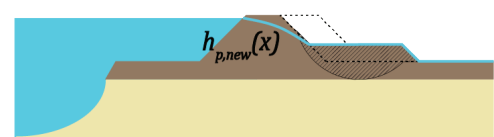
C. Fully saturated

Assumption-step 5:
Blanket layer thickness
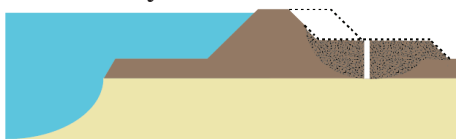
A. Only intact thickness
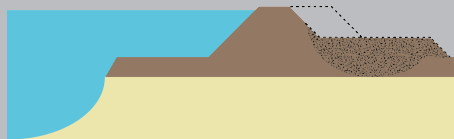
B. Partly remoulded
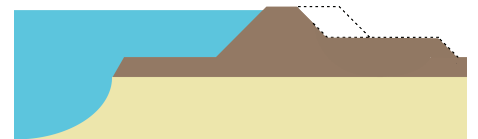
C. Full thickness

Assumption-step 6:
Critical Heave gradient

i_{ch}

A. $i_{ch}=0.1$

i_{ch}

B. $i_{ch}=0.3$

i_{ch}
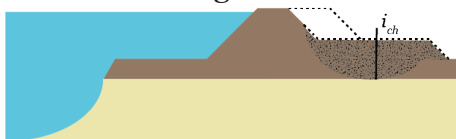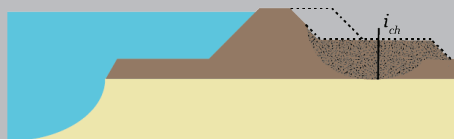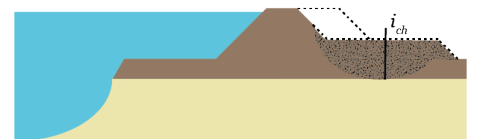
C. $i_{ch}=0.5$

Assumption-step 7:
Seepage path

Base-case

X_f $L_{seepage}$ X_{exit} d

A. Straigth up

X_f $L_{seepage}$ X_{exit} d
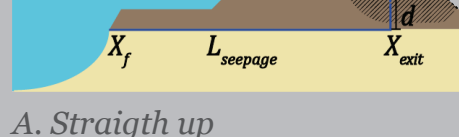
B. Along the sliding plane

4.10. Sensitivity analysis

To quantify the sensitivity of the input parameters on the interaction, different input cases are created, which deviate from the Grebbendijk case on one or two variables. The following deviations are accounted for:

- *Grebbendijk Original case*, see Figure 4.3
- *Thin blanket layer*: $d = 0.5$ m, see Figure 4.18a
- *Thick blanket layer*: $d = 7.0$ m, see Figure 4.18b
- *No foreshore*: $L_f = 0.0$ m, see Figure 4.18c
- *Long foreshore*: $L_f = 135.0$ m, see Figure 4.18d
- *Wide crest and gentle slope*: $B_c = 8.0$ m and $i = 0.25$, see Figure 4.18e

These cases use a single sliding plane shape, which is obtained through a D-Geo stability calculation, which uses a fixed forbidden line and a minimal circle depth of 3 m. The calculated sliding plane falls within one of the six assumption-options of the first assumption-step, because of the different geometries. Therefore, the assumption-scenarios for every input case only consider variations within assumption-step 2 to 7, which limit the number of calculated scenarios within each input case to 486.i

In addition to the first six input cases, a seventh case implies an alternative fixed assumption on the shape of the remaining profile after SI in the Grebbendijk case.

- *Triangular berm*: $H_{berm} = \frac{2*A_{berm}}{L_{berm}}$ at the left side and $H_{berm} = 0$ at the right side, see Figure 4.18f

The seven assumption-steps for this *Triangular berm* case remain unchanged, which also results in 486 scenarios in this analysis.

The original situation ($FoS_{x,original}$) used to determine the difference (ΔFoS_x) also changes in the first six input cases. This can give a distorted picture of the interaction, for example with a large original safety factor (=4) and a safety factor of two for the remaining profile then the negative interaction is minus two ($\Delta FoS_x = -2$). Compared to, for example, a small original safety factor (=0.5) and a safety factor of zero for the remaining profile, the negative interaction is minus 0.5 ($\Delta FoS_x = -0.5$). Therefore, for the sensitivity analysis, the interaction is expressed as a percentage of the original situation. This would give a percentage of -50% and -100% for the two examples.

$$Interaction \quad [\%] = \frac{\Delta FoS_x}{FoS_{x,original}} \tag{4.33}$$

Similar to the original case, the interaction percentages of all failure (sub-)mechanisms (BEP, Uplift, Heave, Piping) for these six input cases are visualised with boxplots. These boxplots will be compared to the boxplots of the original Grebbedijk case.
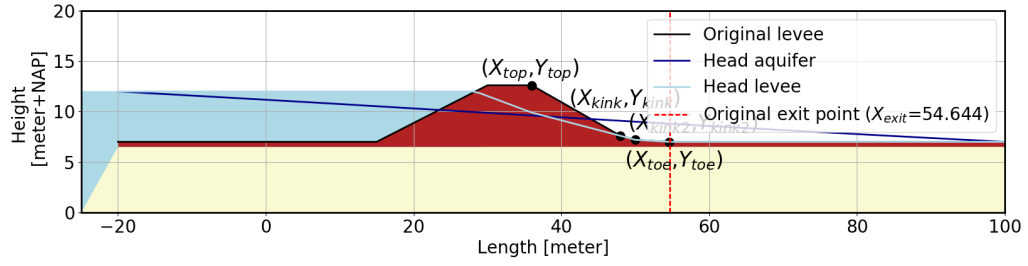
(a) Thin blanket layer case
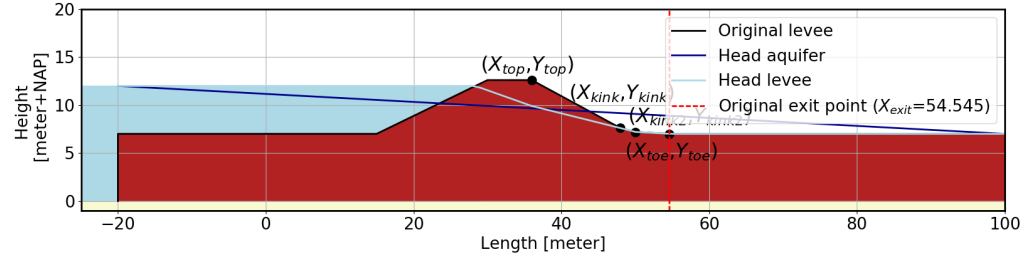
(b) Thick blanket layer case
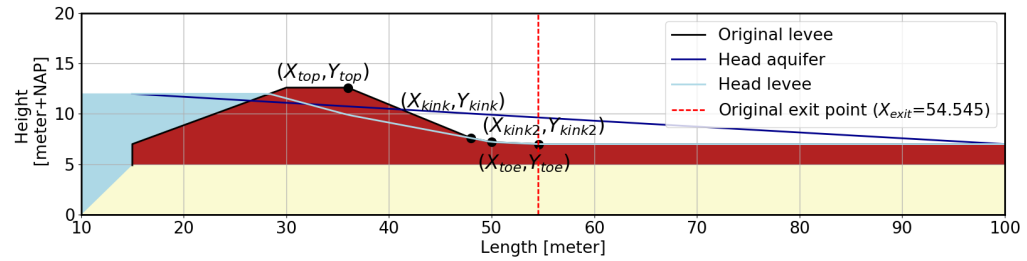
(c) No foreshore case
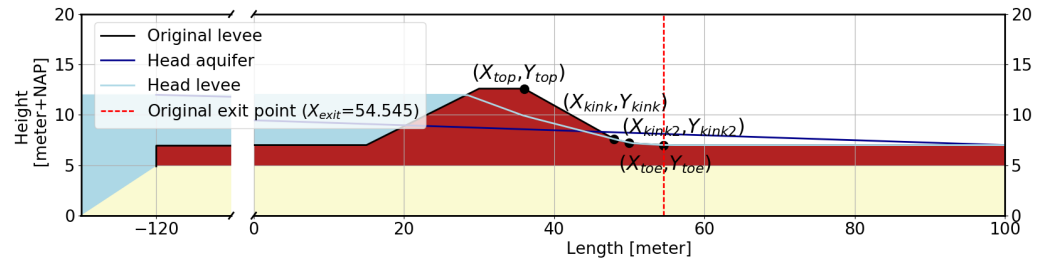
(d) Long foreshore case
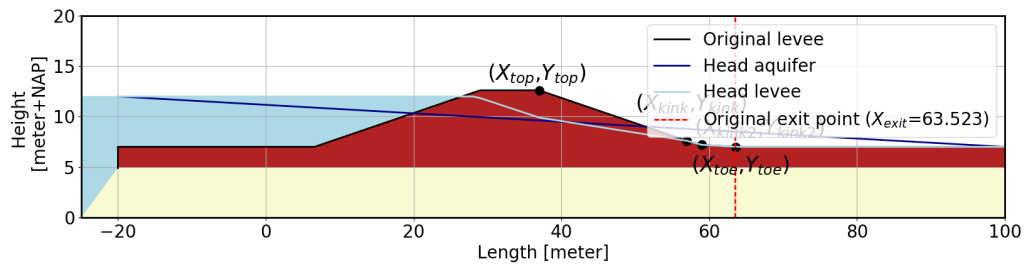
(e) Wide crest and gentle slope case
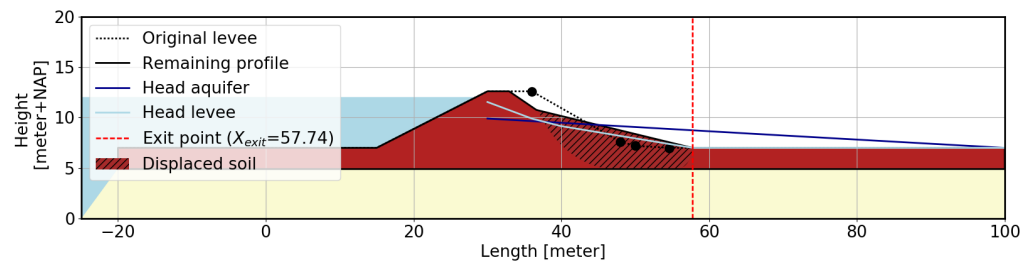
(f) Triangular berm case remaining profile

Figure 4.18: Original situations for different input cases

5

Results: Quantification of interaction

This chapter aims to present and elaborate on the results of quantification of the interaction from slope instability (SI) to backward erosion piping (BEP). Please note, the interaction from BEP to SI is not quantified in this study. The model described in the model framework (Chapter 4) is executed for all possible assumption-scenarios. In section 5.1 the original Grebbedijk case is discussed. This discussion includes the results from the BEP analysis and the values used for this calculation. In section 5.2, the interaction for BEP of the base case is elaborated on in detail. Section 5.3 presents the interactions of all assumption-scenarios in boxplots for the sub-mechanism uplift, heave and piping as well as for the combined BEP. Based on these plots, the most important conditions and assumptions governing the interactions are highlighted. The sensitivity analysis (section 5.4) is discussed in detail to explore how the Grebbedijk results relate to other levees.

The stability analysis interim result are presented in Appendix C for the Grebbedijk case and in Appendix C.2 for the sensitivity analysis. Table D.1 in Appendix D shows the values of the non-variable parameters that are used throughout the complete quantification. The complete table of the results can be found in Appendix E. The complete elaboration of the cases in the sensitivity analysis can be found in Appendix F.

5.1. Backward erosion piping analysis - Original levee

The original combined BEP safety factors of the Grebbedijk levee are needed to assess the interaction from SI to BEP. These factors are used to indicate the difference in combined BEP between the original situation and the situation where SI has occurred, as described in Section 4.6. This combined BEP analysis is carried out using the same method as described in section 4.5, except that the original profile is used and the assumption-steps are not taken into account. Resulting from this analysis are the values for the combined BEP safety factors shown in Table 5.1. The order of magnitude of the results is in line with the assessment results of the Grebbedijk (Hop and Rijneveld, 2018b). In the original situation, BEP is likely to occur because all three sub-mechanisms are below the unity check of 1.

Table 5.1: Factors of safety for combined BEP for the original situation

Factor of safety	Symbol	Value $[-]$
Uplift	$FoS_{u,original}(X_{exit})$	0.93
Heave	$FoS_{h,original}(X_{exit})$	0.36
Piping	$FoS_{p,original}(X_{exit})$	0.65
combined BEP	$FoS_{BEP,original}(X_{exit})$	0.93

Table 5.2: Parameter used in combined BEP analysis of the original levee

Parameter	Value	Unit
X_{exit}	X=54.55,Y=7.00	[m]
$h_p(X_{exit})$	7.00	[m + NAP]
$\phi(X_{exit})$	8.87	[m + NAP]
$\Delta\phi(X_{exit})$	1.87	[m]
$\Delta\phi_{c,u}(X_{exit})$	1.73	[m]
$d(X_{exit})$	2.10	[m]
$i_h(X_{exit})$	0.82	[-]
$i_{c,h}$	0.30	[-]
$L(X_{exit})$	74.54	[m]

Table 5.2 shows the values used for the original combined BEP analysis. It starts with the location of the exit point. This location is determined via the distribution of the FoS of Uplift which was derived from dividing the weight of the blanket distribution of the entire levee ($\Delta\phi_{c,u}(x)$) with the head difference distribution ($\Delta\phi(x)$). Figure 5.1 shows the distribution of FoS of Uplift and the corresponding cross-section of the original levee. The grey area in the Figure indicates the range of possible exit points ($FoS_u < 1$) and possible initial failure locations. The location of the lowest FoS-value is defined as the exit point location (red dotted line). The exit point location is just left of the toe of the levee.
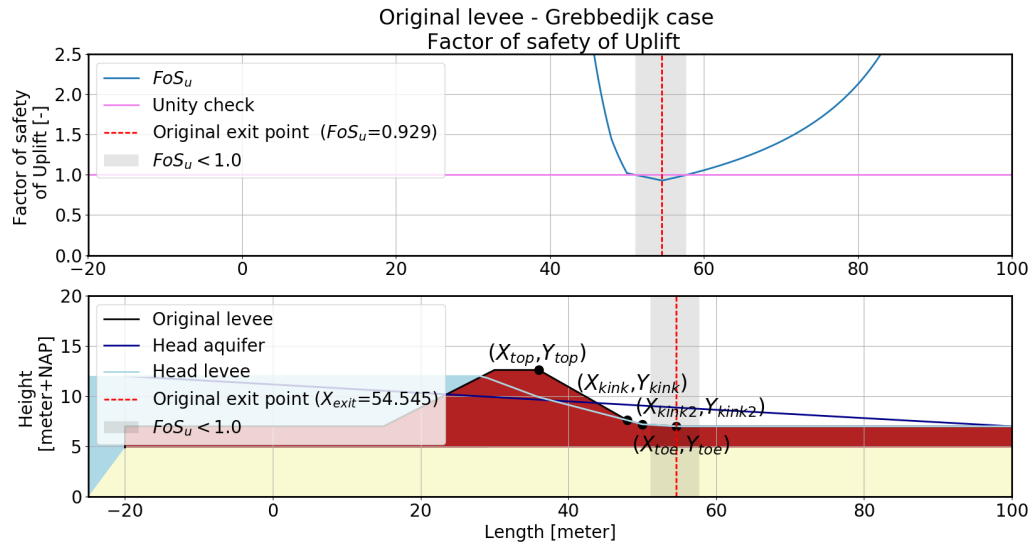
Figure 5.1: Factor of safety of uplift of the original levee (Grebbedijk levee)

5.2. Base case

In Section 4.8, the base case of the assumption-scenario is introduced. From this base case, the first estimate is made of the magnitude of the interaction. The base case (assumption-scenario = 1E, 2B, 3B, 4B, 5B, 6B, 7A.) is run through the model, as described in Chapter 4. Herein, the Grebbedijk case is still used for the input parameters. For the base case, a sliding plane that enters the levee in the crest and reaches the interface between the blanket and sand layer was forced in D-Geo stability as described in Section 4.3. This resulted in a sliding plane with a factor of safety (FoS_s) of 0.53. The results of D-Geo stability for all used sliding planes are shown in Appendix C. The values of the characteristic point of the sliding plane are provided in Table D.2 in green writing. The sliding plane is displaced to form the remaining profile shown in the lower Figure in Figure 5.2, the values used in this calculation are also shown in Table D.2. Figure 5.2 presents the distribution of the FoS-values of uplift along the remaining profile. The exit point location is defined as the location of the

lowest FoS_u-value, which for the base case is at the end of the berm. The FoS-values of heave and piping are determined at this exit location.
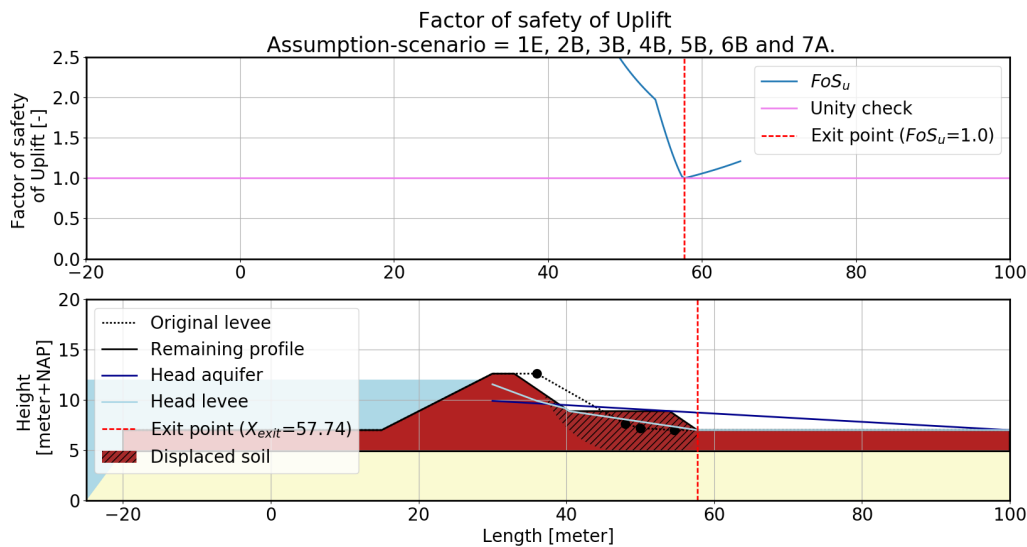
Figure 5.2: Factor of safety of uplift of the remaining profile, base case (assumption-scenario = 1E, 2B, 3B, 4B, 5B, 6B, 7A.)

Table 5.3 presents the results of this computation and the difference shown as the original FoS-values subtracted from the FoS-values of the base case. This difference is the indication for the interaction. For the base case, the sub-mechanism uplift experiences the most prominent change due to the SI (0.07). After this, piping experiences the most difference (0.03) and finally heave experiences a tiny difference (0.01). All three differences are positive, which indicates a positive interaction.

Table 5.3: Results for Grebbedijk base case (Original, remaining profile (assumption-scenario = 1E, 2B, 3B, 4B, 5B, 6B, 7A.))

Factor of safety	Original case	Value $[-]$	Remaining profile	Value $[-]$	Difference (Δ)	Value $[-]$
Uplift	$FoS_{u,original}(X_{exit})$	0.93	$FoS_u(X_{exit})$	1.00	ΔFoS_u	0.07
Heave	$FoS_{h,original}(X_{exit})$	0.36	$FoS_h(X_{exit})$	0.37	ΔFoS_h	0.01
Piping	$FoS_{p,original}(X_{exit})$	0.65	$FoS_p(X_{exit})$	0.68	ΔFoS_p	0.03
BEP	$FoS_{BEP,original}(X_{exit})$	0.93	$FoS_{BEP}(X_{exit})$	1.00	ΔFoS_{BEP}	0.07

If these numbers are translated back to what happens in the remaining profile compared to the original profile, it is noticed that the exit point location shifts 3.16 m more land-inward. The blanket layer is undisturbed at this new exit point location and is the same as in the original profile. However, in the original profile, the exit point was located closer to the river. Therefore, the head difference is smaller at the remaining profile exit point location compared to the head difference in the original profile exit point. Due to this smaller head difference ($\phi(X_{exit}) - h_p(X_{exit})$), there is a difference in the uplift FoS-value and in the heave FoS-value. The difference in the piping FoS-value can be assigned to the increase in seepage length ($L_{seepage}$) which is again caused by the shift due to the SI in the exit point location because the other values in the factor of safety equation of piping do not change compared to the original situation. This way of interaction is often seen in the upcoming assumption-scenarios results, most (about two-thirds) of the interactions found, occur in this form.

5.3. Assumption-scenarios

In the previous section, the interaction of SI to BEP was elaborated using the base case. This base case (1E, 2B, 3B, 4B, 5B, 6B, 7A.) is just one assumption-scenario. However, the consequences of the assumptions made

in the assumption-steps on the interaction are also relevant. Appendix D elaborates upon several (17) of the 2916 scenarios to describe in detail how interaction can take place in these scenarios.

In this section, all the interaction from SI to BEP is examined for all 2916 scenarios through the use of boxplots. The summary of how the assumption scenario codes work can be found in section 4.9, it is useful to keep this page near when reading this chapter. The first section shows the summary of the results for the three sub-mechanisms and the combined effect of these three mechanisms. The Subsections 5.3.2 to 5.3.5 will go into more detail on which scenarios steps have the most influence on the factor of safety (of combined BEP, uplift, heave and piping respectively). For this purpose, the scenarios are regrouped into groups in which one scenario step option (for example 5A) is fixed. This regrouping leads to different sample sizes with only scenarios including the chosen scenario-option of which a new boxplot is created, the corresponding values Tables (minimum, median and maximum) can be found in Appendix E.2.

5.3.1. Interaction of combined BEP, piping, heave and uplift

Figure 5.3 shows boxplots, which indicate the degree of interaction from SI to BEP for all scenarios. These boxplots show the difference in the safety factor for uplift, heave, piping and BEP between the remaining profile and the original situation of the Grebbedijk. A boxplot has the following features:

- The median value (second quartile): Orange vertical line
- Interquartile range (50% of the data, between the first quartile and the third quartile): Black rectangle
- Data below the first quartile and above the third quartile: Whiskers
- Outliers: Black markers

Because a safety factor cannot be lower than 0.0, the difference in safety factor between a scenario and the original situation (ΔFoS) is bounded by the safety factor of the scenario and that of the original situation, according to $-FoS_{x,original} \leq \Delta FoS_x \leq FoS_x$, where x is one of the failure (sub-)mechanisms (combined BEP, uplift, heave or piping). The original safety factors are presented in Table 5.1.
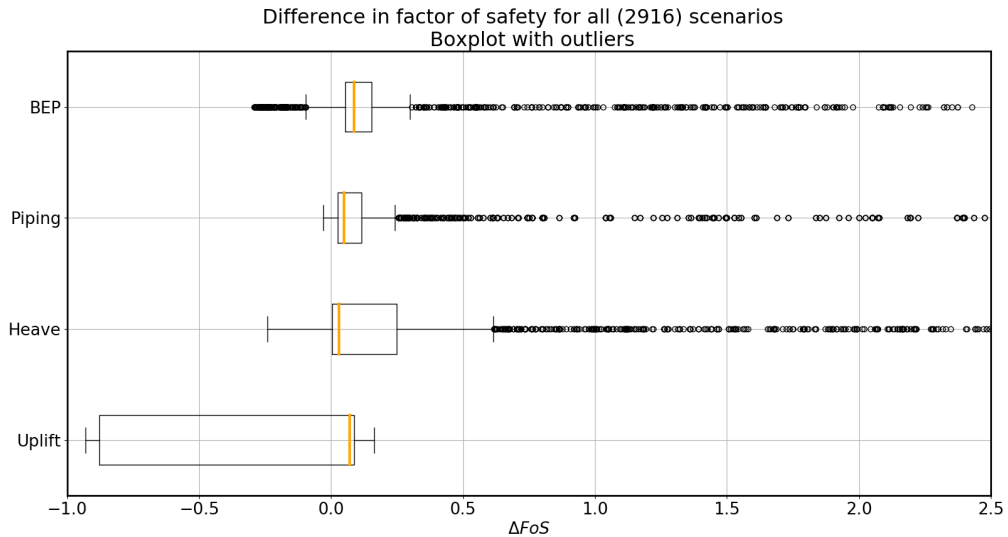
Figure 5.3: The range in the differences in FoS between combined BEP, piping, heave and uplift of the remaining profile and the original situation for all 2916 scenarios. The $FoS_{original}(X_{exit})$ for uplift, heave, piping and combined BEP are 0.93, 0.36, 0.65 and 0.93 respectively.

Figure 5.3 shows that the degree of interaction for combined BEP is between -0.10 and 0.30 (excluding outliers) and between -0.29 and 442,500 (including outliers). This is an indication of how extensive the interaction can be from SI to BEP. In more than three-quarters of the scenarios a positive interaction occurs.

Interestingly, a relatively large fraction of the scenarios lead to a negative interaction for uplift, while only a small fraction gives a negative interaction for heave and piping. Many negative interactions for uplift stem from scenarios that contain assumption-option 5A. This option assumes that rupture automatically occurs in the remoulded soil, and a large crack appears. Therefore, the uplift mechanism is skipped, and FoS_u is set to 0.0. This effect is further elaborated upon in Sections 5.3.2 and 5.3.5.

The majority of scenarios lead to a positive interaction for heave because the exit point is either located at the end of the berm, where the head difference is smaller, or in the berm, where the blanket layer is thicker. This is further elaborated upon in Section 5.3.3. Because both optional exit point locations increase the seepage path (either in the vertical or horizontal direction), the interaction for piping is also predominantly positive. This is explained in Section 5.3.4.

The majority of the positive interactions for heave and piping correspond to the scenarios where the interaction for uplift is negative (the scenarios which contain 5A), which is explained in Sections 5.3.3 and 5.3.4. Because the highest safety factor of the three sub-mechanisms is decisive in the combined BEP mechanism, ΔFoS_{BEP} is also positive for the majority of the scenarios.

5.3.2. Interaction of uplift

This section gives a detailed look at the sensitivity of the uplift mechanism for which the boxplot from Figure 5.4 and Table E.2 are used. In the boxplot, the scenarios are regrouped into groups that contain a given scenario-option. For example, the boxplot at 1A has a group size of 486 scenarios and only contains scenarios which include scenario-option 1A. This regrouping allows the main drivers of the interaction for uplift to be identified. The group size is shown on the right side of the Figure, and the fixed scenario-option is shown on the left.
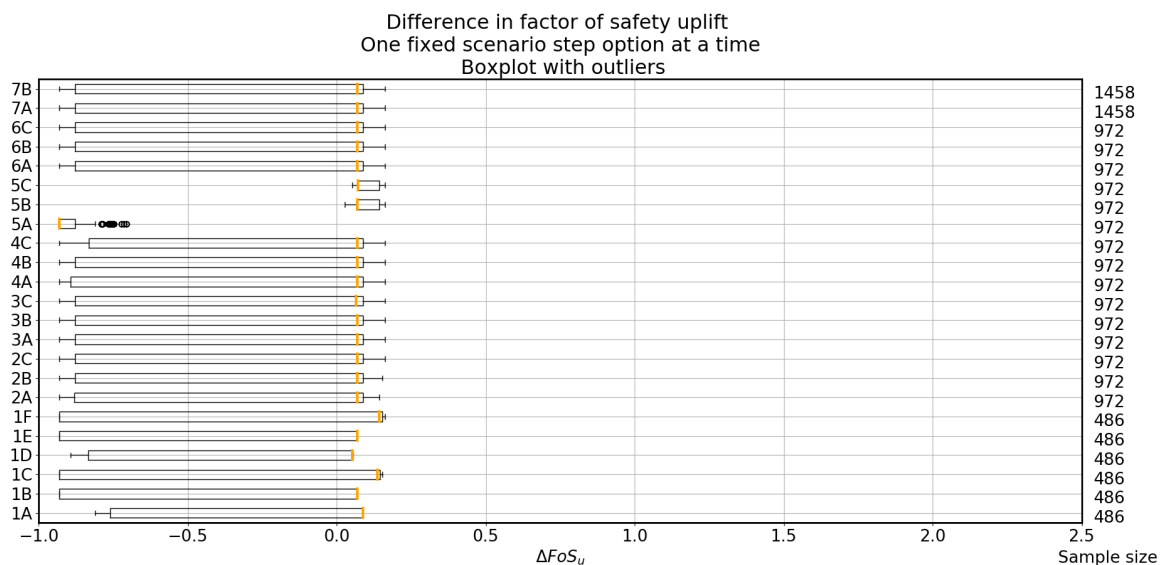
Figure 5.4: The degree of interaction for uplift with fixed scenario-options. The $FoS_{original}(X_{exit})$ for uplift is 0.93.

Most striking is the difference in the boxplots of scenario-options 5A, 5B and 5C. This clearly indicates that the negative interactions for uplift arise from assumption 5A. In this option, it is assumed that the remoulded soil in the berm offers no resistance due to cracks in the soil. When there is no intact layer left in the berm, uplift occurs (FoS_u = 0.0, and therefore ΔFoS_u = -0.93). This is illustrated in one of the worst-case scenario for uplift is 1B, 2A, 3A, 4A, 5A, 6A ,7A, in which only step 1 and 5 affect the minimum, see Table 5.4 and Figure 5.5. The other steps do not influence this most negative interaction. In this scenario, it can be seen that first uplift was the leading mechanism (It had the highest safety factor of the three sub-mechanisms) and that after the displacement piping became the leading mechanism. As a result, the combined BEP has less interaction (-0.26) than the uplift mechanism (-0.93).

Table 5.4: Safety factors for the worst-case interaction for uplift (assumption-scenario: 1B, 2A, 3A, 4A, 5A, 6A, 7A.)

(Sub-)mechanism	$FoS(X_{exit})$	$FoS_{original}(X_{exit})$	ΔFoS
Uplift	0	0.93	-0.93
Heave	0.16	0.36	-0.2
Piping	0.67	0.65	0.02
combined BEP	0.67	0.93	-0.26
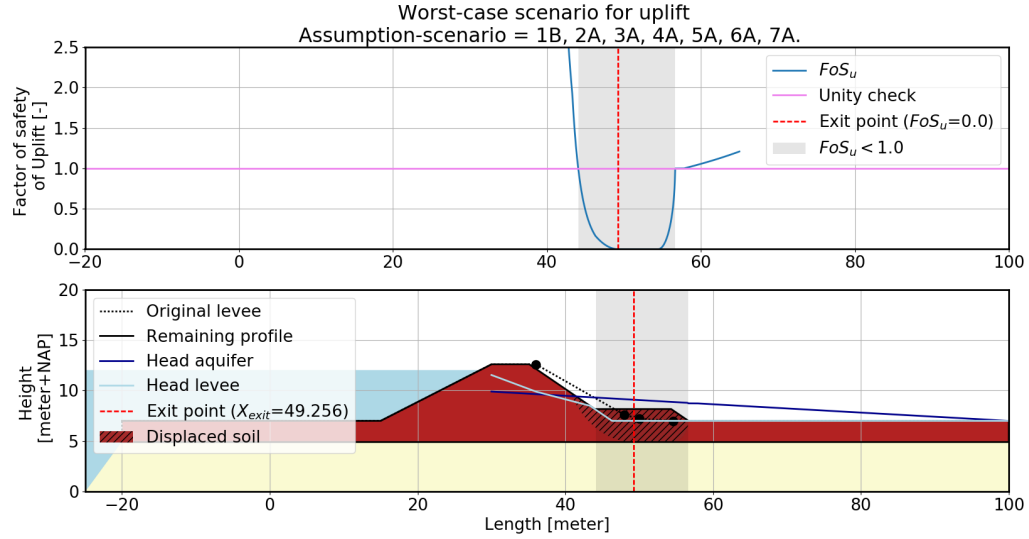
Figure 5.5: Worst-case interaction for uplift (assumption-scenario: 1B, 2A, 3A, 4A, 5A, 6A, 7A.)

Because the berm offers resistance in scenario-options 5B and 5C, even more, resistance than the original case without SI, ΔFoS_u is positive for scenarios including these steps. This also explains why the majority of ΔFoS for all other scenario-options is positive (the median for every option is positive, indicated by the orange line): Two-thirds of all scenarios contain either 5B or 5C and, therefore, have no negative interaction for uplift.

One of the best-case scenario for uplift is 1F, 2C, 3A, 4A, 5B, 6A ,7A in which only changes in assumption-steps 1, 2 and 5 decrease the maximum, see Table 5.5 and Figure 5.6. This best-case scenario for uplift experiences a similar interaction as described in the base-case only with a slightly larger sliding plane, which enlarges the positive effect. What stands out in the maximums in Table E.3 and can also be seen in Figure 5.4 is that step 1, 2 and 5 affect the maximum. The other steps do not influence the most positive interaction. This best-case for uplift has experienced a large displacement. In the case of combined BEP, this situation would be an improvement on the original; only it could be more prone to other failure mechanisms (e.g. overtopping).

Table 5.5: Safety factors for the best-case interaction for uplift (assumption-scenario: 1F, 2C, 3A, 4A, 5B, 6A, 7A.)

(Sub-)mechanism	$FoS(X_{exit})$	$FoS_{original}(X_{exit})$	ΔFoS
Uplift	1.09	0.93	0.16
Heave	0.4	0.36	0.04
Piping	0.71	0.65	0.06
combined BEP	1.09	0.93	0.16
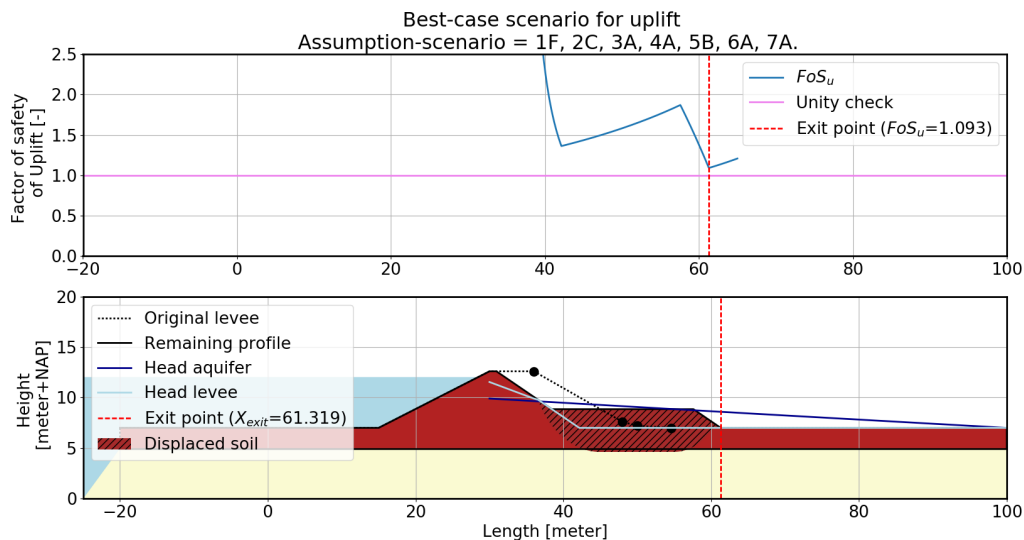
Figure 5.6: Best-case interaction for uplift (assumption-scenario: 1F, 2C, 3A, 4A, 5B, 6A, 7A.)

The boxplots of step 1 (sliding plane location and shape) show that 1B, 1C, 1E and 1F reach to the maximum negative interaction, namely -0.93 because the safety factor for uplift in these scenarios is 0.0. This can be linked to the depth of the sliding plane: When the sliding plane reaches or perforates the blanket layer, it is assumed that there is no resistance against uplift for option 5A, automatically resulting in a safety factor of 0.0. For options 1A and 1D, there is a small intact layer that provides a small resistance against uplift leading to less negative interaction. The positive interaction side has a similar pattern, as seen in Section D. The right side of the boxplots of 1C and 1F contain the scenarios that include step 5B or 5C. These sliding planes perforate the blanket layer and are large. In those cases, the new exit point is located even more landward than all those of all other scenario-options for step 1. This leads to a decrease in load, hence a higher safety factor of uplift.

In the boxplots of assumption-options 4A, 4B and 4C (phreatic line in the berm), the scenarios that lead to positive interactions are similar to each other. However, the lower negative interactions show a gradual increase in the third quartile from option 4A to 4C. Only if the scenario includes option 5A, which leads to an exit point in the berm, step 4 makes a difference. In step 4C, the head difference is the smallest and, therefore, the boxplot of 4C has the highest first quartile of the three options.

Assumption-steps 6 (critical heave gradient) and 7 (seepage path) do not affect uplift. Therefore, they have no shift in the boxplot of the partial sample size compared to the boxplot of all scenarios. The boxplots within assumption-steps 2 and 3 slightly deviate from each other, but these deviations are insignificantly small.

5.3.3. Interaction of heave

In order to find the drivers behind the interaction with heave, the scenarios are regrouped. Figure 5.7 shows how the difference in heave is distributed when one scenario step is fixed. The corresponding values can be found in Appendix E.2. The first thing that stands out in this Figure is a larger number of outliers. This is mainly caused by the scenarios in which step option 5A (large crack) occurs. This can be seen in the boxplot of step 5A, because it is the widest.
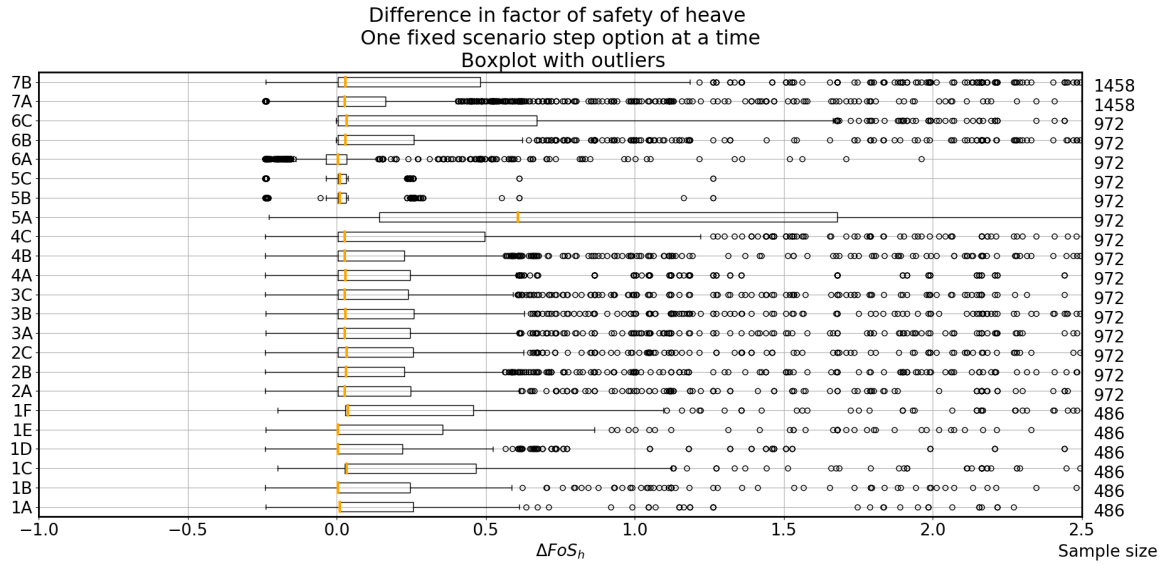
Figure 5.7: The degree of interaction for heave with fixed scenario-options. The $FoS_{original}(X_{exit})$ for heave is 0.36.

What is also striking about this boxplots is that all scenario steps give different size boxplots. From this, it can be concluded that all steps have a certain influence on the interaction with heave. This makes combinations of several scenario-options important.

For example step 6 (critical heave gradient), only option A can lead to negative interaction. This means that only scenarios that contain assumption-option 6A can have a negative interaction. Options B and C both provide only positive interactions, where the range of option C is greater than that of option B. In 6A-scenarios, the critical heave gradient (i_{ch}) is set to a value 0.1. This critical heave gradient could occur if the porosity of the remoulded soil increases. This only affects the interaction if the exit point is located in the remoulded soil. This is the case in 5A-scenarios (exit point in the berm), although this also happens in the exceptional case where the exit point is located a little bit before the end of the berm. For example, one of the worst-case scenarios for heave shown in Figure 5.8, where only 50 cm of blanket layer soil is remoulded.

Table 5.6: Safety factors for the worst-case interaction for heave (assumption-scenario: 1B, 2C, 3C, 4A, 5C, 6A, 7A.)

(Sub-)mechanism	$FoS(X_{exit})$	$FoS_{original}(X_{exit})$	ΔFoS
Uplift	0.98	0.93	0.05
Heave	0.12	0.36	-0.24
Piping	0.67	0.65	0.02
combined BEP	0.98	0.93	0.05
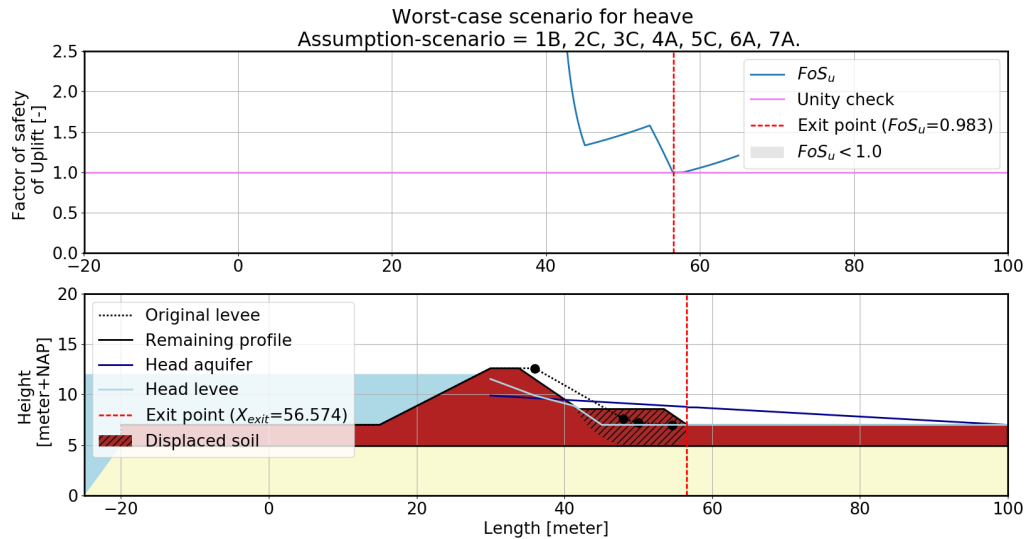
Figure 5.8: Worst-case interaction for heave (assumption-scenario: 1B, 2C, 3C, 4A, 5C, 6A, 7A.)

Option 7B (alternative seepage path) gives a wide range in the interaction for heave. 7B-scenarios only give a change in safety factor if they are combined with assumption-option 5A. Here, the seepage path is elongated and follows the curve of the sliding plane, which leads to higher safety factors. In this model, this alternative path is forced at each sliding plane. However, assuming 5A, in cases where the blanket is perforated (1B, 1C, 1E and 1F), a large crack would have occurred. This means that the alternative path becomes more unlikely.

In case of a 5A-scenario (large crack), the combination with step 4 (phreatic line in the berm) is important. In 5A, the exit point is located in the berm. At this location, the head difference is relevant. In scenarios that contain option 4A, there is a more significant head difference than scenarios that contain option 4C. In case of a scenario with 5A and 4C, the head difference approaches 0 m. This means that i_h approaches zero. This implies that FoS_h would become infinitely large, see equation 4.18, and that ΔFoS_h would also become infinitely large. Table E.3 shows that indeed, only scenarios with 6A give negative interactions and that the scenarios with 5A and 4C give the most prominent positive interactions. So, the worst-case interaction for heave includes options 6A and not options 1C or 1F and 5A. The choice of steps 2, 3, 4 does not influence the worst-case scenario. The best-case scenario for heave contains steps 1E, 2C, 3B, 4C, 5A, 6C and 7B.

Table 5.7: Safety factors for the best-case interaction for heave (assumption-scenario: 1E, 2C, 3B, 4C, 5A, 6C, 7B.)

(Sub-)mechanism	$FoS(X_{exit})$	$FoS_{original}(X_{exit})$	ΔFoS
Uplift	0.0	0.93	-0.93
Heave	442500	0.36	442500
Piping	16.78	0.65	16.13
BEP	442500	0.93	442500

The best-case scenario is shown in Table 5.7, and Figure 5.9. The head difference in the berm is very small (due to option 4C), but because the sliding plane in this scenario does perforate the blanket layer (option 1E), there is still an exit point in the berm due to option 5A, as seen in Figure 5.9. Because the head difference is so small, the safety factor for piping and heave will be very high.
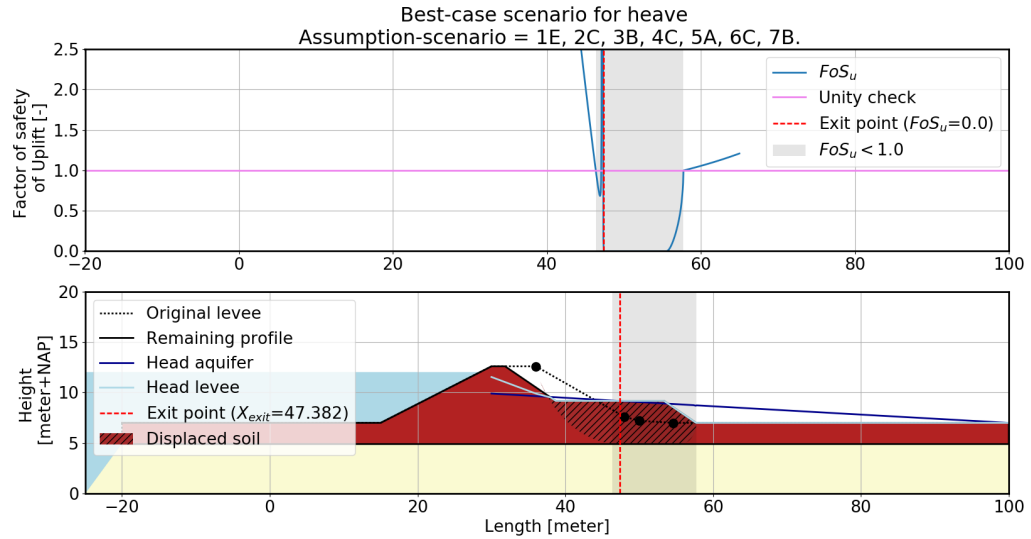
Figure 5.9: Best-case interaction for heave (assumption-scenario: 1E, 2C, 3B, 4C, 5A, 6C, 7B.)

5.3.4. Interaction of piping

Figure 5.10 shows the difference in the factor of safety of piping for the scenario groups with one fixed assumption-option, the supplement table with the corresponding values can be found in E.2. The first thing to notice in Figure 5.10 is that the interaction for sub-mechanism piping is mainly positive and that there are a lot of positive outliers.

Figure 5.10: The degree of interaction for piping with fixed scenario-options. The $FoS_{original}(X_{exit})$ for piping is 0.65.

Step 6 (critical heave gradient) does not influence the interaction of piping and therefore, the options 6A, 6B and 6C show the same boxplot. 7B-scenarios (alternative seepage path) are always positive and only make a difference when the exit point is located in the remoulded soil. The alternative seepage path is in all scenarios longer than the straight up through the blanket layer path. A lot of the higher outliers stem from 7B-scenarios.

Step 5A (large cracks) has a wide range, and this could be explained by the fact that the ratio between the

thickness of the blanket layer and the seepage length is essential to the occurrence of piping. In step 5A the exit point location is located in the berm, so there is a thicker blanket layer than in the original situation but also a shorter seepage length because the exit point is closer to the river. Depending on the ratio between these two and the way it is combined with the other step can lead to this widespread. For example, a scenario including 5A combined with 4C (high phreatic line in the berm) en 7B (based on Table E.4), in this scenario the exit point is located in the berm (due to 5A). The head difference is minimal through 4C, and the seepage path is prolonged due to 7B. This scenario has thus larger safety factor and a larger positive interaction. The positive interactions of step 4 increase in size, which can be explained by the decreasing difference in aquifer head. 4A-scenarios (low phreatic line) contain negative interactions for piping as opposed to 4B and 4C scenarios.

What is remarkable is that the smallest sliding plane (1A-scenarios) contains the most negative interactions compared to the other step 1 options, what causes this can be seen in the worst-case scenario. The worst-case scenario of piping includes 1A, 2A, 4A, 7A, and either 5B or 5C. The choice for scenario-step 3 and 6 are irrelevant for the safety factor of the worst-case scenario. The uplift distribution and remaining profile of this worst-case scenario are shown in Figure 5.11.

Table 5.8: Safety factors for the worst-case interaction for piping (assumption-scenario: 1A, 2A, 3B, 4A, 5B, 6B, 7A.)

(Sub-)mechanism	$FoS(X_{exit})$	$FoS_{original}(X_{exit})$	ΔFoS
Uplift	0.96	0.93	0.03
Heave	0.39	0.36	0.03
Piping	0.62	0.65	-0.03
combined BEP	0.96	0.93	0.03
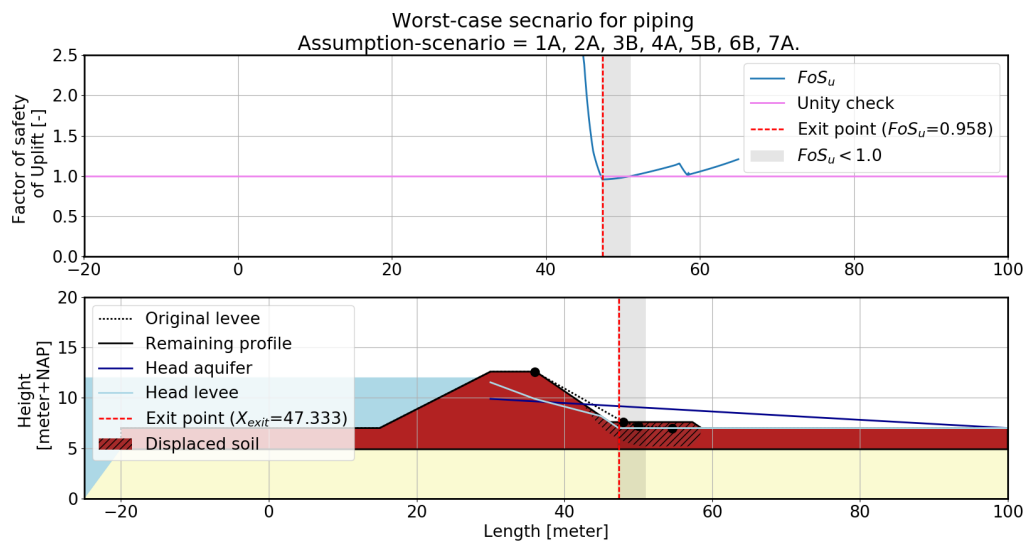
Figure 5.11: Worst-case interaction for piping (assumption-scenario: 1A, 2A, 3B, 4A, 5B, 6B, 7A.)

In this scenario, there is a small sliding plane, which has led to the formation of a thin berm. In addition, it is assumed that there is a low phreatic line in the berm. This gives a more substantial head difference at the location of the berm, and in this case also larger than the original head difference at the location of the berm. At the kink between the new slope and the beginning of the berm, the thickness of the blanket layer is smaller than in the original situation. This, together with an increased head difference, leads to possible uplift at this location. This is an exceptional case where the exit point is located in the berm without the remoulded soil giving no more resistance against uplift. In this case, the exit point is closer to the river than in the original situation and the increase in the blanket layer is small at the beginning of the berm is not even an increase but a decrease compared with the original situation. Therefore, there is a negative interaction possible, although in this case, it is minimal.

Table 5.9: Safety factors for the best-case interaction for piping (assumption-scenario: 1E, 2C, 3B, 4C, 5A, 6A, 7B.)

(Sub-)mechanism	$FoS(X_{exit})$	$FoS_{original}(X_{exit})$	ΔFoS
Uplift	0	0.93	-0.93
Heave	88500	0.36	88500
Piping	16.78	0.65	16.13
BEP	88500	0.93	88500
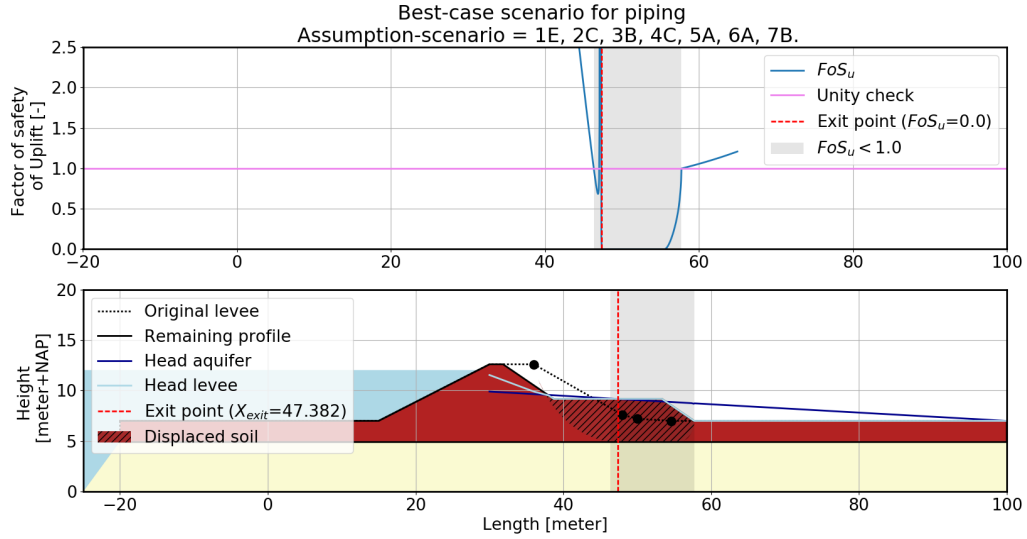
Figure 5.12: Best-case interaction for piping (assumption-scenario: 1E, 2C, 3B, 4C, 5A, 6A, 7B.)

The best-case interaction for piping is shown in Figure 5.12 and Table 5.9. This scenario is similar to the best-case interaction for heave, so again, the exit point is located in the berm, and there is a small head difference. For piping, it is important that this scenario contains assumption-option 7B and therefore follows the extended seepage path, which leads to a high safety factor for piping and thus a large positive interaction for piping. Although piping gives a great positive interaction, it is not the leading mechanism for combined BEP. This is caused by an even higher interaction for heave, in which heave also follows this alternative seepage path.

5.3.5. Interaction of combined backward erosion piping

Figure 5.13 presents the boxplots of the degree of interaction of combined BEP for fixed scenario groups, including a particular scenario-option, Table 5.10 shows the corresponding values. The combined BEP boxplot shows the combined effect of the three sub-mechanisms (uplift, heave and piping) as the difference in factors of safety BEP (ΔFoS_{BEP}). The first thing to notice is that none of the interactions for BEP reaches the maximum negative interaction for BEP (-0.93). This is due to combined BEP being determined by taking the maximum of the three safety factors of sub-mechanism. This ensures that if one of the mechanisms experiences a large negative interaction, the other mechanisms partially compensate for this. For example assumption-scenario 1B, 2A, 3A, 4A, 5A, 6A, 7A (the worst-case situation of uplift), in this scenario uplift has the maximum negative interaction but piping experiences a small positive interaction and has the highest safety factor of the three sub-mechanisms for this scenario and is, therefore, the leading mechanism for the interaction in the combined BEP.
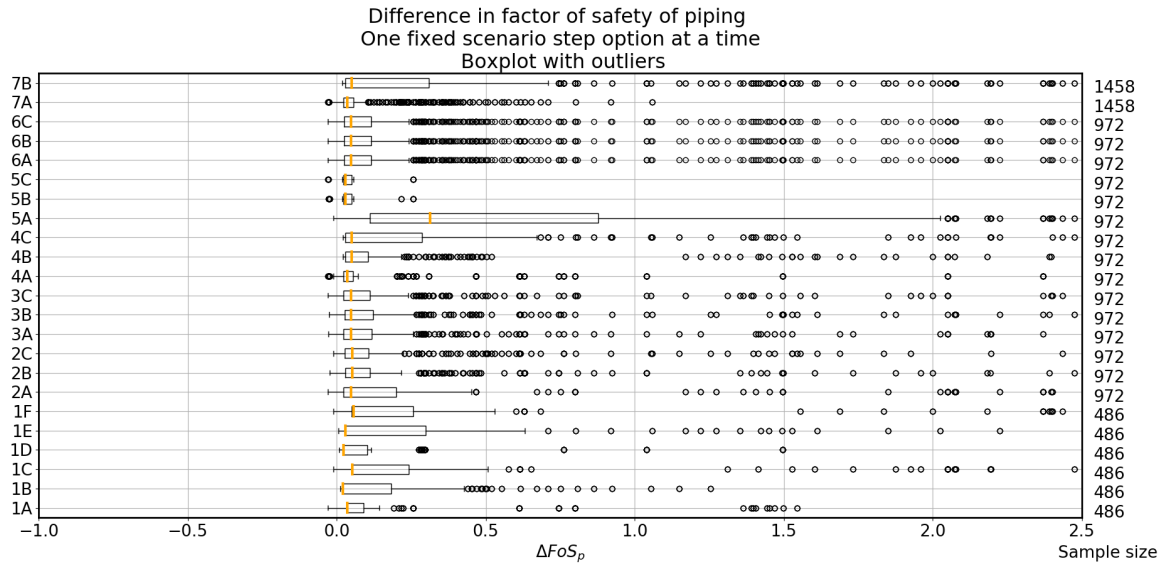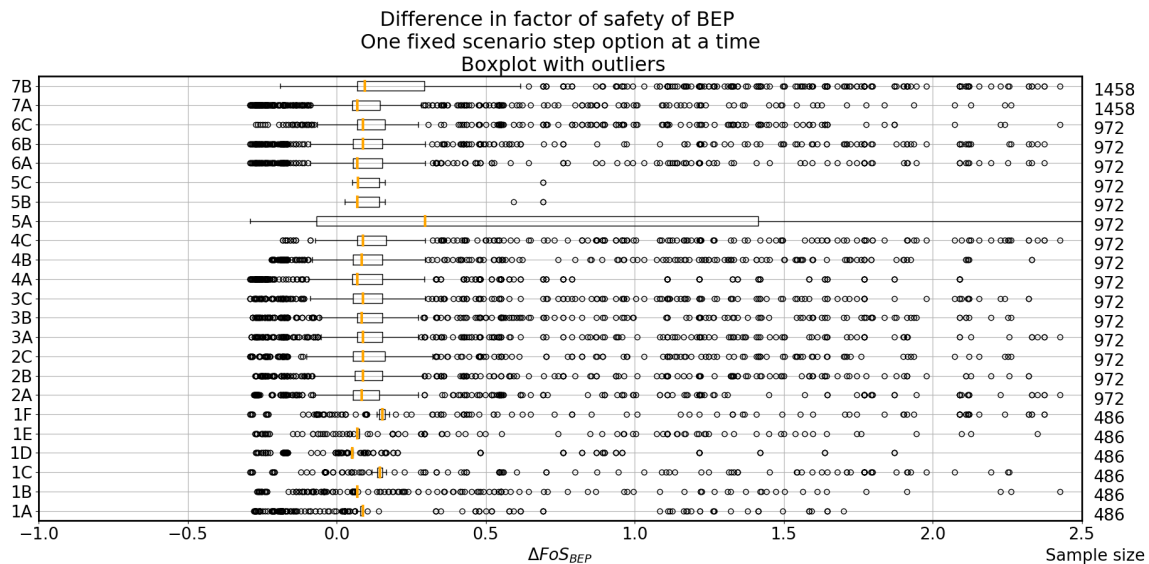
Figure 5.13: The degree of interaction for BEP with fixed scenario-options. The $FoS_{original}(X_{exit})$ for BEP is 0.93.

Striking is that only the first quartile of 5A (large crack) is negative and that the scenarios including 5B or 5C are all positive interactions. Assumption-option 5A gives the biggest range in the degree of interaction of combined BEP. By looking at the all boxplots in Figure 5.13, it seems like option 5A provides the outliers for the other steps. This is an indication that, if it can be precluded that large cracks may occur after sliding, the interaction is mainly positive. Where only negative interaction can occur with a deep but very small sliding plane, resulting in a very thin berm and the exit point can still relocate into this berm. This is an important finding and will, therefore, be further explored in Section 5.4.5.

The options in step 1 (sliding plane location and shape) have a very narrow boxplot. This means that most of the scenarios including one step 1 option are close to each other in terms of value except for a few outliers. This would mean that if 5A provides for the outliers that the most important other factor is the size of the sliding plane. This hypothesis is also tested in the sensitivity analysis.
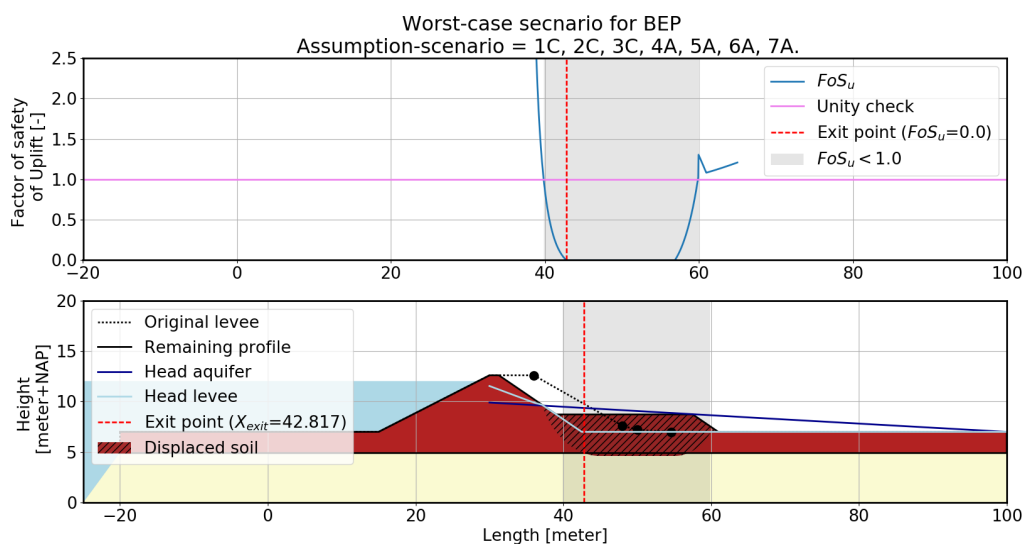
Figure 5.14: Worst-case interaction (assumption-scenario: 1C, 2C, 3C, 4A, 5A, 6A, 7A.)

The worst-case negative interaction occurs in scenarios which include 1C or 1F, 2C, 3C, 4A, 5A, 6A and 7A. In this scenario, the sliding plane passes through the blanket layer, and it is assumed that this blanket layer is ruptured (due to step 1 option C or F). Option 2C (amount of lowering) and 3C (volume change) lead to the largest berm that is possible within the scenarios. The head difference in the berm is largest with option 4A (low phreatic line), and due to 5A (large crack) the exit point is located in the berm as shown in Figure 5.14. The option 6A gives low resistance against heave and 7A is the shortest seepage path.

Table 5.10: Safety factors for the worst-case interaction (assumption-scenario: 1C, 2C, 3C, 4A, 5A, 6A, 7A.)

(Sub-)mechanism	$FoS(X_{exit})$	$FoS_{original}(X_{exit})$	ΔFoS
Uplift	0	0.93	-0.93
Heave	0.16	0.36	-0.2
Piping	0.64	0.65	-0.01
combined BEP	0.64	0.93	-0.29

In the original case, the sub-mechanism uplift is the leading mechanism for the occurrence of combined BEP. In this scenario, the leading sub-mechanism is piping, as seen in Table 5.10. This is due to the fact that the uplift mechanism is skipped because the sliding plane perforates the blanket layer and because FoS_h decreases. This reduction is caused by the low resistance due to 6A and by the higher head difference due to 4A. The piping mechanism itself experiences only a very small negative interaction despite this change in the situation. This is probably because the ratio between the thickness of the blanket layer and the horizontal seepage length compensates each other. This is a good example where the change of the leading sub-mechanism limits the interaction to only -0.29 instead of -0.93, which it would have been if the uplift had remained the leading sub-mechanism.

Table 5.11: Safety factors for the best-case interaction (assumption-scenario: 1E, 2C, 3B, 4C, 5A, 6C, 7B.)

(Sub-)mechanism	$FoS(X_{exit})$	$FoS_{original}(X_{exit})$	ΔFoS
Uplift	0.0	0.93	-0.93
Heave	442500.0	0.36	442499.64
Piping	16.78	0.65	16.13
BEP	442500.0	0.93	442499.07
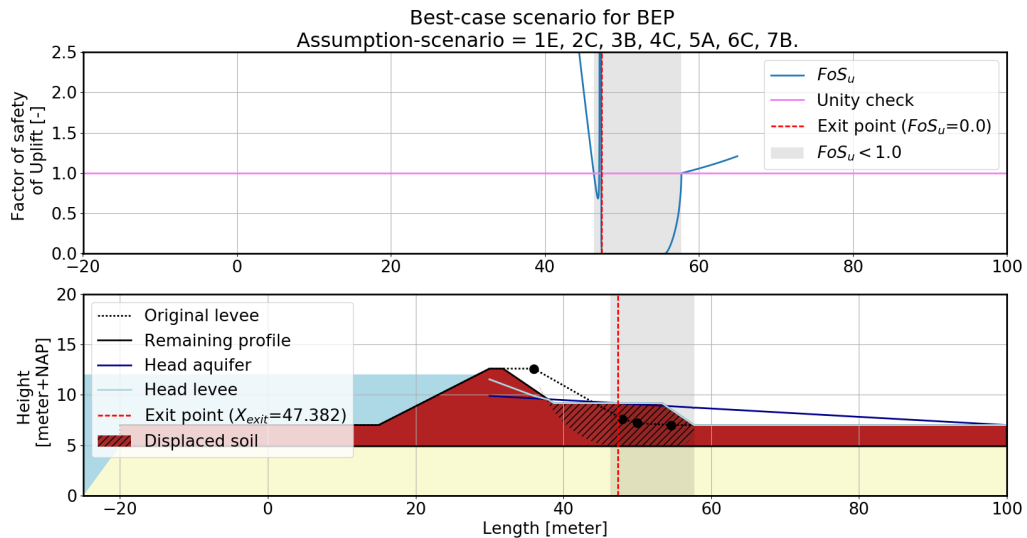
Figure 5.15: Best-case interaction (assumption-scenario: 1E, 2C, 3B, 4C, 5A, 6C, 7B.)

The best-case scenario for BEP is 1E, 2C, 3B, 4C, 5A, 6C, 7B. In this scenario, the exit point is located in the berm, the head difference over the blanket layer is very small, it has a long seepage path (7B) and a high critical heave gradient.

5.3.6. Conclusions

Based on the results of this analysis, the following conclusions can be drawn:

- The degree of interaction for combined BEP is between -0.29 and +442,500 (including outliers), as shown in Figure 5.13. In more than three-quarters of the scenarios, a positive interaction for combined BEP occurs. None of the interactions for BEP reaches the maximum negative interaction for BEP (-0.93), because combined BEP is determined by taking the maximum of the three safety factors of its sub-mechanisms, which allows the sub-mechanisms to compensate for each other. The most prominent assumption that affects the interaction of combined BEP is assumption-option 5A (large cracks), which provides the largest negative interactions and simultaneously also the largest positive interactions. In this option, it is assumed that the remoulded soil in the berm offers no resistance due to large cracks in the soil. The second most important factor is the size of the sliding plane (assumption-step 1). The six options provide the rest of the range of interaction.
- The majority of the positive interactions for heave and piping correspond to the scenarios where the interaction for uplift is negative (the scenarios which contain 5A (large cracks)).
- The degree of interaction for uplift is between -0.93 and +0.16, and a large fraction of the scenarios have a negative interaction for uplift. This negative fraction arises from assumption-option 5A (large cracks in remoulded soil). When there is no intact layer left in the berm, rupture occurs ($FoS_u = 0.0$, and therefore $\Delta FoS_u = -0.93$). Because the berm offers resistance in scenario-options 5B and 5C, even more resistance than the original case without SI, ΔFoS_u is positive. In addition, in 5A-scenarios assumption-step 1 gets the maximum negative interaction for uplift in the case when the sliding plane perforates the blanket layer. If the sliding plane does not perforate the blanket layer, this negative interaction will not give the maximum possible interaction. In the case of 5C and 5B-scenarios, larger sliding planes have a more positive interaction than smaller sliding planes, because the size of the slip plane is correlated to the size of the berm. Only if the scenario includes option 5A, which leads to an exit point in the berm, step 4 makes a difference.
- The degree of interaction for heave is between -0.24 and +442500 with outliers, and the majority of the scenarios leads to positive interaction. All assumption-steps influence heave, therefore combinations of several scenario-options are important for the interaction for heave (as seen in Figure 5.7). Only 6A-scenarios give negative interactions. This step only gives an effect when the exit point is located in the remoulded soil. This is usually the case for 5A-scenarios but can also occur in 5B- and 5C-scenarios. A scenario containing the combination 5A and 4C will lead to the maximum positive interaction for Heave
- The degree of interaction for piping is between -0.03 and +16.13, and the interaction is predominately positive. Scenarios including option 5A (large cracks) give a wide range of interaction because the location of the exit point is located in the berm and closer to the river than in the original situation. Depending on the ratio between the changed thickness of the blanket layer, the changed horizontal seepage length and the combination with the other assumption-steps, especially step 4, the interaction for piping is positive or just negative. Assumption-option 7B (the alternative seepage path) leads to only positive interactions, and this is because the seepage path length is extended in this option. To get a negative interaction for piping, the assumption-scenario must contain 4A and 7A.
- Because a safety factor cannot be lower than 0.0, the limits of the interaction are always bounded by $-FoS_{x,original} \leq \Delta FoS_x \leq FoS_x$, where x is one of the failure (sub-)mechanisms (combined BEP, uplift, heave or piping).

Most common interaction situation description
The assumption scenarios studied have shown that in many cases, a similar interaction takes place. Namely, that sliding occurs, that does not lead to failure but does form a berm. The weight of this extra soil causes the exit point to move further inland. This displacement leads to lower head differences and a longer seepage length. All this has a positive effect on remaining profile safety factor of BEP, and thus a positive interaction.

Worst-case interaction situation description

The modelled most negative interaction from SI to BEP (ΔFoS_{BEP} = -0.29) contains a large sliding plane that perforates the blanket layer. This results in a large berm of remoulded soil that contains large cracks, which ensures the occurrence of uplift. The exit point after sliding is located in the largest of these cracks, while the original exit point is located at the toe of the levee. The phreatic line in the berm is at polder level. The aquifer head does not reach the limit potential at the exit point, because the blanket layer, including the remoulded soil, is thick. Even though the blanket layer thickness has increased, the occurrence of heave increases, because the large cracks in the remoulded soil give a lower critical heave gradient than that of the original soil. The horizontal seepage path is short because the exit point after sliding is located closer to the river than the original case. Because the vertical seepage length has increased due to the presence of the berm, the occurrence of piping has not changed significantly. The degree of interaction results from the change of leading mechanism: While uplift was the leading mechanism in the original profile, piping determines the safety factor for combined BEP for the remaining profile. The difference in safety factor between these mechanisms defines the degree of interaction.

5.4. Sensitivity analysis

The previous Section described how sensitive the interaction is to the assumptions-scenarios. This Section looks at how sensitive the interaction is to changes in the input case. In Section 4.10 is written, which changes in the input case are considered and what has changed in these input case. In this Section, the sensitivity is assessed per input case using the sub-mechanisms uplift, heave and piping and their combined effect (combined BEP). This sensitivity analysis is conducted in order to assess whether the interaction can be applied in general or whether it should be considered on a case-by-case basis.

The sliding plane shapes of the different cases, which are determined with a D-Geo calculation, are shown in Appendix C.2. The detailed results of this analysis can be found in Appendix F. This appendix contains per input case:

- A figure of the original situation of the input case with uplift distribution;
- A figure for the base case with remaining profile and uplift distribution;
- A table with the results for uplift, heave, piping and the combined BEP of the original situation, the remaining profile base case and the interaction in the base case;
- The boxplots of the results for uplift, heave, piping and combined BEP;
- The boxplots of the results for one fixed scenario-option for uplift, heave, piping and combined BEP.

In order to compare all these results, the resulting boxplots of all the different input cases are analysed per uplift, heave, piping and combined BEP. These boxplots show the degree of interaction [%] from SI to BEP by comparing the original situation (case-dependent) with the corresponding remaining profile for the different assumption-scenarios. The boxplot shows the median value (orange line), the interquartile range which is 50% of the data (the 'box'), the data below the first quartile and above the third quartile (Whiskers) and the outliers (Black markers). The interaction is shown as a percentage to prevent the result from being dependent on the factor of safety of the original situation. However, it is essential to keep in mind what the original value for the BEP analysis is for the different cases; therefore, they can be found in Table 5.12.

Table 5.12: The original safety factors for the different input cases

Input case	$FoS_{u,original}$	$FoS_{h,original}$	$FoS_{p,original}$	$FoS_{BEP,original}$
Grebbedijk original case	0.93	0.36	0.65	0.93
Thin blanket layer	0.23	0.36	0.59	0.59
Thick blanket layer	3.07	1.12	0.99	3.07
No foreshore	0.66	0.36	0.38	0.66
Long foreshore	1.57	0.57	1.4	1.57
Wide crest and gentle slope	1.15	0.42	0.72	1.15
Triangular berm	0.93	0.36	0.65	0.93

5.4.1. Uplift

Figure 5.16 shows the boxplots for uplift of the different input cases: *Grebbendijk Original case, Thin blanket layer, Thick blanket layer, No foreshore, long foreshore, Wide crest and gentle slope*, and *Triangular berm*. What is immediately noticeable in this figure is that the range of the *Thin blanket layer* is the largest of all and that the boxplot of the input case *Thick blanket layer* is very narrow.
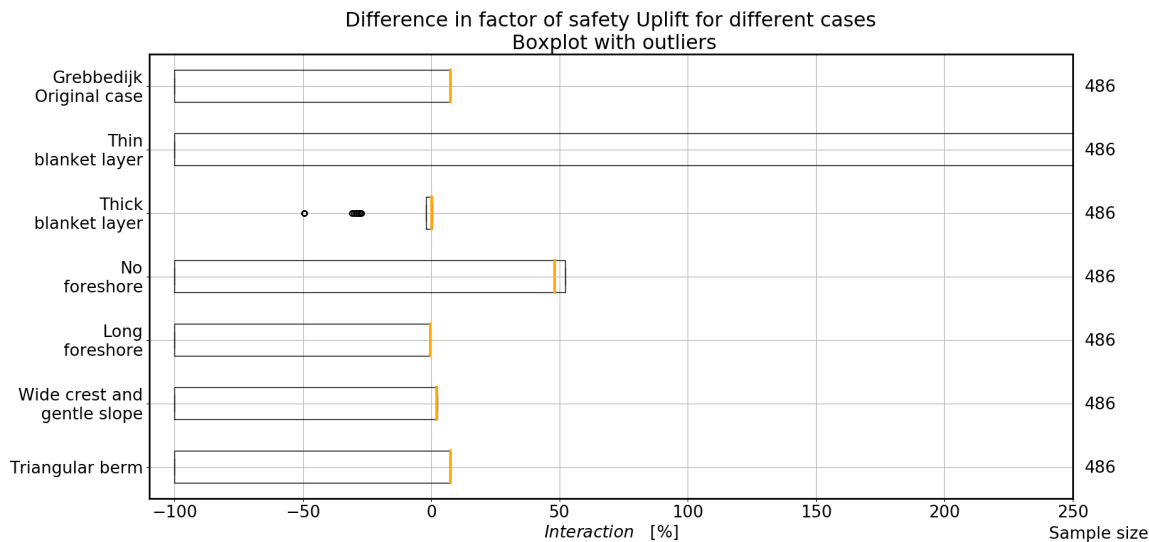
Figure 5.16: The range in the interaction of uplift for different cases with outliers.

With a thin blanket layer, the sliding plane perforates the blanket more easily than with a very thick blanket. Once the blanket layer has been perforated, the head in the aquifer ($\phi_{(}x)$) drops to its limit potential ($\phi_{limit}(x)$) for the remaining profile. When an uplift calculation is performed where the aquifer head is on the limit of the blanket layer, a safety factor of 1 will result from the calculations. In the case of the thin blanket layer, the original safety factor for uplift was 0.23, after the sliding plane perforating the blanket layer, this safety factor becomes 1, which is an increase of almost 500%. On the other hand, if an assumption-scenario, in this case, contains option 5A, the safety factor will go to zero, which is a minus 100% interaction.

The *Thick blanket layer* case gives a different kind of outcome to the other cases. This is because there is no scenario in which the blanket layer is fully perforated, as opposed to the other cases in which this does occur in some scenarios. Therefore, the interaction of the *Thick blanket layer* case does not reach the minus 100 %.

When comparing the *Grebbedijk Original case* to the *Triangular berm*, it is noticeable that they are the same for the uplift mechanism. In both cases, the place where the sliding plane perforates through the blanket layer is in the same place. For this location, by coincidence, the height of the berm is as high in the case of the triangular berm as in the case of a parallelogram berm.

Furthermore, it is known from Figure F.33 that two-thirds of the scenarios in a long foreshore do not interact and one-third provides minus one hundred percent interaction. For the situation with a wide crest and gentle slope, one-third of the scenarios have minus one hundred percent interaction, and two-thirds of the scenarios have a 2.6 percent positive interaction. This one-third, two-thirds ratio results from scenario-options 5A versus 5B and 5C and can be found in all results for uplift.

5.4.2. Heave

The box plots for all the different input case of the interaction with heave are given in Figure 5.17. What is immediately noticeable is that none of these cases reaches the maximum negative interaction of minus 100%.

The cases *Thin blanket layer, Thick blanket layer* and *No foreshore* have a more negative minimum interaction than the *Grebbendijk original case*. The *Thick blanket layer* case has a relatively small range compared to the other cases.

Figure 5.17: The range in the interaction of heave for different cases with outliers.

In the *Thin blanket layer* case large positive interaction for heave arise as a result of the drop in aquifer head caused by the rupture of the blanket layer due to sliding. For the 5A-scenarios, this drop leads to a smaller head difference at the exit point, which gives higher safety factors for heave.

The *Thick blanket layer* case has a small range because most of the assumptions-scenarios only give a small difference (5B and 5C-scenarios). Only approximately half of the blanket layer is affected by the sliding in all scenarios in this case, and only the remoulded soil can have a change in critical heave gradient. Thus, even if the entire resistance of the remoulded soil is zero, the safety factor cannot be lower than half of the original safety factor due to the thickness of the blanket layer and the sliding plane depth.

When comparing *Grebbendijk original case* with *Triangular berm* case, it can be seen that the *Triangular berm* has less negative interactions. In the *Grebbedijk original case*, the 5B- and 5C-scenarios also contain a negative interaction. This is not the case for the *Triangular berm* case. In the *Triangular berm*, the only negative interactions are caused by 5A-scenarios in combination with a low critical heave gradient (6A-scenarios). In the 5B and 5C scenarios, the exit point of the triangular berm is always outside the remoulded soil.

In all cases except *No foreshore*, three-quarters of the scenarios do not show any interaction or show a positive interaction. Figure F.27 compared to Figure F.6 shows that in the case of *No foreshore*, the scenarios including 5A and 4A exhibit more negative interaction than in the *Grebbendijk original case*. This is because 4A gives the biggest head difference when the exit point is in the berm (5A). This applies to both cases, only in the case of *No foreshore* the head differences are bigger due to the higher aquifer head due to the shorter foreshore.

5.4.3. Piping

Figure 5.18 displays the different boxplots for piping for the seven cases considered in the sensitivity analysis. The first thing that can be seen right away is that only the input cases, *No foreshore* gives negative interactions for piping. These negative interactions occur in the scenarios in which a small berm is formed, and the exit point location is in this berm. Subsequently, the seepage length is small, and the thickness of the blanket layer is small, so there is a lower resistance to piping than in their original situations.
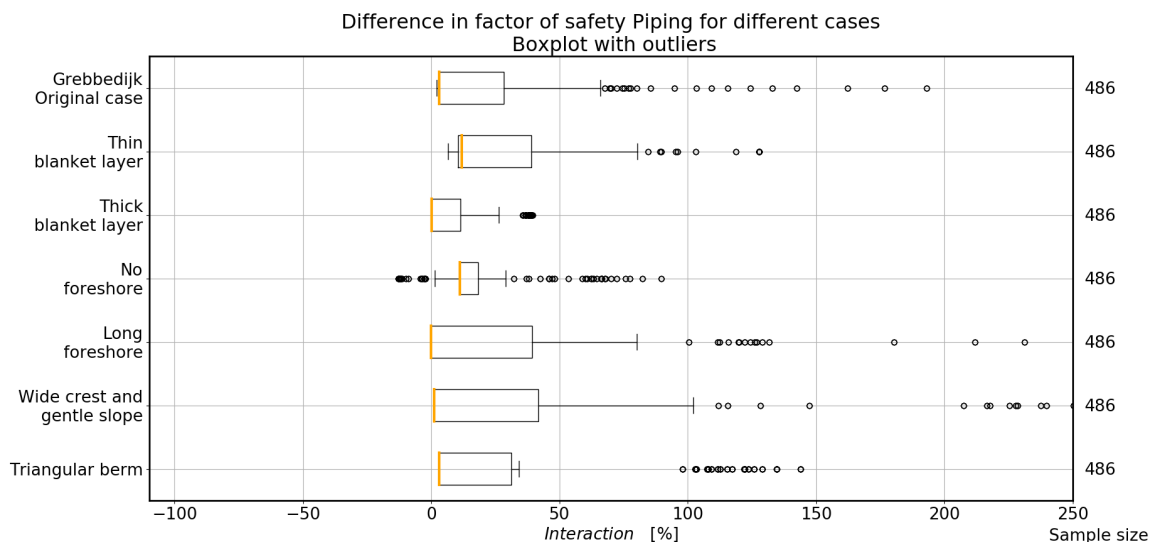
Figure 5.18: The range in interaction of piping for different cases with outliers.

In the case with a *Thick blanket layer*, the interaction is zero in approximately two thirds of the scenarios, the other one-third of the scenario it is positive, and the same applies to the case with a *long foreshore* (see Figures F.21 and F.35, fixed scenario steps 5B and C). In the scenarios including 5B and 5C, the berm ensures that the exit point is at approximately the same location as in the original situation of the cases, which leads to no interaction or a minimal interaction.

The cases *Grebbendijk original case, Thin blanket layer, Wide crest and gentle slope* and *Triangular berm* only experience positive interactions for piping.

In the *Thin blanket layer* case for 5B and 5C-scenarios, the exit point is at the end of the small berm, which means that the horizontal seepage length is longer than in the original situation. The head in the aquifer is reduced to the limit potential of the thin blanket layer due to the rupture of the blanket layer, which is caused by the depth of the sliding plane. This reduction results in a smaller head difference. These two factors both lead to an increase in the safety factor. In the 5A-scenarios, the exit point is located in the berm, which implies a shorter horizontal seepage path. This shorter seepage path is compensated by extra thickness of the blanket layer due to the berm at the exit point and the reduced aquifer head.

For the *Wide crest and gentle slope*, most of the scenarios only experience a small positive change due to the relocation of the exit point to the end of the berm and thus elongation of the horizontal seepage length. There are no negative interactions due to assumption-option 5A, mainly because of the extra thickness of the blanket layer in the berm.

For piping, it is visible that a triangular berm shape has a similar effect on the interaction, with less positive outliers. The positive outliers in the *Grebbedijk original case* are caused by the 5A and 4C combination, which in the triangular berm the effect of a change in phreatic line is less than in the *Grebbedijk original case* due to the smaller difference between the height of the phreatic line in 4B and 4C.

5.4.4. Combined BEP

Figure 5.19 shows the combined effect of the sub-mechanisms uplift, heave and piping on the different input cases. This figure shows that all cases, except the *Thick blanket layer* case, have a broader boxplot than the *Grebbedijk original case*. The cases *Thick blanket layer No foreshore* and *Wide crest and gentle slope* contain scenarios with a more negative value for the interactions than the *Grebbedijk original case*.
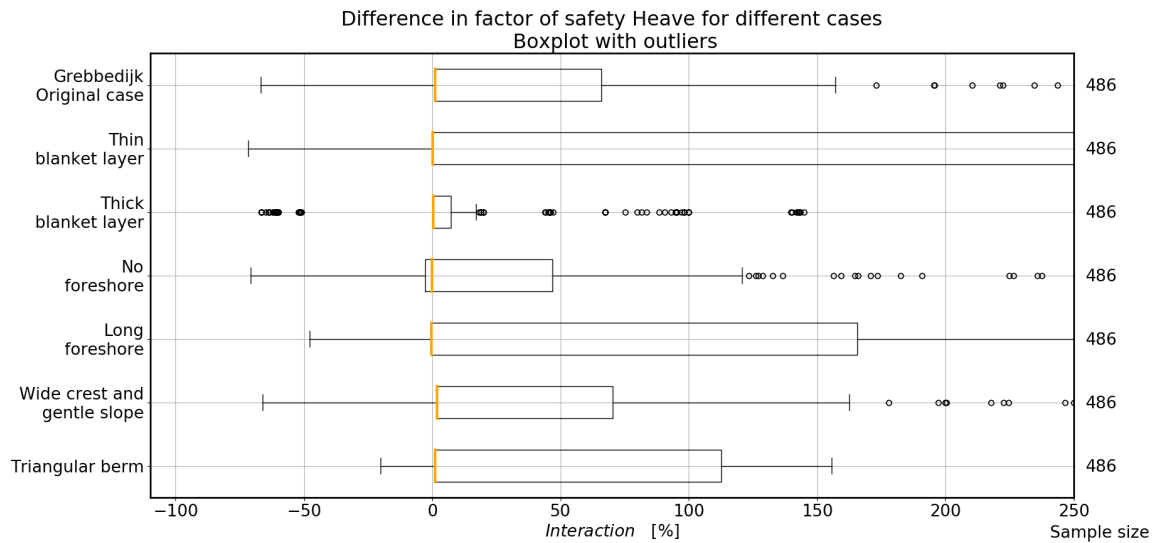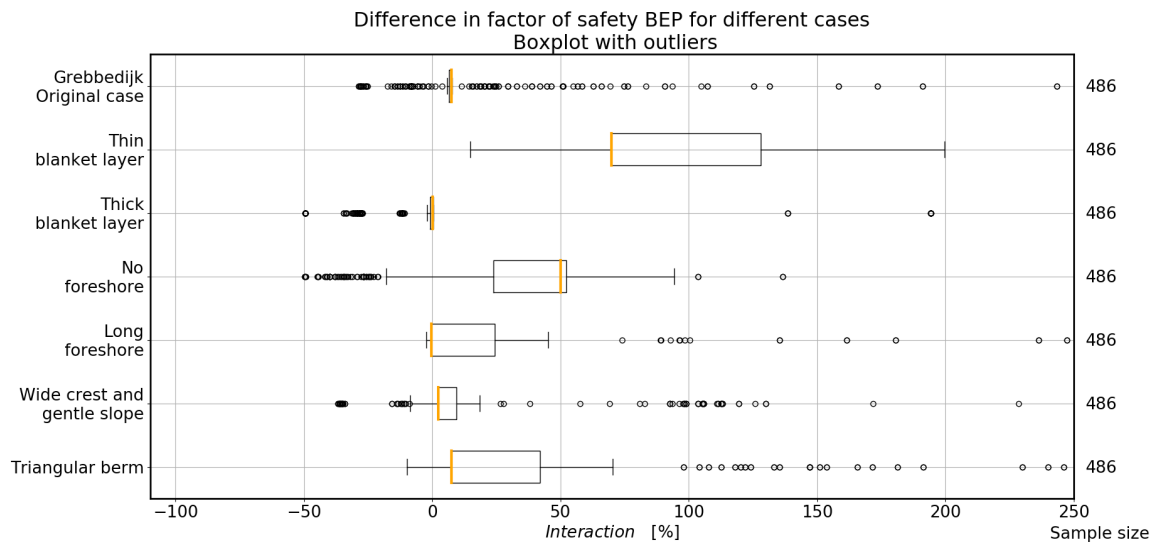
Figure 5.19: The range in the interaction of combined BEP for different cases with outliers.

In the *Thick blanket layer* case, the negative interaction is not caused by a change of leading mechanism, but by a large reduction of the leading mechanism uplift (FoS_u from 3.07 to 1.55). This is probably caused by the big difference between the leading mechanism and the non-leading mechanisms, in which the leading mechanism has to undergo a huge negative interaction or the non-leading mechanism has to undergo a huge positive interaction in order to change the interaction of the leading mechanism. The mechanisms are already far apart in the original situation (by a factor of 3), and all have a high original safety factor ($FoS_x >$ 0.99).

In the *Grebbedijk original case*, the interaction can be determined very precise once the exact sliding plane location and shape is known. This is not the case with the triangular berm. This could be caused by the greater variation in 5A-scenarios, in which the height of the berm is important, which is the difference between these two cases.

The *Wide crest and gentle slope* has some more negative interaction than the *Grebbendijk original case*. The most negative interaction results from the combination of 4A, 5A, 6A or 6B and 7A, which is comparable to the negative interaction of the *Grebbendijk original case*. In the individual mechanisms, the same interactions occur in both cases. However, there is a difference in original safety factors, where in both cases the leading mechanism changes from uplift to piping, the difference in safety factors is greater between these leading mechanisms in the case of the *Wide crest and gentle slope*. This greater difference leads to more negative interactions.

The *Thin blanket layer* case shows an all positive and broader boxplot. This case is the only one in which the base case involves a change in the leading mechanism, from piping to uplift, as can be seen in Table F.2. In the 5B- and 5C-scenarios, this shift in leading mechanism always gives a more positive interaction, and this shift is always from piping to uplift. In the 5A-scenarios, where uplift cannot take over because the safety factor becomes zero, the interaction is still positive because the leading piping mechanism also undergoes an increase in safety factor. Therefore, the *Thin blanket layer* case is all positive interactions for combined BEP.

The negative interactions in the *No foreshore* case arise from scenarios that include assumption-option 5A. In these scenarios, the FoS_u goes from 0.66 to 0.0, making piping the leading mechanism. However, the original factor of safety of piping is already low, as the seepage path is short. The interaction for piping can be a small negative interaction due to a high head difference in the combination of 5A and 4A, in which the safety factor of piping can drop to 0.33. This results in large negative interaction (of approximately −50%) for combined BEP (from leading with $FoS_{u,original} = 0.66$ to leading with $FoS_p = 0.33$).
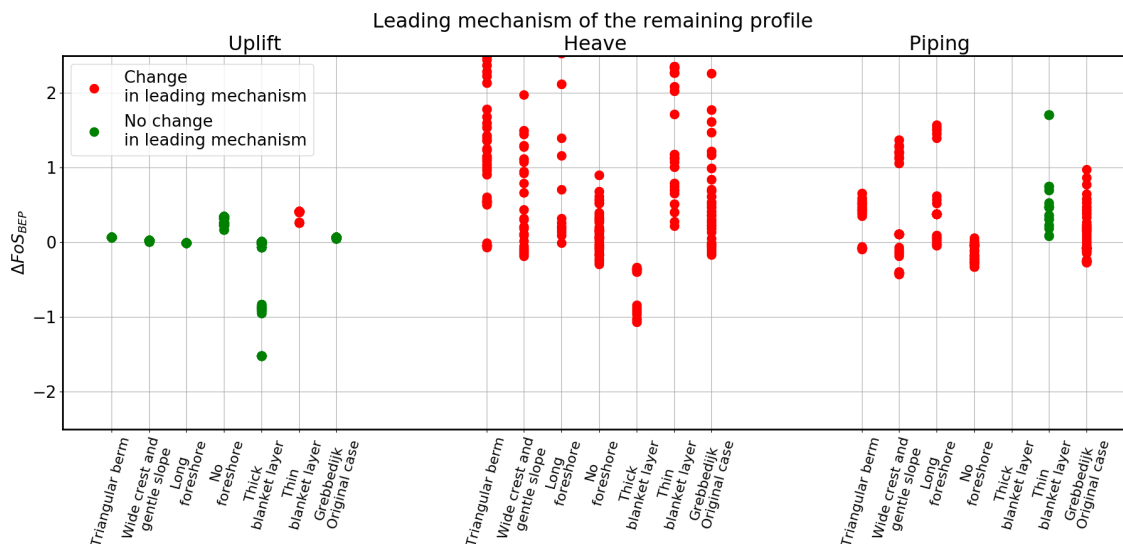
Figure 5.20

Figure 5.20 shows the degree of interaction for combined BEP for all cases, in which the leading mechanism of the remaining profile (uplift, heave or piping) is plotted for each scenario. The highest safety factor of the three sub-mechanism of the remaining profile is the leading mechanism. It is the mechanism that determines the safety factor of combined BEP. If the leading mechanism of the remaining profile has not changed compared to the original profile, it is depicted as a green dot. When it did change, it is depicted as a red dot.

A change in the leading mechanism can have a major effect on the interaction of combined BEP, herein the original situation is essential. If uplift is leading in this original situation, the difference in a safety factor for uplift and that of heave and piping can give an indication of the magnitude of the negative interaction for combined BEP. However, this only applies if the original leading mechanism is uplift because, in some of the assumption-scenarios, the safety factor for uplift may go to zero.

When changing from leading mechanism uplift to heave or piping or staying with the leading mechanism, uplift leads to the negative interactions in the figure. The change in leading mechanism from piping to uplift only shows positive interactions. Whether there is a connection is difficult to determine from these case studies since only one out of the seven starts with a leading mechanism other than uplift.

Table 5.13: The minimum and maximum of the interaction in combined BEP compared to the original situation per input case, no exclusion of outliers

Case	Minimum interaction [%]	Median interaction [%]	Maximum interaction [%]
Grebbedijk Original case	-29	8	472
Thin blanket layer	15	70	17240477
Thick blanket layer	-49	0	6509
No foreshore	-50	50	136
Long foreshore	-2	0	15525844
Wide crest and gentle slope	-37	2	2382
Triangular berm	-10	8	385

The amount of interaction is sensitive to change in the input case in which changes towards a thicker blanket layer or a shorter foreshore lead to the most negative interactions. Note, in the negative interaction of the thick blanket layer case (-49.44%), the unity check ($FoS_{BEP} \geq 1$) is still achieved.

5.4.5. Excluding assumption-option 5A

Section 5.3 showed that the scenario-option 5A has a major effect on the overall interaction. In this scenario-option, it is assumed that an enormous crack in the blanket layer has occurred due to the deformation as a result of the sliding. In Section 5.3.5, a hypothesis is introduced: If the option 5A can be excluded, then the range of the interaction becomes much narrower, and consequently, the interaction can be predicted more accurately.

The boxplots presented in section 5.3 are remade with the same data excluding option 5A (1944 scenarios remaining) to test this hypothesis. The boxplots that result from this can be found in Appendix E.3. These plots confirm that most of the outliers in the boxplots (in section 5.3) emerge from scenarios containing 5A. By estimating the probability of the occurrence of this assumption-option through, for example, research into the existence of deep cracks after a sliding, the range around the interaction could be reduced. The current range in combined BEP lies between the -0.29 and +442,500. If the existence of option 5A in practice can be excluded entirely, then this range could be reduced to an only positive range between 0.03 and 0.69 (see Table E.6). When step 5A has been omitted from this plot (see Figure 5.21), it can be seen that the range of the interaction is mainly caused by (step 1) the different sliding plane location and shapes. However, this option cannot be excluded without further investigation, as the occurrence of cracks cannot yet be excluded. In addition, it is important to look at the effect of smaller cracks and how they affect the interaction.
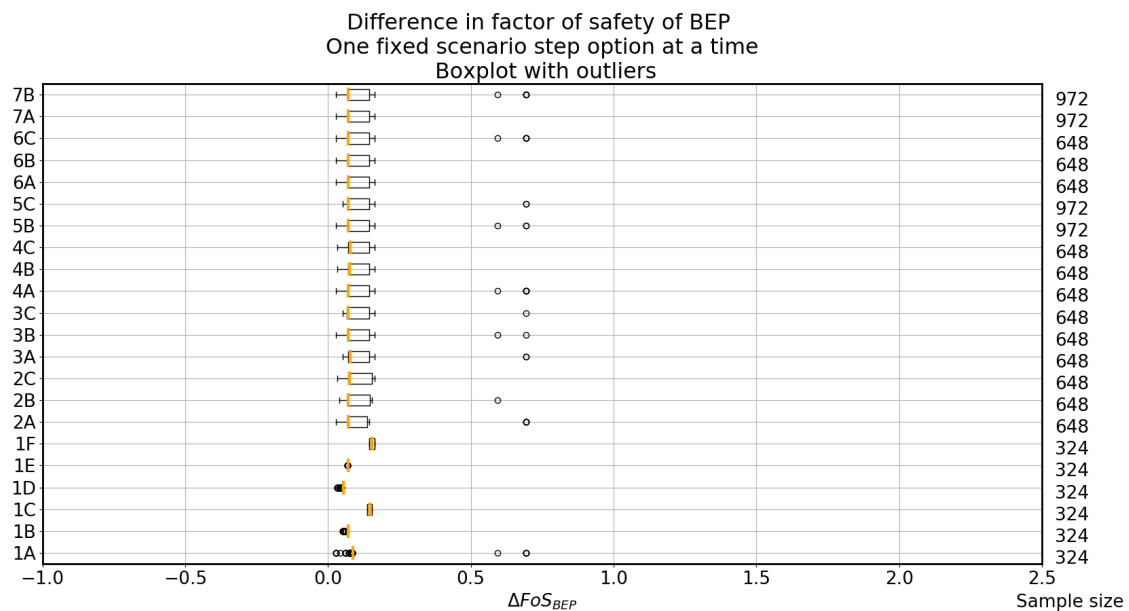
Figure 5.21: The degree of interaction for BEP with fixed scenario-options, without all scenarios that included option 5A. The $FoS_{original}(X_{exit})$ for BEP is 0.93.

The alternative seepage path (assumption-option 7B) are the two outliers in this figure. If the alternative seepage path (7b) could also be excluded, then the range of the interaction is between the +0.03 and +0.016. The same effect is seen in Figure 5.22, where the 5A-scenarios are excluded from the sensitivity analysis results for combined BEP.
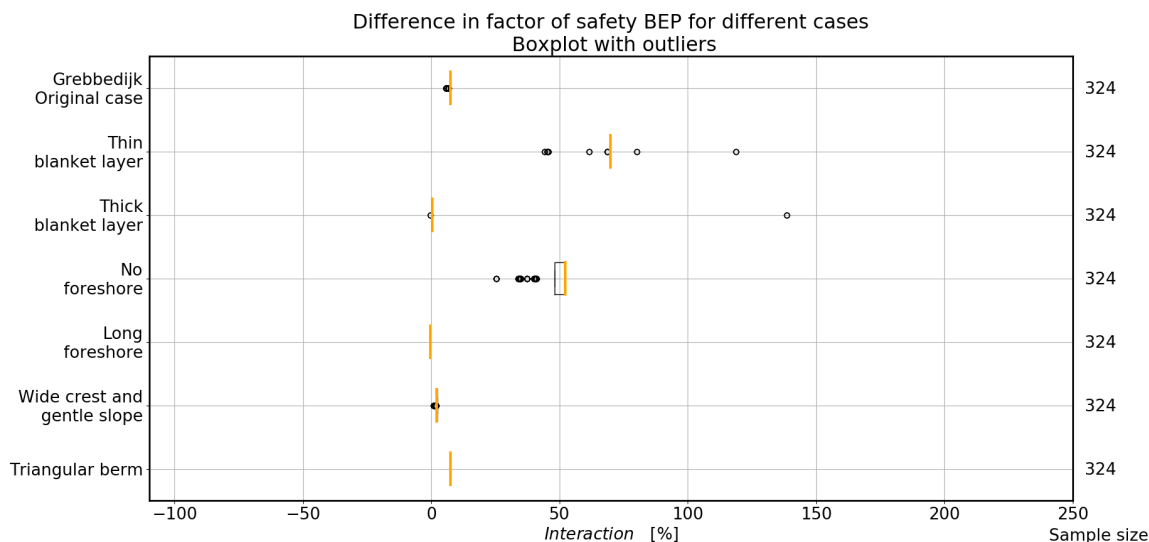
Figure 5.22: The degree of interaction for combined BEP for the seven different cases, without all scenarios that included option 5A.

5.4.6. Conclusion

The degree of interaction for combined BEP for all considered cases varies between -50 % and more than 2000%. The degree of interaction is in almost all cases for three-quarters positive, except for the case with a thick blanket layer (7m), for which half of the scenarios studied are still positive. The cases *Thick blanket layer*, *No foreshore* and *Wide crest and gentle slope* contain scenarios with a more negative value for the degree of interactions (-30% versus -50%) than the original case.

A change in leading mechanism between the original situation and the remaining profile situation for all cases is of importance for the negative interaction for combined BEP, especially when in the original situation the uplift mechanism is leading because it can reduce to a FoS_u of zero. The relationships between the three sub-mechanisms remain, as with the failure mechanism BEP, essential for the interaction. The system operation of the sub-mechanism determines how negative the value of the interaction can become.

If the Grebbedijk case is equipped with a thinner blanket layer in the sensitivity analysis, the sliding plane is more likely to perforate the sand layer. This causes a pressure relieve in the sand layer, which results in higher safety factors for heave and piping. The pressure relieve reduces the head difference, and due to the formation of the berm, the blanket layer is reinforced with more soil and becomes thicker, which makes heave and piping less likely to occur.

The *Thick blanket layer* case has a small range because the sliding plane only reaches approximately halfway through the blanket layer. Two-thirds of the scenarios only experience a small change in safety factors. In these cases, the exit point location is located slightly beyond the original exit point location, at the end of the berm. In the remaining one-third of the scenarios, the exit point is located at the location of the deepest point of the sliding plane, where the blanket layer has approximately half of its original thickness. Thus, even if the total resistance of the remoulded soil is zero, the safety factor cannot be lower than approximately half of the original safety factor due to the thickness of the remaining blanket layer and the sliding plane depth.

The original Grebbedijk case of section 5.3 shows that assumption-option 5A gives the biggest range in the degree of interaction of combined BEP. The difference between assumption-option 5A and assumption-option 5B or 5C is also clearly visible in all cases of the sensitivity analysis. Therefore, it was tested what the degree of interaction would be if assumption-option 5A could be excluded. When excluding assumption-option 5A from the scenarios, the degree of interaction is between +0.03 and +0.69, while it initially was between -0.29 and +442,500. The main motivation for this new range is the size and depth of the sliding plane, together with the alternative seepage path (scenario-option 7B). In case the alternative seepage path could be excluded, the range of the interaction is between +0.03 and +0.16.

6

Discussion

This study presents an overview of the possible interactions between the failure mechanisms backward erosion piping (BEP) and slope instability (SI). First, a qualitative study for both interactions was preformed and subsequently the interaction from SI to BEP was quantified in a model developed for this purpose. This chapter discusses the results of the research, as well as the limitations and assumptions that were required or made. It starts with the general consideration fo further research, after which the discussion points from the identification of the interaction of Chapter 3 are described. After this, the results of the quantification of the interaction is discussed.

6.1. Considerations for further research

This study focusses on cases where a single failure mechanism (A) occurs, which does not lead to the breaching of a levee but could affect the occurrence of a second failure mechanism (B). However, interactions between two failure mechanisms are more likely for levees where the individual failure mechanisms are already likely to occur. Therefore, failure mechanism B of the model, developed in this study (which was initiated as a result of failure mechanism A of the model) can, in reality, already have taken place before the failure mechanism A of the model in sense of sequence (this is the case for *thin blanket layer* in the sensitivity analysis, see Table F.2). Firstly, this indicates that it is necessary to consider whether failure mechanism A is the most likely failure mechanism to trigger the interaction. This is currently not implemented in the model itself, although it can be deduced by looking at the initial safety factors. Secondly, an interaction between two failure mechanisms is no single event. It is a time- and space-dependent process and its leading failure mechanism can continuously change between failure mechanism A and B. It is essential to investigate the interaction between failure mechanisms with a broader view because the interaction is a highly alternating process. When interpreting the results of the developed model, it is necessary to consider whether the initiating mechanism is the most logical starting mechanism, as the developed model does not include this.

A real-life case of the interaction between SI and BEP has never been proven. However, Kolb et al. (1962) suspected an interaction during a breach of the Hohenwisch in 1962. Furthermore, in 2011, the berm of the Hondsbroekschepleij presumably contained hollow spaces due to piping, which hypothetically reduced the shear strength of the soil (Koopmans, 2011). The interaction has never been observed apart from these two cases, likely due to the lack of available data on the late stage of levee failures, emergency measures have already been undertaken, or the experts have not been present at the levee site during failure. More field observations are required to be able to provide evidence for the interaction between SI and BEP. These observations should also be measured on a frequent basis in order to validate the model developed in this study. However, it is difficult to find these observations in reality. Therefore, it is advised to start with more detailed modelling and have the probability of occurrence estimated by experts, in order to determine the relevance of the interaction. Full-scale tests can be carried out if necessary.

The assumption-scenario that resulted in the most positive interaction from SI to BEP contains a large berm and, therefore, a narrow crest after SI. Although this remaining profile has a high safety factor for BEP, it is relatively unsafe, because other failure mechanisms could take over the failure process. For example, the cover material on the inner slope has slid away, so the inner slope is more prone to erosion. When the remaining crest is very narrow, only a small volume needs to erode to result in a lowering of the crest level. Consequently, the levee is more likely to fail due to overtopping or overflow. This highlights the importance of not overlooking the other failure mechanisms that may also interact and, in the end, may dominate the failure process of the levee after the initial interaction.

6.2. Identification of the interaction

It is important to include a flood wave in the river because this influences the continuation of the BEP process. In Chapter 3, only one load case is considered: permanent state extreme high water level. This extreme water level, which corresponds to the norm of the Grebbedijk, is also considered in the model study. BEP and SI both depend on the duration of the flood wave because it affects the head in the aquifer and the phreatic line. The worst-case scenario for the head in the aquifer and the phreatic line can develop some time after the peak of the flood wave. Another load-related point to consider in further studies is a lower high water level, which can lead to uplift and heave without growing until progressive piping occurs. The resulting boil can already influence the shear strength in the soil at lower water levels and thus the interaction from BEP to SI.

Time is an essential factor during the interaction and needs to be included in further studies. For example, the interaction between SI and BEP will stop as soon as the water level of the river drops to non-threatening levels. If the levee has been repaired before the next high water wave, the interaction will not proceed, although it may recur. Another situation emerges when a pipe is formed during a flood wave, which did not breach the levee. When this pipe is not discovered, a lower high water level can already initiate an interaction with SI because the levee is weakened by the presence of the pipe. There is no shear strength in the pipe which means that with a lower load sliding can occur, given that the pipe did not collapse or has not been repaired in the meantime.

The scale difference between BEP and SI is important. SI has a longitudinal width of 30-100 meters, while BEP has an influential area of one pipe of, a few meters after widening and a few centimetres before widening. In reality, a network of smaller pipes will first be created, after this one or more of them grow to a larger size pipe. Although the specific influential area remains unknown, it will still not be in the same order of magnitude as SI. Due to these scale differences, it is uncertain whether these small pipes can reduce the shear strength of the levee to such a degree that it influences the occurrence of SI. In Section 3.3, two cross-sections in the longitudinal direction were considered: In the pipe and next to the pipe. These cross-sections showed the importance of the 3D–effect of the interaction, as the presence of pipes in the levee affects the longitudinal distribution of the shear strength. However, the question remains whether the area of influence of BEP is sufficiently large to influence SI, which has a much larger scale.

In the interaction from BEP to SI, the 3D-effects are described through the different 2D cross-sections and the flow patterns in Section 3.2. However, in the interaction from SI to BEP, the 3D-effect is not described (only one 2D cross-section is considered). In this interaction, the cross-section next to the SI (next to the berm formation) may experience a different interaction. For example, it can become a weak spot because it can experience rupture but does not get the positive effect of the extra weight of the soil. This interaction is not included in the current identification of the interaction, although this interaction will have to be included in order to get a complete overview of the interaction. This is a very local effect, which is why it is expected that it has less influence on the total interaction.

In this study, the failure mechanisms are reviewed with the limit state functions and limit equilibrium model. Herein, only the limit of the different process phases (uplift, heave, piping) are taken into account, which strongly simplifies reality. As a result of this simplification, the interaction is only considered at a certain point in time and space, although in reality, the interaction would be a continuous and spatially varying process. Secondly, some variables are not considered in the calculations of the limit state functions and limit equilibrium model. Extensive models, like a finite element model, would allow for the inclusion of many, possibly relevant processes in the calculation.

6.3. Quantification of the interaction

The discussion of the quantification of the interaction from SI to backward erosion is subdivided into two parts. First, the results and considerations of the study are discussed. Secondly, the limitations of the, in this study developed, model and the limitations of the assumptions made are elaborated.

6.3.1. Results

Considerations for this research

The probability of occurrence of every scenario-option is currently not considered. For example, small sliding planes are more likely to occur in the Grebbendijk than large ones. If a scenario with a large positive inter-action is less likely to occur than another scenario with a much smaller interaction, more weight should be given to the modelling of the smaller interactions within the study. The results of the study can be significantly affected if large interactions occur less frequently and are therefore included less heavily in the study.

In the quantification of the interaction (Chapters 4 and 5), the safety factors are calculated in a deterministic calculation using the mean value for every variable. This gives a good estimate of the interaction. However, it can be further expanded by performing a full probabilistic calculation in which all variables have a distribution, other combinations of parameters can become normative for the degree of interaction.

There are matching parameters between the safety factors of the sub-mechanism that form a dependency, such as the blanket layer thickness (see Section 4.7). The effect of these correlations between matching parameters has not been researched. However, it is important to further investigate this in order to better predict the interaction.

The majority of the modelled assumption-scenarios (50%) only contains small interactions ($0.05 \leq \Delta FoS \leq 0.15$). These arise from cases where the initial safety factors are low and therefore have a high probability of occurrence. The negative side of the degree of interaction (ΔFoS) is limited by the height of the original leading failure mechanisms' safety factor because a safety factor cannot become less than 0. It would be interesting to look at the effect of the interaction at higher initial safety factors, where more and larger interactions might be discovered.

The original Grebbedijk levee does not meet the required factor of safety for all sub-mechanisms of BEP (uplift, heave and piping) using mean values. The percentage-based degree of interaction are not expected to deviate from those of the sensitivity analysis. However, strong negative interactions will not cause failure of a strong levee, while it will for weak ones. For strong levees, the probability of occurrence of a single failure mechanism already is very small, which makes the probability of occurrence of an interaction between two mechanisms even smaller. The qualitative study identified several possible interactions, without considering the initial safety of a levee. Therefore, it is not expected that other interactions were not accounted for, although this possibility cannot be excluded. However, it is possible that another combination of parameters initiates an interaction, as explained in the discussion of the full probabilistic analysis above.

In the SI analysis in the developed model, the uplift Van method is used, together with a critical state drained analysis, as recommended by Hop and Rijneveld (2018a, p. 127). Stuij et al. (2017a) evaluated drained and undrained sliding planes for multiple cross-sections of the Grebbendijk. These sliding planes show that the safety factor of slope instability is lower with an undrained analysis than with a drained analysis. However, the shape of the sliding plane is important for the degree of interaction. The undrained analysis results in longer sliding planes that do not reach a deeper position. The berm that forms from these sliding planes will also be elongated, depending on the thickness of the resulting berm. This elongation will have a positive effect on the interaction with BEP, except when the berm is not thick enough to move the exit point to the end of the berm. This exception will only happen with small sliding planes. However, this only gives a preliminary indication of the possible effects. The exact impact of the (drained or undrained) shear strength model on the outcome of the interaction should also be assessed if a more comprehensive analysis of the interaction is executed.

Assumption-scenarios

The main finding of the quantification of the interaction from SI to BEP of the Grebbedijk is that the extreme negative and positive interactions are dependent on the assumption that large cracks can occur in the remoulded soil. However, the existence of these extreme cracks in reality is questionable. Although the assumption of large cracks is very extreme, there is a supposition that cracks may indeed occur in remoulded soil, but that these may be of a smaller size. These smaller cracks can probably cause negative interactions as well, but the question remains how negative these interactions are.

In creating the scenarios, the three options of step 5 were chosen with the idea that a reduction in soil strength (5B) through the change of specific weight would be a good estimate of the reality. However, the results show that step 5B is always close to step 5C (no physical change of the soil due to sliding) and that the assumptions of a large crack in the remoulded soil (5A) are significantly different from 5B and 5C. This has also been emphasized in the sensitivity analysis by looking at the interaction without this assumed crack. The question remains how a fourth scenario-option with small cracks relates to the other options in scenario-step 5.

The model assumes that rupture occurs if the sliding plane perforates the blanket layer, regardless of the assumption-scenario (except the option for scenario-step 1: Size and shape sliding plane). This rupture implies a reduction of the aquifer head to the limit potential of the blanket layer if this potential is lower than the original aquifer head. This lowering results in a safety factor of uplift FoS_u of 1.0 at those locations, except for scenarios that include assumption-option 5A (large crack). However, it is unknown whether this full reduction takes place in reality. Without this assumed rupture, more assumption-scenarios could have an exit point located in the berm. The *no foreshore* and *thin blanket* case from the sensitivity analysis clearly illustrate the decrease of the head to the limit potential, see Figures F.23 and F.9. The exit point of these cases would be located in the berm if the assumption on rupture was excluded, which can potentially negatively affect the degree of interaction.

Sensitivity analysis

The sensitivity analysis uses the safety factors, which are calculated as the ratio between a resistance and a load, so it is limited by $0 \leq FoS \leq \infty$. Consequently, it is unclear what the effect of the original safety factor on the degree of interaction from SI to BEP is because a positive interaction ($\Delta FoS > 0$) appears more extreme than a negative interaction ($\Delta FoS < 0$). For example, the original safety factor for the case *thick blanket layer* is already very high, which causes the degree of interaction for this case to be low. This could be solved by scaling the safety factors, or by taking the difference instead of the ratio. However, this requires variables with the same unit, such as energy on a micro scale.

In determining the degree of the negative interaction of combined BEP, a change of leading mechanism is essential. The sensitivity analysis shows larger negative interactions for combined BEP if the original safety factor for uplift is leading, because there is a possibility that the assumption-scenarios contain an assumption in which there is a large crack in the blanket layer, and as a consequence, the safety factor of uplift goes to zero. The plausibility of this assumption has already been discussed above. However, for the sub-mechanisms heave and piping, there is no assumption-scenario in which the safety factors are reduced to zero. This raises new questions such as whether assumptions have been overlooked that could also reduce the heave and piping safety factors to zero and would they then, as leading mechanisms have the same effect as uplift as the leading mechanism on the interaction.

For simplicity, the critical sliding planes in the five cases of the sensitivity analysis are determined through a D-Geo Stability calculation (considering the restrictions from Section 4.10) and subsequently subdivided in one of the six sliding plane shapes of assumption-step 1. This approach is different from that of the original Grebbendijk case, where all six different sliding plane shapes are considered for this scenario-step. Therefore, the results of the sensitivity analysis are based on different sample sizes and different sliding plane shapes. This leads to a distorted comparison of the cases, however the most probable of the six sliding planes is accounted for in every case of the sensitivity analysis, thus the effect is expected to be limited.

6.3.2. Limitations of and additions to the developed model

Some assumptions made in the assumption-scenarios are implausible in reality.

- The degree of interaction from SI to BEP is very dependent on whether scenario-option 5A (large crack) or one of the other step 5 options is chosen. However, the occurrence of this option in reality is debatable, because this option requires the unlikely event of a vertical crack through the entire remoulded soil. This debates also holds for scenario-options 4C and 7B. Option 4C requires an addition of water to the system, while option 7B involves a longer seepage path than necessary.
- Because clay already is densely packed, and the formation of a berm creates chunks of clay with cracks, the berm cannot be more densely packed than the initial profile. However, this is one of the options within assumption-step 3 (3C. Volume decrease).
- The critical heave gradient depends on the porosity and not the permeability of the soil in equation 4.20. However, although the porosity of the chunks of clay does not change, the permeability of the clay layer (with cracks) increases, which reduces the resistance of the soil against heave and therefore a decrease in the critical heave gradient can be expected. Within assumption-step 6, there is an option that offers an arbitrary increase in critical heave gradient which must be linked to the chunk formation.
- The alternative seepage path (assumption-option 7B) is hinted at in the literature (Knoeff et al., 2018, p. 23). In the model used (Sellmeijer), it is not possible to implement this other seepage path properly. The way it is incorporated in the model is not a good approximation of this possible alternative seepage path.
- The combination of scenario-options 5A and 7B is highly unlikely to occur in reality, because option 5A implies a large vertical crack through the remoulded soil, while option 7B implies that the seepage path does not go vertical through the remoulded soil but follows the interface of the sliding plane. In scenarios that contain option 5A, the path of least resistance always goes vertically through the vertical crack in the remoulded soil.
- Because the volumetric weight of the berm and the critical heave gradient are no fully independent variables (are correlated by the porosity of the remoulded soil), the calculations in scenario-step 3 and 6 need to be correlated. This relation is not yet quantified, and every combination of options for these two scenario-steps can currently be chosen in the model.

Some additions to the developed model need to be considered:

- The difference in the resulting interactions between these two options is considerably large and more options should be added between option 5A and 5B, for example, an option with a smaller vertical crack or the presence of large hollow spaces in the remoulded soil.
- For scenario-option 7B (alternative seepage path along the sliding plane), it is also possible that the seepage still continuous straight up through the blanket layer, only it will experience more resistance to the compacted layer of soil that lies at the interface of the sliding plane. This could be an addition to the currently just method, or it could be researched in a more comprehensive flow model.

<div style="text-align: right; font-size: 3em;">7</div>

Conclusion and Recommendations

This chapter derives the conclusion of this study and answers the research questions, based on the results of a qualitative and quantitative analysis, given in Chapters 3, 4 and 5. Next, recommendations for future design and assessment of levees, as well as recommendations for future research, are given, based on the conclusions and the discussion in Chapter 6.

7.1. Conclusions

The conclusions of this study are based on a qualitative assessment of the possible interactions between backward erosion piping and slope instability from Chapter 3, and a quantitative assessment of the one-sided interaction from slope instability to backward erosion piping from Chapters 4 and 5.

An interaction is defined as one failure mechanism influencing the probability of another failure mechanism in a positive or negative sense, where positive interaction is defined as a reduction and a negative interaction as an increase of the failure probability. The main research question of this study is:

How do interactions between backward erosion piping and slope instability affect the safety of a levee?

The main research question is answered by answering the sub-questions:

1. *How are interactions between failure mechanisms currently assessed?*

The current assessment and design method of levees (Rijkswaterstaat WVL, 2017a,d) does not include the interactions between failure mechanisms for all possible combinations. Currently, it only includes the effects of overtopping on slope instability (de Visser et al., 2018) and a reduction of the shear strength in slope instability due to uplift (Kanning and van der Krogt, 2016). At the moment, there is ongoing research on interactions between failure mechanisms and whether these should be included in a method for the design and assessment of levees (Knoeff et al., 2018). Although these methods are currently still in the trial phase, it is suggested to use the event tree method to visualize interactions.

The USACE uses the event tree method. However, they do not include interactions in the event tree.

2. *How do interactions between backward erosion piping and slope instability occur?*

An interaction between backward erosion piping and slope instability can take place in both directions (from and to) and can change from direction several times in the failure process of a levee. A parametric study provided an overview of the parameters that influence the interaction, in which the limit state functions (for uplift, heave, piping and slope instability) act as a guide.

The influence of backward erosion piping on slope instability
The enumeration summarises the influence of backward erosion piping on slope instability.

- Due to rupture of the blanket layer, there is a reduction of shear strength in the soil surrounding the rupture point at the interface between the clay and sand layer. The shear strength can reach zero landward of the rupture point.
- Due to the presence of seepage, there is a slightly lower head in the sand layer.
- Due to the presence of hollow space or pipes filled with water or fluidised sand, there is no shear strength in these pipes or hollow spaces.
- Due to the pipe acting as a drain, there is an increase in shear strength of the soil surrounding the pipes.
- Due to the drainage effect of pipes, there is a decrease in saturation in the levee which results in a reduction of the specific weight in the levee, reducing the driving moment of the soil equilibrium.

Therefore, it seems that, in the case of a thin blanket layer, there is a decrease in the probability of occurrence of slope instability due to rupture. It is important to note that the interaction is governed by the 3D-effect, as different locations in and adjacent to the location of a pipe have contradictory effects on slope instability.

The influence of slope instability on backward erosion piping
After the sliding of a section of the levee due to slope instability, this study assumed that a berm has formed and the levee has not yet failed due to this sliding. The exit point relocates due to the formation of the berm, depending on the soil properties of the berm. There are two possible new locations: in the berm or at the end of the berm. The enumeration summarises the influence of slope instability on backward erosion piping.

- Due to sliding, the blanket layer can be ruptured, which can cause a valve effect, lowering the head in the aquifer.
- A berm can locally increase the blanket layer thickness, affecting the height of the limit potential.
- The porosity and permeability of the soil in the berm can either increase due to the formation of cracks or decrease due to compaction of the soil. As a result, both the critical heave gradient and the specific weight of the soil in the berm can be affected.
- The saturation of the berm and the phreatic line location in the berm are unknown. However, they are either on polder level or higher.
- Due to a possible change in the exit point location, there is a change in seepage length, which can also affect the occurrence of piping.

If the exit point is located at the end of the berm, the properties of the berm do not influence the occurrence of backward erosion piping. It only depends on the valve effect due to sliding, the thickness of the blanket layer and the length of the berm which determines the seepage length. These will lead to a decrease in the occurrence of backward erosion piping. When the exit point is located in the berm, the occurrence of backward erosion piping is influenced by the properties of the berm. This parametric study on itself cannot determine the entire influence, because these properties are uncertain.

3. *How can the interaction from slope instability to backward erosion piping be quantified?*

A 2D-model is developed to enable quantification of the interaction from slope instability to backward erosion piping. This model consists of three consecutive analyses: A stability analysis, displacement analysis of the sliding plane and a backward erosion piping analysis. The model uses a representative cross-section of the Grebbedijk levee as input. In addition, the three analyses require an assumption-scenario, which contains seven assumption-steps. As every assumption-step contains two to six options, a total of 2,916 assumption-scenarios are created. The model calculates a safety factor for slope instability, as well as for uplift, heave, piping and combined backward erosion piping (hereafter referred to as 'combined BEP') of the remaining profile for each assumption-scenario. Combined BEP in the model is the maximum safety factor of the three sub-mechanisms (uplift, heave and piping). The degree of interaction is defined as the difference between the safety factor of the original profile (prior to sliding) and the safety factor of the remaining profile (after sliding).

A sensitivity analysis is conducted to get insight into the case-dependent sensitivity of the interaction. The input cases within this analysis are based on the Grebbendijk case, however they vary on one or two variables (*Thin blanket layer, Thick blanket layer, No foreshore, long foreshore, Wide crest and gentle slope*, and *Triangular berm*). These input cases are analyzed with the same three analyses and assumption-steps. All input cases give a degree of interaction, based on all assumption-scenarios.

4. *What is the range of the degree of interaction from slope instability to backward erosion piping and which conditions and assumptions govern this range?*

The degree of interaction (ΔFoS) for combined BEP is between minus 0.29 and more than plus 20 for the Grebbedijk case on the safety factor of combined BEP. The median degree of interaction is +0.09. In more than three-quarters of the scenarios, a positive interaction for combined BEP occurs for the Grebbedijk case. There are significant differences between the modelled scenarios which stem from the presence of possible large cracks in the remoulded soil. Without cracks, only moderate interactions have been found, while with cracks the interaction becomes more significant, on both the positive and negative side. The largest positive and negative contributions to the degree of interaction stem from the following properties:

1. The assumption of large cracks in the remoulded soil gives the most negative interactions (-0.29), but also the most positive interactions (>20). In case of a large crack, the properties of the remoulded soil are essential because the crack ensures that the exit point location is in the berm.
    a. There is a large negative interaction when the leading mechanism changes to piping and a large positive interaction when the leading mechanism changes to heave. This change is determined by the effect of the interaction on the safety factor of heave. The behaviour of the critical heave gradient together with the occurring head difference is decisive in this respect.
    b. If it is assumed that the occurrence of large cracks reduces the critical heave gradient and there is a large head difference at the crack because it is assumed that the phreatic line is at polder level, then, the safety factor of heave is lower than the safety factor of piping and piping becomes leading.
    c. If it is assumed that the occurrence of large cracks does not affect the critical heave gradient and the head difference at the crack is small because the berm is not drained, and the phreatic line is high, then, the safety factor of heave will be higher than that of piping and thus leading.
2. If it is assumed that no large cracks occur, the size of the sliding plane will determine the degree of interaction.
    a. The most negative degree of interaction that occurs without cracks is +0.03, where there is a small sliding that does not penetrate the blanket layer. Therefore, the aquifer head will not reduce to the limit potential due to sliding. In addition, there is an extra thickness of the blanket layer due to the formation of the berm. This extra thick blanket layer is not thick enough to move the exit point to the end of the berm. However, it is thick enough to increase safety against uplift. This increases the safety factor for uplift, resulting in no change between leading mechanism and thus an increase in the interaction.
    b. The most positive interaction comes from a large sliding plane that perforates the blanket layer but causes such a thicker blanket layer that the limit potential is higher than the head in the aquifer. This thick blanket layer ensures that the exit point is relocated to the end of the berm. Due to the increased distance from the river, there will be a smaller head difference at the end of the berm than in the original situation. As a result, the safety factor of uplift increased and uplift remains the leading mechanism.

5. *Which (environmental) circumstances affect the degree of interaction?*

The degree of interaction for combined BEP for all considered cases in the sensitivity analysis varies between -50 % and more than 2000%. In order to arrive at these percentages, the calculated degree of interaction (ΔFoS) per scenario is divided by the original safety factors. The degree of interaction is positive in three-quarters of the scenarios for almost all cases, except for the case with a levee with a thick blanket layer (7m). In that case, half of the scenarios are positive.

Even more negative interactions were found (-30% versus -50%) in the cases with a thick blanket layer, no foreshore and a wide crest and a gentle slope compared to the original Grebbedijk case. However, these negative interactions stem from the same assumption-option as in the original Grebbedijk case, namely the possibility of a large crack in the remoulded soil after sliding. These results can be seen in all situations considered and, therefore, it is expected that they will be present in all interactions between SI and BEP for different types of river levees with a blanket layer. The number of negative interactions are expected to decrease considerably if the assumption of large cracks can be excluded or nuanced, which on average results in a more positive degree of interaction. The relationship between the three sub-mechanisms remains, as with the failure mechanism BEP, essential for the interaction. The system operation of the sub-mechanism determines how negative the value of the interaction can become.

The thickness of the blanket layer is a defining parameter for the interaction because it provides a significant variation in the results. For instance, it appears that, with a thick blanket layer, fewer positive and larger negative interactions are found, whereas, with a thin blanket layer, all interactions are positive. The most critical condition herein is whether or not the blanket layer is perforated by the sliding plane, which affects the head in the aquifer so that it may or may not approach the limit potential. It is expected that the dependence of the degree of interaction on the thickness of the blanket layer also applies to other river levees.

7.2. Recommendations

This section describes the recommendations that follow from the discussion and conclusions.

General recommendations
Large interactions ($\Delta FoS \geq -0.3$ and $\Delta FoS \geq +20$) from SI to BEP have been found in this study, both positive and negative, that can make a significant difference for levees that do not comply or only just comply with the new standard. Therefore, further research into this interaction is needed. The focus of this further research should be on determining the effect of different sizes of cracks in the remoulded soil, especially on the weight of the blanket, aquifer head and the critical heave gradient. These cracks have a large effect on the interaction through these parameters and are still unknown. Subsequently, the interaction from backward erosion piping to slope instability, which is only described qualitatively in this study, also has to be investigated, as possible interactions were identified in the parametric study. It is essential to directly account for 3D and scale effects in this interaction, as these effects are decisive for the size and direction of the interaction. In addition, research on the remaining combinations of failure mechanisms that may interact and the significance of their contribution to the failure process needs to be performed.

It is recommended to omit the quantitative interaction from slope instability to backward erosion piping from this study in the assessment and design of levees for the foreseeable future. As mentioned above, a start must be made on researching other possible interactions with a significant contribution to the failure process, then comparing their respective significance, ensuring that only those interactions that really contribute to the levee failure can be identified, quantified and ultimately implemented in the assessment and design of levees. Secondly, Rijkswaterstaat is advised to translate the interaction found into a simplified guideline.

In addition, the current method (WBI and OI) focuses on preventing individual failure mechanisms. A hypothesis from this study is that by doing so, a majority of the interactions will also be prevented indirectly. Firstly, because the interactions occur later in the failure process secondly, because measures are taken to prevent one of the failure mechanisms often reduce one of the parameters that are relevant to both mechanisms. For example, relieve wells can have an effect on backward erosion piping, but also on slope instability, because they lower the head in the aquifer.

Improvements
The following recommendations are given to increase the quality and reliability of further research:

- The probability of occurrence of every scenario-option must be quantified in order to allow the inclusion of interaction in the assessment and design of levees. Only interactions with a significant probability of occurrence should be included in this assessment.
- A future study investigating properties of the remoulded soil should be carried out, which focusses on the effect the remoulded soil has on the resistance against uplift of the blanket layer. This could elaborate on the effect of the remoulded soil on the head in the aquifer and if the remoulded soil contains possible ruptures, small fractures or a large cracks. In the first instance, the effect can be studied on a modelling basis by adding an additional scenario-options in step 5 with a low resistance of the remoulded soil to the current model to account for these possible effects of small fractures. If this results in a more negative interaction, laboratory tests with remoulded soil are needed to validate if this reduction is implemented correctly.
- A better understanding of the dependence of the critical heave gradient on the permeability of clay after deformation needs to be developed in order to improve predictions on the occurrence of heave in remoulded soil after slope instability.
- The full failure process of a levee that experiences an interaction between slope instability and back-

ward erosion piping needs to be researched in 3D, including time-dependence, to get the full potential of the interaction. The full failure process refers to the alternating interaction that changes during the failure process. This could be achieved by creating a 3D-model of the interaction that is alternating between different failure mechanisms and depends on the initial situation. In this model, the failure process starts with the most likely failure mechanism to occur, looking at the probability of occurrence of both failure mechanisms. The next steps of the failure process depend on the most likely failure mechanism to occur, considering space- and time-dependency.

Bibliography

Art. 1.1 Water Act (1 July (2018). `https://wetten.overheid.nl/BWBR0025458/2018-07-01`. [Online; accessed 27-06-2019].

Bishop, A. W. (1955). The use of the Slip Circle in the Stability Analysis of Slopes. *Géotechnique*, 5(1):7–17.

Breteler, M. K., Hart, R. t., Verheij, H., and Knoeff, H. (2010). Reststerkte van dijken na initiële schade, SBW-reststerkte fase 1: inventarisatie. Technical report, Deltares. 1200393-002-HYE-0010.

Calle, E. (2002). Dijkdoorbraakprocessen. Technical report, GeoDelft. 720201/39.

de Loor, D. (2018). An Analysis Phreatic Surface of the of Primary Flood Defences. Master's thesis, Delft University of Technology.

de Visser, M., Jongejan, R., and Bisschop, Cor Tigchelaar, J. (2018). KPR factsheet werkwijze macrostabiliteit i.c.m. golfoverslag OI2014v4. Kpr memo, KPR - Kennisplatform Risicobenadering.

Deltares (2007). Finite Element Model DgFlow in delta Shell - Manual. Technical report, Deltares.

Den Haan, d., Rozing, i. A., and van Hoven, i. A. (2014). Residual dike strength after macro-instability. Technical report, Deltares. 1207811-013-HYE-0001.

ENW, Fugro, GeoDelft, Grontmij, and Rijkswaterstaat (2009). Actuele sterkte van dijken. Technical report, Expertise Netwerk Waterveiligheid.

Evers, W. (2018). Waterkeringbeheer. Presentation, Drentse Overijsselse Delta.

Förster, U., van den Ham, G., Calle, E., and Kruse, G. (2012). Onderzoeksrapport Zandmeevoerende Wellen. Technical report, Deltares and Rijkswaterstaat.

Helpdesk Water and Rijkswaterstaat (2018). Nieuwe Normering. `https://www.helpdeskwater.nl/onderwerpen/waterveiligheid/primaire/nieuwe-normering/`. [Online; accessed 06-04-2018].

Hop, M. and Rijneveld, B. (2018a). Karakterisering Grebbedijk. Technical report, Waterschap Vallei en Veluwe, LievenseCSO and Fugro. 17M3041-R-006-V02.

Hop, M. and Rijneveld, B. (2018b). Technisch ontwerp zeef 1 verkenning Grebbedijk. Technical report, Waterschap Vallei en Veluwe, LievenseCSO and Fugro. 17M3041-R-007-V01.

Hop, M. and Rijneveld, B. (2018c). Uitgangspuntendocument zeef 1 Verkenning Grebbedijk. Technical report, Waterschap Vallei en Veluwe, LievenseCSO and Fugro. 17M3041-R-005-V02.

Hoven, A. V., Hardeman, B., van der Meer, J., and Steendam, G. (2011). SLIDING STABILITY OF LANDWARD SLOPE CLAY COVER LAYERS OF SEA DIKES SUBJECT TO WAVE OVERTOPPING. *Coastal Engineering Proceedings*, 1(32):5.

ICTdijk (2009). Ijdijk experment september 2008 video. `https://www.youtube.com/watch?v=lwBrJi9ly5c`. [Online; accessed 4-09-2018].

Jonkman, S., Jorissen, R., Schweckendieck, T., and van den Bos, J. (2017). *Flood defences*. Department of Hydraulic Engineering Faculty of Civil Engineering and Geosciences, second edition.

Jonkman, S. N., Vrouwenvelder, A. C. W. M., Steenbergen, R. D. J. M., Morales-nápoles, O., and Vrijling, J. K. (2015). *Probabilistic Design : Risk and Reliability Analysis in Civil Engineering*. Department of Hydraulic Engineering Faculty of Civil Engineering and Geosciences, third edition.

Kanning, W. and van der Krogt, M. (2016). Memo: Pore water pressure uncertainties for slope stability. Technical report, Deltares.

KNAG (2018). Overstromingsrisicoatlas. https://www.overstromingsrisicoatlas.nl/WSVV/index-west.html.

Knoeff, H., Kok, M., and Pol, J. (2018). Bijdrage aan discussie faalpaden - interne notitie. Technical report, Deltares and HKV and TU Delft and Rijkswaterstaat WVL. 12200575-003.

Knoeff, H., Sellmeijer, H., Lopez, J., Luijendijk, S., and van Beek, V. (2009). SBW Piping - Hervalidatie piping, HP1. Ontwikkeling nieuwe rekenregel and HP1.2 Uitbreiding en aanpassing van de pipingregel. Technical report, Deltares. 1200187-015-GEO-0004.

Koelewijn, d. (2009). SBW Hervalidatie piping - E. Evaluatie 0,3d rekenregel. Technical report, Deltares.

Kok, M., van Damme, M., and Kanning, W. (2017). Samenhang tussen Faalmechanismen. Technical report, TU Delft. Memo.

Kolb, L., Otremba, E., and Brunger, W. (1962). STURMFLUT 17. FEBRUAR 1962- Morphologie der deich-unf flurbeschadigungen zwischen moorburg and cranz. Technical report, Instituts fur Geographie un Wirtschaftsgeographie der Universitat Hamburg. 17M3041-R-007-V01.

Koopmans, R. (2011). Hondsbroeksche Pleij DP-220-223 Hoogwater januari 2011. Technical report, Waterschap Rijn en IJssel and Arcadis. Ref number: 075347595:A - Definitief C03011.000135.0120.

Margo, D. A. (2018). Personal E-mail. Answer to the question: Does USACE take interactions between failure modes into account.

Murthy, D. N. P. and Nguyen, D. G. (1985). Study of two-component system with failure interaction. *Naval Research Logistics Quarterly*, 32(2):239–247.

Parekh, M. L., Asce, S. M., Kanning, W., Ph, D., Bocovich, C., Mooney, M. A., Ph, D., Koelewijn, A. R., and Ph, D. (2016). Backward Erosion Monitored by Spatial – Temporal Pore Pressure Changes during Field Experiments. *Journal of Geotechnical and Geoenvironmental Engineering*, 142(10):1–10.

Rijkswaterstaat (2016). Schematiseringshandleiding macrostabiliteit. Technical report, Ministerie van Infrastructuur en Milieu. WBI 2017.

Rijkswaterstaat (2017). Schematiseringshandleiding piping. Technical report, Ministerie van Infrastructuur en Milieu. WBI 2017.

Rijkswaterstaat WVL (2017a). Handreiking ontwerpen met overstromingskansen: Veiligheidsfactoren en belastingen bij nieuwe overstromingskansnormen. Technical report, Rijkswaterstaat.

Rijkswaterstaat WVL (2017b). Regeling Veiligheid primaire waterkeringen 2017 - Bijlage I Procedure. Technical report, Ministerie van Infrastructuur en Milieu. WBI 2017.

Rijkswaterstaat WVL (2017c). Regeling Veiligheid primaire waterkeringen 2017 - Bijlage II Voorschriften bepaling hydraulische belasting primaire waterkeringen. Technical report, Ministerie van Infrastructuur en Milieu. WBI 2017.

Rijkswaterstaat WVL (2017d). Regeling Veiligheid primaire waterkeringen 2017 - Bijlage III Sterkte en veiligheid. Technical report, Ministerie van Infrastructuur en Milieu. WBI 2017.

Robbins, B. A., van Beek, V., Lopez, J., Montalvo Bartolomei, A., and Murphy, J. (2017). A novel laboratory test for backward erosion piping. *Under Review*, pages 1–14.

Rosenbrand, E. (2017). *Achtergrondrapport WBI - piping bij dijken*. Deltares. 1230086-021-GEO-0001.

Sellmeijer, H., de la Cruz, J. L., van Beek, V. M., and Knoeff, H. (2011). Fine-tuning of the backward erosion piping model through small-scale, medium-scale and ijkdijk experiments. *European Journal of Environmental and Civil Engineering*, 15(8):1139–1154.

Stuij, S., de Wit, T., and Huting, R. (2017a). Dijkversterking Grebbedijk - Nadere Veiliheidsanalyse. Technical report, RoyalHaskoningDHV.

Stuij, S., de Wit, T., and Huting, R. (2017b). Ontwerp en toetsrekensheet waterkeringen Royal Haskoning DHV Bijlage IV GR 22-33. Technical report, Royalhaskoning DHV.

't Hart, R., de Bruijn, H., and de Vries, G. (2016). Fenomenologische beschrijving - Faalmechanismen WTI. Technical report, Deltares. 1220078-000.

TAW (1985). Leidraad voor het ontwerpen van rivierdijken. Technical report, Technische advies commissie waterkeringen.

TAW (1994). Handreiking Constructief ontwerpen. Technical report, Technische adviescommissie voor de waterkeringen.

TAW (2004). Technisch Rapport Waterspanningen bij dijken. Technical Report september, Technische advies commissie waterkeringen.

USACE (1956). *Investigation of underseepage and its control – Lower Mississippi river Levees*, volume 1. Waterways Experiment Station, Vicksburg, Mississippi.

Van, M., Koelewijn, A., and B. J. Barends, F. (2005). Uplift Phenomenon: Model, Validation, and Design. *International Journal of Geomechanics*, 5.

Van Beek, V. (2015). *Backward Erosion Piping: Initiation and Progression*. PhD thesis, Technische Universiteit Delft.

Van Beek, V., Bezuijen, a., Sellmeijer, J., and Barends, F. (2014). Initiation of backward erosion piping in uniform sands. *Géotechnique*, 64(12):927–941.

van Beek, V., van Essen, H., Van den boer, K., and Bezuijen, A. (2015). Developments in modelling of backward erosion piping. *Géotechnique*, 65(9):740–754.

van der Krogt, M., Schweckendiek, T., and Kok, M. (2019). Do all dike instabilities cause flooding?

Van Hemert, H., Igigabel, M., Pohl, R., Sharp, M., Simm, J., Tourment, R., and Wallis, M. (2013). *The International Levee Handbook*. CIRIA, Griffin Court, 15 Long Lane, London, EC1A 9PN, UK CIRIA.

Van Montfoort, M. (2018). *Safety assessment method for macro- stability of dikes with high foreshores*. PhD thesis, Delft university of technology.

Vandenboer, K., van Beek, V., and Bezuijen, A. (2014). 3D finite element method (FEM) simulation of groundwater flow during backward erosion piping. *Frontiers of Structural and Civil Engineering*, 8(2):160–166.

Verruijt, A. (2001). *Grondmechanica*. Technische Universiteit Delft.

Wikipedia, the free encyclopedia (2009). Schematic of the method of slices showing rotation center. `https://en.wikipedia.org/wiki/Slope_stability_analysis`. [Online; accessed July 26, 2018].

Zwanenburg, C., van Duinen, A., and Rozing, A. (2013). Technisch Rapport Macrostabiliteit. Technical report, Deltares. 1204203-007-GEO-0003- gbh.

Nomenclature

Greek symbols

Symbol	Description	Unit
σ'_{vy}	Vertical yield stress	[kN/m^2]
α	Angle of slice	[°]
β	Angle of the sloping surface	[kg/m^3]
ΔFoS	Difference in factor of safety between remaining profile and original profile	[−]
$\Delta\phi$	Head difference	[m]
$\Delta\phi_{c,u}$	Critical head difference	[m]
η	Constant of White	[−]
γ'_p	Submerged specific weight sand	[kN/m^3]
γ_p	Saturated volumetric sand grains	[kN/m^3]
γ_w	Volumetric weight water	[kN/m^3]
$\gamma_{sat,remoulded}$	Volumetric weight of remoulded soil	[kN/m^3]
γ_{sat}	Saturated volumetric weight blanket	[kN/m^3]
γ_{unsat}	Unsaturated volumetric weight blanket	[kN/m^3]
κ	Intrinsic permeability coefficient	[m^2]
ν	Kinematic viscosity water	[m^2/s]
ϕ	Friction angle	[°]
ϕ'	Effective friction angle	[°]
ϕ'_{cz}	Angle of internal friction	[°]
$\phi(x)$	Head in aquifer	[m + NAP]
ϕ_{exit}	Head at the exit point	[m + NAP]
ϕ_{limit}	Limit head/potential of the blanket layer	[−]
$\phi_{new}(x)$	Head in aquifer after sliding	[m + NAP]
ρ_s	Soil density	[kg/m^3]
ρ_w	Water density	[kg/m^3]
σ'	Effective normal stress	[kN/m^2]
$\sigma'_{v,i}$	In situ effective vertical stress	[kN/m^2]
σ'_{vy}	Vertical yield stress	[kN/m^2]
τ	Shear stress	[kN/m^2]
θ	Bedding angle	[°]

Roman symbols

Symbol	Description	Unit
A	Amount of lowering	[m]
A_{berm}	Area of the berm	[m^2]
B	Width of the levee	[m]
B_c	Width of the crest of the levee	[m]
c	Cohesion	[kN/m^2]
c'	Cohesion	[kN/m^2]
d	Thickness of the blanket	[m]
D	Aquifer thickness	[m]
d_f	Thickness foreland blanket	[m]
d_h	Thickness hinterland blanket	[m]
d_i	Thickness of the intact blanket layer	[m]
d_r	Thickness of the remoulded blanket layer	[m]
d_{70m}	Reference value for d_{70}	[m]

d_{70}	70%-fractile of the grain size distribution	[m]
d_{70}	70% fractile of grain size distribution	[m]
FoS_h	Factor of safety of heave	[−]
FoS_p	Factor of safety of piping	[−]
FoS_s	Factor of safety slope instability	[−]
FoS_u	Factor of safety of uplift	[−]
$FoS_{BEP,original}$	Factor of safety of combined BEP, original profile	[−]
$FoS_{h,original}$	Factor of safety of heave, original profile	[−]
$FoS_{p,original}$	Factor of safety of piping, original profile	[−]
$FoS_{u,original}$	Factor of safety of uplift, original profile	[−]
g	Gravitational constant	[m^2/s]
h	Outside waterlevel	[m + NAP]
H_c	Level of the levee	[m + NAP]
H_c	Critical head difference	[m]
h_g	Ground level polder	[m + NAP]
h_p	Hinterland phreatic level	[m + NAP]
h_p	Hinterland phreatic level	[m + NAP]
$h_p(x)$	Phreatic line	[m + NAP]
h_s	Ground level start sand layer	[m]
H_{berm}	Height of the berm	[m]
$H_{c,p}$	Critical head difference piping	[m]
$h_{p,new}(x)$	Phreatic line after sliding	[m + NAP]
H_{sp}	Heigth of the sliding plane	[m]
i	Exit gradient	[−]
$i_{c,h}$	Critical heave gradient	[−]
i_{ch}	Critical heave gradient	[−]
j	Slice index	[−]
k	Permeability aquifer	[m/s]
k_f	Permeability blanket foreland	[m/s]
k_h	Permeability blanket hinterland	[m/s]
L	Seepage length	[m]
l	Width of each slice	[m]
L_f	Length (effective) foreshore	[m]
L_h	Length of the hinterland	[m]
L_{berm}	Length of the berm	[m]
$L_{seepage}$	Seepage length	[m]
m	Stress increase exponent	[−]
M_d	Driving moment	[kNm]
M_r	Resisting moment	[kNm]
n	Soil porosity	[−]
OCR	Over-consolidation ratio	[−]
POP	Pre-overburden pressure	[kN/m^2]
R	Resistance	[−]
R	circle radius	[m]
S	Load	[−]
S	Undrained shear strength ratio	[−]
s'	Mean effective principal stress ($\frac{\sigma'_v + \sigma'_h}{2}$)	[kN/m^2]
$S1$	Slope between the entry sliding plane and centre slip circle	[m]
$S2$	Slope between the exit sliding plane and centre slip circle	[m]
s_u	Undrained shear strength	[kN/m^2]
T	Traffic loads	[kN/m^2]
t_{max}	Maximum mobilizable shear stress ($\frac{\sigma'_v - \sigma'_h}{2}$)	[kN/m^2]
v	Kinematic viscosity	[m^2/s]
V_s	Total volume consists of the solids	[m^3]
V_t	Total volume of the soil	[m^3]

V_v	Total volume consists of the voids	[m^3]
V_v	Volume of the voids	[m^3]
W	Weight of each slice	[kg/m^3]
X_m	X-coordinate centre point slip circle	[m]
X_r	Length of the sliding planes entry point after displacement	[m]
X_{exit}	Exit point location	[−]
$X_{r,exit}$	Length of the sliding planes exit point after displacement	[m]
$X_{sp,exit}$	X-coordinate sliding plane exit point	[m]
Y_m	Y-coordinate centre point slip circle	[m]
Y_r	Height of the sliding planes entry point after displacement	[m]
Y_{polder}	Polder level	[m]
$Y_{r,exit}$	Height of the sliding planes exit point after displacement	[m]
$Y_{sp,entry}$	Height of the sliding planes entry point	[m]
$Y_{sp,exit}$	Y-coordinate sliding plane exit point	[m]
Z	Limit state function	[−]
Z_h	Limit state function for heave	[−]
Z_p	Limit state function for piping	[−]
Z_s	Limit state function for slope instability	[−]
Z_u	Limit state function of uplift	[−]

A
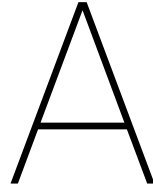
Theoretical background

A.1. Hydraulic loads on levee

Depending on the location of the levee, the loads on the levee differ. For levees at sea loads consist of the still water level, the tide, storms, waves and seiches. The focus in this study is on river levee, so only the relevant loads for river levees are described below. The river water level is mainly dependent on the river discharges and the characteristics of the river. Wind waves can develop on the river as well but will only give a short load on the levee. For the failure mechanisms, backward erosion piping and slope stability the long duration high water levels are of more importance, such as a flood wave. This flood wave is the result of rainfall, rainwater run-off and ice melt. The duration of the flood wave depends on several aspects like the length of the river and the rain durations. A flood wave can be represented in the discharge or water level at a certain point in the river, as shown in figure. The peak of the flood wave is used to predict extreme water level and get the corresponding return period of the water level. Depending on the location of the levee and the safety standard of that location a design water level is appointed for the semi- probabilistic calculations as a load on the levee. The water level influences the saturation of the levee and therefore the pore water pressures in the levee.

A.2. Groundwater

Groundwater plays an imported role in the failure mechanisms backward erosion piping and inner slope stability as well as failure mechanisms micro stability and outer slope stability which are not included in the scope of this thesis.

Internal soil equilibrium
The internal soil equilibrium is an equilibrium between the soil grains and the groundwater, described by Terzaghi as, (Verruijt, 2001):

$$\sigma' = \sigma_n - u \tag{A.1}$$

Where			
	σ_n	Total normal stress	[N/m^2]
	σ'	Effective stress	[N/m^2]
	u	Pore water pressure	[N/m^2]

When there is no groundwater flow the pore water pressure distribution is hydrostatic. Groundwater flow can change the pore water pressure, when the total normal stress, load on the soil and the specific weight of the soil, remains constant. This change in pore water pressure can only be compensated with the effective stress. The change in effective stress is essential for the shear strength of the soil TAW (2004). Pore water pressure can also be a result from soil stresses like creep and consolidation or due to soil deformations. TAW (2004)

focusses on the groundwater flow induced pore water pressures to schematised the hydraulic head in and around the levee.

These pore water pressures create the hydraulic head (see equation A.2) in the soil.

$$\Phi = z + \frac{u}{\rho_w g} \tag{A.2}$$

Where	Φ	Hydraulic head	[m]
	z	Elevation head	[m]
	ρ_w	Specific weight water	[kg/m^3]
	g	Acceleration due to gravity	[m/s^2]

Groundwater flow

In Figure A.1, the groundwater flow in a typical Dutch levee is outlined. Three flows are defined: A. two dimensional flow through the levee, B. one dimensional flow through the blanket, infiltration at outer side and seepage at the inner side of the levee. C. one dimensional horizontal flow in the aquifer. (Zwanenburg et al., 2013)
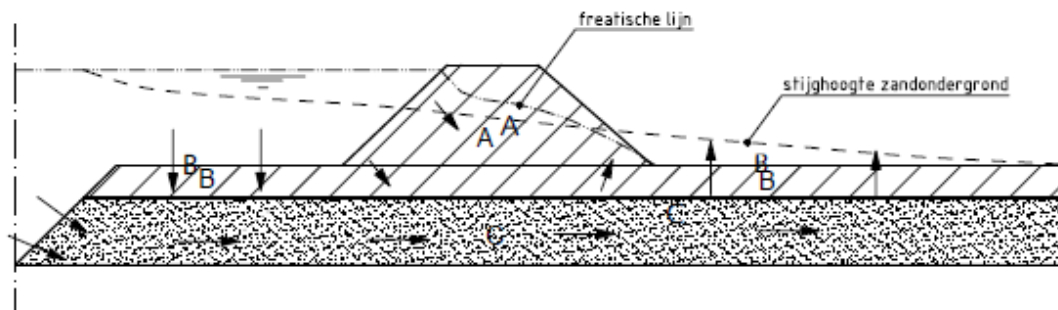
Figuur 2.2b Grondwaterstroming in dijkprofiel en ondergrond

Figure A.1: Possible groundwater flow through and beneath levee based on a Holland profile (TAW, 2004, p. 17)

Analytical model ground water flow

The fundamental equations behind the calculation of the groundwater flow are Dacry's law and the conversation of mass. Darcy's law describes flow in saturated soil (TAW, 2004), see equation A.3.

$$q_x = -k * \frac{\partial \Phi}{\partial x} \tag{A.3}$$

$$q_y = -k * \frac{\partial \Phi}{\partial y} \tag{A.4}$$

$$q_z = -k * \frac{\partial \Phi}{\partial z} \tag{A.5}$$

Where	q	Specific discharge	[m/s]
	k	Permeability	[m/s]
	$\frac{d\Phi}{dx}$	Hydraulic gradient	[-]

The law of conservation of mass A.6 for (quasi-) stationary flow gives the continuity equation:

$$\frac{\partial \Phi}{\partial x} + \frac{\partial \Phi}{\partial y} + \frac{\partial \Phi}{\partial z} = 0 \tag{A.6}$$

With non stationary flow the continuity equation for the phreatic storage follows:

$$n\frac{\partial h}{\partial t} + \frac{\partial(hq_x)}{\partial x} + \frac{\partial(hq_y)}{\partial y} = N \tag{A.7}$$

Where	h	head relative to top aquifer	[m]
	N	Net infiltration precipitation	[m/s]
	n	Phreatic porosity	[-]

and for elastic storage:

$$(m_v + n\beta)\frac{\partial u}{\partial t} = \frac{\partial \Phi}{\partial x} + \frac{\partial \Phi}{\partial y} + \frac{\partial \Phi}{\partial z} \tag{A.8}$$

Where	m_v	Compressibility of the soil	[m^2/N]
	β	Compressibility water	[m^2/N]

There are three important hydraulic heads to consider for failure mechanisms backward erosion piping and slope stability; The phreatic line in the levee, the head distribution in the blanket layer, and the head in the sand layer. In Rijkswaterstaat WVL (2017c) the pore water pressures are schematized following TAW (2004).

TAW (2004) defines four base cases of levees:

1. Clay core on clay/peat subsoil
2. Clay core on sand subsoil
3. Sand core on clay/peat subsoil
4. Sand core on sand subsoil

Consolidation loads and undrained loading (like traffic loads and creep) are not taken into account, these are implement via other methods like in the momentum equilibrium for slope stability or in the undrained shear strength.

A.3. Phreatic line

The distribution of the head (phreatic line) in the levee depends on: the saturation of the levee before an extreme high water level and during an extreme high water level,The permeability of the levee and if the ground water flow can be considered stationary, quasi-stationary or non-stationary. The soil above the phreatic line is assumed unsaturated (expectation of capillary rise) below is assumed saturated. The higher the phreatic line at the inside of the levee, the more pore pressure and thus less shear strength.

Saturation
The base saturation of the levee depends on the amount of phreatic and elastic storage and the amount of precipitation and overtopping. For the later, TAW (2004) assumes that the extreme precipitation thus not occur at the same time as the high water level, the phreatic line in the middle of the levee rises in-between the 0.5 meter and 1 meter, the ground water level in the polder will rise to the ground level and the precipitations does not influences the head in the aquifer. More recent study by de Loor (2018) suggest that the influence of the extreme precipitation is less important than the small frequent precipitation. de Loor (2018) also shows that the assumed rise in phreatic level is very conservative especially for levees with a clay core. For this research the schematization of the base phreatic line is based on the assumptions of TAW (2004). At the start, a levee has a pre-existing saturation which is the result of infiltration of precipitation and evaporation of the water. After precipitation, the phreatic line can increase inside the levee as shown in Figure A.2.
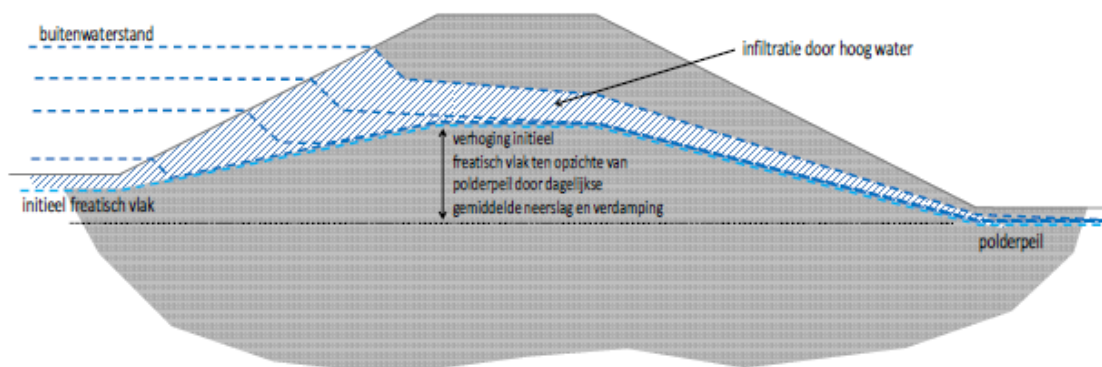
Figure A.2: Phreatic line after precipitation (Rijkswaterstaat, 2016, p. 36)

There are two types of storage in a levee, phreatic and elastic storage. Phreatic storage occurs when the ground water level rises and the pores in the soil fill with water. Elastic storage occurs when the pore water increases in such a way that the effective stress in the soil changes. This stress change changes the pore space in the soil creating more storage room (TAW, 2004). Phreatic storage is bigger than elastic storage, the both only occur in non-stationary ground water flow.

The saturation of the levee during a extreme high water level depends on the duration of the load and the permeability of the levee. Figure A.3 shows the difference between a permanent load and a transient load. The transient load is a short flood wave. It is import to note that at the peak of the flood wave the infiltration of the water into the levee is not at the most critical situation. When there is a long duration flood wave, the steady state can be reached and the load can be considered as a permanent load. To calculate the safety of the levee for the failure mechanisms backward erosion piping and slope stability, the load is assumed as a permanent load by TAW (2004). Note, that this would be an overestimation of the actual situation. Figure A.4 shows that with higher permeability and a transient load, the water infiltrates much faster.
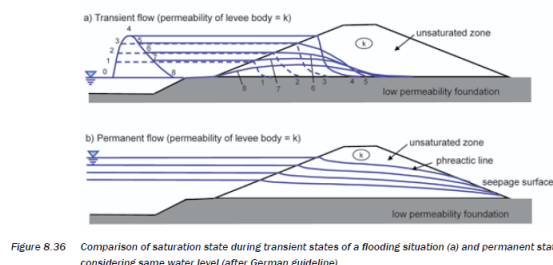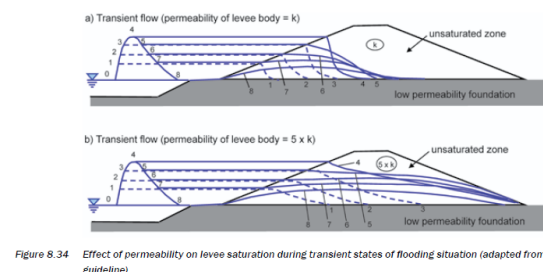
Figure A.3: Transient vs permanent (Van Hemert et al., 2013, p. 797)

Figure A.4: low permeability vs high permeability (Van Hemert et al., 2013, p. 796)

stationary, quasi-stationary or non-stationary
The ground water flow can be stationary, quasi-stationary or non-stationary, which one is used depends on the duration of the high water level, the storage and the permeability of the soil. In weak layers like peat and clay layers (low permeability) the flow is considered non-stationary and in the aquifer it is considered stationary. To account for the non-stationary effect, quasi stationary solutions are used (TAW, 2004).

For "long durations" of high water the ground water flow is considered (quasi-) stationary, for shorter duration of high water the ground water flow is considered stationary or time dependent.(Rijkswaterstaat, 2016)

Determine phreatic line

To model the phreatic line in the levee, the Rijkswaterstaat WVL (2017c) advises to use measurements where possible to estimate the initial phreatic line. If this is not possible, the method to estimated the initial phreatic line is described in TAW (2004). This method gives an overestimation of the load, if this is results in low factor of safety (FoS), a more detailed groundwater flow model can be used. For a detailed assessment of the initial phreatic line the analytical formulas of Dupuit or Hooghoudt can be used.

In the cases 1 and 2 (levee with a clay core) the phreatic line is determined as shown in Figure A.5. For the case with sand core the phreatic line can be schematized via the method described in TAW (2004).
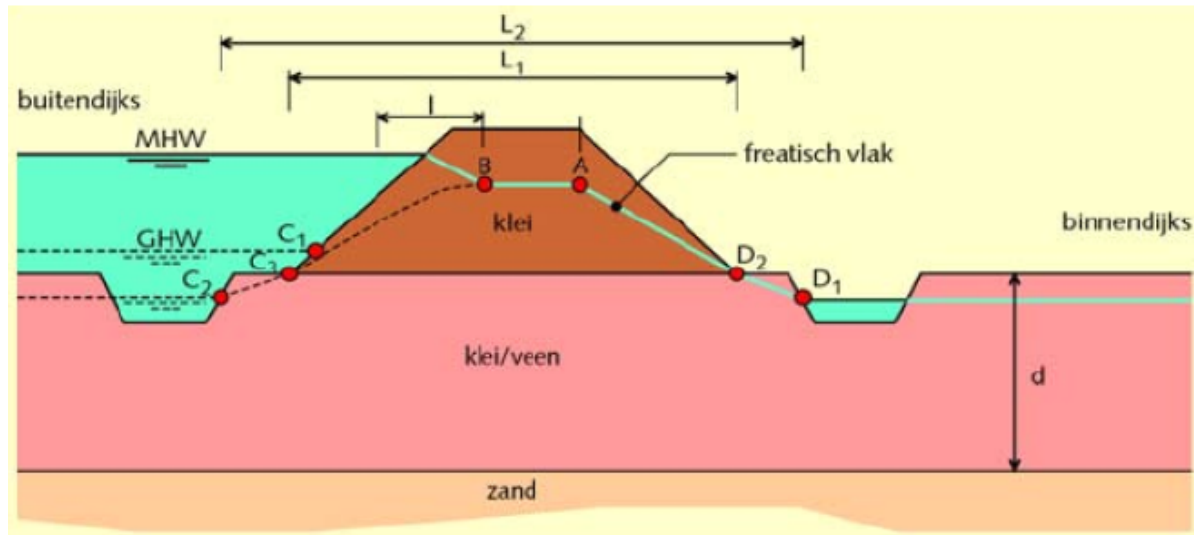
Figure A.5: Phreatic line at design high water level (TAW, 2004, p. 68)

In Figure A.5, the position of A is determined with equation A.9.

$$A = min(C + \frac{L}{x}, \quad D + \frac{L}{x}, \quad h_{crest} - 0.3) \tag{A.9}$$

$$X \quad becomes \quad \begin{aligned} X &= 10 & if & \quad d < 4.0m \\ X &= 8 & if & \quad d > 4.0m \end{aligned}$$

Intrusion length which gives location point B is determine with equation A.10, in TAW (2004).

$$I = \sqrt{\frac{2k_l H_0 t}{n_l}} \tag{A.10}$$

Where			
	I	Intrusion length	[m]
	k_l	Permeability of the levee material	[m/s]
	H_0	Water level compared to level of the blanket layer	[m]
	t	High water duration	[s]
	n_l	Porosity of the levee material	[-]

A.4. Pore water pressure in aquifer

As shown in Figure A.6, the head in the aquifer decreases to the head in the polder at high water. The distances it takes to decreases to this level is determined by the resistance in the sand layer. This resistance can be divided over three sections; The foreland, the levee and the hinterland. It can analytically be expressed as equation A.11 following TAW (2004).
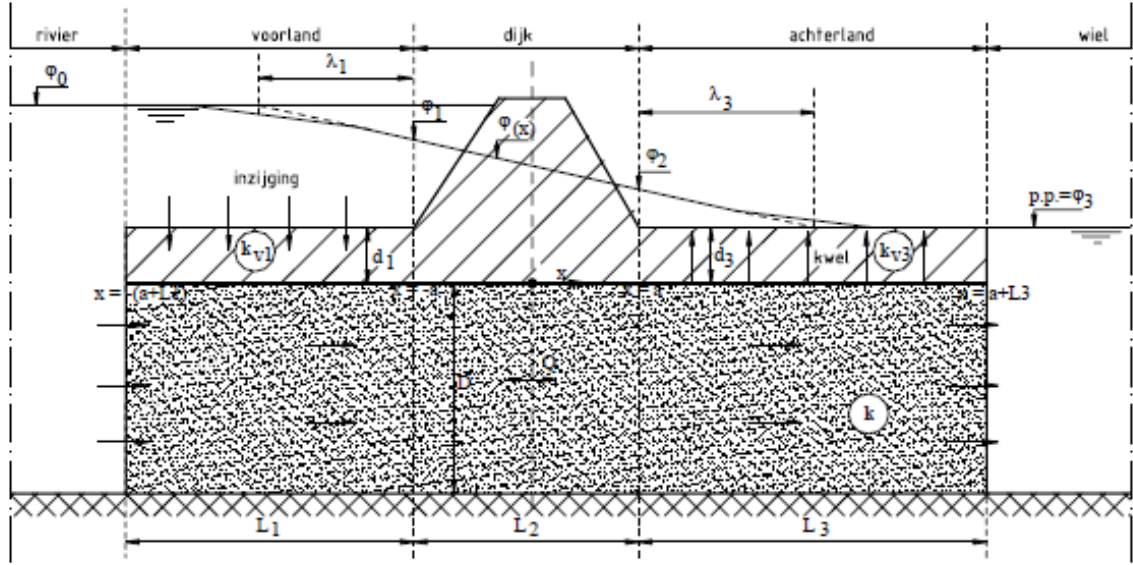
Figure A.6: Head in aquifer (TAW, 2004, p. 145)

$$\sum R = R_1 + R_2 + R_3 \tag{A.11}$$

$$R_1 = \frac{\lambda_f}{kD}\tanh(\frac{L_f}{\lambda_f}) \tag{A.12}$$

$$R_2 = \frac{B}{kD} \tag{A.13}$$

$$R_3 = \frac{\lambda_h}{kD}\tanh(\frac{L_h}{\lambda_h}) \tag{A.14}$$

Where R Resistance   []
         λ_f Leakage factor of foreshore   [m]
         λ_h Leakage factor of hinterland   [m]
         k Hydraulic conductivity of the aquifer   [m/s]
         D Thickness of the aquifer   [m]
         L_f Length of the foreshore   [m]
         B Width of the levee   [m]
         L_h Length of the hinterland   [m]

The leakage factors of the foreshore and hinterland are determined with equation A.15

$$\lambda_f = \sqrt{\frac{kDd_f}{k_{vf}}} \tag{A.15}$$

$$\lambda_h = \sqrt{\frac{kDd_h}{k_{vh}}} \tag{A.16}$$

$$\tag{A.17}$$

Where k_{vf} or k_{vh} Vertical hydraulic conductivity of the blanket at the foreshore or hinterland[m/s]
         d_f or d_h Thickness of the blanket at the foreshore or hinterland   [m]

The head at the levee toe can be determined as is shown in equation A.18. TAW (2004) gives equations to

calculated the head of the aquifer at all locations (for the hinterland equation A.19). .

$$\Phi_2 = h_p + \frac{R_3}{\sum R}(h - h_p) \tag{A.18}$$

Where			
	Φ_2	Head in aquifer at the toe of the levee	[m+NAP]
	h_p	hinterland phreatic level	[m+NAP]
	h	Outside water level	[m+NAP]
	$\frac{R_3}{\sum R}$	Damping factor λ at the toe of the levee	[-]

The damping factor can be determined by flow models, expert judgement or by monitoring. For a safe calculation, a damping factor of 1 can be assumed (Rijkswaterstaat, 2017). This damping factor λ differs per to determine location. When the length of the hinterland (L_h) compared with the leakage length (λ_h) is above the 1.8, the head in the aquifer in the hinterland can be approximated with equation A.19.

$$\phi(x) = h_p + (\Phi_2 - h_p)e^{\frac{B/2-x}{\lambda_h}} \tag{A.19}$$

Where			
	x	location of the head	[m]

$$\phi_{exit} = h_p + \lambda(h - h_p) \tag{A.20}$$

Where			
	ϕ_{exit}	Head at the exit point	[m+NAP]
	h	Outside water level	[m+NAP]
	λ	Damping factor at the exit point	[-]

A.5. Pore water pressure in blanket

As explained above, the pore pressure increase in the aquifer and press against the blanket. The pore water pressures in the blanket react slow to this change due to the low permeability (see Figure A.7). It would be very conservative to assume static pressure distribution in the blanket. So in practices the intrusion length is used to account for this effect. (Jonkman et al., 2017).
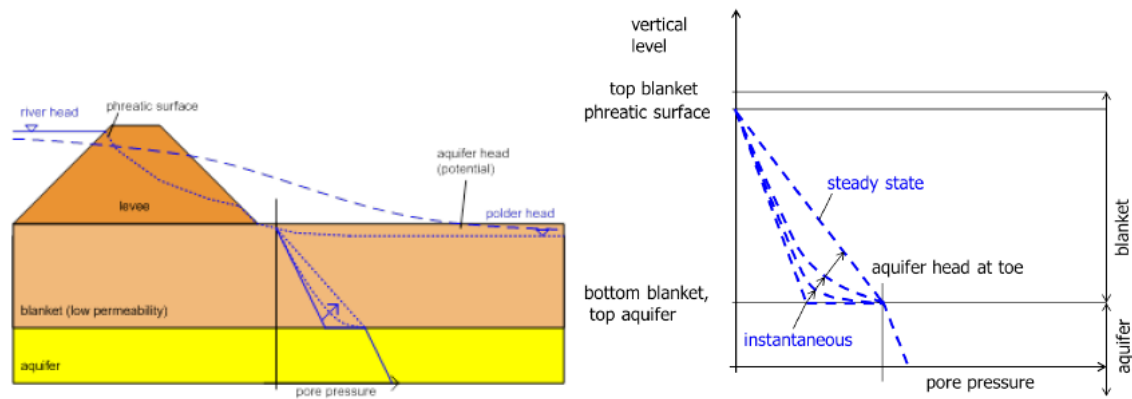
Figure 6.13: Increase of the piezometric head (pore water pressures) in an aquifer underlying a dike.
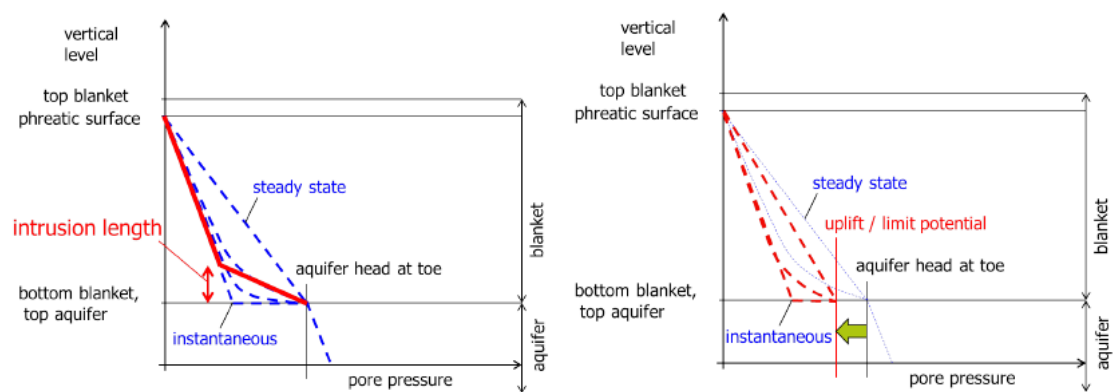
Figure 6.14: Definition of the *intrusion length* in non-uplift conditions (left-hand side) and in uplift conditions (right-hand side).

Figure A.7: Head in the blanket (Jonkman et al., 2017, p. 122)

TAW (2004) describes a analytical way to determine the intrusion length but also states that in practice it is assumed to be 3.0 meter for the the northern river levees in the Netherlands and 1.0 meter for the southern river levees.

Modelling groundwater flow D-Geo flow is used to model the pore water pressures (Deltares, 2007) based on the way decibed in TAW (2004). It is a finite element model, which uses the mass balance equation and Darcy's law to calculated the subsurface flow.

<div align="right">

B

</div>

Case study: Grebbedijk

B.1. Case description

The Grebbedijk is an earthen levee that is located between Rhenen and Wageningen along the river Nederrijn. The levee protects the Gelderse vallie, which is in-closed by the Utrechtse hills (Utrechtse Heuvelrug) and the Veluwe highlands. If the levee fails there is flooding all the way to the former Zuiderzee, see Figure B.1. The levee is approximately 5.5 kilometres (Hop and Rijneveld, 2018c). The safety standard for the levee is set on 1/100,000 per year.
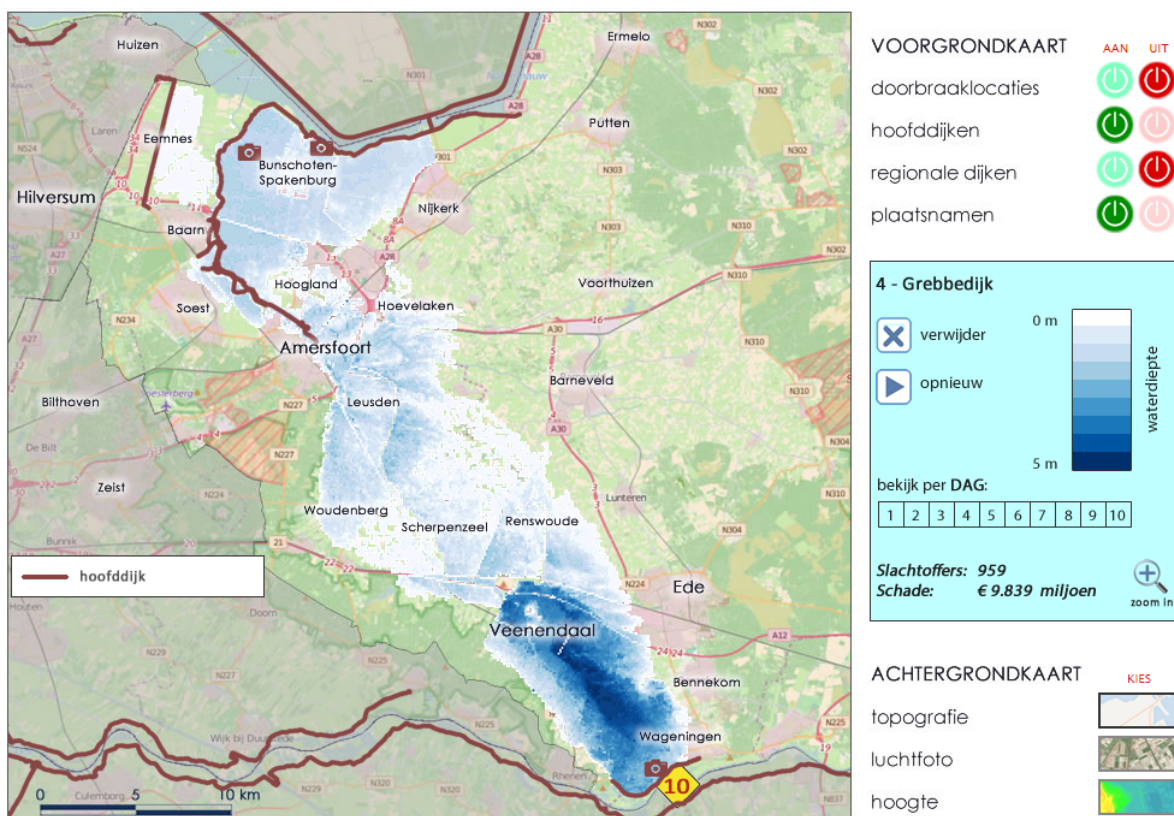
Figure B.1: Flooding due to Grebbedijk breach (KNAG, 2018)

The Grebbedijk did not pass the assessment of 2017. In Stuij et al. (2017a) an extended safety assessment was executed. The levee fails the assessment on almost all failure mechanism and levee section, only the levee section 013-022 has passed. For backward erosion piping the seepage lengths are to short and should be extended 30 to 90 meters to pass the assessment. For slope stability the slopes of the levee are too steep to pass. The Undrained shear strength calculation were normative.

The case of the Grebbedijk is suitable for research of the interactions because it has both backward erosion piping problems and slope stability problems at the same locations. For this thesis uses the levee profile of dp 20-52 as starting point for the schematization. This schematization was made available by Waterschap Vallei en Veluwe (water authority) and is used to calculate the safety factor for inner slope stability (Hop and Rijneveld, 2018a), (Hop and Rijneveld, 2018b). Small change are made to this schematization to make it applicable for a backward erosion piping as well as for slope stability. The main change is made in the schematization of the aquifer head. All assumptions made will be to represent reality as much as possible and remove conservative assumptions. This means that mean values are used when they are available.

B.2. Profile

Figure B.2 shows a typical cross section of the Grebbedijk. All previous levee improvement are shown in the figure. The schematization in Figure B.3 is based on this typical cross section in combination with the received schematization from the water authority. The foreland is set on 35 meter, the levee width on 35m and the hinterland length on 50m due to the presence of canals (Hop and Rijneveld, 2018a, p. 62). The location and name of the characteristic points of the profile are summarized in table B.1.
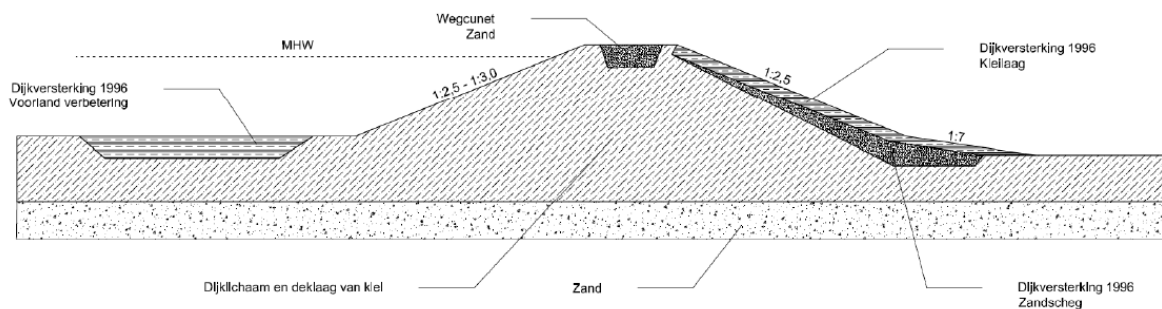
Figure B.2: Typical cross-section of the Grebbedijk (Hop and Rijneveld, 2018a, p. 13)
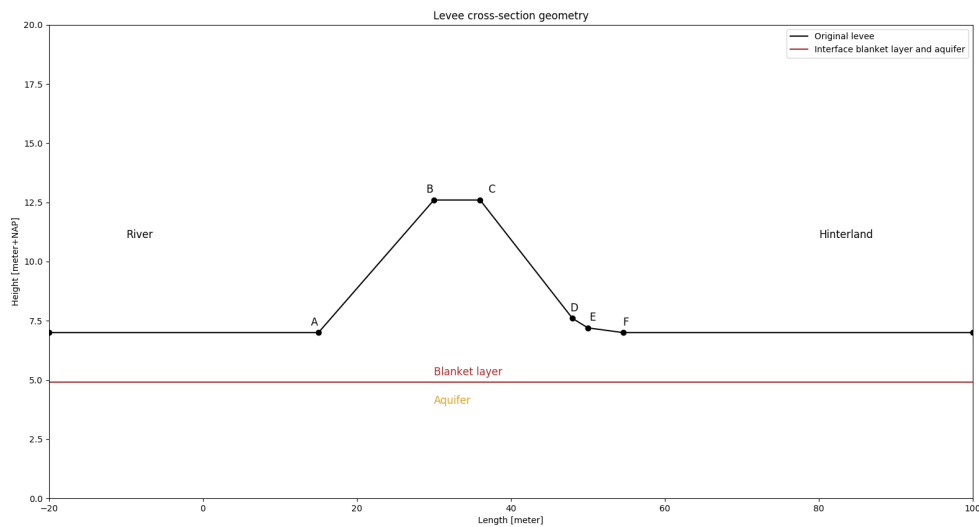
Figure B.3: Used profile of the Grebbedijk

Table B.1: Location of characteristic points in levee profile

Location	Name	Height [m + NAP]	Length [m]
-	Entry point	7.0	-20.0
A	Outer toe	7.0	15.0
B	Outer crest	12.6	30.0
C	Inner crest	12.6	36.0
D	Deflection point	7.6	48.0
E	Inner toe	7.2	50.0
F	Start polder	7.0	54.5

B.3. Loads

The water level of 11.99 m +NAP, which corresponds with the set standard of the levee (1/30.000 year) (Stuij et al., 2017a, p. 25), is the starting point for the load condition. The phreatic surface and the head in the aquifer are determined following the method of TAW (2004) as described in A. At the location of the inner crest line, the location of the phreatic line is at 9.9 m+NAP and an aquifer head of 9.6 m+NAP. At the inner toe the phreatic line has a level of 7.2 m+NAP and an aquifer head of 9.0 m+NAP. This corresponds with the results from measurements done in Hop and Rijneveld (2018a) (page 56 and 57), where the aquifer head varies between 8.8 m +NAP and 9.7 m +NAP at the toe and the phreatic level at the inner crest line varies between 9.5 m +NAP and 9.9 m +NAP. This load condition is the only one that will be considered here. Another load condition, which includes overtopping and thus a fully saturated levee, is not considered because this takes into account interaction between overtopping and slope stability.

There is an road on the levee therefore an traffic load is applied in the slope stability analysis (Hop and Rijneveld, 2018c, p. 31).
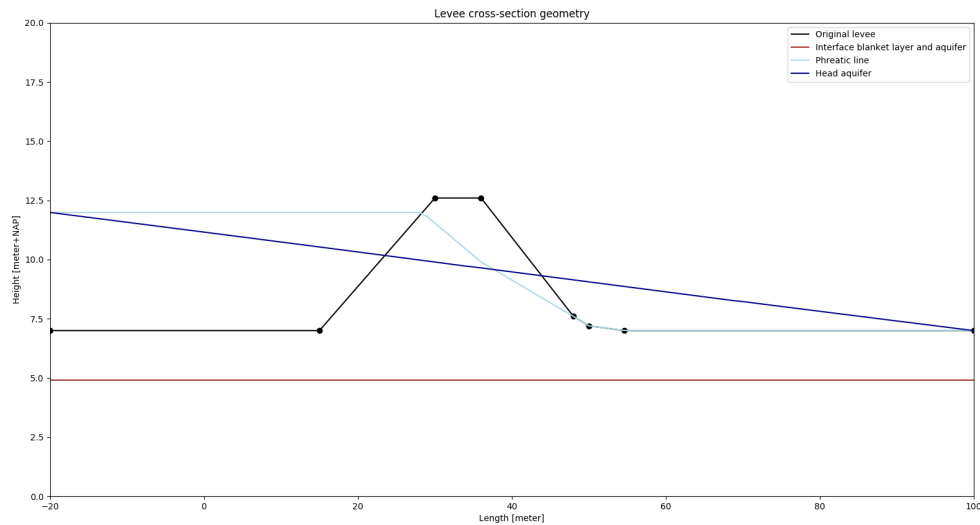
Figure B.4: The phreatic line and head in the aquifer

B.4. Soil characteristics

The permeability of the blanket hinterland, blanket foreland and levee resulted from the fit of the hydro-metric measurements. Here, only a characteristic value is mentioned and no corresponding distribution is mentioned. The value is set on the characteristic value of 0.05 m/day. (Hop and Rijneveld, 2018a, p. 64)

The mean values of the aquifer thickness and the permeability of the aquifer are known (Hop and Rijneveld, 2018a, p. 55). In between the DP20-52, it is uncertain if the clay layer at a depth of -15 m+NAP till -25 m+NAP continues (Hop and Rijneveld, 2018a, p. 16). It is here for assumed it does continue underneath the levee used here.

The saturated volumetric weight of the blanket layer the mean value is 17.9 kN/m^3 (Hop and Rijneveld, 2018a, p. 124).

B.5. Shear strength model

The consideration behind the choice for drained strength parameters is discussed by Hop and Rijneveld (2018a). The soil type of the soil in the levee is silty clay, the behaviour of silty clay is not standard defined as undrained or drained. The permeability results would imply the use of undrained behaviour. Hop and Rijneveld (2018a) states three reasons for choosing drained behaviour: The CPT shows low normalised water-pressure which implies almost non overpressure or underpressures which is similar to drained soil behaviour. The experiments show underspresurres by large strains, this means that the undrained strength is higher than the drained strength. And last, the uncertainty surrounding the drained shear strength is lower. Critical state drained shear strength is used in this thesis.

Table B.2: Soil properties needed in stability analysis,(Hop and Rijneveld, 2018a, p. 127)

Soil type	γ_{unsat}	γ_{sat}	ϕ'_{cs} [deg]	$c\ [kN/m^2]$
Clay, blanket layer	17.40	17.90	31.80	0.0
Sand, aquifer	18.00	20.00	31.30	0.0
Clay, levee material	18.50	18.80	28.00	0.0

B.6. Input parameters

In table B.3 shows all values of the input parameters of the Grebbedijk. The head in the aquifer and the phreatic level are separately explained, as well as the friction angle and cohesion of the different soil layers. The values of the parameters are the mean values, unless otherwise indicated.

Table B.3: Input parameters Grebbedijk for the model

Input parameters	Symbol	Value	Unit	Source
Geometry of the levee				
Height of the levee	H_c	12.6	$[m + NAP]$	(Hop and Rijneveld, 2018a, p. 13)
Width of the levee	B	35.0	$[m]$	(Hop and Rijneveld, 2018a, p. 13)
Width of the crest of the levee	B_c	6.0	$[m]$	(Hop and Rijneveld, 2018a, p. 13)
Hinterland phreatic level	h_p	7.0	$[m + NAP]$	(Hop and Rijneveld, 2018a, p. 13)
Length of the hinterland	L_h	50.0	$[m]$	(Hop and Rijneveld, 2018a, p. 62)
Length (effective) foreshore	L_f	35.0	$[m]$	(Hop and Rijneveld, 2018a, p. 59)
Soil characteristics and structure				
Soil layer build up	-	Simple	[-]	
Aquifer thickness	D	22	$[m]$	(Hop and Rijneveld, 2018a, p. 55)
Thickness foreland blanket	d_f	2.3	$[m]$	(Hop and Rijneveld, 2018a, p. 119)
Thickness hinterland blanket	d_h	2.3	$[m]$	(Hop and Rijneveld, 2018a, p. 119)
Permeability aquifer	k	39	$[m/day]$	(Hop and Rijneveld, 2018a, p. 55)
Permeability blanket hinterland	k_h	0.05^*	$[m/day]$	(Hop and Rijneveld, 2018a, p. 64)
Permeability blanket foreland	k_f	0.05^*	$[m/day]$	(Hop and Rijneveld, 2018a, p. 64)
Saturated volumetric weight blanket	γ_{sat}	17.9	$[kN/m^3]$	(Hop and Rijneveld, 2018a, p. 124)
Unsaturated volumetric weight blanket	γ_{sat}	17.4	$[kN/m^3]$	(Hop and Rijneveld, 2018a, p. 124)
Saturated volumetric weight water	γ_w	9.81	$[kN/m^3]$	
Load on the levee				
Outside waterlevel	h	11.99	$[m + NAP]$	(Hop and Rijneveld, 2018a, p. 56)
Phreatic line	h_p	-	$[m + NAP]$	see section B.3
Head in aquifer	Φ	-	$[m + NAP]$	see section B.3
Specific for backward erosion piping				
Saturated volumetric sand grains	γ_p	20	$[kN/m^3]$	(Hop and Rijneveld, 2018a, p. 127)
Critical heave gradient	i_{ch}	0.3	[-]	(Hop and Rijneveld, 2018c, p. 28)
Bedding angle	θ	37	$[deg]$	(Förster et al., 2012),(Stuij et al., 2017b)
Kinematic viscosity water	ν	1.33×10^{-6}	$[m^2/s]$	
Constant of White	η	0.25	[-]	(Förster et al., 2012),(Stuij et al., 2017b)
Gravitational constant	g	9.81	$[m^2/s]$	
70% fractile of grain size distribution	d_{70}	$0.208 \times 10^{-3*}$	$[m]$	(Förster et al., 2012),(Stuij et al., 2017b)
Reference value for d70	d_{70m}	$0.307 \times 10^{-3*}$	$[m]$	(Hop and Rijneveld, 2018a, p. 38)
Specific for slope stability analysis				
Shear strength model	-	Critical State C-ϕ model	[-]	(Hop and Rijneveld, 2018a, p. 127)
Stability model	-	Uplift Van	[-]	
Traffic loads	T	13.30	$[kN/m^2]$	(Hop and Rijneveld, 2018c, p. 31)
Friction angle	ϕ_{cs}	-	$[deg]$	see section B.5
Cohesion	c	-	$[kN/m^2]$	see section B.5

C
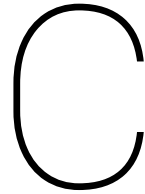
Stability analysis results

This appendix is a supplement to chapter 5, where the results of model calculation are discussed.

C.1. Sliding plane exact location and shape: Grebbedijk case

The stability analysis is conducted for the six options for scenario step I: sliding plane location and shape. (see chapter 4).

1. *Slope- blanket* The sliding plane starts in the slope and reaches into the blanket layer.
2. *Slope- interface* The sliding plane starts in the slope and reaches to the interface between the blanket layer and the sand layer.
3. *Slope- sand* The sliding plane starts in the slope and reaches into the sand layer.
4. *Crest- blanket* The sliding plane starts in the crest and reaches into the blanket layer.
5. *Crest- interface* The sliding plane starts in the crest and reaches to the interface between the blanket layer and the sand layer.
6. *Crest- sand* The sliding plane starts in the crest and reaches into the sand layer.

The result drawings of the calculated scenario step options are shown in sequence. The sliding plane follows the Uplift-Van shape, which consist of two circles connected by a pressure bar. The sliding planes vary in sliding depth. The values of the sliding planes locations are depicted in table C.1. The table shows for each option, the left and right circle centre point coordinates and the radius, as well as the locations of the entry and exit point of the sliding plane. All of the used scenarios have a safety factor below 1 as can be seen in table C.1 and can therefore occur.

Table C.1: Details on the calculate sliding plane locations

Assumption - step 1: Sliding plane description	A. Slope-blanket	B. Slope-interface	C. Slope-sand	D. Crest-blanket	E. Crest-interface	F. Crest-sand
Left circle:						
X-coordinate centre point	51.36	49.25	45.02	45.02	47.34	45.02
Y-coordinate centre point	16.55	14.94	13.33	15.74	17.35	14.13
Radius	11.36	10.04	8.72	10.74	12.45	9.52
Right circle:						
X-coordinate centre point	56.6	54.45	54.99	54.99	55.53	54.99
Y-coordinate centre point	7.11	7.11	10.97	7.11	7.11	11.46
Radius	1.92	2.21	6.36	2.11	2.21	6.84
Left entry point:						
X-coordinate	42.005	40.05	36.35	34.75	35.62	35.62
Y-coordinate	10.04	10.86	12.38	12.6	12.6	12.6
Right exit point:						
X-coordinate	58.53	56.66	59.96	57.1	57.73	60.18
Y-coordinate	7	7	7	7	7	7
Safety factor:	0.42	0.53	0.91	0.84	0.71	0.91

Slip Plane Uplift Van

Layers

6. Klei, deklaag
5. Zand, antropogeen
4. Klei, dijksmateriaal
3. Klei, deklaag
2. Opbarstzone
1. Zand

Radius : 11,36 [m]
Safety : 0,42

Xm : 51,36 [m]
Ym : 16,55 [m]

D-Geo Stability 18.1 : STBI normaal dp 20-52-PLlineseigen-slope-blanket.sti

<Not Registered> <Not Registered>	<Not Registered> <Not Registered> <Not Registered>	Phone Fax	<Not Registered> <Not Registered>	date 8-11-2018
Sliding plane location: Through the slope and in the blanket layer				
Grebbedijk case				Annex

Slip Plane Uplift Van

Layers

- 6. Klei, deklaag
- 5. Zand, antropogeen
- 4. Klei, dijksmateriaal
- 3. Klei, deklaag
- 2. Opbarstzone
- 1. Zand

T1

2

4

Xm : 49,25 [m]
Ym : 14,94 [m]

Radius : 10,04 [m]
Safety : 0,53

D-Geo Stability 18.1 : STBI normaal dp 20-52-PLlineseigen-forbiddenlineincrest-slope-interface-slidingdepth300.sti

			date
<Not Registered>	<Not Registered>	Phone <Not Registered>	8-11-2018
<Not Registered>	<Not Registered> <Not Registered>	Fax <Not Registered>	

Sliding plane location:

Through the slope and at the interface

Grebbedijk case

Annex

Slip Plane Uplift Van

Layers

- 6. Klei, deklaag
- 5. Zand, antropogeen
- 4. Klei, dijksmateriaal
- 3. Klei, deklaag
- 2. Opbarstzone
- 1. Zand

Radius : 8,72 [m]
Safety : 0,91

Xm : 45,02 [m]
Ym : 13,33 [m]

D-Geo Stability 18.1 : STBI normaal dp 20-52-PLlineseigen-forbiddenlineinfullcrest-slidingplanedepth470.sti

<Not Registered> <Not Registered>	<Not Registered> <Not Registered> <Not Registered>	Phone Fax	<Not Registered> <Not Registered>	date 8-11-2018
Sliding plane location: Through the slope and in the sand layer				
Grebbedijk case				Annex

Slip Plane Uplift Van

Layers

- 6. Klei, deklaag
- 5. Zand, antropogeen
- 4. Klei, dijksmateriaal
- 3. Klei, deklaag
- 2. Opbarstzone
- 1. Zand

Radius : 10,74 [m]
Safety : 0,84

Xm : 45,02 [m]
Ym : 15,74 [m]

D-Geo Stability 18.1 : STBI normaal dp 20-52-PLlineseigen-crest-blanket.sti

<Not Registered> <Not Registered>	<Not Registered> <Not Registered> <Not Registered>	Phone Fax	<Not Registered> <Not Registered>	date 8-11-2018

Sliding plane location:

Through crest and in the blanket layer

Grebbedijk case

Annex

Slip Plane Uplift Van

Layers

6. Klei, deklaag
5. Zand, antropogeen
4. Klei, dijksmateriaal
3. Klei, deklaag
2. Opbarstzone
1. Zand

Radius : 12,45 [m]
Safety : 0,71

Xm : 47,13 [m]
Ym : 17,35 [m]

D-Geo Stability 18.1 : STBI normaal dp 20-52-PLlineseigen_crest_interface_forbiddenline.sti

<Not Registered> <Not Registered>	<Not Registered> <Not Registered> <Not Registered>	Phone <Not Registered> Fax <Not Registered>	date 8-11-2018

Sliding plane location:

Through the crest and at the interface

Grebbedijk case

Annex

Slip Plane Uplift Van

Layers

- 6. Klei, deklaag
- 5. Zand, antropogeen
- 4. Klei, dijksmateriaal
- 3. Klei, deklaag
- 2. Opbarstzone
- 1. Zand

T1

5

4

2

Xm : 45,02 [m]
Ym : 14,13 [m]

Radius : 9,52 [m]
Safety : 0,91

D-Geo Stability 18.1 : STBI normaal dp 20-52-PLlineseigen-forbiddenlineincrest-crest-sand-slidingdepth500.sti

			date
<Not Registered> <Not Registered>	<Not Registered> <Not Registered> <Not Registered>	Phone <Not Registered> Fax <Not Registered>	8-11-2018

Sliding plane location:

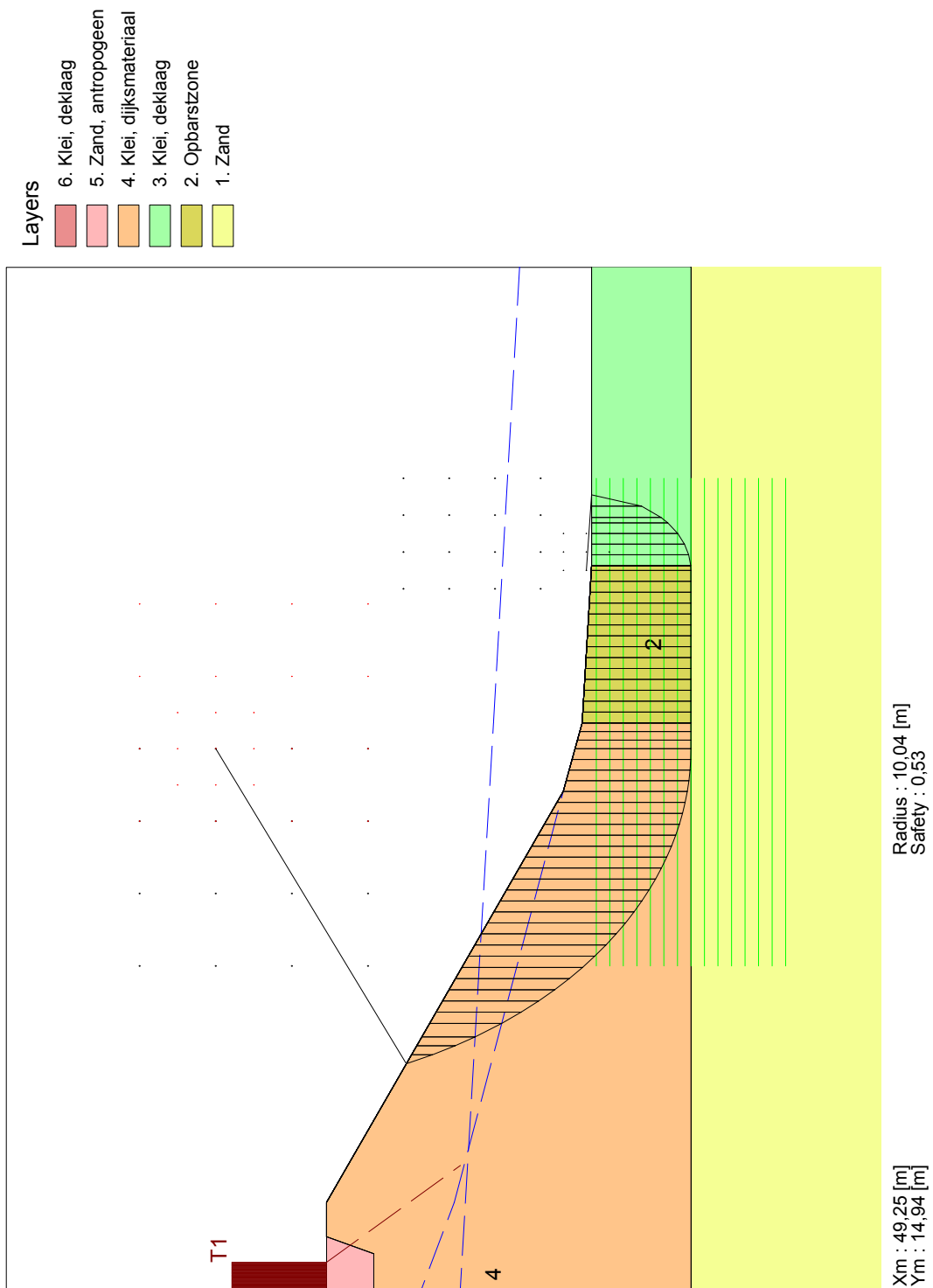Through the crest and in the sand layer

Grebbedijk case

Annex

C.2. Sensitivity analysis

The sliding planes used in the sensitivity analysis (section 5.4) are presented below.

Table C.2: Details on the calculate sliding plane locations

Assumption - step 1: Sliding plane description	Grebbendijk Original case	Thin blanket layer	Thick blanket layer	No foreshore	Long foreshore	Wide crest and gentle slope
Assumption-option	1B	1C	1A	1C	1B	1B
Left circle:						
X-coordinate centre point	49.25	44.49	49.25	47.13	47.13	53.47
Y-coordinate centre point	14.94	13.95	17.35	10.92	16.55	18.16
Radius	10.04	8.23	13.35	6.52	11.65	13.26
Right circle:						
X-coordinate centre point	54.45	54.63	50.69	57.14	51.76	61.98
Y-coordinate centre point	7.11	19.74	8.07	7.11	7.59	7.11
Radius	2.21	14.03	4.07	2.71	2.69	2.21
Left entry point:						
X-coordinate	40.04	36.4	36.92	40.625	36.21	42.12
Y-coordinate	10.86	12.36	12.15	10.67	12.45	11.28
Right exit point:						
X-coordinate	56.66	60.5	54.62	59.85	54.395	64.19
Y-coordinate	7	7	7	7	7.02	7
Safety factor:	0.53	0.86	0.82	0.43	0.94	1.07

Slip Plane Uplift Van

Layers

- 6. Klei, deklaag
- 5. Zand, antropogeen
- 4. Klei, dijksmateriaal
- 3. Klei, deklaag
- 2. Opbarstzone
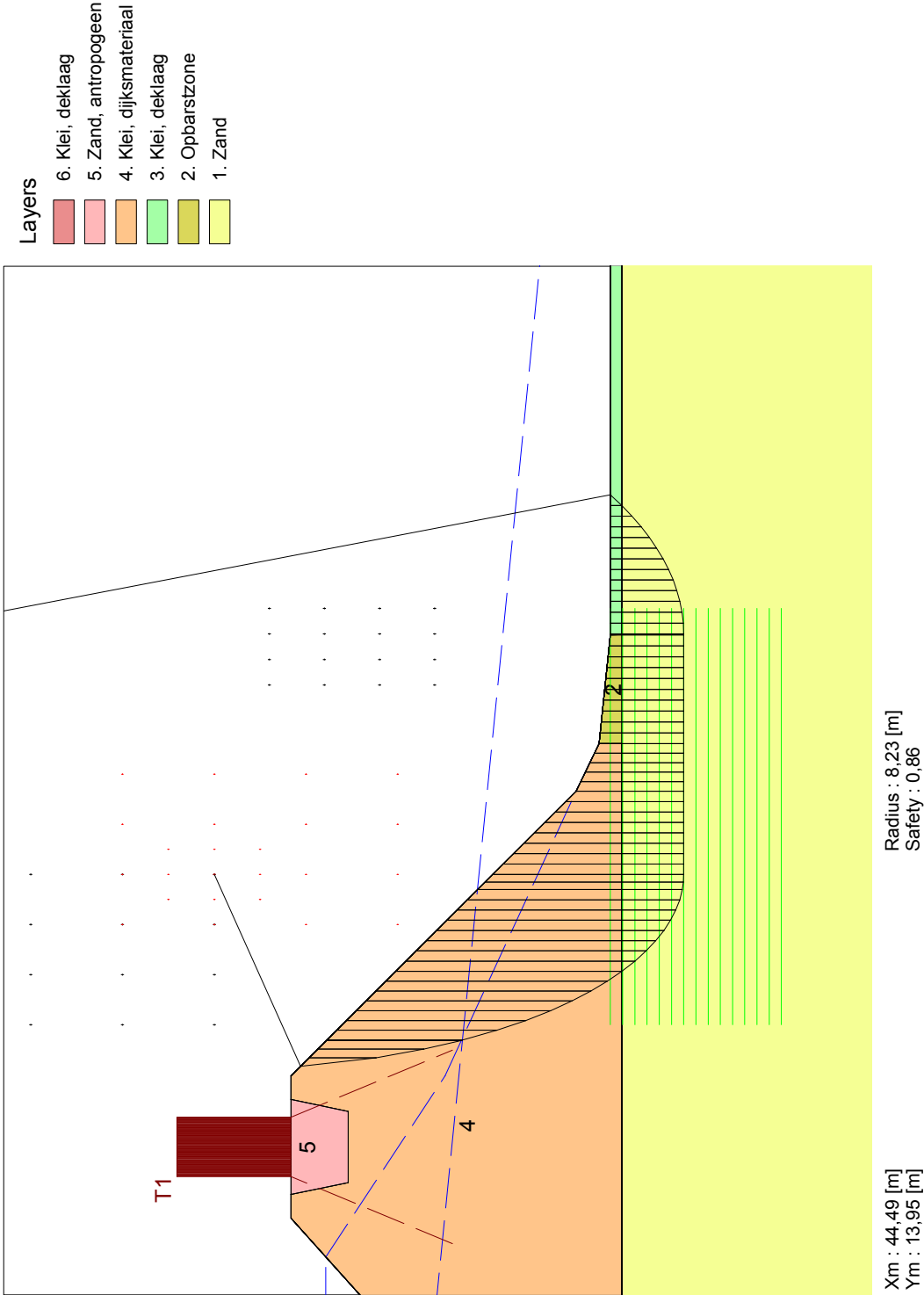- 1. Zand

T1

2

4

Radius : 10,04 [m]
Safety : 0,53

Xm : 49,25 [m]
Ym : 14,94 [m]

D-Geo Stability 18.1 : STBI normaal dp 20-52-PLlineseigen-forbiddenlineincrest-slope-interface-slidingdepth300.sti

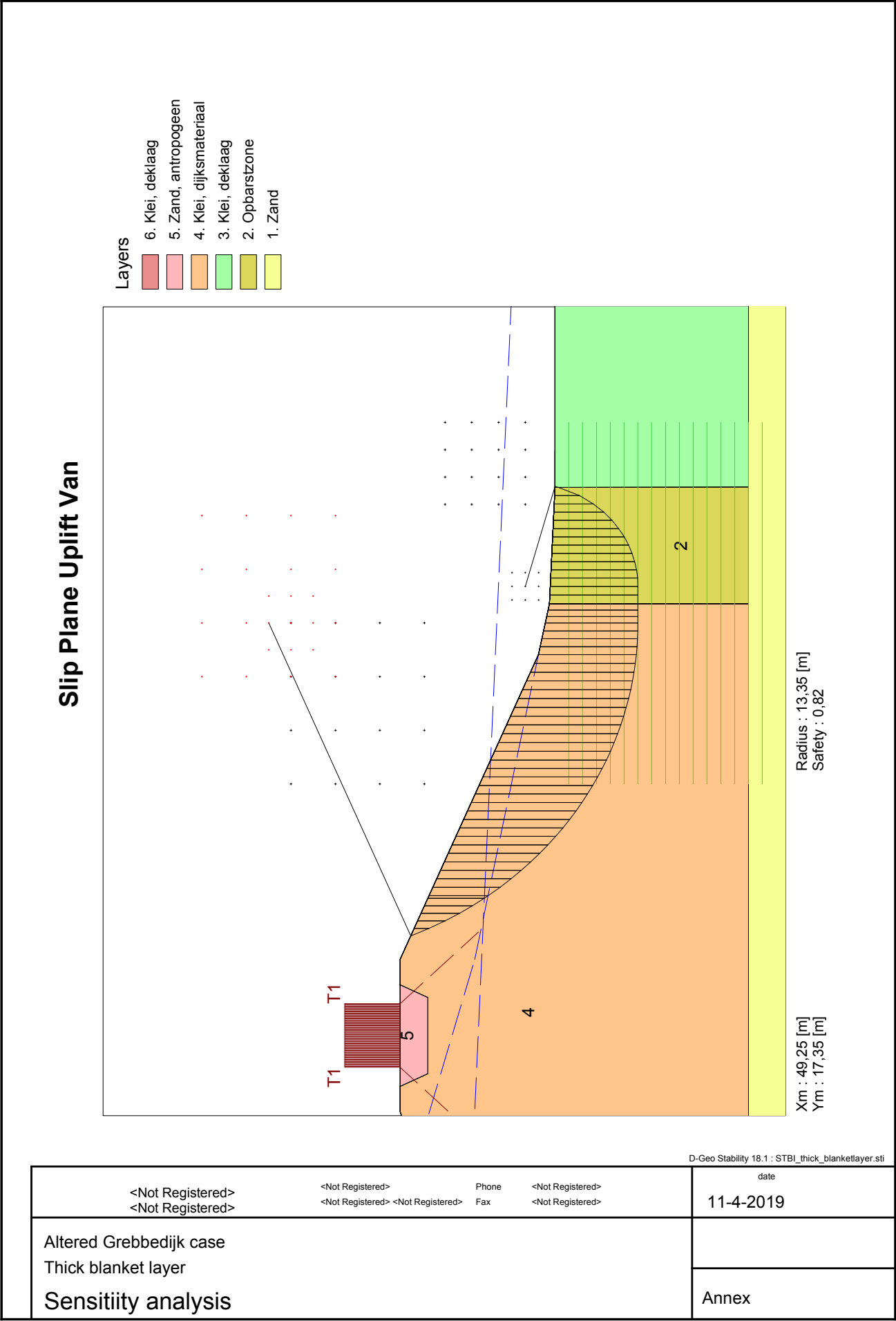|				date
<Not Registered> <Not Registered>	<Not Registered> <Not Registered> <Not Registered>	Phone Fax	<Not Registered> <Not Registered>	8-11-2018

Sliding plane location:

Through the slope and at the interface
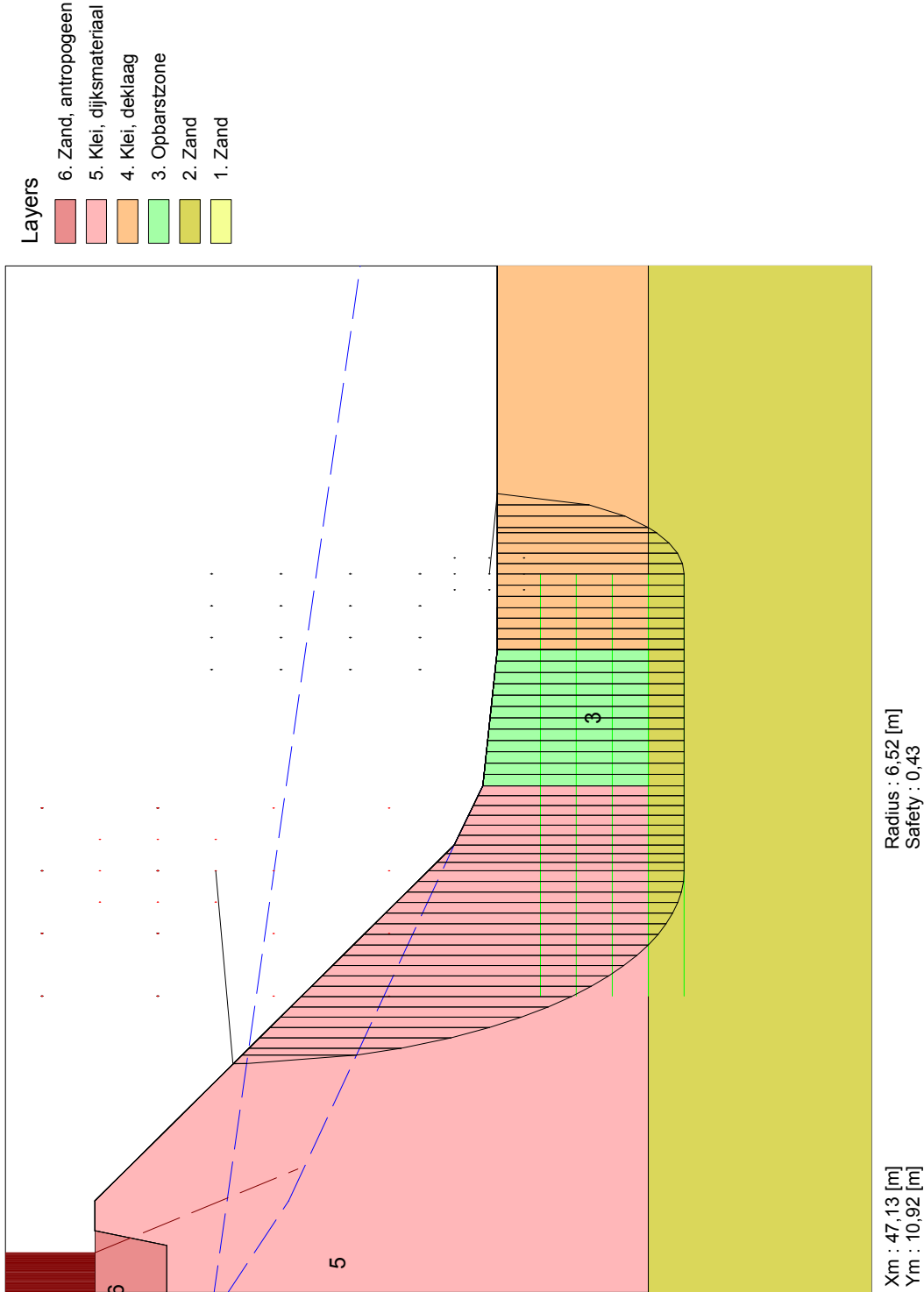
Grebbedijk case

Annex

Slip Plane Uplift Van

Layers

6. Klei, deklaag
5. Zand, antropogeen
4. Klei, dijksmateriaal
3. Klei, deklaag
2. Opbarstzone
1. Zand

T1

5

4

2

Radius : 8,23 [m]
Safety : 0,86

Xm : 44,49 [m]
Ym : 13,95 [m]

D-Geo Stability 18.1 : STBI_thin_blanketlayer.sti

				date
<Not Registered> <Not Registered>	<Not Registered> <Not Registered> <Not Registered>	Phone Fax	<Not Registered> <Not Registered>	11-4-2019
Altered Grebbedijk case Thin blanket layer				
Sensitivity analysis				Annex

Slip Plane Uplift Van

Layers

6. Klei, deklaag
5. Zand, antropogeen
4. Klei, dijksmateriaal
3. Klei, deklaag
2. Opbarstzone
1. Zand

Radius : 13,35 [m]
Safety : 0,82

Xm : 49,25 [m]
Ym : 17,35 [m]

D-Geo Stability 18.1 : STBI_thick_blanketlayer.sti

				date
<Not Registered> <Not Registered>	<Not Registered> <Not Registered> <Not Registered>	Phone Fax	<Not Registered> <Not Registered>	11-4-2019
Altered Grebbedijk case Thick blanket layer				
Sensitiity analysis				Annex

Slip Plane Uplift Van

Layers

6. Zand, antropogeen
5. Klei, dijksmateriaal
4. Klei, deklaag
3. Opbarstzone
2. Zand
1. Zand

3

5

6

Radius : 6,52 [m]
Safety : 0,43

Xm : 47,13 [m]
Ym : 10,92 [m]

D-Geo Stability 18.1 : STBI_short_seepagelength.sti

	<Not Registered>	Phone	<Not Registered>	date
<Not Registered> <Not Registered>	<Not Registered> <Not Registered>	Fax	<Not Registered>	11-4-2019

Altered Grebbedijkcase

No foreshore

Sensitivity analysis

Annex

Slip Plane Uplift Van

Layers

6. Klei, deklaag
5. Zand, antropogeen
4. Klei, dijksmateriaal
3. Klei, deklaag
2. Opbarstzone
1. Zand

Radius : 11,65 [m]
Safety : 0,94

Xm : 47,13 [m]
Ym : 16,55 [m]

D-Geo Stability 18.1 : STBI_long_seepagelength.sti

			date
<Not Registered> <Not Registered>	<Not Registered> <Not Registered> <Not Registered>	Phone <Not Registered> Fax <Not Registered>	11-4-2019
Altered Grebbedijk case Long foreshore			
Sensitivity analysis			Annex

Slip Plane Uplift Van

Layers

- 6. Klei, deklaag
- 5. Zand, antropogeen
- 4. Klei, dijksmateriaal
- 3. Klei, deklaag
- 2. Opbarstzone
- 1. Zand

Radius : 13,26 [m]
Safety : 1,07

Xm : 53,47 [m]
Ym : 18,16 [m]

D-Geo Stability 18.1 : STBI_brederedijk.sti

			date
<Not Registered> <Not Registered>	<Not Registered> <Not Registered> <Not Registered>	Phone <Not Registered> Fax <Not Registered>	15-4-2019
Altered Grebbedijk case Wider crest and fainter slope			
Sensitivity analysis			Annex

D
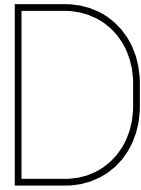
17 detailed assumption-scenarios descriptions

This appendix is a supplement to chapter 5. In this appendix, 17 assumption-scenarios are compared with the base case. In the first section D.1, the effect of the interaction is discussed using the sub mechanisms (uplift, heave and piping). The second section D.2 lists all the calculation values used for this analysis.

These scenarios deviate from the base case by one assumption-step. For example, the base case uses option B (0.35 H lowering) for assumption-step 2. When this assumption-step is changed to option A (1m lowering), this leads to a new assumption-scenario (1E, 2A, 3B, 4B, 5B, 6B, 7A.) and when it is changed to option C (0.5 H lowering) it leads to scenario (1E, 2C, 3B, 4B, 5B, 6B, 7A.). This allows seventeen assumption-scenarios to be compared simultaneously.

Table D.1 shows the values of the non-variable parameters that are used throughout the complete quantification.

Table D.1: Non-variable parameters used throughout calculation

Parameter	Value	Unit
(X_{top}, Y_{top})	(36.0, 12.6)	[m]
(X_{knik}, Y_{knik})	(48.0, 7.6)	[m]
(X_{knik2}, Y_{knik2})	(52.0, 7.2)	[m]
(X_{toe}, Y_{toe})	(54.58, 7.0)	[m]
Y_{polder}	7.0	[m]
$Y_{blanketlayer}$	4.9	[m]
L_f	35.0	[m]
γ_{sat}	17.90	[kN/m^3]
γ_{water}	9.81	[kN/m^3]
η	0.25	[-]
γ_p	20.00	[kN/m^3]
g	9.81	[m^2/s]
Θ	37.00	[°]
d_{70m}	3.07E-04	[m]
d_{70}	2.08E-04	[m]
ν_{water}	1.33E-06	[m^2/s]
k	4.51E-04	[m/day]
D	22.00	[m]
$\phi(x)$	distribution	[-]
$h_p(x)$	distribution	[-]
h	11.99	[m + NAP]

D.1. Results of 17 assumption-scenarios

In the section 5.2, the interaction of slope stability to backward erosion piping was elaborated using the base case. This base case is one assumption scenario. However, we are also interested in the consequences of the assumptions made in the assumption steps on the interaction. Plots are made of the range of FoS-values to illustrate these consequences, in which the range is created by taking the base case and changing one assumption-step-option at the time. For example, the base case (1E, 2B, 3B, 4B, 5B, 6B, 7A.) uses option B (0.35 H lowering) for assumption-step 2. When this assumption-step is changed to option A (1m lowering), this leads to a new assumption-scenario (1E, 2A, 3B, 4B, 5B, 6B, 7A.) and when it is changed to option C (0.5 H lowering) it leads to scenario (1E, 2C, 3B, 4B, 5B, 6B, 7A.). By repeatedly changing one assumption step from the base case, a total of seventeen assumption scenarios are created. This allows this seventeen assumption-scenarios to be compared simultaneously. For each of these scenarios, the values used for calculation are shown in section D.2.

Figure D.1 shows the range of the interaction of uplift in these 17 scenarios. The assumption scenarios in which the option of step 1 are varied and the other step options remain the same as the base case are shown in the first six bars in this figure. The values used in the calculation of these six scenarios are presented in Table D.3 in the section D.2. The corresponding figures with the remaining profile and FoS uplift distribution can also be found in this section D.2 (Figures D.5, D.6, D.7, D.8, D.9 and D.10).

In Figure D.1 can be seen that in two scenario steps, the options chosen for the assumption-scenario result in a range in the interaction for the sub-mechanism of uplift. These two steps are step 1: Sliding plane location, and shape and step 5: Blanket layer thickness. The range created by step 5 is significantly larger than the range created in step 1.

For step 5, option A (only intact thickness) shows a negative difference, which indicates a negative interaction for assumption scenario 1E, 2B, B, 4B, 5A, 6B, 7A. In this option, it is assumed that the remoulded soil in the berm offers no resistance due to cracks in the soil. So, when there is no intact layer left in the berm (as is the case in the scenarios which include 1E.), uplift occurs ($FoS_u = 0$) in the berm. Figure D.17 shows the uplift distribution over the levee cross-section for this scenario. In the options B and C of step 5, the berm does

offer a resistance against uplift, which makes that the lowest point in the uplift distribution is at the end of the berm.

Step 1 consists of different sized sliding planes. In Figure D.1, the options C. and F. give a peak in the difference. These two options have in common that they reach into the sand layer and that they displace more soil as shown in figures D.7 and D.10. This leads to a larger and longer berm. So, when the exit point is located at the end of this berm, it is located even more land-inward than in the base case. This explains why there is an increase in the difference of FoS_u.
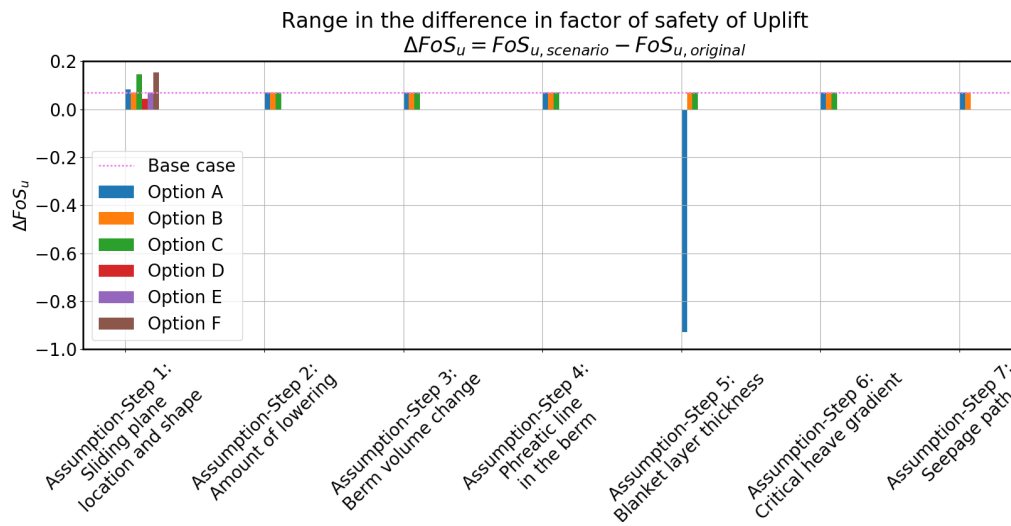
Figure D.1: Range in factor of safety uplift FoS_u due to a change of a single assumption option from the base case

Figure D.1 depicts no changes in the difference in uplift compared to the base case, for the scenarios including the options of steps 2, 3, 4, 6 and 7. This is due to the fact that for these scenarios the exit point is located at the end of the berm and these steps only affect the properties of the remoulded soil in the berm, except for step 2. This step can change the length of the berm (via the rotation angle (δ) and $X_{r,exit}$) which affects the uplift distribution via the blanket layer thickness. However, for these scenarios the changes in exit point location are so small (order of centimetres) and still at the end of the berm.

When looking at these 17 scenarios for uplift, it can be concluded that the assumptions of steps 1 and 5 have the most significant effect on the total interaction from uplift. Both steps influence the uplift distribution through the size and the resistance of the berm, which leads to a change in exit point location compared to the original exit point location.
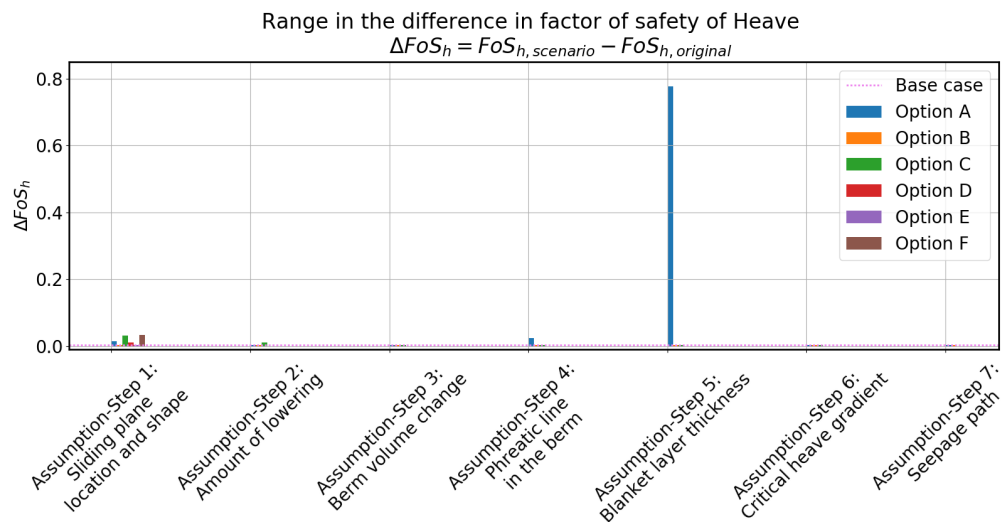
Figure D.2: Range in factor of safety heave FoS_h due to a change of a single assumption option from the base case

Figure D.2 presents the range created by the seventeen scenarios for the factor of safety of heave. When looking at figure D.2, the first noticeable thing is that the differences for heave for all 17 assumption scenarios are positive and in the order of magnitude of 10^{-2}, except for assumption scenario including option 5A. The difference between scenario (1E, 2B, 3B, 4B, 5A, 6B, 7A) and the other 16 scenarios is the location of the exit point (Figure D.17 and Appendix D.2). In the 16 scenarios, the exit point is behind the berm, but the exit point for 5A is in the berm. If the exit point is located in the berm, the height of the berm will add resistance to heave apart from the original blanket layer thickness. This leads to a higher FoS_h which in turn leads to a higher difference of ΔFoS_h.

In addition, Figure D.2 shows that the scenarios including assumption steps 1 and 4 give small differences compared to the base case.

The different exit point locations mainly cause the differences in step 1, which depends on the length of the berm, which is related to the size of the sliding plane. In this step, it also depends on whether the blanket layer is perforated or not and thus whether the head in the aquifer has dropped to its limit.

In the scenario including 4A, the exit point is located just in the berm (30 cm from the end). Because of this, the thickness of the blanket layer used to calculate heave gradient is thicker (13 cm). The head difference is also slightly larger (1 cm) because the exit point is closer to the river. Because of the ratio of these two parameters, the heave gradient is larger (0.02).

However, the small order of magnitude makes the results sensitivity to rounding errors. Depending on the length of the berm and the original location of the exit point the difference can be small (as is the case for these 16 scenarios)
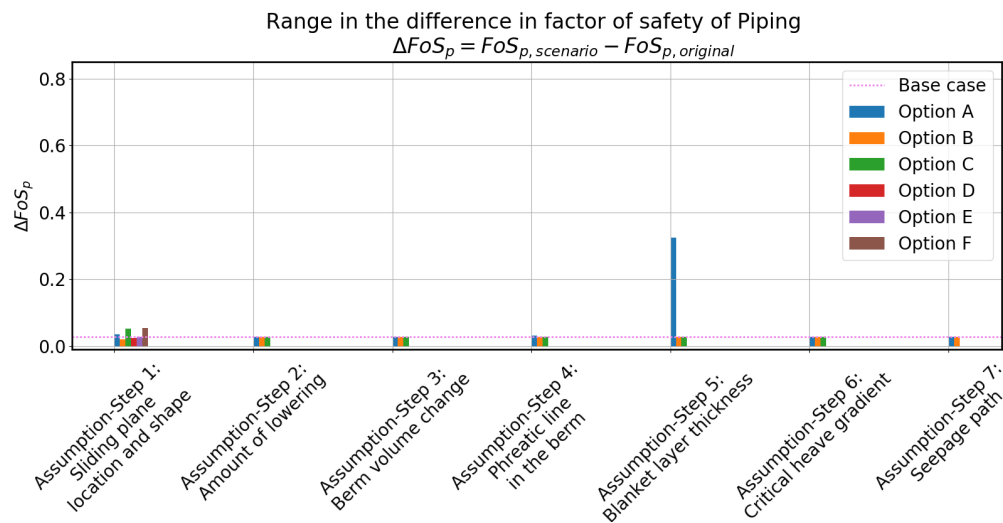
Figure D.3: Range in factor of safety piping FoS_p due to a change of a single assumption option from the base case

The range of differences in the factor of safety of piping is the smallest of the three ranges. Figure D.3 shows that the range is caused by step 1 and 5. Herein, step 5 stands out the most.

The difference in step 5 is caused by the ratio of the seepage length (in this case shorter due to the location of the exit point on the berm) and the blanket layer thickness (in this case thicker due to the position of the exit point), which in this case is positive.

The differences in scenario step 1 can be explained by the different exit point locations that directly influence the seepage length. The sliding planes influence the size and length of the berm, which alters the exact position of the exit point. This location affects the seepage length. If the seepage length is larger than the original, the FoS_p is larger when the other parameters stay the same.

What is also striking is that the scenario options of step 7 (seepage path) do not give a range. This is also due to the exit point location together with the fixed underlying assumptions that the seepage path will only be able to follow the sliding plane shape if the exit point is located in the berm. This is not the case here, and therefore the step does not lead to deviations from the base case.

D.2. Values used for calculation of the 17 scenarios

D.2.1. Base case
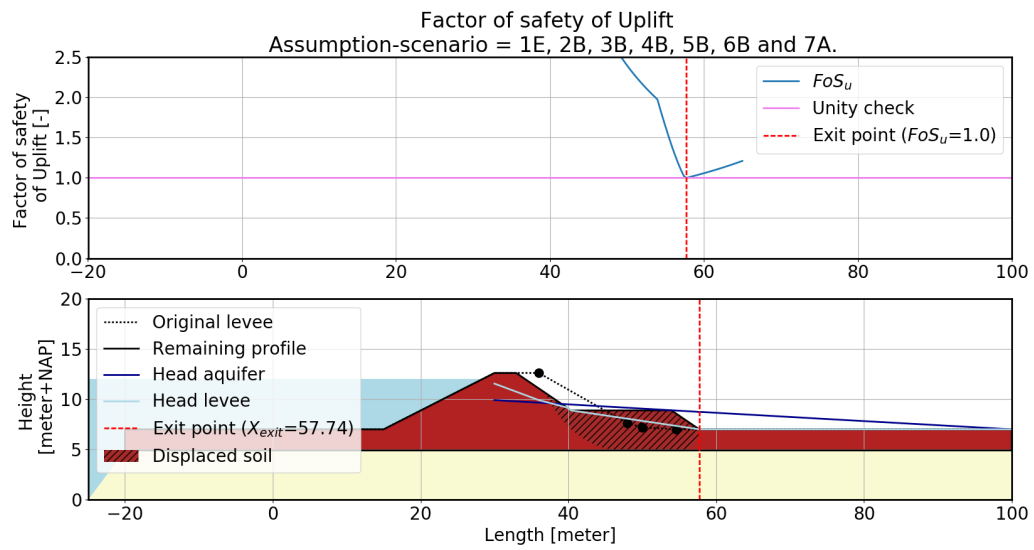
Figure D.4: Factor of safety of uplift of the remaining profile (assumption-scenario = 1E, 2B, 3B, 4B, 5B, 6B, 7A.)

Table D.2: Parameter used in BEP analysis of the assumption-scenario = 1E, 2B, 3B, 4B, 5B, 6B, 7A.

Parameter	Value	Unit	Analysis
$X_{sp,entry}$	35.62	[m]	Stability
$Y_{sp,entry}$	12.60	[m]	Stability
$X_{sp,exit}$	57.73	[m]	Stability
$Y_{sp,exit}$	7.00	[m]	Stability
$X_{m,circle1}$	47.34	[m]	Stability
$Y_{m,circle1}$	17.35	[m]	Stability
$R_{circle1}$	12.45	[m]	Stability
$X_{m,circle2}$	55.53	[m]	Stability
$Y_{m,circle2}$	7.11	[m]	Stability
$R_{circle2}$	2.21	[m]	Stability
H_{sp}	5.60	[m]	Displacement
$A(2)$	1.96	[m]	Displacement
(X_r, Y_r)	(36.85, 10.64)	[m]	Displacement
(X_{newtop}, Y_{newtop})	(32.93, 12.6)	[m]	Displacement
(X_{newtoe}, Y_{newtoe})	(44.13, 7.0)	[m]	Displacement
$S1$	0.41	[−]	Displacement
$S2$	0.64	[−]	Displacement
δ	10.55	[°]	Displacement
$(X_{r,exit}, Y_{r,exit})$	(57.71, 7.4)	[m]	Displacement
$Area$	24.27	[m^2]	Displacement
L_{berm}	13.58	[m]	Displacement
$A_{berm}(3)$	25.49	[m^2]	Displacement
$(X_{bermstart}, Y_{bermstart})$	(40.38, 8.88)	[m]	Displacement
$(X_{bermend}, Y_{bermend})$	(53.96, 8.88)	[m]	Displacement
$(X_{bermendlow}, Y_{bermendlow})$	(57.71, 7.0)	[m]	Displacement
$d(X_{exit}), d_i(X_{exit}), d_r(X_{exit})$	2.1, 2.1, 0.0	[m]	Displacement
$\phi_{new}(X_{exit})$	8.73	[m + NAP]	Displacement
$h_{p,new}(X_{exit})(4)$	7.00	[m + NAP]	Displacement
$\Delta\phi(X_{exit})$	1.73	[m]	Backward erosion piping
$\Delta\phi_{c,u}(X_{exit})(5)$	1.73	[m]	Backward erosion piping
$FoS_u(X_{exit})$	1.00	[−]	Backward erosion piping
X_{exit}	57.74	[m]	Backward erosion piping
$i_h(X_{exit})$	0.82	[−]	Backward erosion piping
$i_{c,h}(X_{exit})(6)$	0.30	[−]	Backward erosion piping
$FoS_h(X_{exit})$	0.37	[−]	Backward erosion piping
$H_p(X_{exit})$	4.36	[m]	Backward erosion piping
$H_{c,p}(X_{exit})$	2.96	[m]	Backward erosion piping
$d_{seepage}$	2.10	[m]	Backward erosion piping
$L(X_{exit})$	77.74	[m]	Backward erosion piping
$FoS_p(X_{exit})(7)$	0.68	[−]	Backward erosion piping

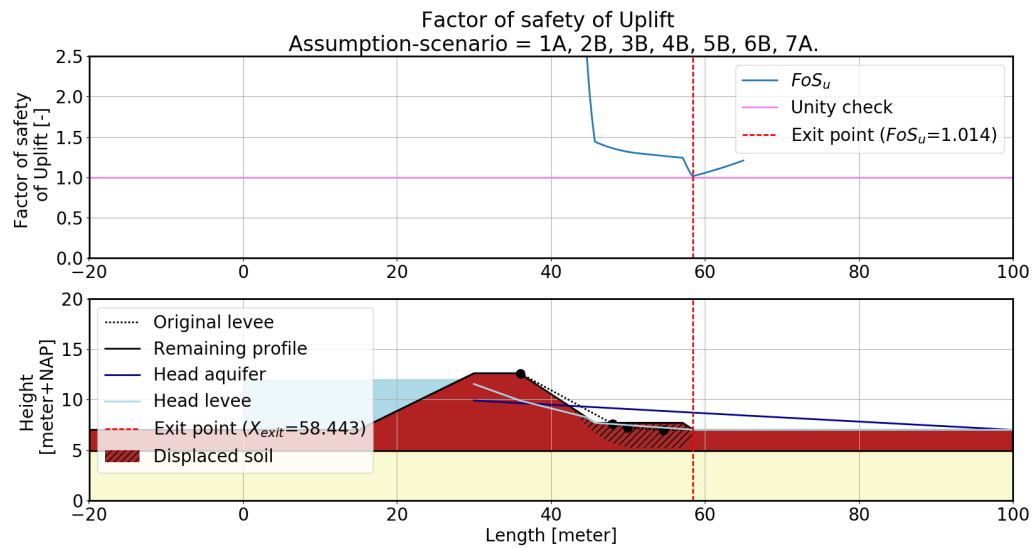## D.2.2. Base case with different scenario step 1 options

Figure D.5: Factor of safety of uplift of the remaining profile (assumption-scenario = 1A, 2B, 3B, 4B, 5B, 6B, 7A.)
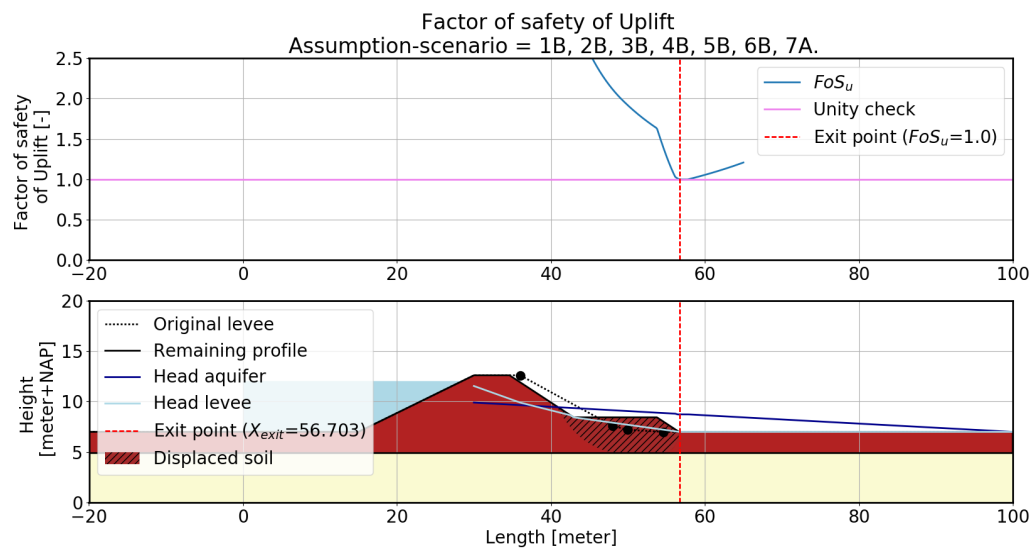

Figure D.6: Factor of safety of uplift of the remaining profile (assumption-scenario = 1B, 2B, 3B, 4B, 5B, 6B, 7A.)
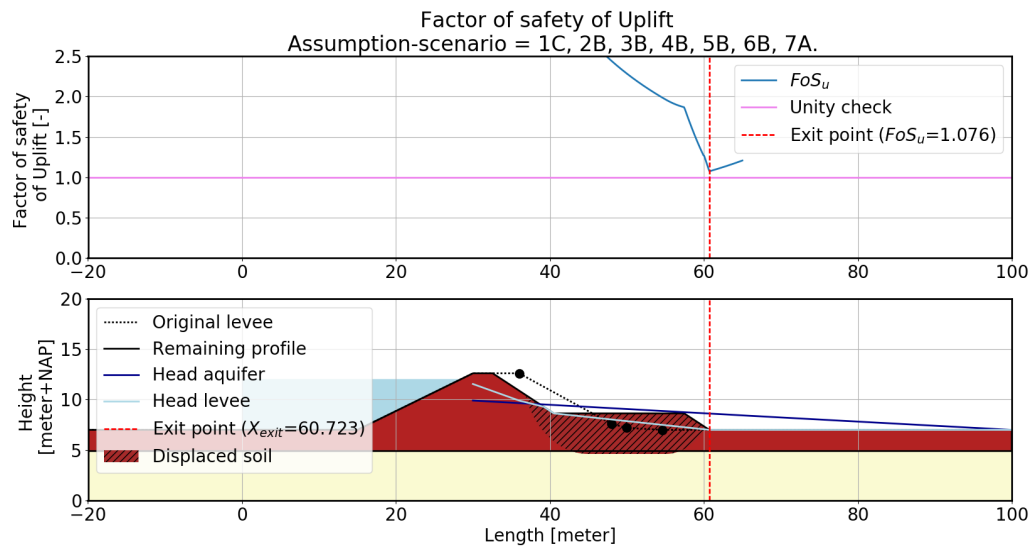
Figure D.7: Factor of safety of uplift of the remaining profile (assumption-scenario = 1C, 2B, 3B, 4B, 5B, 6B, 7A.)
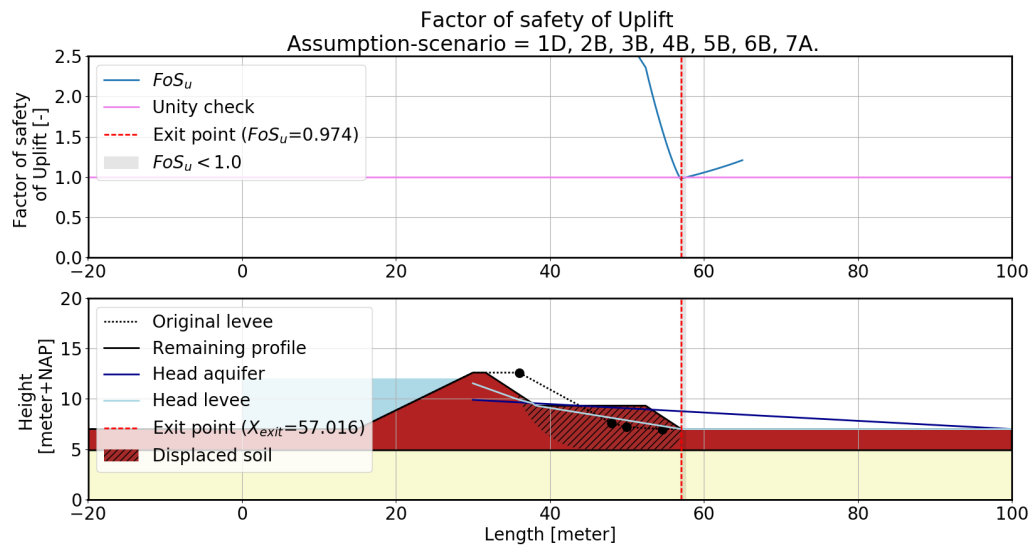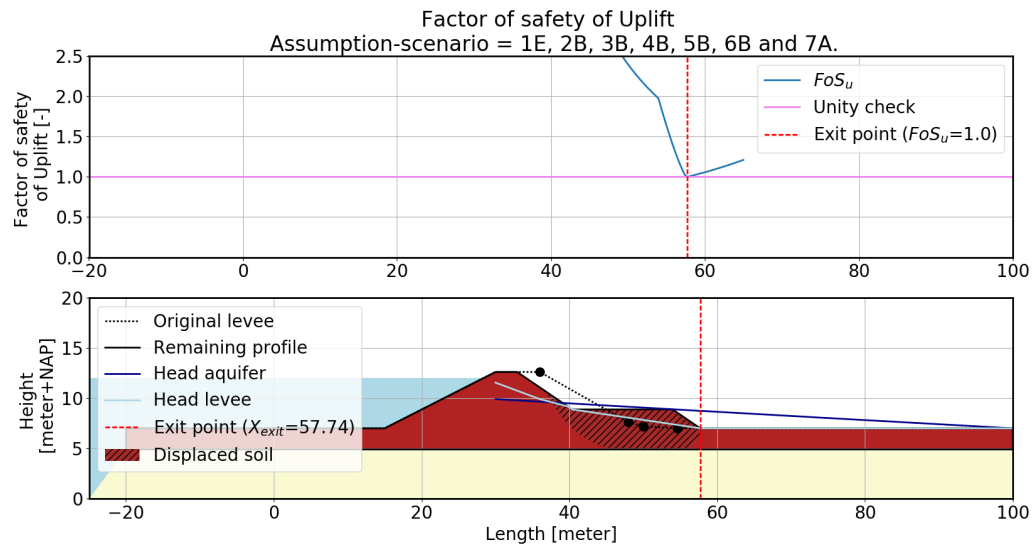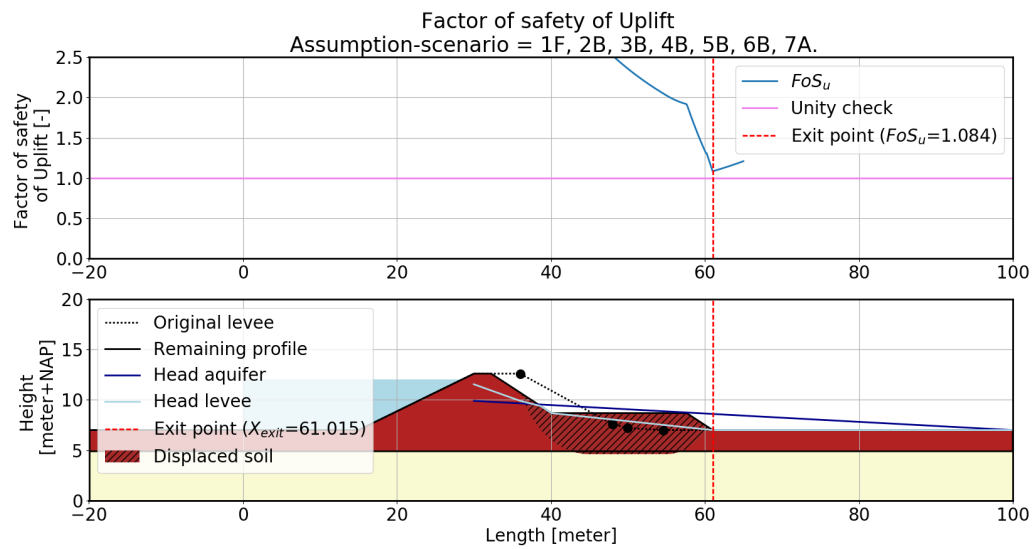

Figure D.8: Factor of safety of uplift of the remaining profile (assumption-scenario = 1D, 2B, 3B, 4B, 5B, 6B, 7A.)

Figure D.9: Factor of safety of uplift of the remaining profile (assumption-scenario = 1E, 2B, 3B, 4B, 5B, 6B, 7A.)

Figure D.10: Factor of safety of uplift of the remaining profile (assumption-scenario = 1F, 2B, 3B, 4B, 5B, 6B, 7A.)

Table D.3: Parameter used to calculated interaction base case and different assumption-option in step 1

Parameter	Unit	Analysis	1A, 2B, 3B, 4B, 5B, 6B, 7A.	1B, 2B, 3B, 4B, 5B, 6B, 7A.	1C, 2B, 3B, 4B, 5B, 6B, 7A.	1D, 2B, 3B, 4B, 5B, 6B, 7A.	Values base-case	
							1E, 2B, 3B, 4B, 5B, 6B, 7A.	1E, 2B, 3B, 4B, 5B, 6B, 7A.
Assumption-scenario								
$X_{sp,entry}$	[m]	4.3	42.01	40.05	36.35	34.75	35.62	35.62
$Y_{sp,entry}$	[m]	4.3	10.40	10.86	12.38	12.60	12.60	12.60
$X_{sp,exit}$	[m]	4.3	58.52	56.66	59.96	57.10	57.73	60.18
$Y_{sp,exit}$	[m]	4.3	7.00	7.00	7.00	7.00	7.00	7.00
$X_{m,circle1}$	[m]	4.3	51.36	49.25	45.02	45.02	47.34	45.02
$Y_{m,circle1}$	[m]	4.3	16.55	14.94	13.33	15.74	17.35	14.13
$R_{circle1}$	[m]	4.3	11.36	10.04	8.72	10.74	12.45	9.52
$X_{m,circle2}$	[m]	4.3	56.60	54.45	54.99	54.99	55.53	54.99
$Y_{m,circle2}$	[m]	4.3	7.11	7.11	10.97	7.11	7.11	11.46
$R_{circle2}$	[m]	4.3	1.92	2.21	6.36	2.11	2.21	6.84
H_{sp}	[m]	4.4	3.40	3.86	5.38	5.60	5.60	5.60
$A(2)$	[m]	4.4	1.19	1.35	1.88	1.96	1.96	1.96
(X_r, Y_r)	[m]	4.4	(42.69, 9.21)	(40.81, 9.51)	(36.77, 10.5)	(35.57, 10.64)	(36.85, 10.64)	(36.16, 10.64)
(X_{newtop}, Y_{newtop})	[m]	4.4	(35.91, 12.6)	(34.62, 12.6)	(32.57, 12.6)	(31.65, 12.6)	(32.93, 12.6)	(32.24, 12.6)
(X_{newtoe}, Y_{newtoe})	[m]	4.4	(47.11, 7.0)	(45.82, 7.0)	(43.77, 7.0)	(42.85, 7.0)	(44.13, 7.0)	(43.44, 7.0)
$S1$	[-]	4.4	0.66	0.44	0.11	0.31	0.41	0.16
$S2$	[-]	4.4	0.85	0.64	0.34	0.54	0.64	0.39
δ	[°]	4.4	0.12	0.15	0.22	0.20	10.55	0.21
$(X_{r,exit}, Y_{r,exit})$	[m]	4.4	(58.52, 7.23)	(56.65, 7.34)	(60.71, 8.19)	(57.08, 7.42)	(57.71, 7.4)	(61.01, 8.2)
$Area$	[m^2]	4.4	7.60	14.81	26.32	31.47	24.27	28.14
L_{berm}	[m]	4.4	11.41	10.82	16.94	14.23	13.58	17.57
$A_{berm}(3)$	[m^2]	4.4	7.98	15.55	27.64	33.04	25.49	29.55
$(X_{bermstart}, Y_{bermstart})$	[m]	4.4	(45.71, 7.7)	(42.95, 8.44)	(40.5, 8.63)	(38.2, 9.32)	(40.38, 8.88)	(40.08, 8.68)
$(X_{bermend}, Y_{bermend})$	[m]	4.4	(57.13, 7.7)	(53.77, 8.44)	(57.45, 8.63)	(52.43, 9.32)	(53.96, 8.88)	(57.64, 8.68)
$(X_{bermendlow}, Y_{bermendlow})$	[m]	4.4	(58.52, 7.0)	(56.65, 7.0)	(60.71, 7.0)	(57.08, 7.0)	(57.71, 7.0)	(61.01, 7.0)
$d(X_{exit}), d_l(X_{exit}), d_r(X_{exit})$	[m]	4.4	2.1, 2.1, 0.0	2.1, 2.1, 0.0	2.1, 2.1, 0.0	2.12, 1.72, 0.4	2.1, 2.1, 0.0	2.1, 2.1, 0.0
$\phi_{new}(X_{exit})$	[m + NAP]	4.4	8.43	8.43	8.43	8.76	8.73	8.60
$h_{p,new}(X_{exit})(4)$	[m + NAP]	4.4	7.00	7.00	7.00	7.00	7.00	7.00
$\Delta\phi(X_{exit})$	[m]	4.5	1.43	1.43	1.43	1.76	1.73	1.60
$\Delta\phi_{c,u}(X_{exit})(5)$	[m]	4.5	1.73	1.73	1.73	1.71	1.73	1.73
$FoS_u(X_{exit})$	[-]	4.5	1.21	1.21	1.21	0.97	1.00	1.08
X_{exit}	[m]	4.5	58.44	56.70	60.72	57.04	57.74	61.02
$i_h(X_{exit})$	[-]	4.5	0.79	0.82	0.77	0.81	0.82	0.76
$i_{c,h}(X_{exit})(6)$	[-]	4.5	0.30	0.30	0.30	0.30	0.30	0.30
$FoS_h(X_{exit})$	[-]	4.5	0.38	0.36	0.39	0.37	0.36	0.39
$H_p(X_{exit})$	[m]	4.5	4.34	4.36	4.36	4.35	4.36	4.36
$H_{c,p}(X_{exit})$	[m]	4.5	2.98	2.92	3.06	2.94	2.96	3.07
$d_{seepage}$	[m]	4.5	2.10	2.10	2.10	2.12	2.10	2.10
$L(X_{exit})$	[m]	4.5	78.44	76.70	80.72	77.04	77.74	81.02
$FoS_p(X_{exit})(7)$	[-]	4.5	0.69	0.67	0.70	0.67	0.68	0.70

D.2.3. Base case with different scenario options for step 2, 3, 4, 5, 6, 7

Table D.4: Parameter used to calculated interaction base case and different assumption-option in step 2

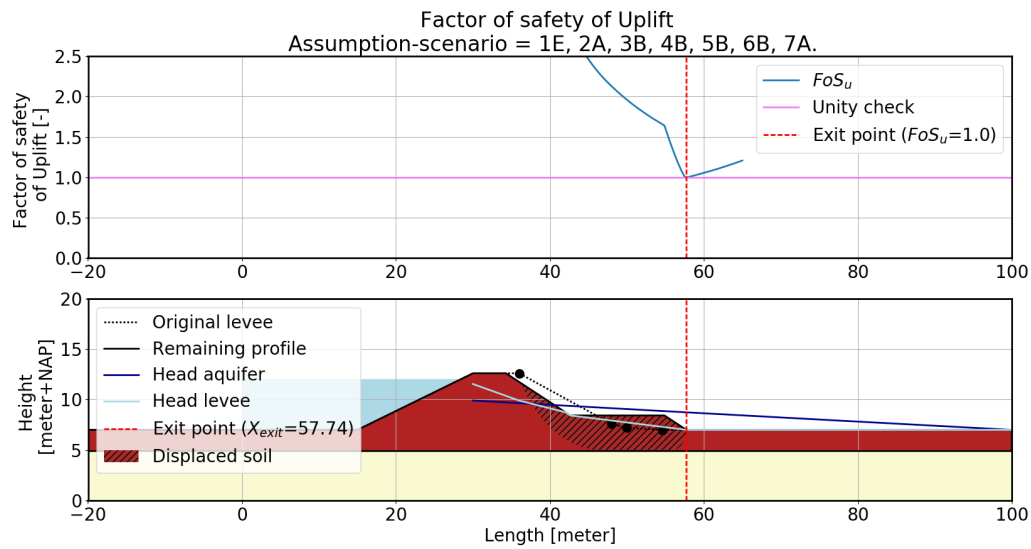| Parameter	Unit	Section		Values base-case	
Assumption-scenario	[−]	-	1E, 2A, 3B, 4B, 5B, 6B, 7A.	1E, 2B, 3B, 4B, 5B, 6B, 7A.	1E, 2C, 3B, 4B, 5B, 6B, 7A.
$X_{sp,entry}$	[m]	4.3	35.62	35.62	35.62
$Y_{sp,entry}$	[m]	4.3	12.60	12.60	12.60
$X_{sp,exit}$	[m]	4.3	57.73	57.73	57.73
$Y_{sp,exit}$	[m]	4.3	7.00	7.00	7.00
$X_{m,circle1}$	[m]	4.3	47.34	47.34	47.34
$Y_{m,circle1}$	[m]	4.3	17.35	17.35	17.35
$R_{circle1}$	[m]	4.3	12.45	12.45	12.45
$X_{m,circle2}$	[m]	4.3	55.53	55.53	55.53
$Y_{m,circle2}$	[m]	4.3	7.11	7.11	7.11
$R_{circle2}$	[m]	4.3	2.21	2.21	2.21
H_{sp}	[m]	4.4	5.60	5.60	5.60
$A(2)$	[m]	4.4	1.00	1.96	2.80
(X_r, Y_r)	[m]	4.4	(36.3, 11.6)	(36.85, 10.64)	(37.44, 9.8)
(X_{newtop}, Y_{newtop})	[m]	4.4	(34.3, 12.6)	(32.93, 12.6)	(31.84, 12.6)
(X_{newtoe}, Y_{newtoe})	[m]	4.4	(45.5, 7.0)	(44.13, 7.0)	(43.04, 7.0)
$S1$	[−]	4.4	0.41	0.41	0.41
$S2$	[−]	4.4	0.52	0.64	0.76
δ	[°]	4.4	5.44	10.55	15.27
$(X_{r,exit}, Y_{r,exit})$	[m]	4.4	(57.73, 7.21)	(57.71, 7.4)	(57.68, 7.58)
$Area$	[m²]	4.4	16.63	24.27	30.39
L_{berm}	[m]	4.4	12.23	13.58	14.64
$A_{berm}(3)$	[m²]	4.4	17.46	25.49	31.91
$(X_{bermstart}, Y_{bermstart})$	[m]	4.4	(42.64, 8.43)	(40.38, 8.88)	(38.68, 9.18)
$(X_{bermend}, Y_{bermend})$	[m]	4.4	(54.88, 8.43)	(53.96, 8.88)	(53.32, 9.18)
$(X_{bermendlow}, Y_{bermendlow})$	[m]	4.4	(57.73, 7.0)	(57.71, 7.0)	(57.68, 7.0)
$d(X_{exit}), d_i(X_{exit}), d_r(X_{exit})$	[m]	4.4	2.1, 2.1, 0.0	2.1, 2.1, 0.0	2.1, 1.75, 0.35
$\phi_{new}(X_{exit})$	[m + NAP]	4.4	8.73	8.73	8.70
$h_{p,new}(X_{exit})(4)$	[m + NAP]	4.4	7.00	7.00	7.00
$\Delta\phi(X_{exit})$	[m]	4.5	1.73	1.73	1.70
$\Delta\phi_{c,u}(X_{exit})(5)$	[m]	4.5	1.73	1.73	1.70
$FoS_u(X_{exit})$	[−]	4.5	1.00	1.00	1.00
X_{exit}	[m]	4.5	57.74	57.74	57.69
$i_h(X_{exit})$	[−]	4.5	0.82	0.82	0.81
$i_{c,h}(X_{exit})(6)$	[−]	4.5	0.30	0.30	0.30
$FoS_h(X_{exit})$	[−]	4.5	0.36	0.36	0.37
$H_p(X_{exit})$	[m]	4.5	4.36	4.36	4.36
$H_{c,p}(X_{exit})$	[m]	4.5	2.96	2.96	2.96
$d_{seepage}$	[m]	4.5	2.10	2.10	2.10
$L(X_{exit})$	[m]	4.5	77.74	77.74	77.69
$FoS_p(X_{exit})(7)$	[−]	4.5	0.68	0.68	0.68

Figure D.11: Factor of safety of uplift of the remaining profile (assumption-scenario = 1E, 2A, 3B, 4B, 5B, 6B, 7A.)
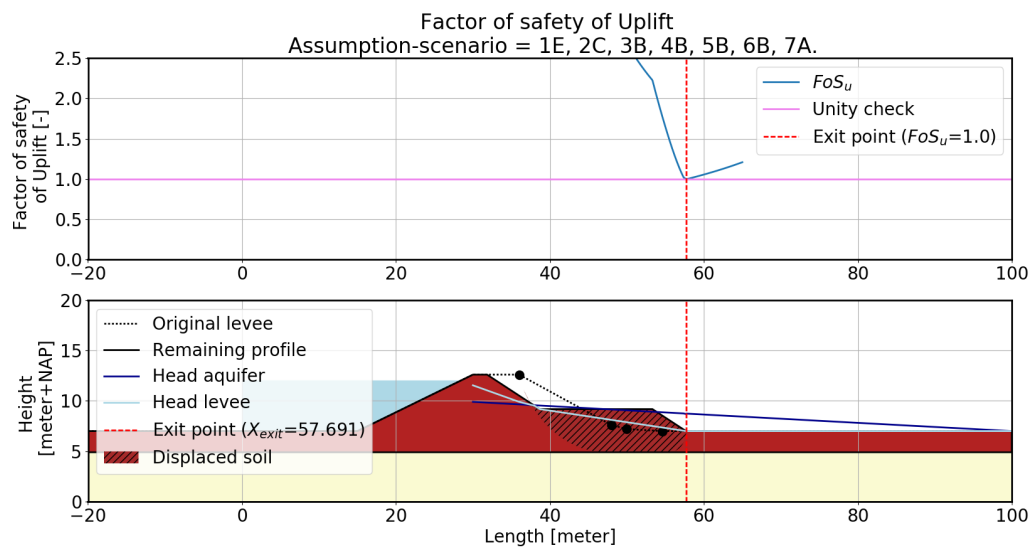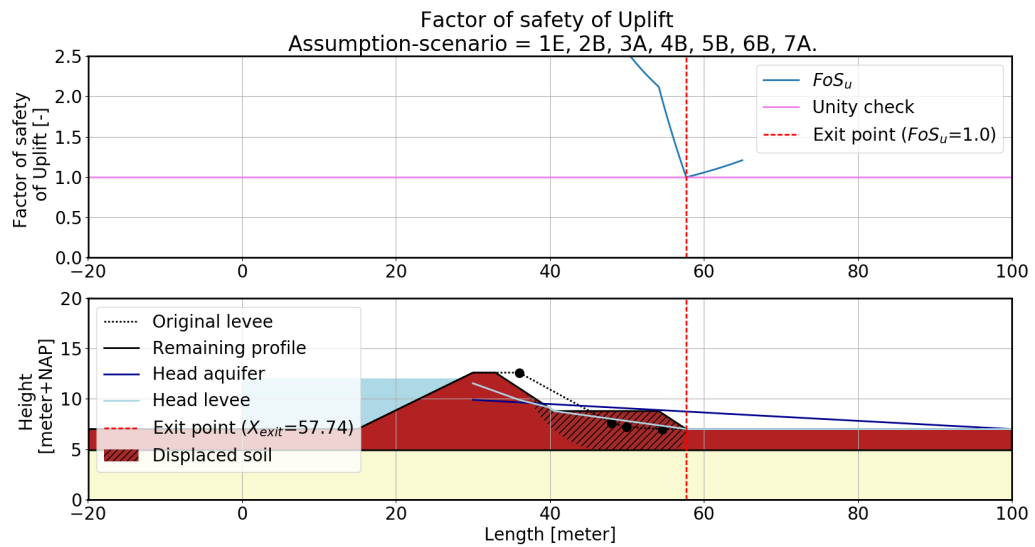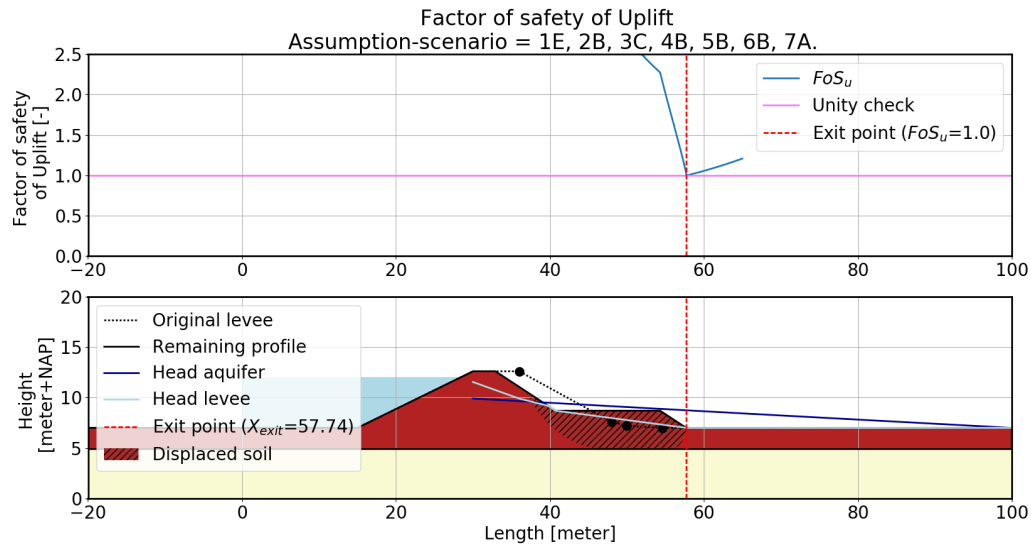

Figure D.12: Factor of safety of uplift of the remaining profile (assumption-scenario = 1E, 2C, 3B, 4B, 5B, 6B, 7A.)

Table D.5: Parameter used to calculated interaction base case and different assumption-option in step 3

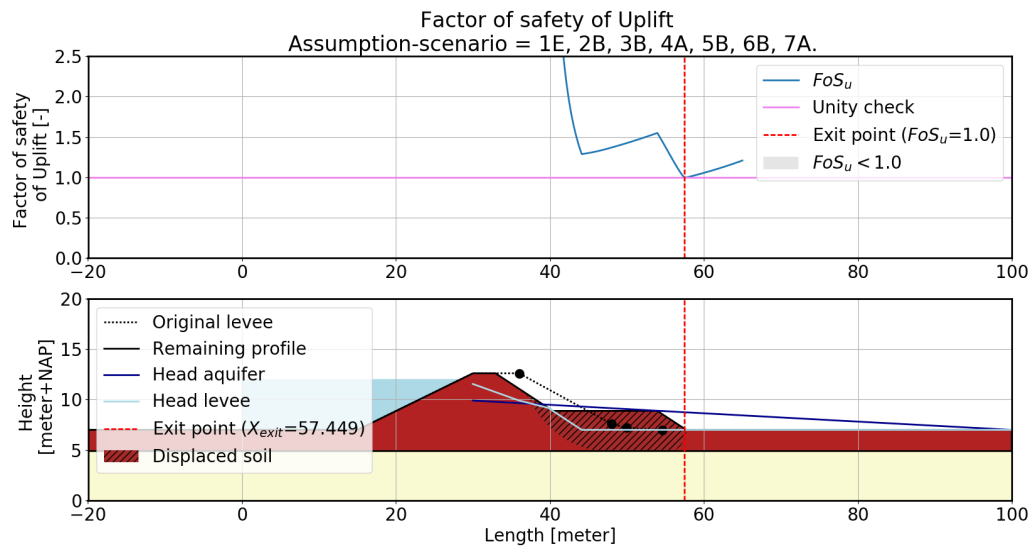| Parameter	Unit	Section		Values base-case	
Assumption-scenario	[−]	-	1E, 2B, 3A, 4B, 5B, 6B, 7A.	1E, 2B, 3B, 4B, 5B, 6B, 7A.	1E, 2B, 3C, 4B, 5B, 6B, 7A.
$X_{sp,entry}$	[m]	4.3	35.62	35.62	35.62
$Y_{sp,entry}$	[m]	4.3	12.60	12.60	12.60
$X_{sp,exit}$	[m]	4.3	57.73	57.73	57.73
$Y_{sp,exit}$	[m]	4.3	7.00	7.00	7.00
$X_{m,circle1}$	[m]	4.3	47.34	47.34	47.34
$Y_{m,circle1}$	[m]	4.3	17.35	17.35	17.35
$R_{circle1}$	[m]	4.3	12.45	12.45	12.45
$X_{m,circle2}$	[m]	4.3	55.53	55.53	55.53
$Y_{m,circle2}$	[m]	4.3	7.11	7.11	7.11
$R_{circle2}$	[m]	4.3	2.21	2.21	2.21
H_{sp}	[m]	4.4	5.60	5.60	5.60
$A(2)$	[m]	4.4	1.96	1.96	1.96
(X_r, Y_r)	[m]	4.4	(36.85, 10.64)	(36.85, 10.64)	(36.85, 10.64)
(X_{newtop}, Y_{newtop})	[m]	4.4	(32.93, 12.6)	(32.93, 12.6)	(32.93, 12.6)
(X_{newtoe}, Y_{newtoe})	[m]	4.4	(44.13, 7.0)	(44.13, 7.0)	(44.13, 7.0)
$S1$	[−]	4.4	0.41	0.41	0.41
$S2$	[−]	4.4	0.64	0.64	0.64
δ	[°]	4.4	10.55	10.55	10.55
$(X_{r,exit}, Y_{r,exit})$	[m]	4.4	(57.71, 7.4)	(57.71, 7.4)	(57.71, 7.4)
$Area$	[m²]	4.4	24.27	24.27	24.27
L_{berm}	[m]	4.4	13.58	13.58	13.58
$A_{berm}(3)$	[m²]	4.4	24.27	25.49	23.06
$(X_{bermstart}, Y_{bermstart})$	[m]	4.4	(40.56, 8.79)	(40.38, 8.88)	(40.74, 8.7)
$(X_{bermend}, Y_{bermend})$	[m]	4.4	(54.14, 8.79)	(53.96, 8.88)	(54.32, 8.7)
$(X_{bermendlow}, Y_{bermendlow})$	[m]	4.4	(57.71, 7.0)	(57.71, 7.0)	(57.71, 7.0)
$d(X_{exit}), d_i(X_{exit}), d_r(X_{exit})$	[m]	4.4	2.1, 2.1, 0.0	2.1, 2.1, 0.0	2.1, 2.1, 0.0
$\phi_{new}(X_{exit})$	[m + NAP]	4.4	8.73	8.73	8.73
$h_{p,new}(X_{exit})(4)$	[m + NAP]	4.4	7.00	7.00	7.00
$\Delta\phi(X_{exit})$	[m]	4.5	1.73	1.73	1.73
$\Delta\phi_{c,u}(X_{exit})(5)$	[m]	4.5	1.73	1.73	1.73
$FoS_u(X_{exit})$	[−]	4.5	1.00	1.00	1.00
X_{exit}	[m]	4.5	57.74	57.74	57.74
$i_h(X_{exit})$	[−]	4.5	0.82	0.82	0.82
$i_{c,h}(X_{exit})(6)$	[−]	4.5	0.30	0.30	0.30
$FoS_h(X_{exit})$	[−]	4.5	0.36	0.36	0.36
$H_p(X_{exit})$	[m]	4.5	4.36	4.36	4.36
$H_{c,p}(X_{exit})$	[m]	4.5	2.96	2.96	2.96
$d_{seepage}$	[m]	4.5	2.10	2.10	2.10
$L(X_{exit})$	[m]	4.5	77.74	77.74	77.74
$FoS_p(X_{exit})(7)$	[−]	4.5	0.68	0.68	0.68

Figure D.13: Factor of safety of uplift of the remaining profile (assumption-scenario = 1E, 2B, 3A, 4B, 5B, 6B, 7A.)
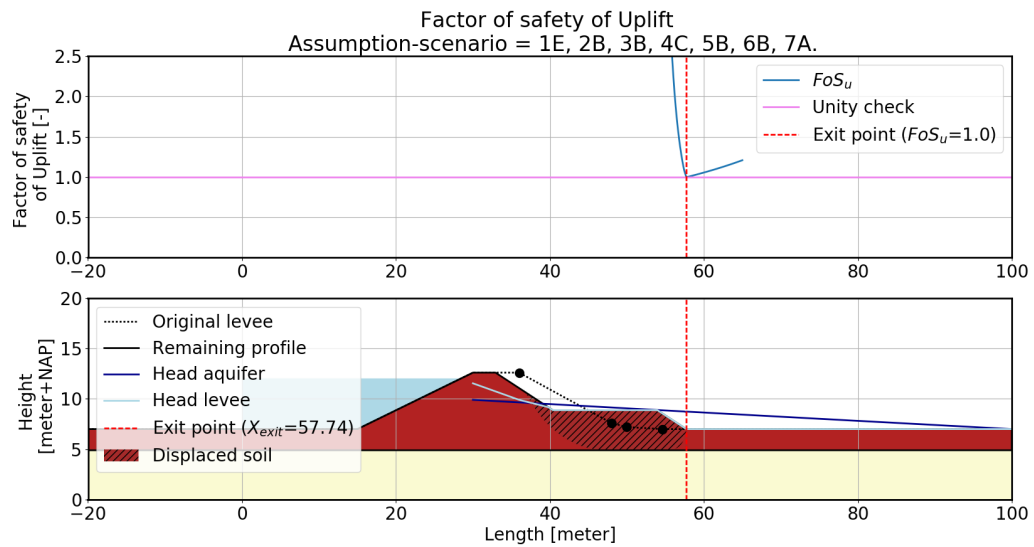
Figure D.14: Factor of safety of uplift of the remaining profile (assumption-scenario = 1E, 2B, 3C, 4B, 5B, 6B, 7A.)

Table D.6: Parameter used to calculated interaction base case and different assumption-option in step 4

| Parameter	Unit	Section		Values base-case	
Assumption-scenario	$[-]$	-	1E, 2B, 3B, 4A, 5B, 6B, 7A.	1E, 2B, 3B, 4B, 5B, 6B, 7A.	1E, 2B, 3B, 4C, 5B, 6B, 7A.
$X_{sp,entry}$	[m]	4.3	35.62	35.62	35.62
$Y_{sp,entry}$	[m]	4.3	12.60	12.60	12.60
$X_{sp,exit}$	[m]	4.3	57.73	57.73	57.73
$Y_{sp,exit}$	[m]	4.3	7.00	7.00	7.00
$X_{m,circle1}$	[m]	4.3	47.34	47.34	47.34
$Y_{m,circle1}$	[m]	4.3	17.35	17.35	17.35
$R_{circle1}$	[m]	4.3	12.45	12.45	12.45
$X_{m,circle2}$	[m]	4.3	55.53	55.53	55.53
$Y_{m,circle2}$	[m]	4.3	7.11	7.11	7.11
$R_{circle2}$	[m]	4.3	2.21	2.21	2.21
H_{sp}	[m]	4.4	5.60	5.60	5.60
$A(2)$	[m]	4.4	1.96	1.96	1.96
(X_r,Y_r)	[m]	4.4	(36.85, 10.64)	(36.85, 10.64)	(36.85, 10.64)
(X_{newtop}, Y_{newtop})	[m]	4.4	(32.93, 12.6)	(32.93, 12.6)	(32.93, 12.6)
(X_{newtoe}, Y_{newtoe})	[m]	4.4	(44.13, 7.0)	(44.13, 7.0)	(44.13, 7.0)
$S1$	$[-]$	4.4	0.41	0.41	0.41
$S2$	$[-]$	4.4	0.64	0.64	0.64
δ	[°]	4.4	10.55	10.55	10.55
$(X_{r,exit}, Y_{r,exit})$	[m]	4.4	(57.71, 7.4)	(57.71, 7.4)	(57.71, 7.4)
$Area$	[m^2]	4.4	24.27	24.27	24.27
L_{berm}	[m]	4.4	13.58	13.58	13.58
$A_{berm}(3)$	[m^2]	4.4	25.49	25.49	25.49
$(X_{bermstart}, Y_{bermstart})$	[m]	4.4	(40.38, 8.88)	(40.38, 8.88)	(40.38, 8.88)
$(X_{bermend}, Y_{bermend})$	[m]	4.4	(53.96, 8.88)	(53.96, 8.88)	(53.96, 8.88)
$(X_{bermendlow}, Y_{bermendlow})$	[m]	4.4	(57.71, 7.0)	(57.71, 7.0)	(57.71, 7.0)
$d(X_{exit}), d_i(X_{exit}), d_r(X_{exit})$	[m]	4.4	2.23, 1.11, 1.12	2.1, 2.1, 0.0	2.1, 2.1, 0.0
$\phi_{new}(X_{exit})$	[m + NAP]	4.4	8.74	8.73	8.73
$h_{p,new}(X_{exit})(4)$	[m + NAP]	4.4	7.00	7.00	7.00
$\Delta\phi(X_{exit})$	[m]	4.5	1.74	1.73	1.73
$\Delta\phi_{c,u}(X_{exit})(5)$	[m]	4.5	1.74	1.73	1.73
$FoS_u(X_{exit})$	$[-]$	4.5	1.00	1.00	1.00
X_{exit}	[m]	4.5	57.45	57.74	57.74
$i_h(X_{exit})$	$[-]$	4.5	0.78	0.82	0.82
$i_{c,h}(X_{exit})(6)$	$[-]$	4.5	0.30	0.30	0.30
$FoS_h(X_{exit})$	$[-]$	4.5	0.38	0.36	0.36
$H_p(X_{exit})$	[m]	4.5	4.32	4.36	4.36
$H_{c,p}(X_{exit})$	[m]	4.5	2.95	2.96	2.96
$d_{seepage}$	[m]	4.5	2.23	2.10	2.10
$L(X_{exit})$	[m]	4.5	77.45	77.74	77.74
$FoS_p(X_{exit})(7)$	$[-]$	4.5	0.68	0.68	0.68

Figure D.15: Factor of safety of uplift of the remaining profile (assumption-scenario = 1E, 2B, 3A, 4B, 5B, 6B, 7A.)
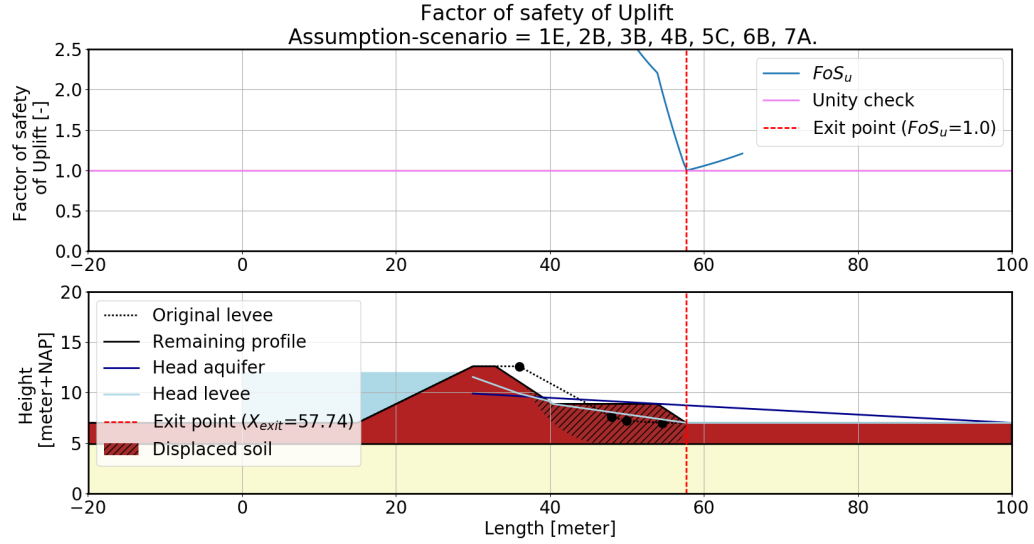

Figure D.16: Factor of safety of uplift of the remaining profile (assumption-scenario = 1E, 2B, 3C, 4B, 5B, 6B, 7A.)

Table D.7: Parameter used to calculated interaction base case and different assumption-option in step 5

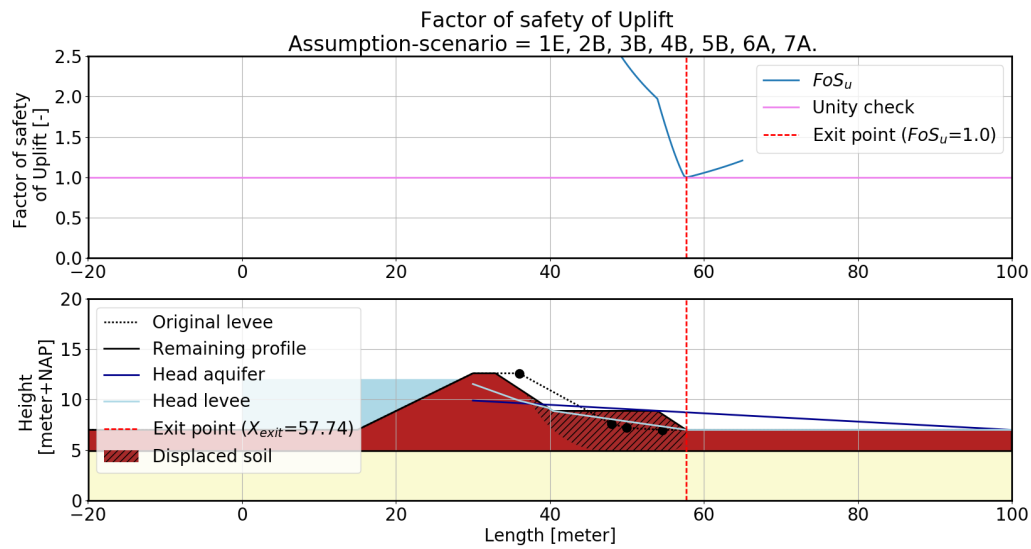| Parameter	Unit	Section		Values base-case	
Assumption-scenario	[−]	-	1E, 2B, 3B, 4B, 5A, 6B, 7A.	1E, 2B, 3B, 4B, 5B, 6B, 7A.	1E, 2B, 3B, 4B, 5C, 6B, 7A.
$X_{sp,entry}$	[m]	4.3	35.62	35.62	35.62
$Y_{sp,entry}$	[m]	4.3	12.60	12.60	12.60
$X_{sp,exit}$	[m]	4.3	57.73	57.73	57.73
$Y_{sp,exit}$	[m]	4.3	7.00	7.00	7.00
$X_{m,circle1}$	[m]	4.3	47.34	47.34	47.34
$Y_{m,circle1}$	[m]	4.3	17.35	17.35	17.35
$R_{circle1}$	[m]	4.3	12.45	12.45	12.45
$X_{m,circle2}$	[m]	4.3	55.53	55.53	55.53
$Y_{m,circle2}$	[m]	4.3	7.11	7.11	7.11
$R_{circle2}$	[m]	4.3	2.21	2.21	2.21
H_{sp}	[m]	4.4	5.60	5.60	5.60
$A(2)$	[m]	4.4	1.96	1.96	1.96
(X_r, Y_r)	[m]	4.4	(36.85, 10.64)	(36.85, 10.64)	(36.85, 10.64)
(X_{newtop}, Y_{newtop})	[m]	4.4	(32.93, 12.6)	(32.93, 12.6)	(32.93, 12.6)
(X_{newtoe}, Y_{newtoe})	[m]	4.4	(44.13, 7.0)	(44.13, 7.0)	(44.13, 7.0)
$S1$	[−]	4.4	0.41	0.41	0.41
$S2$	[−]	4.4	0.64	0.64	0.64
δ	[°]	4.4	10.55	10.55	10.55
$(X_{r,exit}, Y_{r,exit})$	[m]	4.4	(57.71, 7.4)	(57.71, 7.4)	(57.71, 7.4)
$Area$	[m^2]	4.4	24.27	24.27	24.27
L_{berm}	[m]	4.4	13.58	13.58	13.58
$A_{berm}(3)$	[m^2]	4.4	25.49	25.49	25.49
$(X_{bermstart}, Y_{bermstart})$	[m]	4.4	(40.38, 8.88)	(40.38, 8.88)	(40.38, 8.88)
$(X_{bermend}, Y_{bermend})$	[m]	4.4	(53.96, 8.88)	(53.96, 8.88)	(53.96, 8.88)
$(X_{bermendlow}, Y_{bermendlow})$	[m]	4.4	(57.71, 7.0)	(57.71, 7.0)	(57.71, 7.0)
$d(X_{exit}), d_i(X_{exit}), d_r(X_{exit})$	[m]	4.4	3.98, 0.0, 3.98	2.1, 2.1, 0.0	2.1, 2.1, 0.0
$\phi_{new}(X_{exit})$	[m + NAP]	4.4	9.17	8.73	8.73
$h_{p,new}(X_{exit})(4)$	[m + NAP]	4.4	8.12	7.00	7.00
$\Delta\phi(X_{exit})$	[m]	4.5	1.05	1.73	1.73
$\Delta\phi_{c,u}(X_{exit})(5)$	[m]	4.5	0.00	1.73	1.73
$FoS_u(X_{exit})$	[−]	4.5	0.00	1.00	1.00
X_{exit}	[m]	4.5	47.38	57.74	57.74
$i_h(X_{exit})$	[−]	4.5	0.26	0.82	0.82
$i_{c,h}(X_{exit})(6)$	[−]	4.5	0.30	0.30	0.30
$FoS_h(X_{exit})$	[−]	4.5	1.14	0.36	0.36
$H_p(X_{exit})$	[m]	4.5	2.68	4.36	4.36
$H_{c,p}(X_{exit})$	[m]	4.5	2.61	2.96	2.96
$d_{seepage}$	[m]	4.5	3.98	2.10	2.10
$L(X_{exit})$	[m]	4.5	67.38	77.74	77.74
$FoS_p(X_{exit})(7)$	[−]	4.5	0.97	0.68	0.68
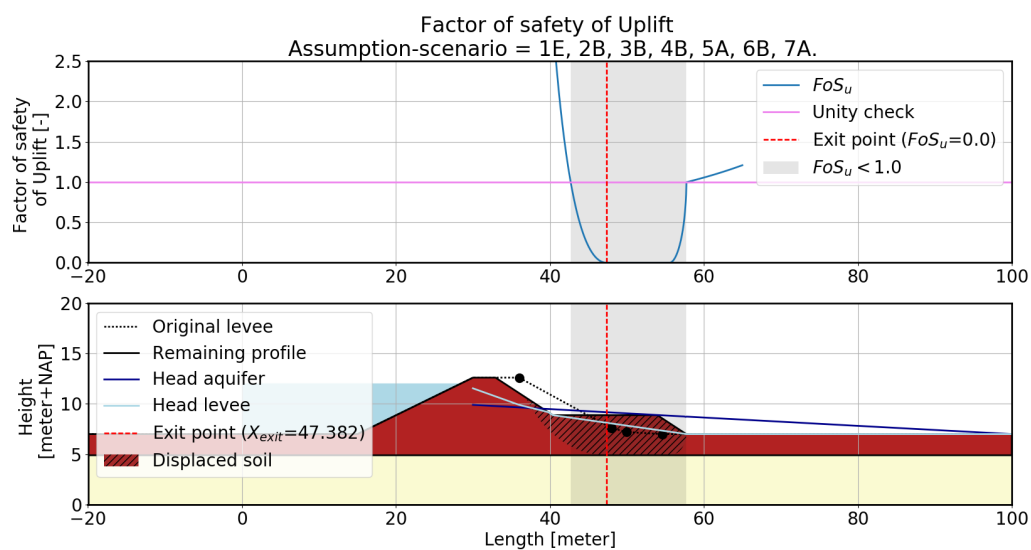
Figure D.17: Factor of safety of uplift of the remaining profile (assumption-scenario = 1E, 2B, 3B, 4B, 5A, 6B, 7A.)
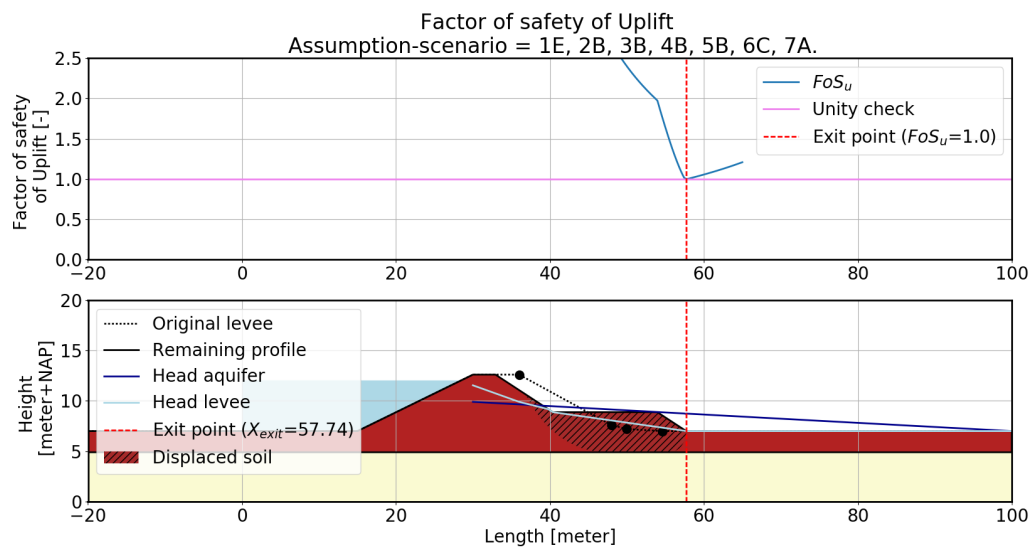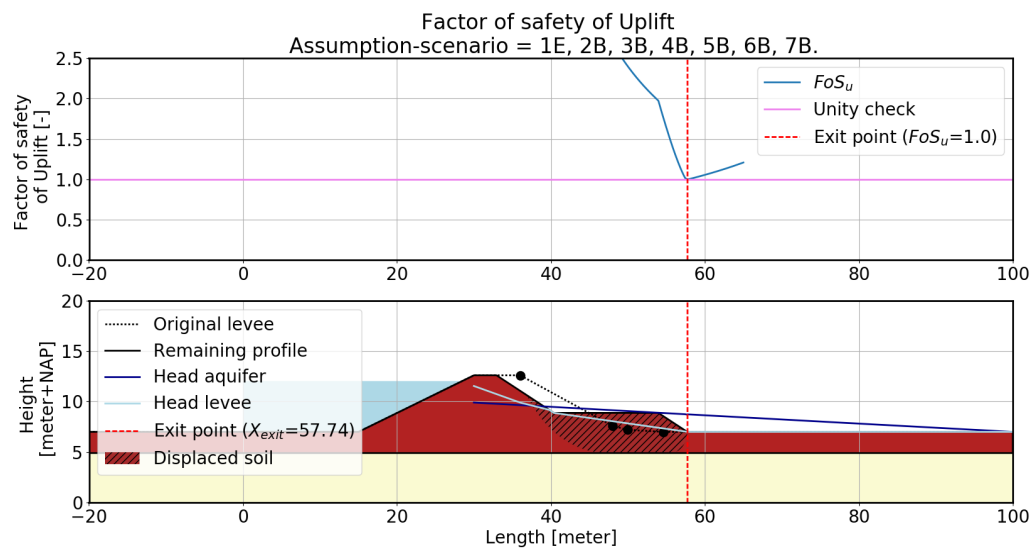
Figure D.18: Factor of safety of uplift of the remaining profile (assumption-scenario = 1E, 2B, 3B, 4B, 5C, 6B, 7A.)

Table D.8: Parameter used to calculated interaction base case and different assumption-option in step 6

Parameter	Unit	Section		Values base-case	
Assumption-scenario	[−]	-	1E, 2B, 3B, 4B, 5B, 6A, 7A.	1E, 2B, 3B, 4B, 5B, 6B, 7A.	1E, 2B, 3B, 4B, 5B, 6C, 7A.
$X_{sp,entry}$	[m]	4.3	35.62	35.62	35.62
$Y_{sp,entry}$	[m]	4.3	12.60	12.60	12.60
$X_{sp,exit}$	[m]	4.3	57.73	57.73	57.73
$Y_{sp,exit}$	[m]	4.3	7.00	7.00	7.00
$X_{m,circle1}$	[m]	4.3	47.34	47.34	47.34
$Y_{m,circle1}$	[m]	4.3	17.35	17.35	17.35
$R_{circle1}$	[m]	4.3	12.45	12.45	12.45
$X_{m,circle2}$	[m]	4.3	55.53	55.53	55.53
$Y_{m,circle2}$	[m]	4.3	7.11	7.11	7.11
$R_{circle2}$	[m]	4.3	2.21	2.21	2.21
H_{sp}	[m]	4.4	5.60	5.60	5.60
$A(2)$	[m]	4.4	1.96	1.96	1.96
(X_r, Y_r)	[m]	4.4	(36.85, 10.64)	(36.85, 10.64)	(36.85, 10.64)
(X_{newtop}, Y_{newtop})	[m]	4.4	(32.93, 12.6)	(32.93, 12.6)	(32.93, 12.6)
(X_{newtoe}, Y_{newtoe})	[m]	4.4	(44.13, 7.0)	(44.13, 7.0)	(44.13, 7.0)
$S1$	[−]	4.4	0.41	0.41	0.41
$S2$	[−]	4.4	0.64	0.64	0.64
δ	[°]	4.4	10.55	10.55	10.55
$(X_{r,exit}, Y_{r,exit})$	[m]	4.4	(57.71, 7.4)	(57.71, 7.4)	(57.71, 7.4)
$Area$	[m^2]	4.4	24.27	24.27	24.27
L_{berm}	[m]	4.4	13.58	13.58	13.58
$A_{berm}(3)$	[m^2]	4.4	25.49	25.49	25.49
$(X_{bermstart}, Y_{bermstart})$	[m]	4.4	(40.38, 8.88)	(40.38, 8.88)	(40.38, 8.88)
$(X_{bermend}, Y_{bermend})$	[m]	4.4	(53.96, 8.88)	(53.96, 8.88)	(53.96, 8.88)
$(X_{bermendlow}, Y_{bermendlow})$	[m]	4.4	(57.71, 7.0)	(57.71, 7.0)	(57.71, 7.0)
$d(X_{exit}), d_i(X_{exit}), d_r(X_{exit})$	[m]	4.4	2.1, 2.1, 0.0	2.1, 2.1, 0.0	2.1, 2.1, 0.0
$\phi_{new}(X_{exit})$	[m + NAP]	4.4	8.73	8.73	8.73
$h_{p,new}(X_{exit})(4)$	[m + NAP]	4.4	7.00	7.00	7.00
$\Delta\phi(X_{exit})$	[m]	4.5	1.73	1.73	1.73
$\Delta\phi_{c,u}(X_{exit})(5)$	[m]	4.5	1.73	1.73	1.73
$FoS_u(X_{exit})$	[−]	4.5	1.00	1.00	1.00
X_{exit}	[m]	4.5	57.74	57.74	57.74
$i_h(X_{exit})$	[−]	4.5	0.82	0.82	0.82
$i_{c,h}(X_{exit})(6)$	[−]	4.5	0.30	0.30	0.30
$FoS_h(X_{exit})$	[−]	4.5	0.36	0.36	0.36
$H_p(X_{exit})$	[m]	4.5	4.36	4.36	4.36
$H_{c,p}(X_{exit})$	[m]	4.5	2.96	2.96	2.96
$d_{seepage}$	[m]	4.5	2.10	2.10	2.10
$L(X_{exit})$	[m]	4.5	77.74	77.74	77.74
$FoS_p(X_{exit})(7)$	[−]	4.5	0.68	0.68	0.68

Figure D.19: Factor of safety of uplift of the remaining profile (assumption-scenario = 1E, 2B, 3B, 4B, 5B, 6A, 7A.)

Figure D.20: Factor of safety of uplift of the remaining profile (assumption-scenario = 1E, 2B, 3B, 4B, 5C, 6B, 7A.)

Table D.9: Parameter used to calculated interaction base case and different assumption-option in step 7

Parameter	Unit	Section	Values base-case	
Assumption-scenario	[−]	-	1E, 2B, 3B, 4B, 5B, 6B, 7A.	1E, 2B, 3B, 4B, 5B, 6C, 7B.
$X_{sp,entry}$	[m]	4.3	35.62	35.62
$Y_{sp,entry}$	[m]	4.3	12.60	12.60
$X_{sp,exit}$	[m]	4.3	57.73	57.73
$Y_{sp,exit}$	[m]	4.3	7.00	7.00
$X_{m,circle1}$	[m]	4.3	47.34	47.34
$Y_{m,circle1}$	[m]	4.3	17.35	17.35
$R_{circle1}$	[m]	4.3	12.45	12.45
$X_{m,circle2}$	[m]	4.3	55.53	55.53
$Y_{m,circle2}$	[m]	4.3	7.11	7.11
$R_{circle2}$	[m]	4.3	2.21	2.21
H_{sp}	[m]	4.4	5.60	5.60
$A(2)$	[m]	4.4	1.96	1.96
(X_r, Y_r)	[m]	4.4	(36.85, 10.64)	(36.85, 10.64)
(X_{newtop}, Y_{newtop})	[m]	4.4	(32.93, 12.6)	(32.93, 12.6)
(X_{newtoe}, Y_{newtoe})	[m]	4.4	(44.13, 7.0)	(44.13, 7.0)
$S1$	[−]	4.4	0.41	0.41
$S2$	[−]	4.4	0.64	0.64
δ	[°]	4.4	10.55	10.55
$(X_{r,exit}, Y_{r,exit})$	[m]	4.4	(57.71, 7.4)	(57.71, 7.4)
$Area$	[m^2]	4.4	24.27	24.27
L_{berm}	[m]	4.4	13.58	13.58
$A_{berm}(3)$	[m^2]	4.4	25.49	25.49
$(X_{bermstart}, Y_{bermstart})$	[m]	4.4	(40.38, 8.88)	(40.38, 8.88)
$(X_{bermend}, Y_{bermend})$	[m]	4.4	(53.96, 8.88)	(53.96, 8.88)
$(X_{bermendlow}, Y_{bermendlow})$	[m]	4.4	(57.71, 7.0)	(57.71, 7.0)
$d(X_{exit}), d_i(X_{exit}), d_r(X_{exit})$	[m]	4.4	2.1, 2.1, 0.0	2.1, 2.1, 0.0
$\phi_{new}(X_{exit})$	[m + NAP]	4.4	8.73	8.73
$h_{p,new}(X_{exit})(4)$	[m + NAP]	4.4	7.00	7.00
$\Delta\phi(X_{exit})$	[m]	4.5	1.73	1.73
$\Delta\phi_{c,u}(X_{exit})(5)$	[m]	4.5	1.73	1.73
$FoS_u(X_{exit})$	[−]	4.5	1.00	1.00
X_{exit}	[m]	4.5	57.74	57.74
$i_h(X_{exit})$	[−]	4.5	0.82	0.82
$i_{c,h}(X_{exit})(6)$	[−]	4.5	0.30	0.30
$FoS_h(X_{exit})$	[−]	4.5	0.36	0.36
$H_p(X_{exit})$	[m]	4.5	4.36	4.36
$H_{c,p}(X_{exit})$	[m]	4.5	2.96	2.96
$d_{seepage}$	[m]	4.5	2.10	2.10
$L(X_{exit})$	[m]	4.5	77.74	77.74
$FoS_p(X_{exit})(7)$	[−]	4.5	0.68	0.68

Figure D.21: Factor of safety of uplift of the remaining profile (assumption-scenario = 1E, 2B, 3B, 4B, 5B, 6B, 7B.)

Results in table

E.1. Grebbedijk case

Tables with all calculated safety factors for the remaining profile and the difference with the original profile are available in excel and PDF. These files are not attached to this report because of the size of these tables. If you are interested in these files, you can retrieve them by contacting Laura van der Doef.

Table E.1: Scenarios abbreviation

Assumption	Description	Number	Option
step 1:	Sliding plane location and shape	1	A = Slope-blanket B = Slope-interface C = Slope-sand D = Crest-blanket E = Crest-interface F = Crest-sand
step 2:	Amount of lowering	2	A = 1m lowering B = $0.35H_{sp}$ lowering C = $0.5H_{sp}$ lowering
step 3:	Berm volume change	3	A = Equal volume B = Increase volume C = Decrease volume
step 4:	Saturation of the berm	4	A = Unsaturated berm B = Partly saturated berm C = Fully saturated berm
step 5:	Blanket layer thickness	5	A = Only intact layer B = Partly remoulded C = Full thickness
step 6:	Critical heave gradient	6	A = i_{ch} = 0.1 B = i_{ch} = 0.3 C = i_{ch} = 0.5
step 7:	Seepage path	7	A = Straight up B = Along sliding plane

E.2. Fixed scenario-options - minimum, median and maximum value

This appendix is an addition to chapter 5.3. It presents the tables showing the values for the box plots.

Table E.2 presents the minimum, maximum and mean ΔFoS_u with their corresponding assumption-scenarios, a supplement to figure 5.4. As explained in Section 5.3.1, the minimum of the boxplot cannot be lower than $-FoS_{u,original}$ (-0.93). This value is shown in many rows in the second column of Table E.2.

Table E.2: The minimum, median and maximum value of the difference in uplift compared to the original situation with the corresponding scenario, no exclusion of outliers

Fixed option	Minimum		Median		Maximum	
	ΔFoS_u	Scenario	ΔFoS_u	Scenario	ΔFoS_u	Scenario
1A	-0.81	1A,2A,3A,4A,5A,6A,7A	0.09	1A,2C,3A,4A,5C,6C,7A	0.09	1A,2B,3A,4A,5B,6A,7A
1B	-0.93	1B,2A,3A,4A,5A,6A,7A	0.07	1B,2A,3B,4A,5C,6A,7A	0.07	1B,2A,3A,4A,5B,6A,7A
1C	-0.93	1C,2A,3A,4A,5A,6A,7A	0.14	1C,2A,3C,4B,5B,6A,7A	0.15	1C,2C,3A,4A,5B,6A,7A
1D	-0.89	1D,2A,3A,4A,5A,6A,7A	0.05	1D,2C,3C,4C,5C,6A,7B	0.05	1D,2A,3C,4A,5B,6A,7A
1E	-0.93	1E,2A,3A,4A,5A,6A,7A	0.07	1E,2A,3B,4B,5B,6B,7B	0.07	1E,2A,3A,4A,5B,6A,7A
1F	-0.93	1F,2A,3A,4A,5A,6A,7A	0.14	1F,2A,3C,4B,5B,6A,7A	0.16	1F,2C,3A,4A,5B,6A,7A
2A	-0.93	1B,2A,3A,4A,5A,6A,7A	0.07	1E,2A,3A,4B,5B,6B,7A	0.14	1F,2A,3A,4A,5B,6A,7A
2B	-0.93	1B,2B,3A,4A,5A,6A,7A	0.07	1E,2B,3C,4A,5B,6B,7A	0.15	1F,2B,3A,4A,5B,6A,7A
2C	-0.93	1B,2C,3A,4A,5A,6A,7A	0.07	1E,2C,3A,4C,5B,6A,7A	0.16	1F,2C,3A,4A,5B,6A,7A
3A	-0.93	1B,2A,3A,4A,5A,6A,7A	0.07	1E,2C,3A,4C,5C,6B,7B	0.16	1F,2C,3A,4A,5B,6A,7A
3B	-0.93	1B,2A,3B,4A,5A,6A,7A	0.07	1B,2A,3B,4A,5B,6C,7A	0.16	1F,2C,3B,4A,5B,6A,7A
3C	-0.93	1B,2A,3C,4A,5A,6A,7A	0.07	1E,2C,3C,4A,5C,6B,7B	0.16	1F,2C,3C,4A,5B,6A,7A
4A	-0.93	1B,2A,3A,4A,5A,6A,7A	0.07	1E,2B,3A,4A,5C,6C,7A	0.16	1F,2C,3A,4A,5B,6A,7A
4B	-0.93	1B,2A,3A,4B,5A,6A,7A	0.07	1E,2B,3B,4B,5B,6B,7A	0.16	1F,2C,3A,4B,5B,6A,7A
4C	-0.93	1B,2A,3A,4C,5A,6A,7A	0.07	1E,2B,3B,4C,5B,6B,7A	0.16	1F,2C,3A,4C,5B,6A,7A
5A	-0.93	1B,2A,3A,4A,5A,6A,7A	-0.93	1B,2A,3C,4C,5A,6C,7A	-0.71	1A,2C,3B,4C,5A,6A,7A
5B	0.03	1A,2A,3B,4A,5B,6A,7A	0.07	1E,2C,3B,4B,5B,6B,7A	0.16	1F,2C,3A,4A,5B,6A,7A
5C	0.05	1D,2C,3A,4A,5C,6A,7A	0.07	1A,2A,3C,4A,5C,6C,7A	0.16	1F,2C,3A,4A,5C,6A,7A
6A	-0.93	1B,2A,3A,4A,5A,6A,7A	0.07	1E,2A,3C,4C,5C,6A,7A	0.16	1F,2C,3A,4A,5B,6A,7A
6B	-0.93	1B,2A,3A,4A,5A,6B,7A	0.07	1E,2A,3C,4C,5C,6B,7A	0.16	1F,2C,3A,4A,5B,6B,7A
6C	-0.93	1B,2A,3A,4A,5A,6C,7A	0.07	1E,2A,3C,4C,5C,6C,7A	0.16	1F,2C,3A,4A,5B,6C,7A
7A	-0.93	1B,2A,3A,4A,5A,6A,7A	0.07	1B,2A,3A,4B,5B,6B,7A	0.16	1F,2C,3A,4A,5B,6A,7A
7B	-0.93	1B,2A,3A,4A,5A,6A,7B	0.07	1B,2A,3A,4B,5B,6B,7B	0.16	1F,2C,3A,4A,5B,6A,7B

Table E.3 presents the minimum, maximum and mean ΔFoS_h with their corresponding assumption-scenarios, a supplement to figure 5.7.

Table E.3: The minimum, median and maximum value of the difference in heave compared to the original situation with the corresponding scenario, no exclusion of outliers

Fixed option	Minimum		Median		Maximum	
	ΔFoS_h	Scenario	ΔFoS_h	Scenario	ΔFoS_h	Scenario
1A	-0.24	1A,2A,3C,4A,5C,6A,7A	0.01	1A,2B,3A,4B,5B,6A,7A	4.03	1A,2C,3B,4C,5A,6C,7B
1B	-0.24	1B,2C,3C,4A,5C,6A,7A	0.00	1B,2A,3A,4C,5B,6B,7A	8.24	1B,2C,3B,4C,5A,6C,7B
1C	-0.20	1C,2C,3C,4A,5A,6A,7A	0.03	1C,2C,3B,4B,5C,6C,7B	8.11	1C,2C,3B,4C,5A,6C,7B
1D	-0.24	1D,2A,3C,4A,5C,6A,7A	0.00	1D,2B,3A,4B,5B,6B,7A	2.44	1D,2A,3A,4A,5A,6C,7A
1E	-0.24	1E,2A,3B,4A,5B,6A,7B	0.00	1E,2A,3A,4B,5C,6A,7A	442499.64	1E,2C,3B,4C,5A,6C,7B
1F	-0.20	1F,2C,3C,4A,5A,6A,7A	0.04	1F,2C,3B,4B,5C,6C,7B	9.25	1F,2C,3B,4C,5A,6C,7B
2A	-0.24	1B,2A,3C,4A,5B,6A,7A	0.03	1C,2A,3C,4B,5C,6C,7A	5.61	1E,2A,3B,4C,5A,6C,7B
2B	-0.24	1B,2B,3C,4A,5B,6A,7A	0.03	1C,2B,3A,4B,5C,6B,7A	14.80	1E,2B,3B,4C,5A,6C,7B
2C	-0.24	1B,2C,3C,4A,5C,6A,7A	0.03	1C,2C,3A,4A,5B,6A,7A	442499.64	1E,2C,3B,4C,5A,6C,7B
3A	-0.24	1B,2A,3A,4A,5B,6A,7A	0.03	1C,2A,3A,4C,5B,6B,7A	47.28	1E,2C,3A,4C,5A,6C,7B
3B	-0.24	1D,2A,3B,4A,5B,6A,7B	0.03	1F,2A,3B,4C,5B,6C,7A	442499.64	1E,2C,3B,4C,5A,6C,7B
3C	-0.24	1B,2C,3C,4A,5C,6A,7A	0.03	1C,2A,3C,4C,5C,6B,7A	22.14	1E,2C,3C,4C,5A,6C,7B
4A	-0.24	1B,2C,3C,4A,5C,6A,7A	0.03	1F,2A,3A,4A,5C,6A,7A	3.85	1C,2A,3A,4A,5A,6C,7B
4B	-0.24	1B,2C,3C,4B,5C,6A,7A	0.03	1C,2A,3C,4B,5C,6B,7A	4.73	1F,2C,3B,4B,5A,6C,7B
4C	-0.24	1B,2C,3C,4C,5C,6A,7A	0.03	1C,2A,3B,4C,5C,6B,7B	442499.64	1E,2C,3B,4C,5A,6C,7B
5A	-0.23	1A,2A,3C,4A,5A,6A,7A	0.61	1C,2B,3A,4A,5A,6C,7A	442499.64	1E,2C,3B,4C,5A,6C,7B
5B	-0.24	1B,2A,3C,4A,5B,6A,7A	0.01	1A,2B,3C,4C,5B,6C,7B	1.26	1A,2A,3A,4A,5B,6C,7B
5C	-0.24	1B,2C,3C,4A,5C,6A,7A	0.01	1A,2C,3B,4C,5C,6B,7A	1.26	1A,2A,3A,4A,5C,6C,7B
6A	-0.24	1B,2C,3C,4A,5C,6A,7A	0.00	1B,2C,3B,4C,5C,6A,7A	88499.64	1E,2C,3B,4C,5A,6A,7B
6B	0.00	1D,2C,3C,4A,5C,6B,7A	0.03	1F,2A,3C,4B,5B,6B,7A	265499.64	1E,2C,3B,4C,5A,6B,7B
6C	0.00	1D,2C,3C,4A,5C,6C,7A	0.03	1F,2B,3C,4B,5B,6C,7B	442499.64	1E,2C,3B,4C,5A,6C,7B
7A	-0.24	1B,2C,3C,4A,5C,6A,7A	0.03	1C,2A,3B,4B,5B,6B,7A	213978.41	1E,2C,3B,4C,5A,6C,7A
7B	-0.24	1B,2C,3A,4A,5B,6A,7B	0.03	1F,2A,3C,4B,5B,6C,7B	442499.64	1E,2C,3B,4C,5A,6C,7B

Table E.4 presents the minimum, maximum and mean ΔFoS_p with their corresponding assumption-scenarios, a supplement to figure 5.10.
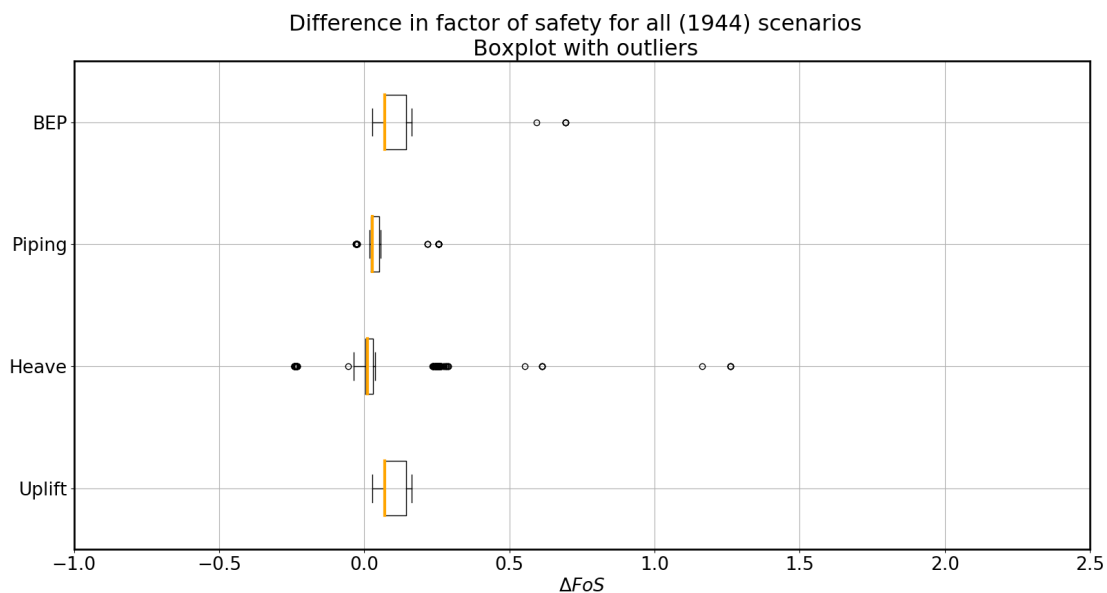
Table E.4: The minimum, median and maximum value of the difference in piping compared to the original situation with the corresponding scenario, no exclusion of outliers

Fixed option	Minimum		Median		Maximum	
	ΔFoS_p	Scenario	ΔFoS_p	Scenario	ΔFoS_p	Scenario
1A	-0.03	1A,2A,3C,4A,5C,6A,7A	0.04	1A,2C,3C,4C,5B,6A,7B	1.55	1A,2C,3B,4C,5A,6A,7B
1B	0.01	1B,2A,3C,4A,5A,6A,7A	0.02	1B,2B,3A,4A,5C,6B,7A	1.26	1B,2C,3B,4C,5A,6A,7B
1C	-0.01	1C,2C,3C,4A,5A,6A,7A	0.05	1C,2C,3B,4A,5C,6B,7B	2.53	1C,2C,3B,4C,5A,6A,7B
1D	0.01	1D,2A,3C,4A,5A,6A,7A	0.02	1D,2A,3C,4A,5B,6C,7B	1.50	1D,2A,3A,4A,5A,6A,7B
1E	0.01	1E,2A,3C,4A,5A,6A,7A	0.03	1E,2B,3A,4A,5C,6A,7A	16.13	1E,2C,3B,4C,5A,6A,7B
1F	-0.01	1F,2C,3C,4A,5A,6A,7A	0.06	1F,2C,3C,4B,5B,6A,7B	3.48	1F,2B,3B,4C,5A,6A,7B
2A	-0.03	1A,2A,3C,4A,5C,6A,7A	0.05	1C,2A,3B,4A,5C,6C,7A	2.95	1F,2A,3B,4C,5A,6A,7B
2B	-0.02	1A,2B,3B,4A,5B,6A,7A	0.05	1C,2B,3B,4B,5B,6C,7A	5.04	1E,2B,3B,4C,5A,6A,7B
2C	-0.01	1C,2C,3C,4A,5A,6A,7A	0.05	1C,2C,3A,4B,5C,6C,7A	16.13	1E,2C,3B,4C,5A,6A,7B
3A	-0.03	1A,2A,3A,4A,5B,6A,7A	0.05	1C,2A,3A,4C,5B,6C,7B	9.41	1E,2C,3A,4C,5A,6A,7B
3B	-0.03	1A,2A,3B,4A,5B,6A,7A	0.05	1C,2A,3B,4C,5B,6C,7A	16.13	1E,2C,3B,4C,5A,6A,7B
3C	-0.03	1A,2A,3C,4A,5C,6A,7A	0.05	1C,2A,3C,4B,5B,6A,7B	6.54	1E,2C,3C,4C,5A,6A,7B
4A	-0.03	1A,2A,3C,4A,5C,6A,7A	0.04	1A,2A,3C,4A,5B,6A,7A	2.37	1F,2A,3A,4A,5A,6A,7B
4B	0.02	1B,2C,3C,4B,5C,6A,7A	0.05	1F,2A,3B,4B,5C,6C,7B	2.86	1F,2A,3B,4B,5A,6A,7B
4C	0.02	1B,2C,3C,4C,5C,6A,7A	0.05	1F,2A,3C,4C,5B,6B,7A	16.13	1E,2C,3B,4C,5A,6A,7B
5A	-0.01	1C,2C,3C,4A,5A,6A,7A	0.31	1B,2A,3B,4C,5A,6C,7A	16.13	1E,2C,3B,4C,5A,6A,7B
5B	-0.03	1A,2A,3A,4A,5B,6A,7A	0.03	1E,2A,3B,4A,5B,6B,7A	0.26	1A,2A,3A,4A,5B,6A,7B
5C	-0.03	1A,2A,3C,4A,5C,6A,7A	0.03	1E,2A,3C,4C,5C,6A,7B	0.26	1A,2A,3A,4A,5C,6A,7B
6A	-0.03	1A,2A,3C,4A,5C,6A,7A	0.05	1C,2A,3C,4B,5C,6A,7A	16.13	1E,2C,3B,4C,5A,6A,7B
6B	-0.03	1A,2A,3C,4A,5C,6B,7A	0.05	1C,2A,3C,4B,5C,6B,7A	16.13	1E,2C,3B,4C,5A,6B,7B
6C	-0.03	1A,2A,3C,4A,5C,6C,7A	0.05	1C,2A,3C,4B,5C,6C,7A	16.13	1E,2C,3B,4C,5A,6C,7B
7A	-0.03	1A,2A,3C,4A,5C,6A,7A	0.04	1A,2C,3B,4B,5B,6B,7A	1.06	1E,2C,3B,4C,5A,6A,7A
7B	0.02	1B,2C,3A,4A,5B,6A,7B	0.05	1F,2A,3A,4B,5C,6A,7B	16.13	1E,2C,3B,4C,5A,6A,7B

Table E.5 presents the minimum, maximum and mean ΔFoS_{bep} with their corresponding assumption-scenarios, a supplement to figure 5.13.

Table E.5: The minimum, median and maximum value of the difference in combined BEP compared to the original situation with the corresponding scenario, no exclusion of outliers

Fixed option	Minimum		Median		Maximum	
	ΔFoS_{bep}	Scenario	ΔFoS_{bep}	Scenario	ΔFoS_{bep}	Scenario
1A	-0.28	1A,2A,3C,4A,5A,6A,7A	0.09	1A,2B,3B,4B,5C,6B,7B	3.46	1A,2C,3B,4C,5A,6C,7B
1B	-0.27	1B,2A,3C,4A,5A,6A,7A	0.07	1B,2B,3A,4A,5C,6B,7B	7.67	1B,2C,3B,4C,5A,6C,7B
1C	-0.29	1C,2C,3C,4A,5A,6A,7A	0.15	1C,2B,3B,4C,5C,6B,7A	7.54	1C,2C,3B,4C,5A,6C,7B
1D	-0.27	1D,2A,3C,4A,5A,6A,7A	0.05	1D,2B,3A,4C,5C,6A,7B	1.87	1D,2A,3A,4A,5A,6C,7B
1E	-0.27	1E,2A,3C,4A,5A,6A,7A	0.07	1E,2C,3A,4B,5B,6B,7A	442499.07	1E,2C,3B,4C,5A,6C,7B
1F	-0.29	1F,2C,3C,4A,5A,6A,7A	0.15	1F,2B,3A,4B,5C,6A,7A	8.68	1F,2C,3B,4C,5A,6C,7B
2A	-0.28	1A,2A,3C,4A,5A,6A,7A	0.08	1A,2A,3A,4A,5B,6B,7A	5.04	1E,2A,3B,4C,5A,6C,7B
2B	-0.27	1A,2B,3C,4A,5A,6A,7A	0.09	1A,2B,3B,4B,5C,6C,7A	14.23	1E,2B,3B,4C,5A,6C,7B
2C	-0.29	1C,2C,3C,4A,5A,6A,7A	0.09	1A,2C,3C,4A,5C,6A,7A	442499.07	1E,2C,3B,4C,5A,6C,7B
3A	-0.29	1C,2C,3A,4A,5A,6A,7A	0.09	1A,2C,3A,4B,5C,6A,7B	46.71	1E,2C,3A,4C,5A,6C,7B
3B	-0.28	1C,2C,3B,4A,5A,6A,7A	0.09	1A,2C,3B,4C,5B,6B,7A	442499.07	1E,2C,3B,4C,5A,6C,7B
3C	-0.29	1C,2C,3C,4A,5A,6A,7A	0.09	1A,2A,3C,4C,5C,6C,7B	21.57	1E,2C,3C,4C,5A,6C,7B
4A	-0.29	1C,2C,3C,4A,5A,6A,7A	0.07	1B,2A,3A,4A,5C,6C,7A	3.28	1C,2A,3A,4A,5A,6C,7B
4B	-0.22	1A,2A,3C,4B,5A,6A,7A	0.08	1A,2A,3B,4B,5B,6C,7B	4.16	1F,2C,3B,4B,5A,6C,7B
4C	-0.18	1A,2A,3C,4C,5A,6A,7A	0.09	1A,2B,3B,4C,5B,6B,7B	442499.07	1E,2C,3B,4C,5A,6C,7B
5A	-0.29	1C,2C,3C,4A,5A,6A,7A	0.30	1C,2C,3C,4B,5A,6B,7A	442499.07	1E,2C,3B,4C,5A,6C,7B
5B	0.03	1A,2A,3B,4A,5B,6A,7A	0.07	1E,2A,3B,4B,5B,6B,7A	0.69	1A,2A,3A,4A,5B,6C,7B
5C	0.05	1D,2C,3A,4A,5C,6A,7A	0.07	1A,2A,3C,4A,5C,6B,7B	0.69	1A,2A,3A,4A,5C,6C,7B
6A	-0.29	1C,2C,3C,4A,5A,6A,7A	0.07	1B,2A,3B,4C,5B,6A,7A	88499.07	1E,2C,3B,4C,5A,6A,7B
6B	-0.29	1C,2C,3C,4A,5A,6B,7A	0.09	1A,2C,3B,4A,5C,6B,7A	265499.07	1E,2C,3B,4C,5A,6B,7B
6C	-0.27	1A,2A,3C,4A,5A,6C,7A	0.09	1A,2A,3C,4C,5B,6C,7B	442499.07	1E,2C,3B,4C,5A,6C,7B
7A	-0.29	1C,2C,3C,4A,5A,6A,7A	0.07	1E,2C,3A,4B,5B,6A,7A	213977.84	1E,2C,3B,4C,5A,6C,7A
7B	-0.19	1A,2A,3C,4B,5A,6A,7B	0.10	1D,2B,3A,4B,5A,6C,7B	442499.07	1E,2C,3B,4C,5A,6C,7B

E.3. Boxplot all scenarios excluding 5A

The boxplots in this appendix correspond to the sensitivity analysis section 5.4.5 and show the results of the Grebbedijk case excluding assumption-option 5A.

Figure E.1

Table E.6: The minimum, maximum and mean value of the difference in BEP compared to the original situation with the corresponding scenario, exclusion of 5A

Fixed option	Minimum	Scenario	Maximum	Scenario	Mean
1A	0.03	1A,2A,3B,4A,5B,6A,7A	0.69	1A,2A,3A,4A,5B,6C,7B	0.10
1B	0.05	1B,2C,3C,4A,5C,6A,7A	0.07	1B,2A,3A,4A,5B,6A,7A	0.07
1C	0.14	1C,2A,3A,4A,5B,6A,7A	0.15	1C,2C,3A,4A,5B,6A,7A	0.15
1D	0.03	1D,2C,3B,4A,5B,6A,7A	0.05	1D,2A,3C,4A,5B,6A,7A	0.05
1E	0.07	1E,2C,3C,4A,5C,6A,7A	0.07	1E,2A,3A,4A,5B,6A,7A	0.07
1F	0.14	1F,2A,3A,4A,5B,6A,7A	0.16	1F,2C,3A,4A,5B,6A,7A	0.15
2A	0.03	1A,2A,3B,4A,5B,6A,7A	0.69	1A,2A,3A,4A,5B,6C,7B	0.10
2B	0.04	1D,2B,3B,4A,5B,6A,7A	0.59	1A,2B,3B,4A,5B,6C,7B	0.10
2C	0.03	1D,2C,3B,4A,5B,6A,7A	0.16	1F,2C,3A,4A,5B,6A,7A	0.10
3A	0.05	1D,2C,3A,4A,5B,6A,7A	0.69	1A,2A,3A,4A,5B,6C,7B	0.10
3B	0.03	1A,2A,3B,4A,5B,6A,7A	0.69	1A,2A,3B,4A,5B,6C,7B	0.10
3C	0.05	1D,2C,3C,4A,5C,6A,7A	0.69	1A,2A,3C,4A,5C,6C,7B	0.10
4A	0.03	1A,2A,3B,4A,5B,6A,7A	0.69	1A,2A,3A,4A,5B,6C,7B	0.10
4B	0.03	1D,2C,3B,4B,5B,6A,7A	0.16	1F,2C,3A,4B,5B,6A,7A	0.10
4C	0.03	1D,2C,3B,4C,5B,6A,7A	0.16	1F,2C,3A,4C,5B,6A,7A	0.10
5B	0.03	1A,2A,3B,4A,5B,6A,7A	0.69	1A,2A,3A,4A,5B,6C,7B	0.10
5C	0.05	1D,2C,3A,4A,5C,6A,7A	0.69	1A,2A,3A,4A,5C,6C,7B	0.10
6A	0.03	1A,2A,3B,4A,5B,6A,7A	0.16	1F,2C,3A,4A,5B,6A,7A	0.10
6B	0.03	1A,2A,3B,4A,5B,6B,7A	0.16	1F,2C,3A,4A,5B,6B,7A	0.10
6C	0.03	1A,2A,3B,4A,5B,6C,7A	0.69	1A,2A,3A,4A,5B,6C,7B	0.10
7A	0.03	1A,2A,3B,4A,5B,6A,7A	0.16	1F,2C,3A,4A,5B,6A,7A	0.10
7B	0.03	1A,2A,3B,4A,5B,6A,7B	0.69	1A,2A,3A,4A,5B,6C,7B	0.10
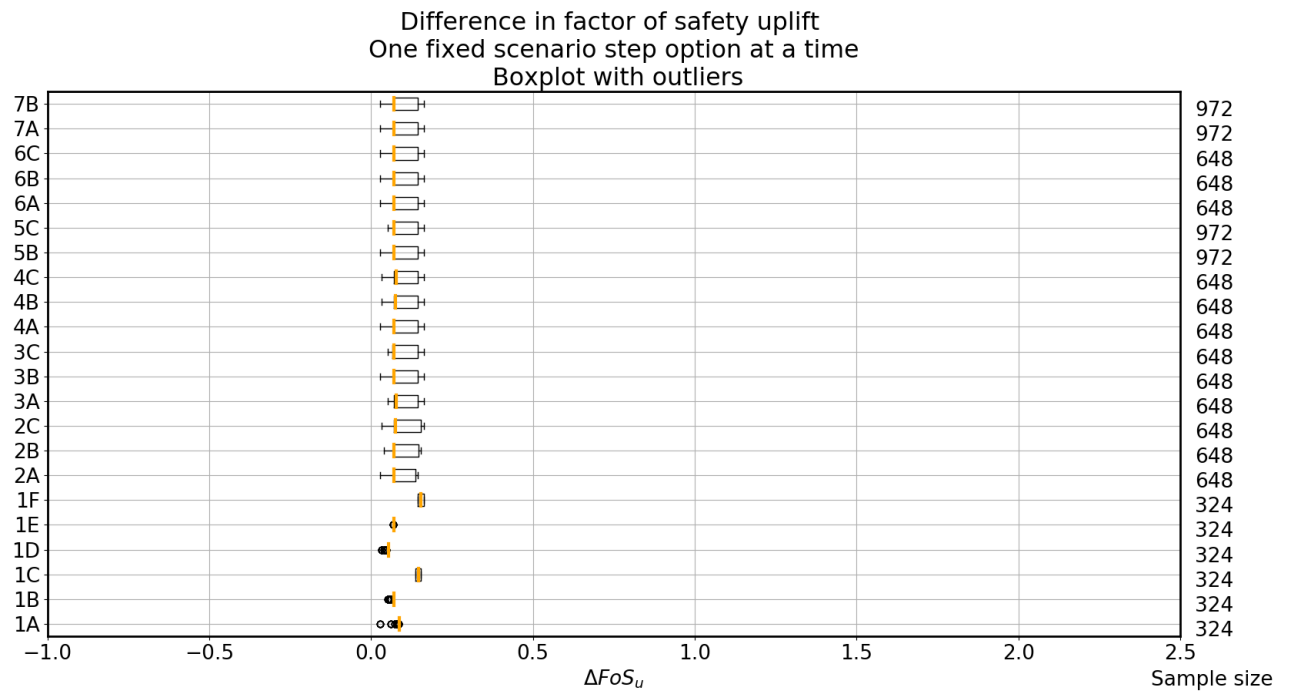
Figure E.2
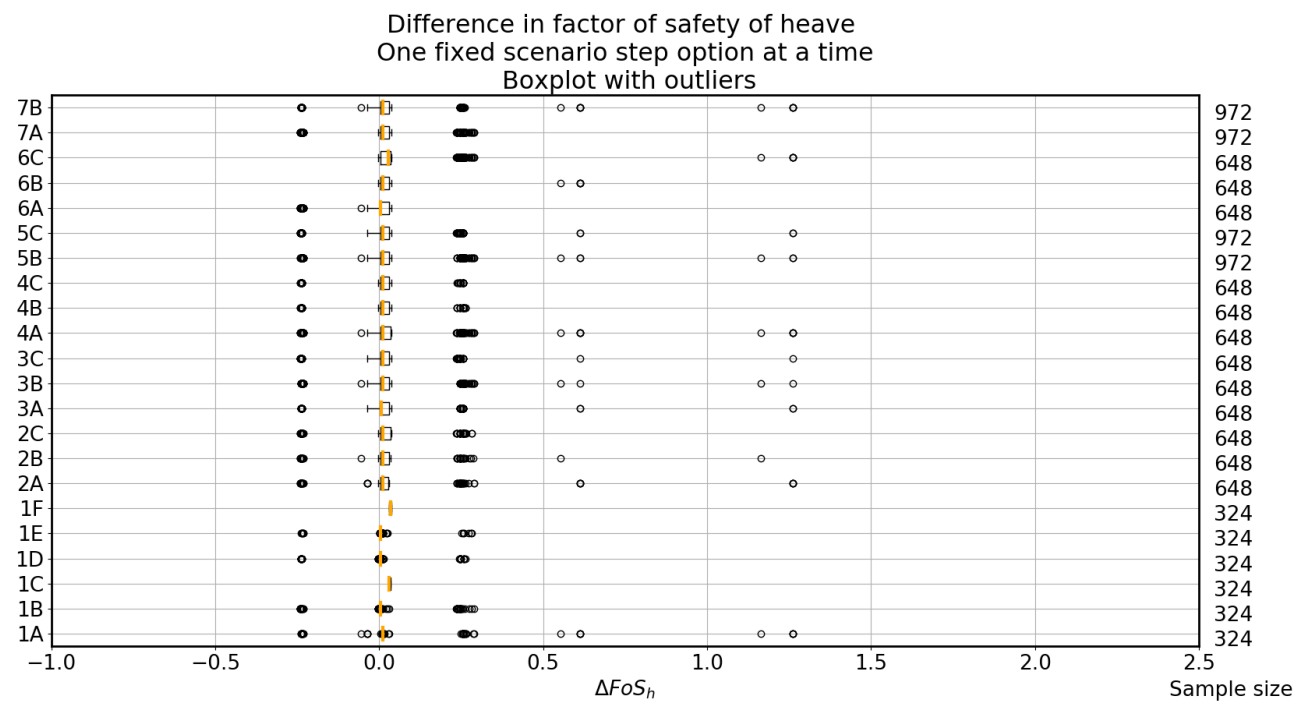
Figure E.3
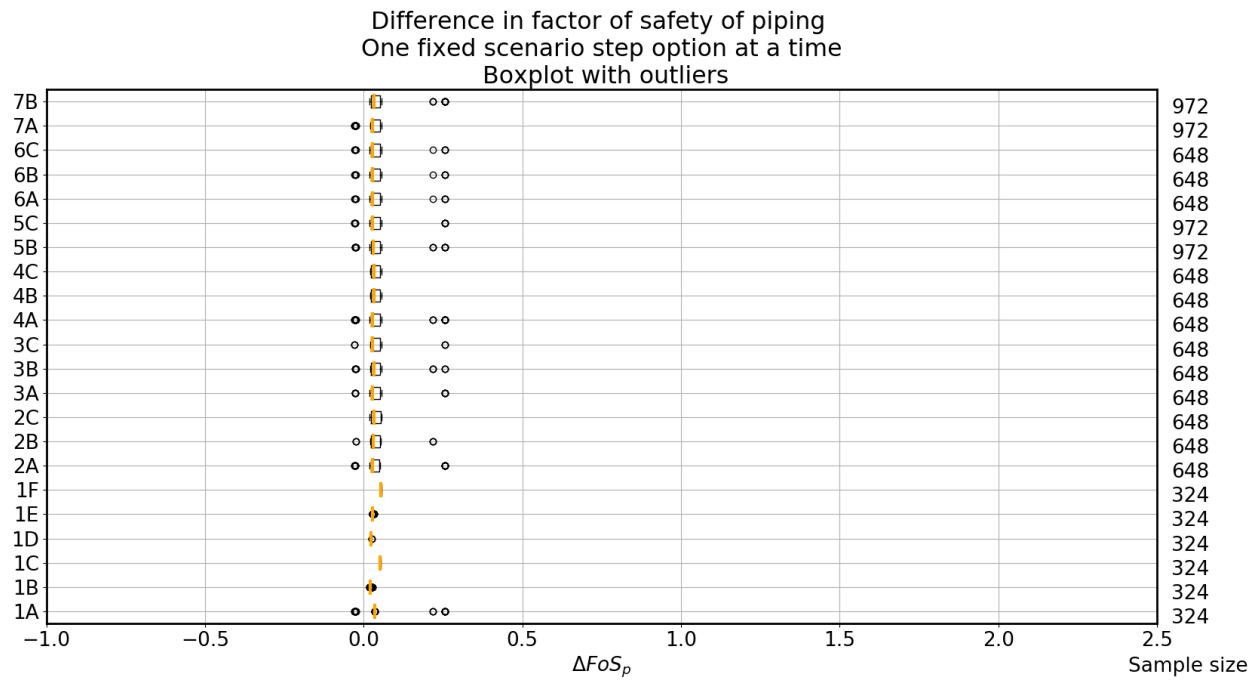
Figure E.4
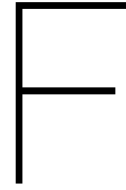
F
Sensitivity analysis results

This appendix shows all results form the different input cases in the same format as the Grebbedijk case was described in chapter 5. This appendix is a supplement to section 5.4.

F.1. Grebbedijk original case
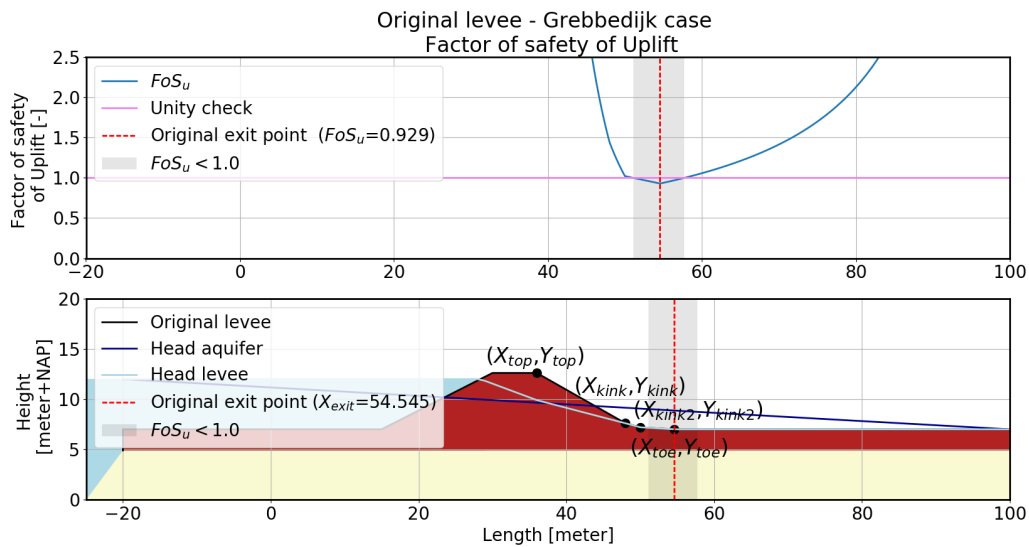
Figure F.1: Factor of safety of uplift of the original levee (Grebbedijk original case)

Table F.1: Results for Grebbedijk original case (Original, remaining profile (assumption-scenario: 1B, 2B, 3B ,4B, 5B, 6B, 7A.))

Factor of safety	Original case	Value $[-]$	Remaining profile	Value $[-]$	Difference (Δ)	Value $[-]$
Uplift	$FoS_{u,original}(X_{exit})$	0.93	$FoS_u(X_{exit})$	1.00	ΔFoS_u	0.07
Heave	$FoS_{h,original}(X_{exit})$	0.36	$FoS_h(X_{exit})$	0.36	ΔFoS_h	0.00
Piping	$FoS_{p,original}(X_{exit})$	0.65	$FoS_p(X_{exit})$	0.67	ΔFoS_p	0.02
BEP	$FoS_{BEP,original}(X_{exit})$	0.93	$FoS_{BEP}(X_{exit})$	1.00	ΔFoS_{BEP}	0.07

Figure F.2: Factor of safety of uplift of the remaining profile, (Grebbedijk original case) base case (assumption-scenario = 1B, 2B, 3B ,4B, 5B, 6B, 7A.)
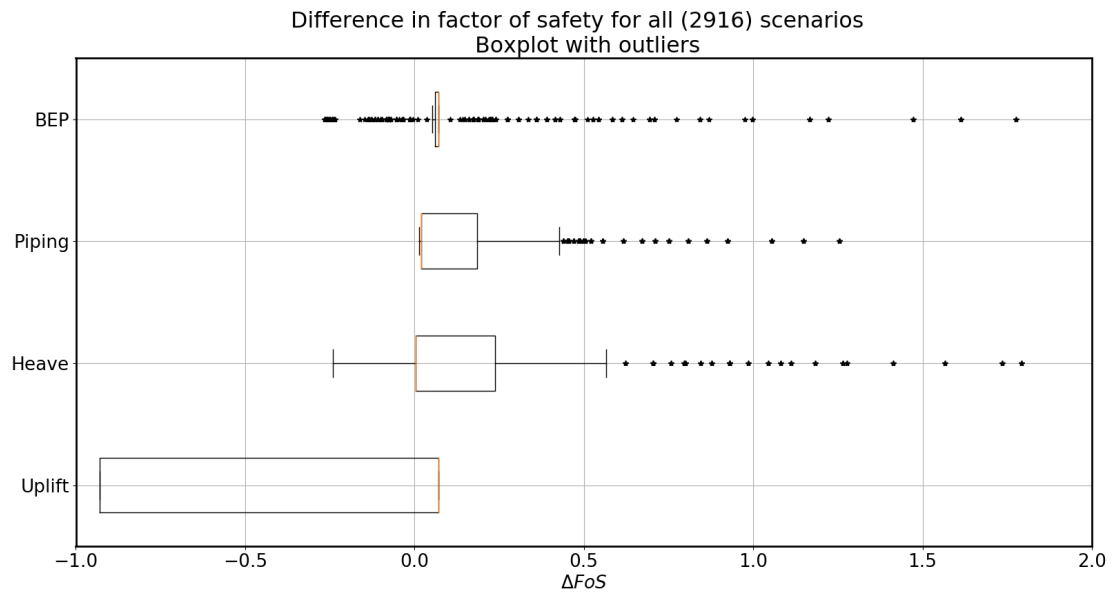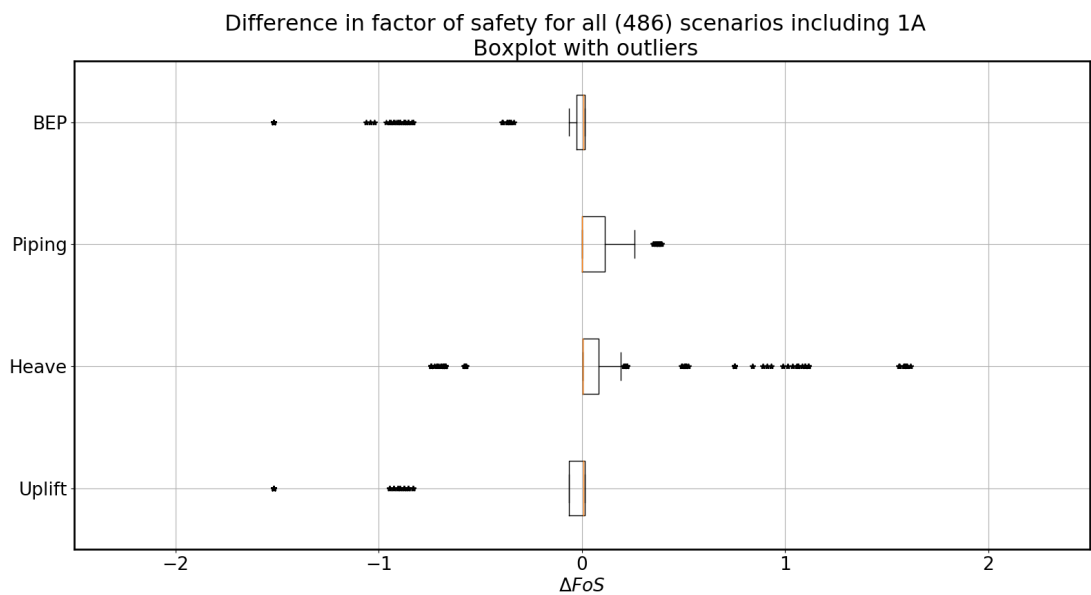

Figure F.3: The range in the differences between BEP, Uplift, Heave and Piping and the original situation for all 486 scenarios with the outliers (Grebbedijk original case)
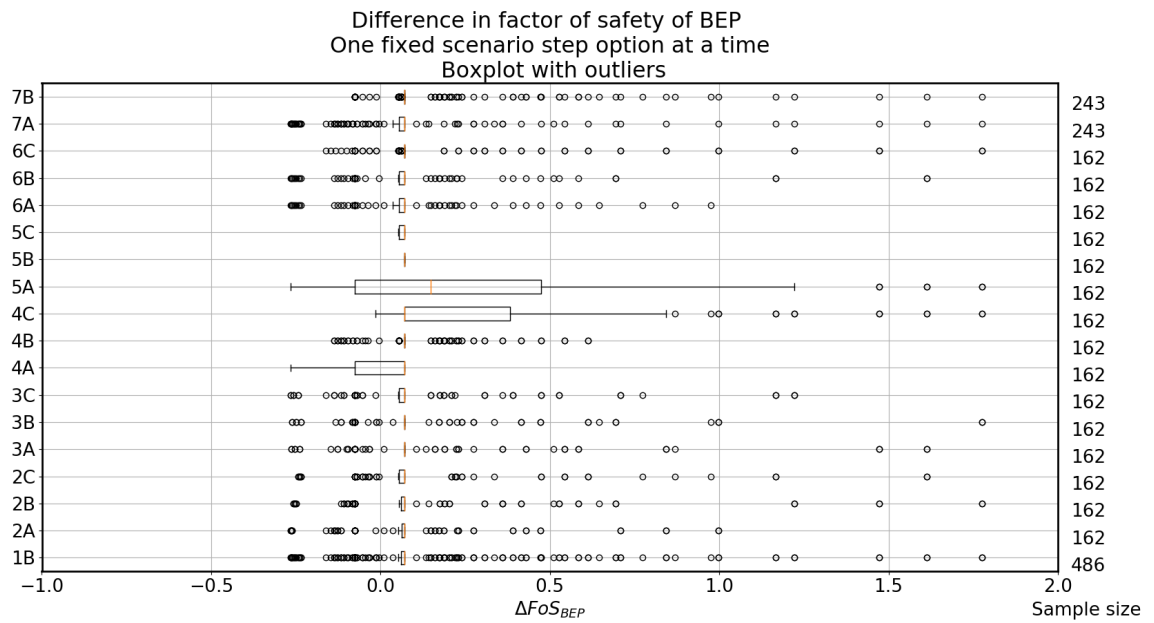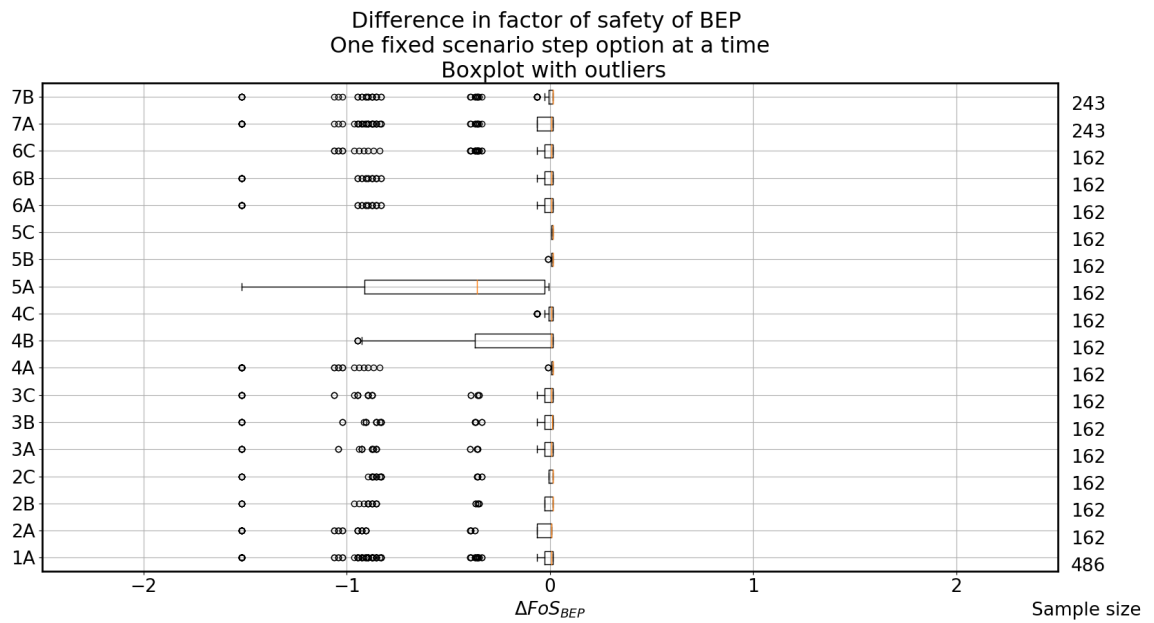
F.1.1. BEP

Figure F.4: The range in difference of BEP for fixed scenario options with outliers (Grebbedijk original case).

F.1.2. Uplift
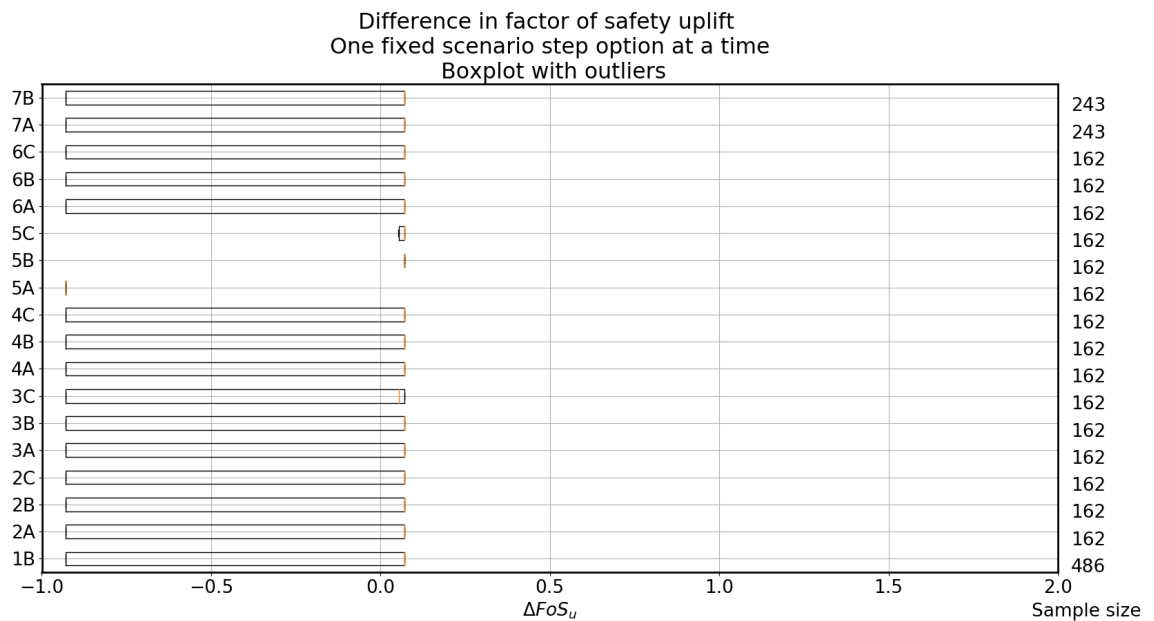
Figure F.5: The range in difference of uplift for fixed scenario options with outliers (Grebbedijk original case).

F.1.3. Heave
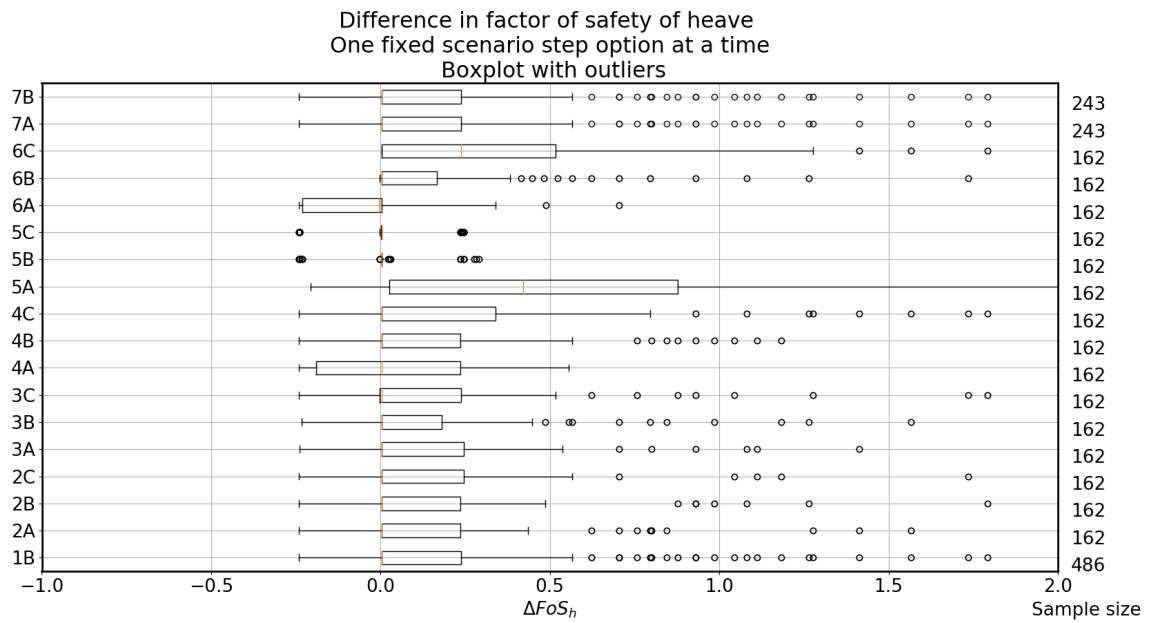
Figure F.6: The range in difference of heave for fixed scenario options with outliers (Grebbedijk original case).
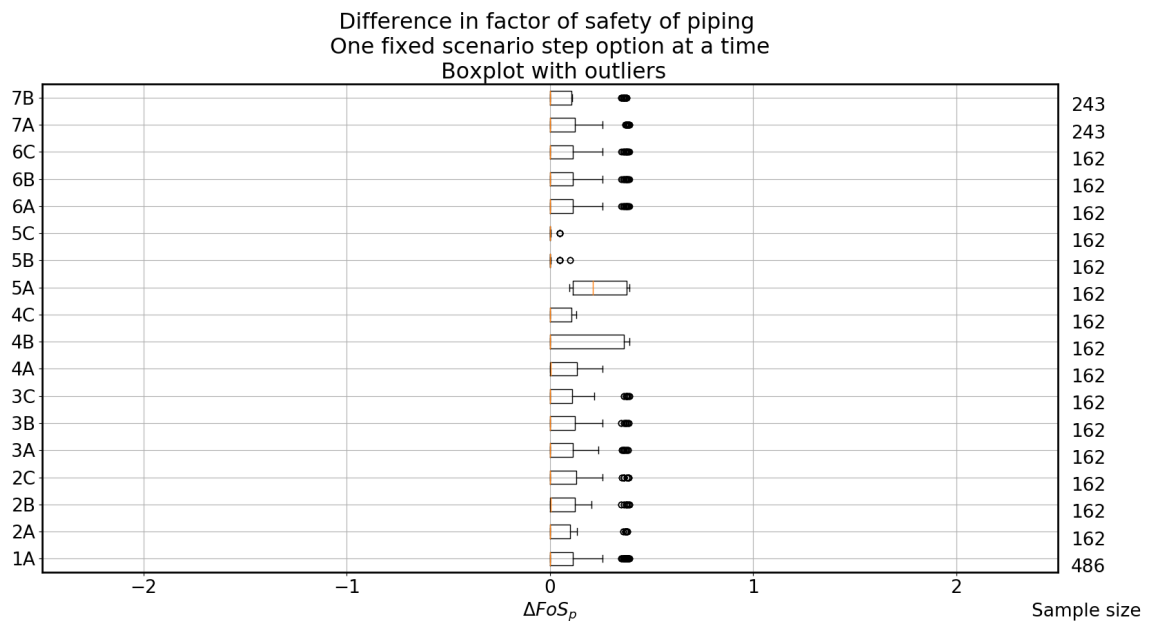
F.1.4. Piping
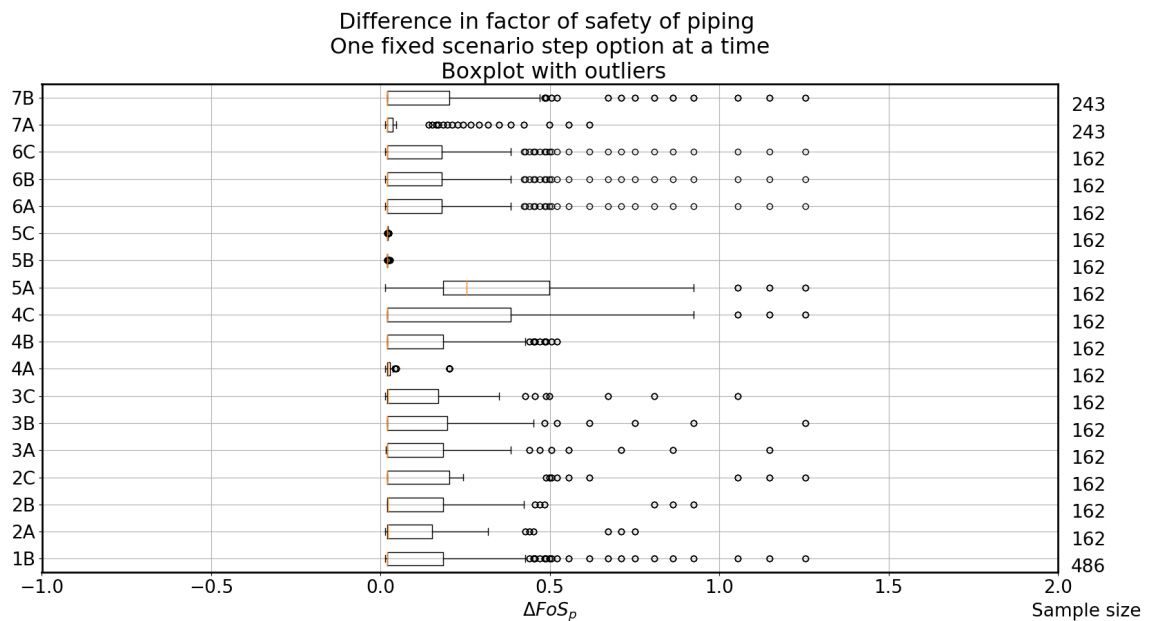
Figure F.7: The range in difference of piping for fixed scenario options with outliers (Grebbedijk original case).

F.2. Thin blanket layer
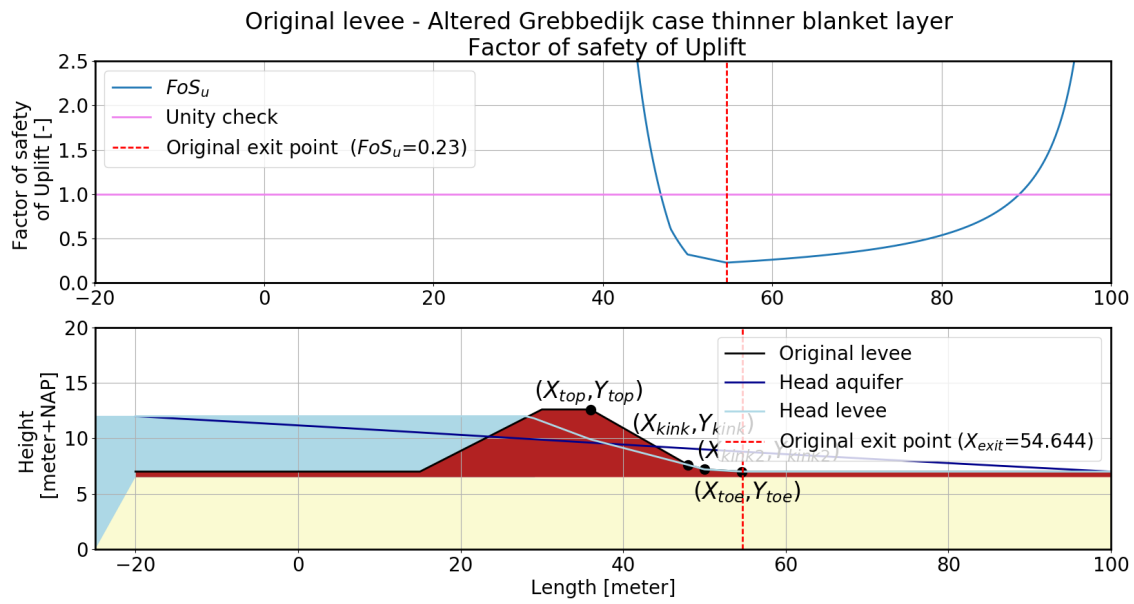
Figure F.8: Factor of safety of uplift of the original levee (Thin blanket layer case)

Table F.2: Results for thin blanket layer case (Original, remaining profile (assumption-scenario: 1C, 2B, 3B ,4B, 5B, 6B, 7A.))

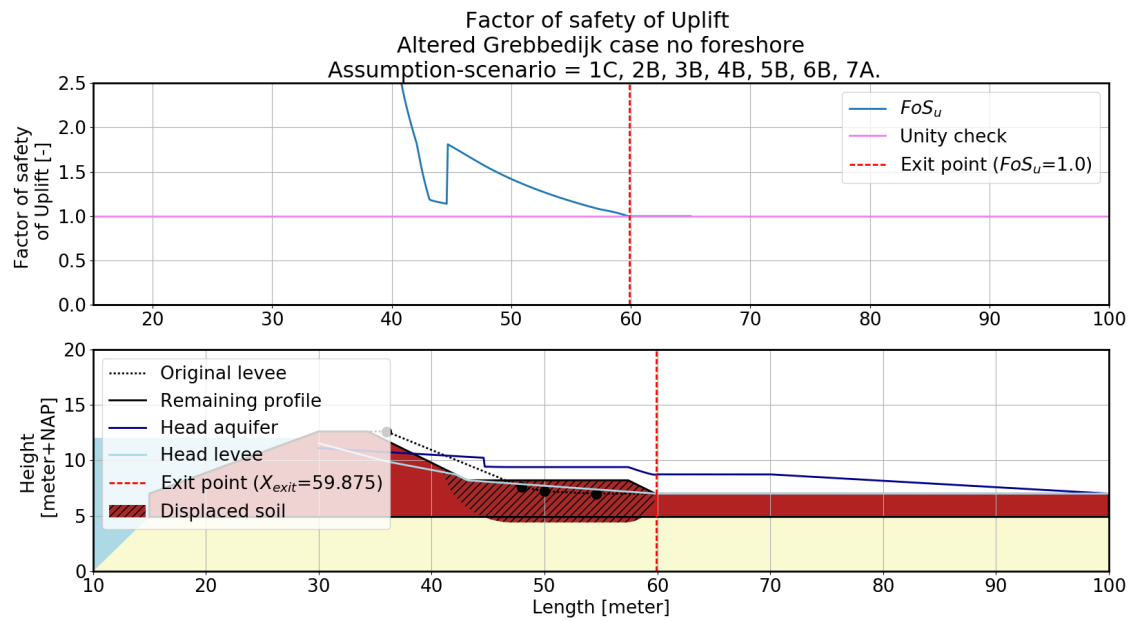| Factor of safety	Original case	Value $[-]$	Remaining profile	Value $[-]$	Difference (Δ)	Value $[-]$
Uplift	$FoS_{u,original}(X_{exit})$	0.23	$FoS_u(X_{exit})$	0.99	ΔFoS_u	0.76
Heave	$FoS_{h,original}(X_{exit})$	0.36	$FoS_h(X_{exit})$	0.36	ΔFoS_h	0.00
Piping	$FoS_{p,original}(X_{exit})$	0.59	$FoS_p(X_{exit})$	0.65	ΔFoS_p	0.06
BEP	$FoS_{BEP,original}(X_{exit})$	0.59	$FoS_{BEP}(X_{exit})$	0.99	ΔFoS_{BEP}	0.40
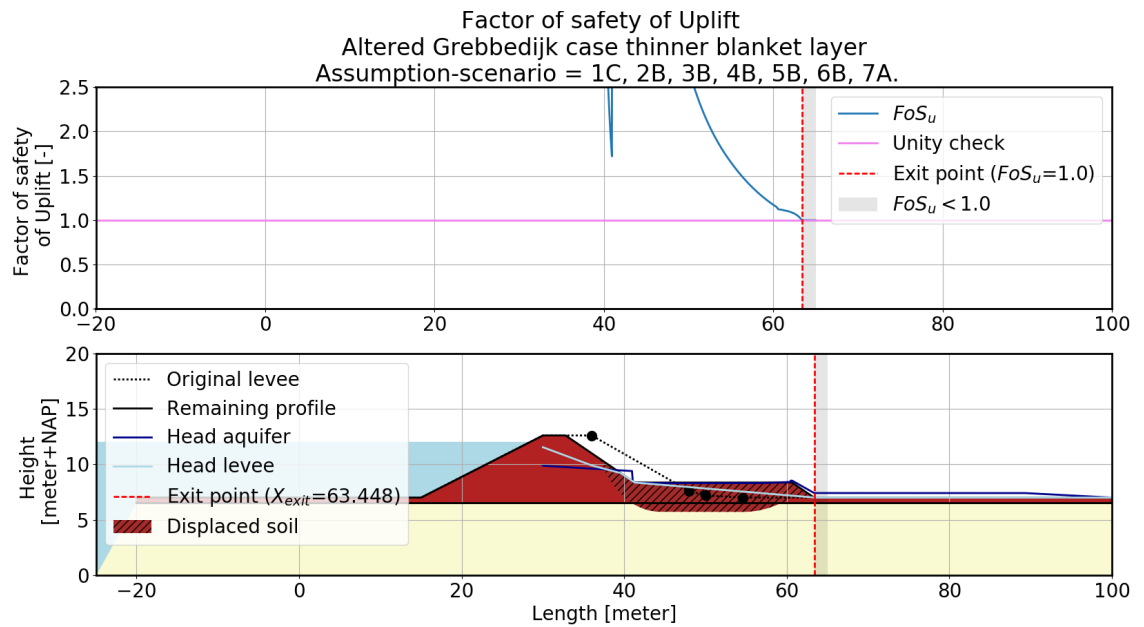
Figure F.9: Factor of safety of uplift of the remaining profile, (Thin blanket layer case) base case (assumption-scenario = 1C, 2B, 3B, 4B, 5B, 6B, 7A.)
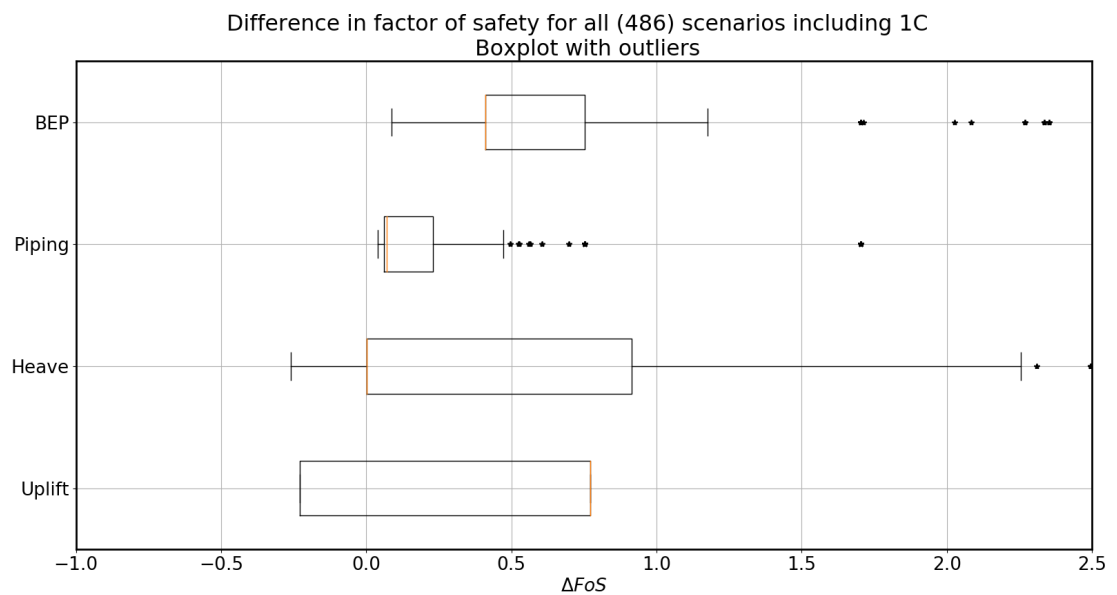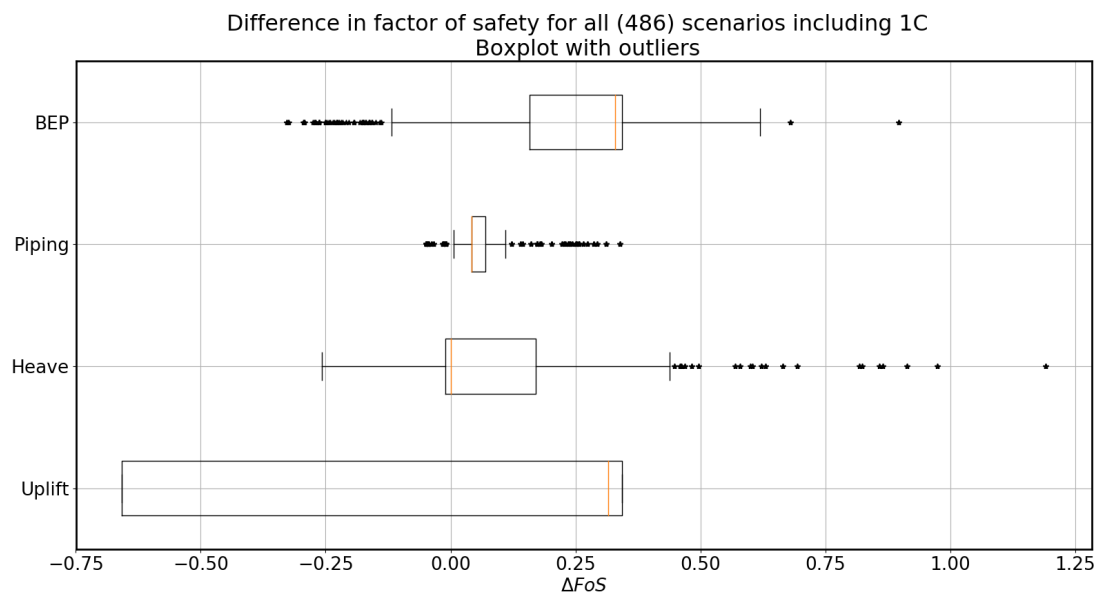

Figure F.10: The range in the differences between BEP, Uplift, Heave and Piping and the original situation for all 486 scenarios with the outliers (Thin blanket layer case)
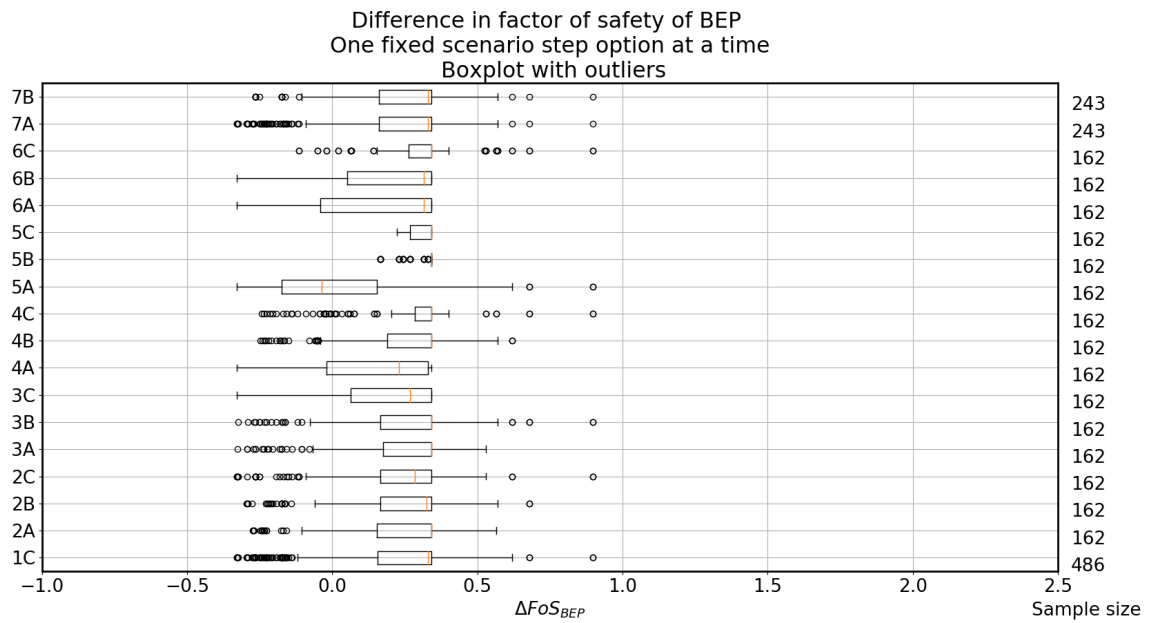
F.2.1. BEP
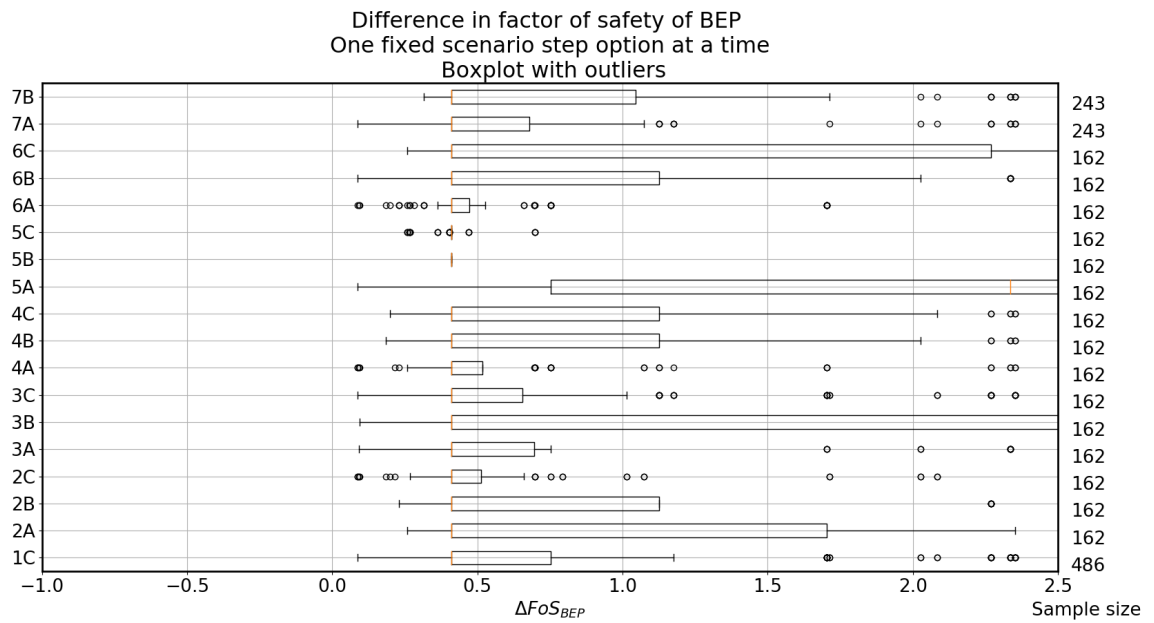
Figure F.11: The range in difference of BEP for fixed scenario options with outliers (Thin blanket layer case).
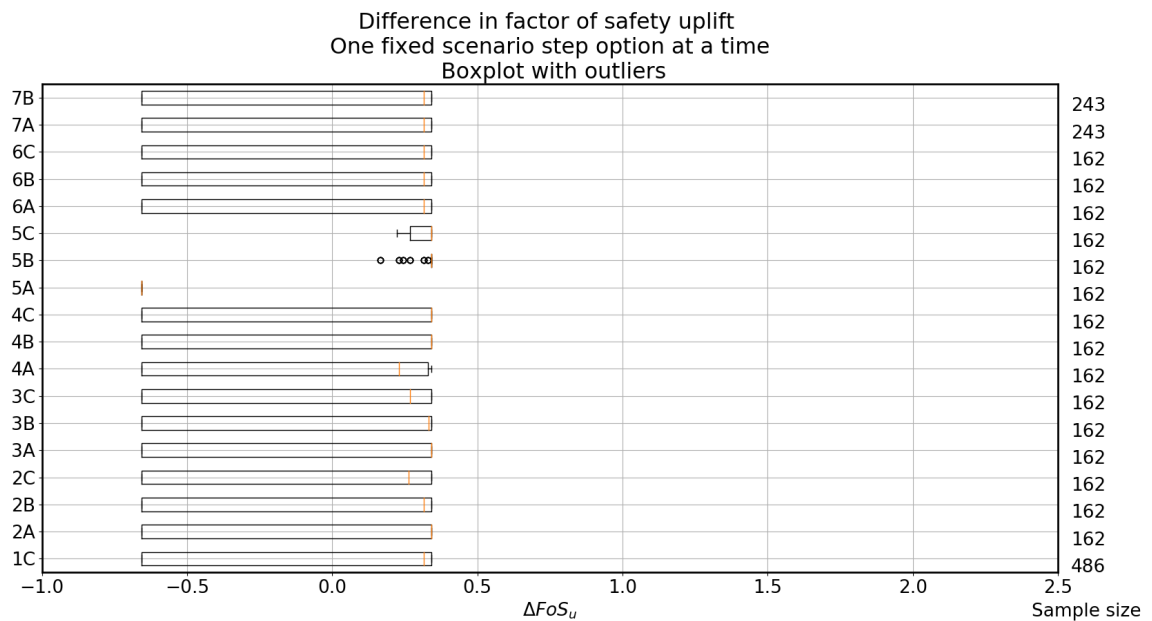
F.2.2. Uplift
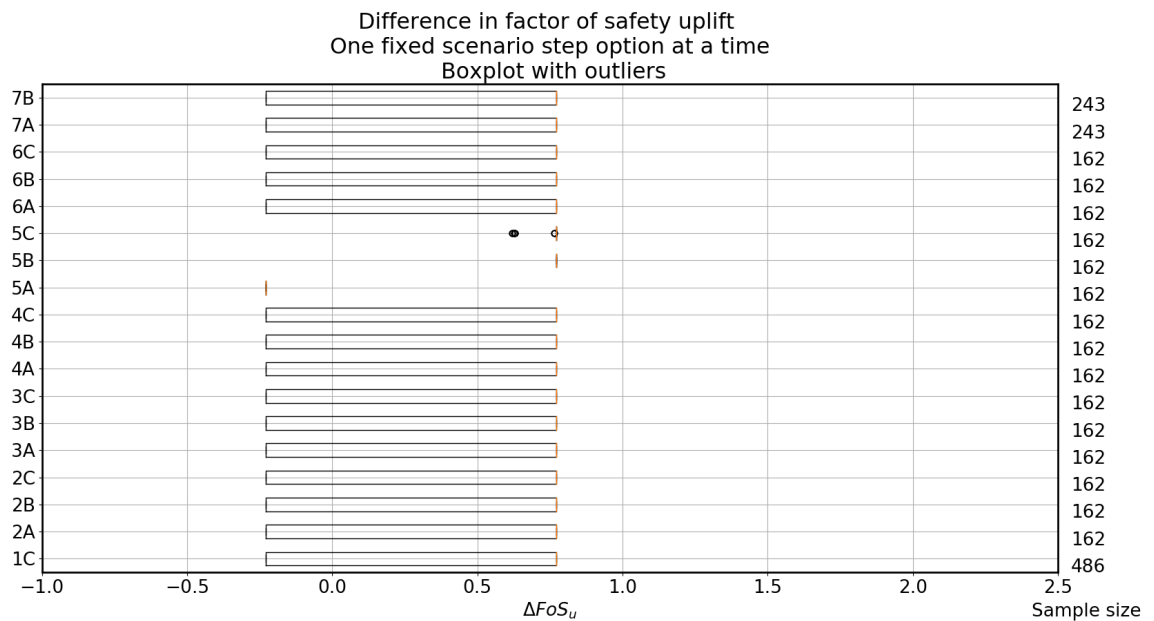
Figure F.12: The range in difference of uplift for fixed scenario options with outliers (Thin blanket layer case).
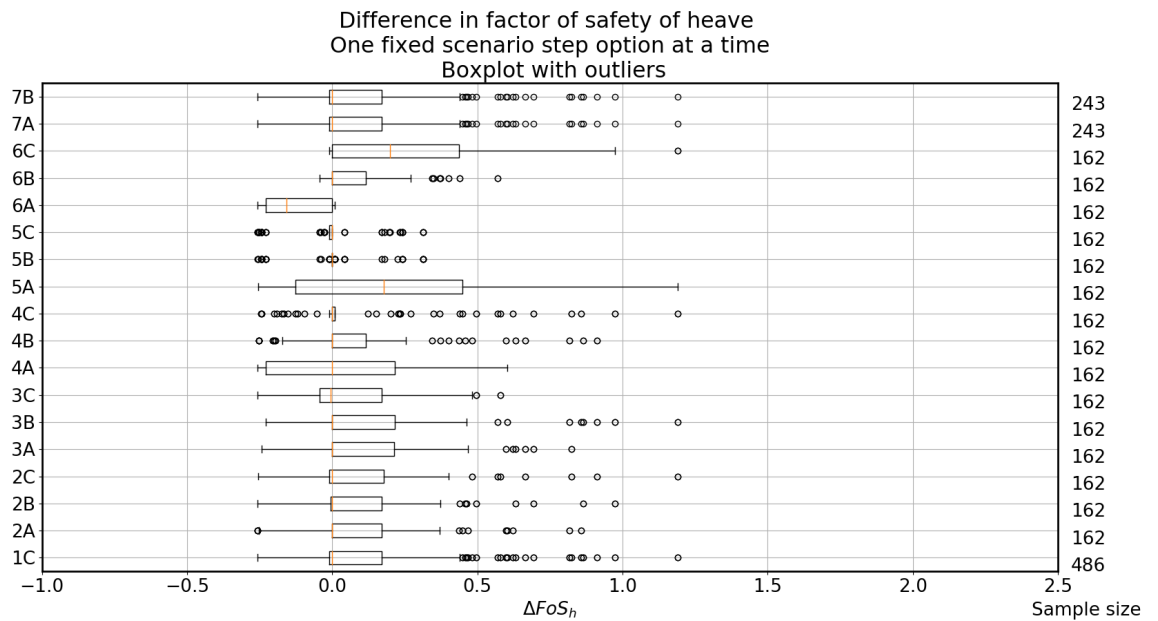
F.2.3. Heave
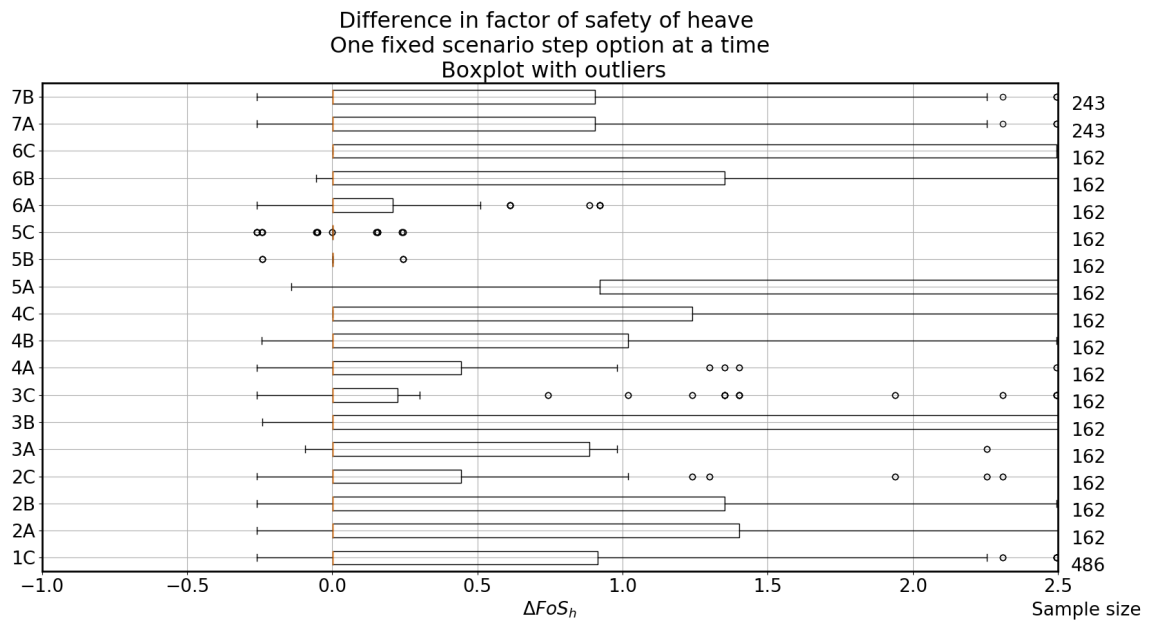
Figure F.13: The range in difference of heave for fixed scenario options with outliers (Thin blanket layer case).
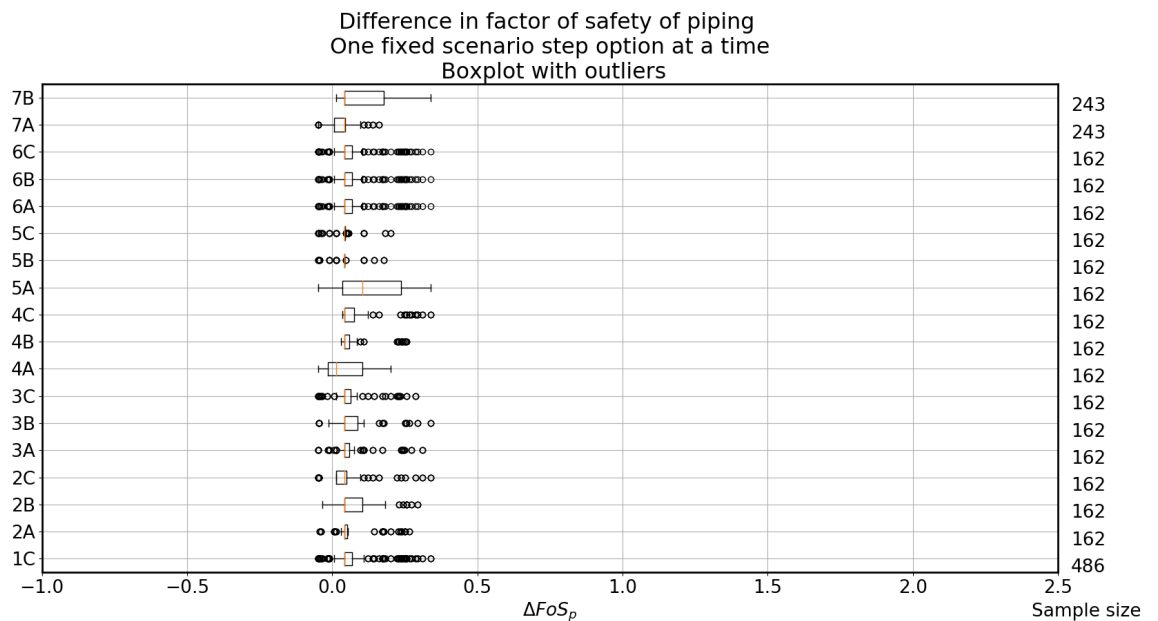
F.2.4. Piping
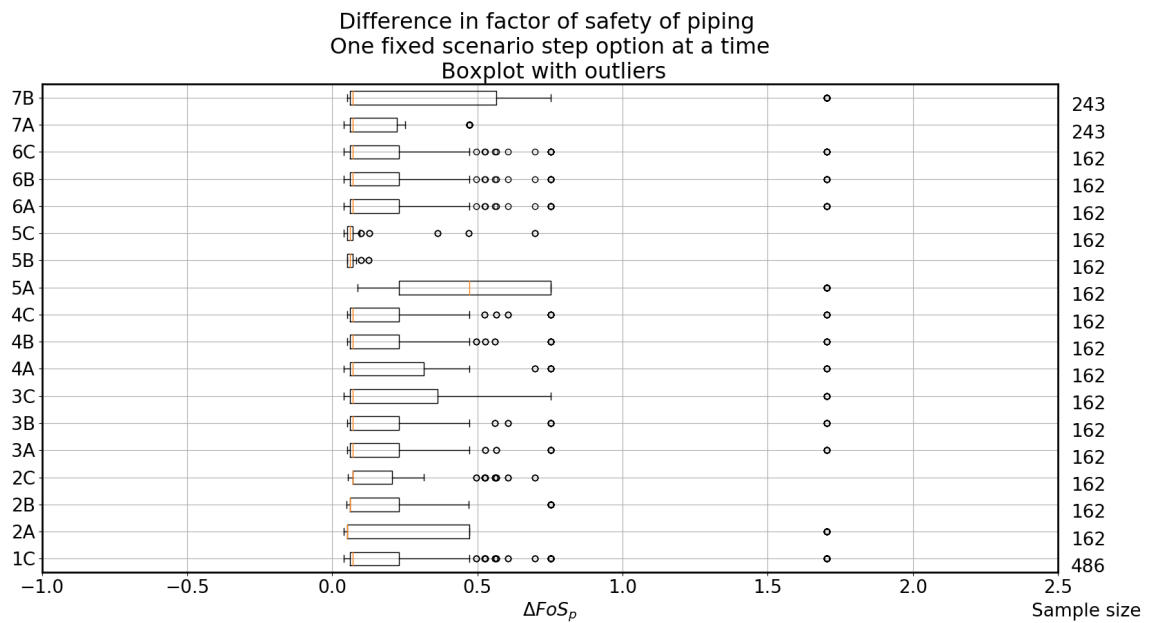
Figure F.14: The range in difference of piping for fixed scenario options with outliers (Thin blanket layer case).
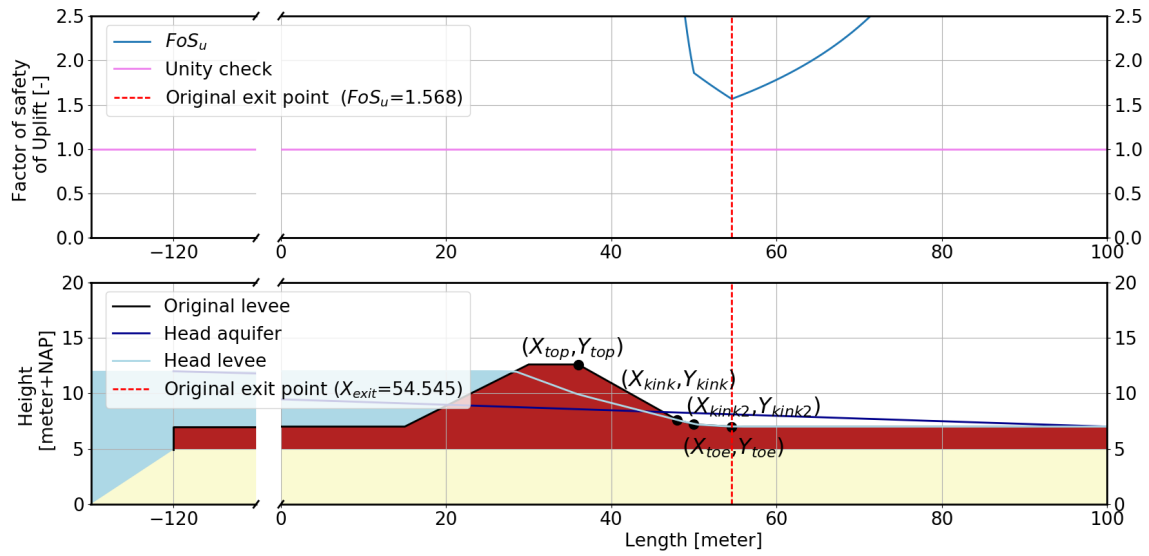
F.3. Thick blanket layer
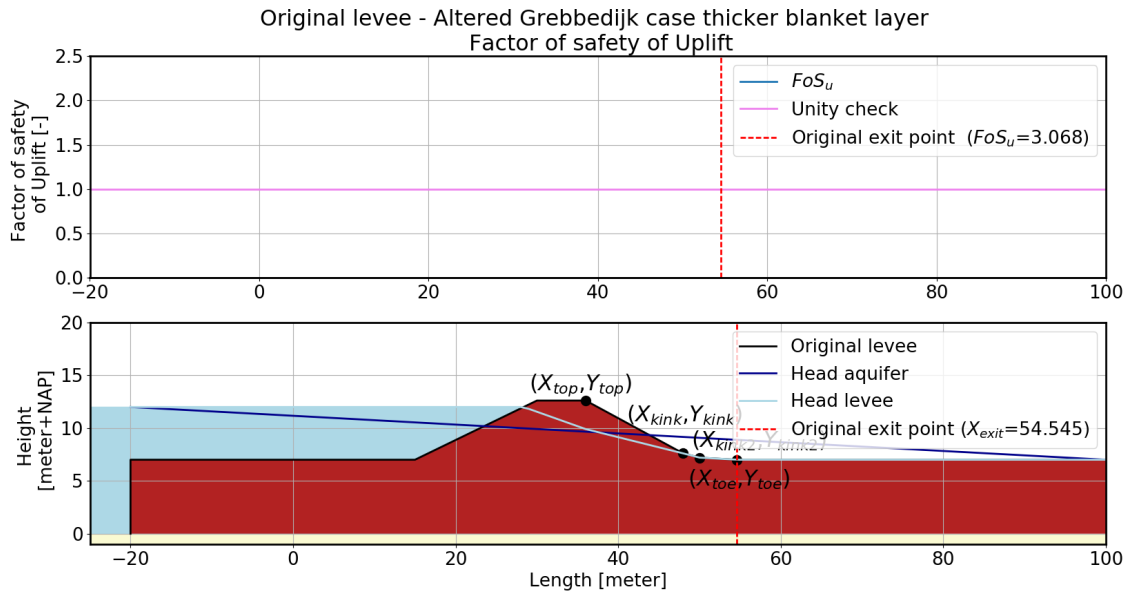
Figure F.15: Factor of safety of uplift of the original levee (Thick blanket layer case)

Table F.3: Results for thin blanket layer case (Original, remaining profile (assumption-scenario: 1A, 2B, 3B ,4B, 5B, 6B, 7A.))

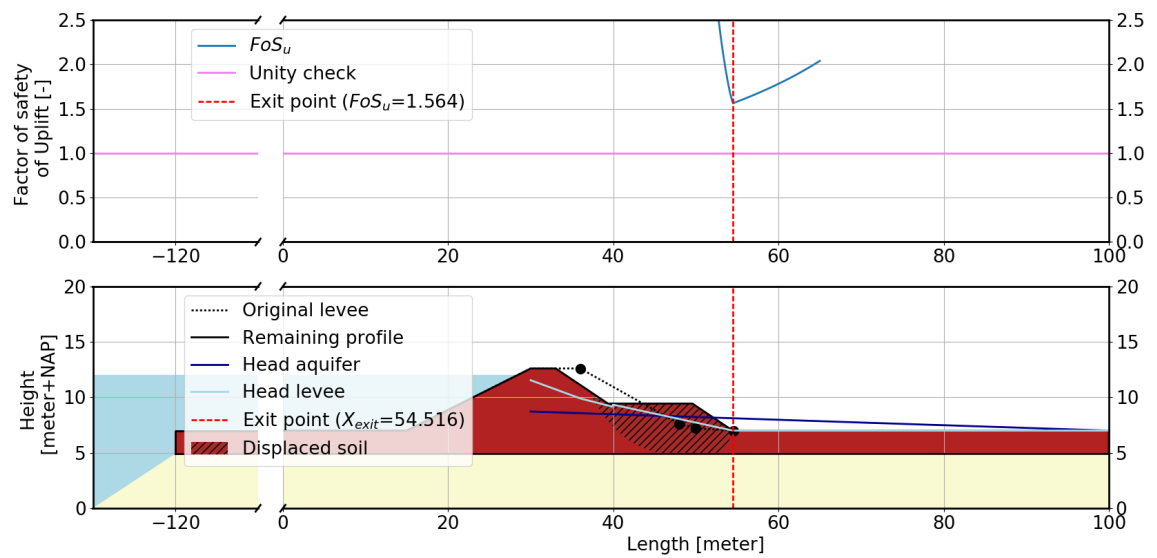| Factor of safety	Original case	Value $[-]$	Remaining profile	Value $[-]$	Difference (Δ)	Value $[-]$
Uplift	$FoS_{u,original}(X_{exit})$	3.07	$FoS_u(X_{exit})$	3.08	ΔFoS_u	0.01
Heave	$FoS_{h,original}(X_{exit})$	1.12	$FoS_h(X_{exit})$	1.12	ΔFoS_h	0.01
Piping	$FoS_{p,original}(X_{exit})$	0.99	$FoS_p(X_{exit})$	0.99	ΔFoS_p	0.00
BEP	$FoS_{BEP,original}(X_{exit})$	3.07	$FoS_{BEP}(X_{exit})$	3.08	ΔFoS_{BEP}	0.01
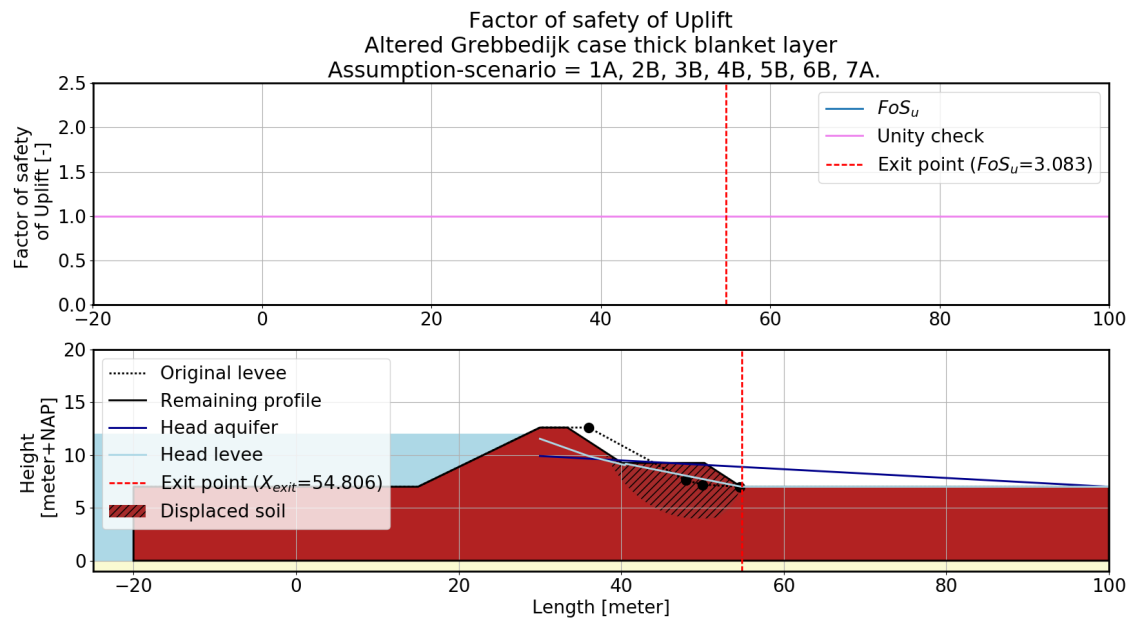
Figure F.16: Factor of safety of uplift of the remaining profile, (Thick blanket layer case) base case (assumption-scenario = 1A, 2B, 3B, 4B, 5B, 6B, 7A.)

Figure F.17: The range in the differences between BEP, Uplift, Heave and Piping and the original situation for all 486 scenarios with the outliers (Thick blanket layer case)

F.3.1. BEP

Figure F.18: The range in difference of BEP for fixed scenario options with outliers (Thick blanket layer case).

F.3.2. Uplift
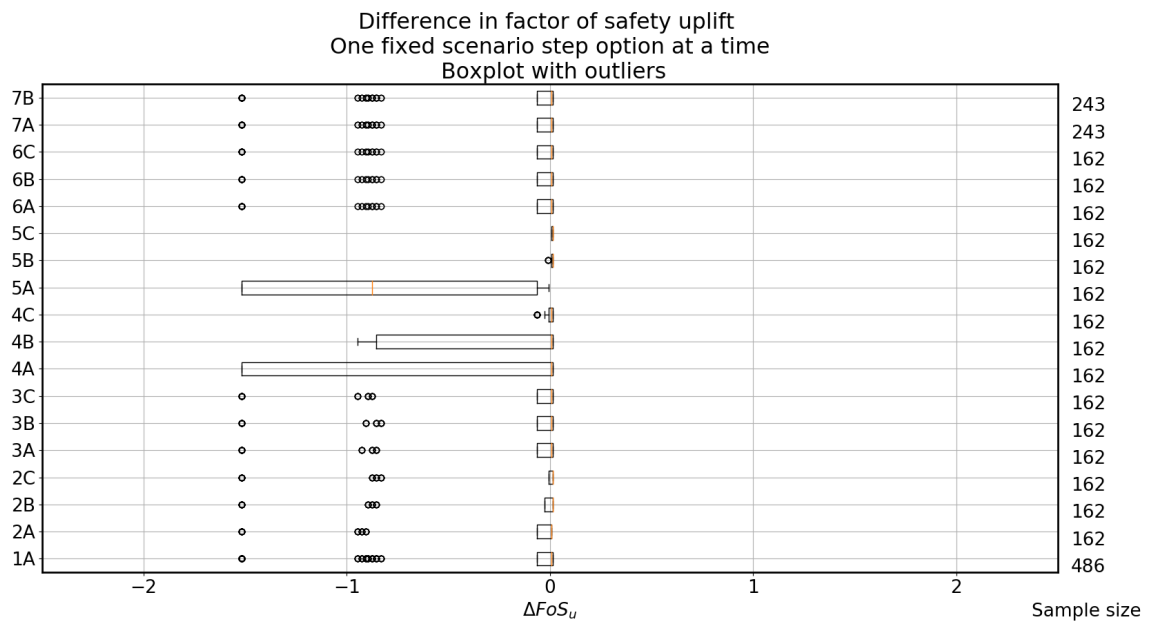
Figure F.19: The range in difference of uplift for fixed scenario options with outliers (Thick blanket layer case).

F.3.3. Heave
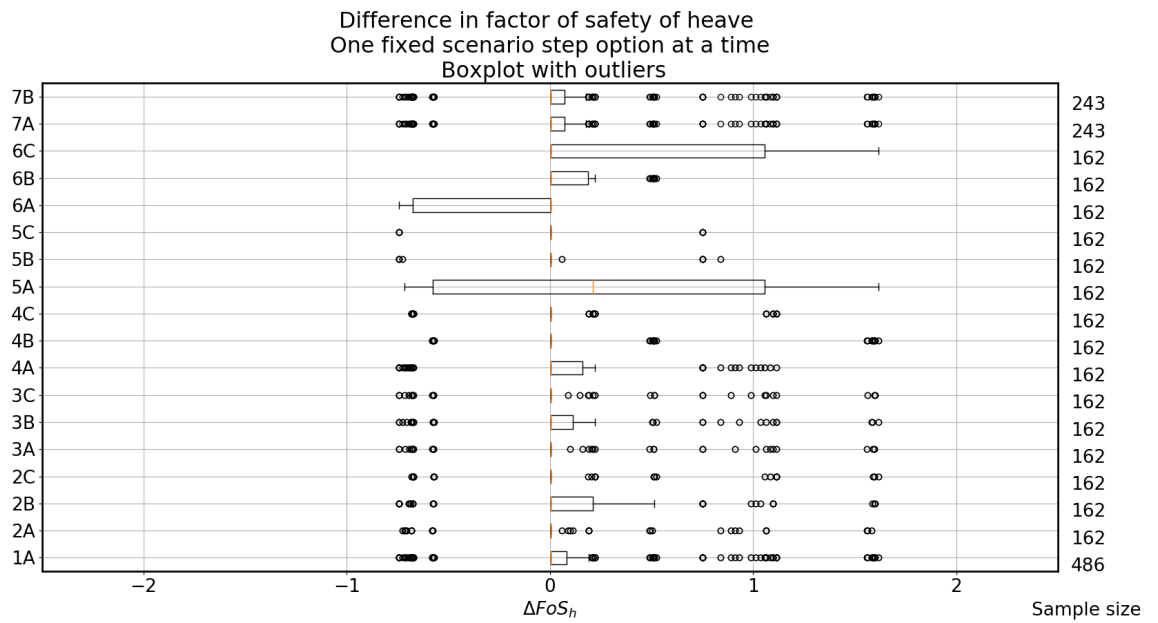
Figure F.20: The range in difference of heave for fixed scenario options with outliers (Thick blanket layer case).

F.3.4. Piping

Figure F.21: The range in difference of piping for fixed scenario options with outliers (Thick blanket layer case).
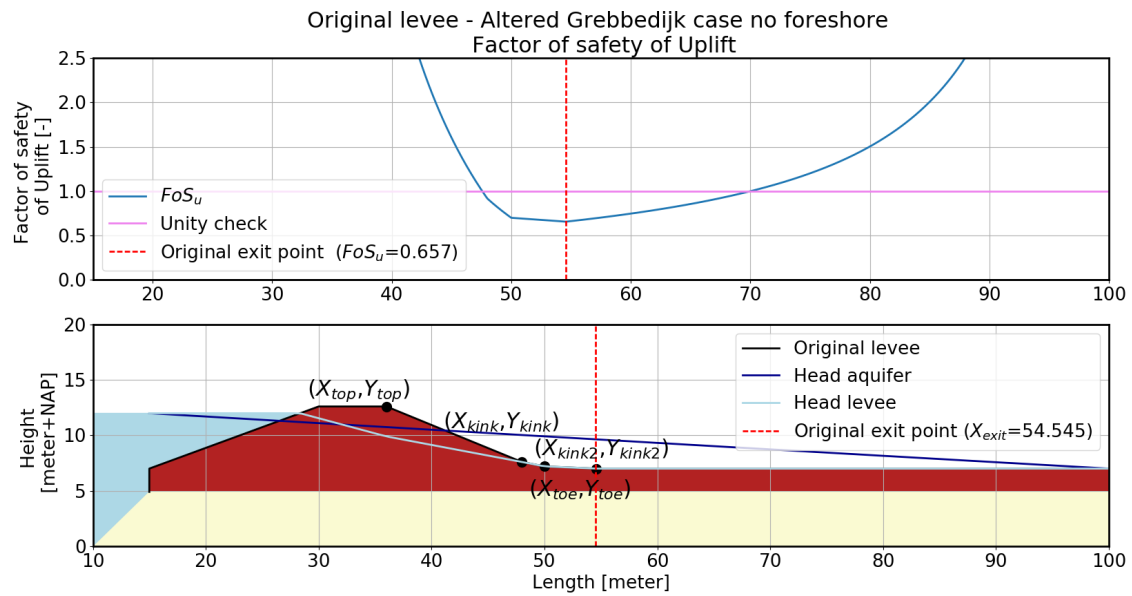
F.4. No foreshore

Figure F.22: Factor of safety of uplift of the original levee (No foreshore case)

Table F.4: Results for no foreshore case (Original, remaining profile (assumption-scenario: 1C, 2B, 3B ,4B, 5B, 6B, 7A.))

Factor of safety	Original case	Value [−]	Remaining profile	Value [−]	Difference (Δ)	Value [−]
Uplift	$FoS_{u,original}(X_{exit})$	0.66	$FoS_u(X_{exit})$	1.00	ΔFoS_u	0.34
Heave	$FoS_{h,original}(X_{exit})$	0.36	$FoS_h(X_{exit})$	0.36	ΔFoS_h	0.00
Piping	$FoS_{p,original}(X_{exit})$	0.38	$FoS_p(X_{exit})$	0.42	ΔFoS_p	0.04
BEP	$FoS_{BEP,original}(X_{exit})$	0.66	$FoS_{BEP}(X_{exit})$	1.00	ΔFoS_{BEP}	0.34

Figure F.23: Factor of safety of uplift of the remaining profile, (No foreshore case) base case (assumption-scenario = 1C, 2B, 3B, 4B, 5B, 6B, 7A.)

Figure F.24: The range in the differences between BEP, Uplift, Heave and Piping and the original situation for all 486 scenarios with the outliers (No foreshore case)
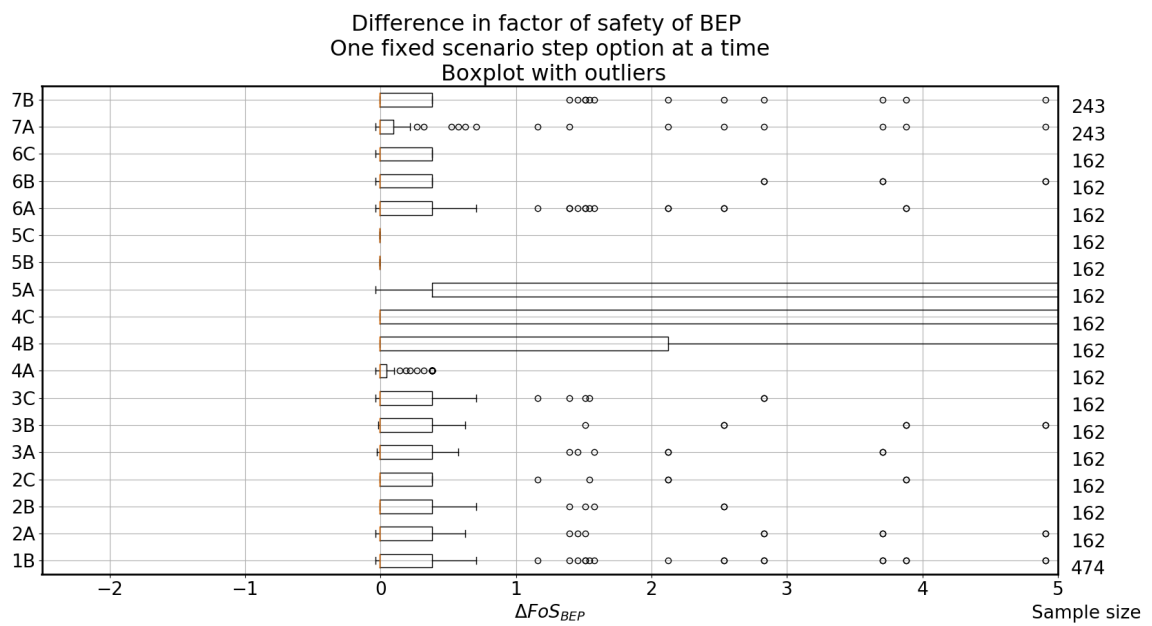
F.4.1. BEP

Figure F.25: The range in difference of BEP for fixed scenario options with outliers (No foreshore case).
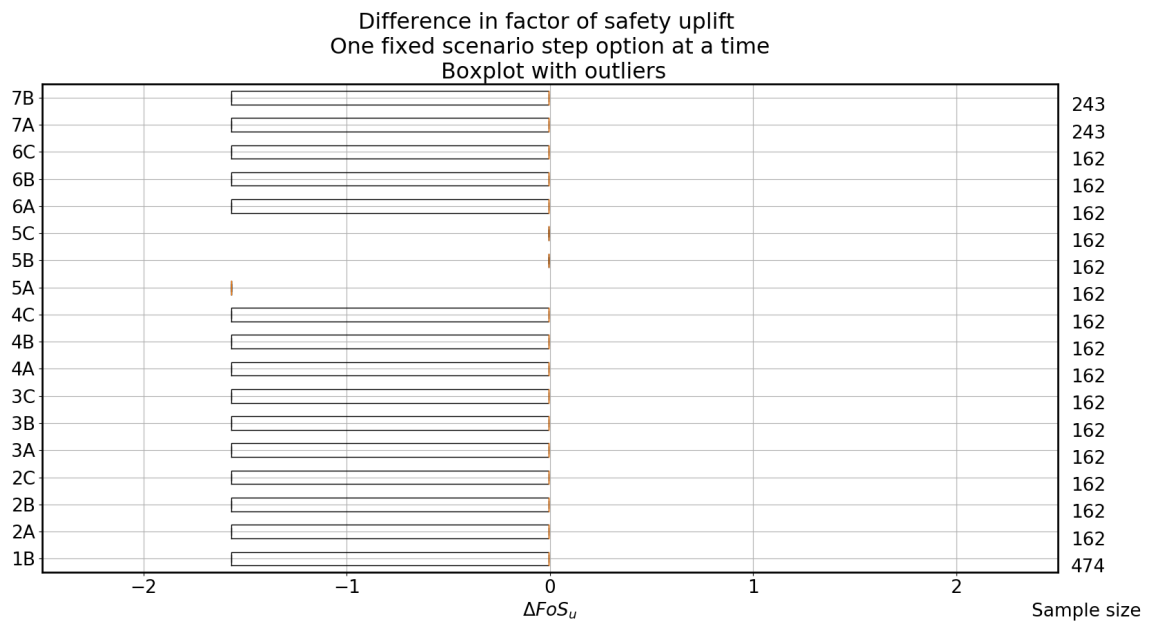
F.4.2. Uplift

Figure F.26: The range in difference of uplift for fixed scenario options with outliers (No foreshore case).
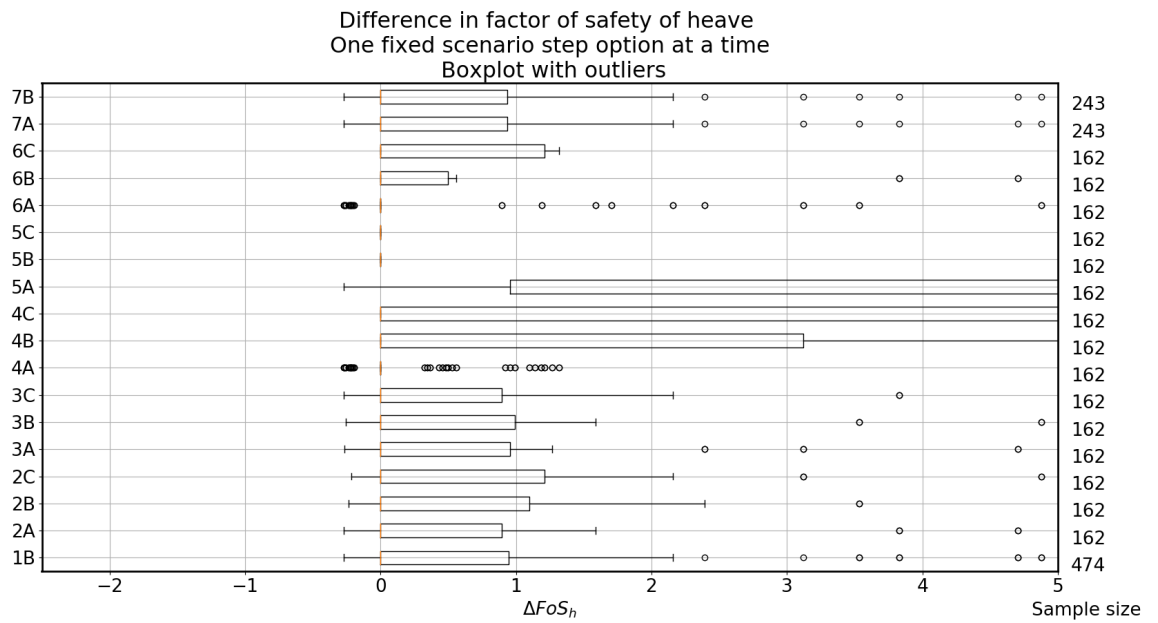
F.4.3. Heave

Figure F.27: The range in difference of heave for fixed scenario options with outliers (No foreshore case).
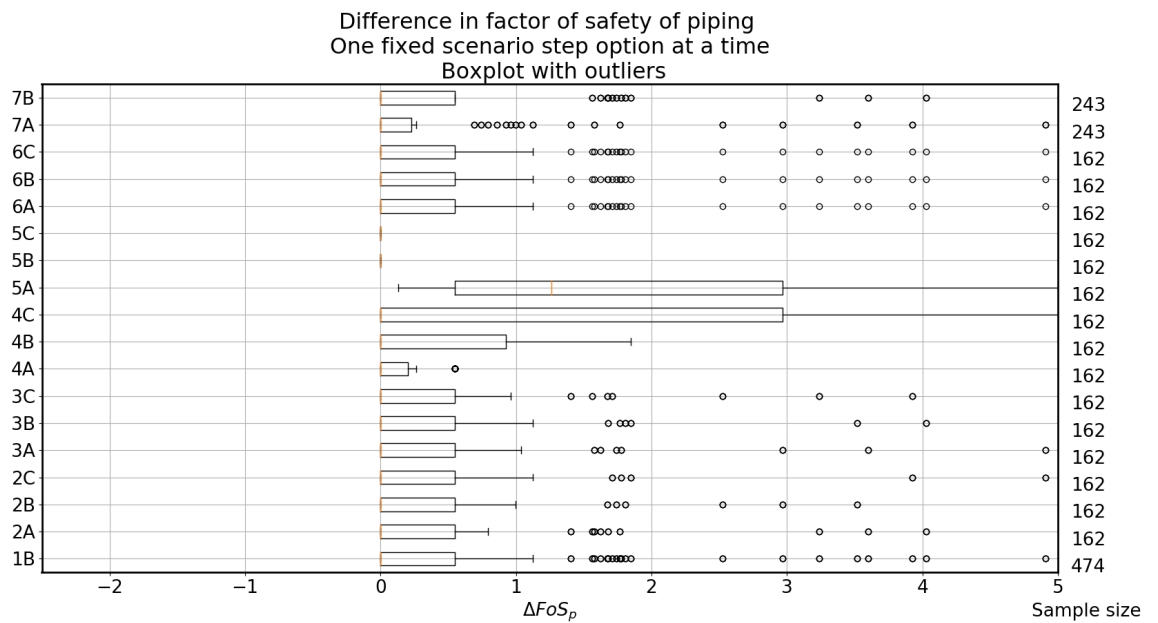
F.4.4. Piping

Figure F.28: The range in difference of piping for fixed scenario options with outliers (No foreshore case).

F.5. Long foreshore
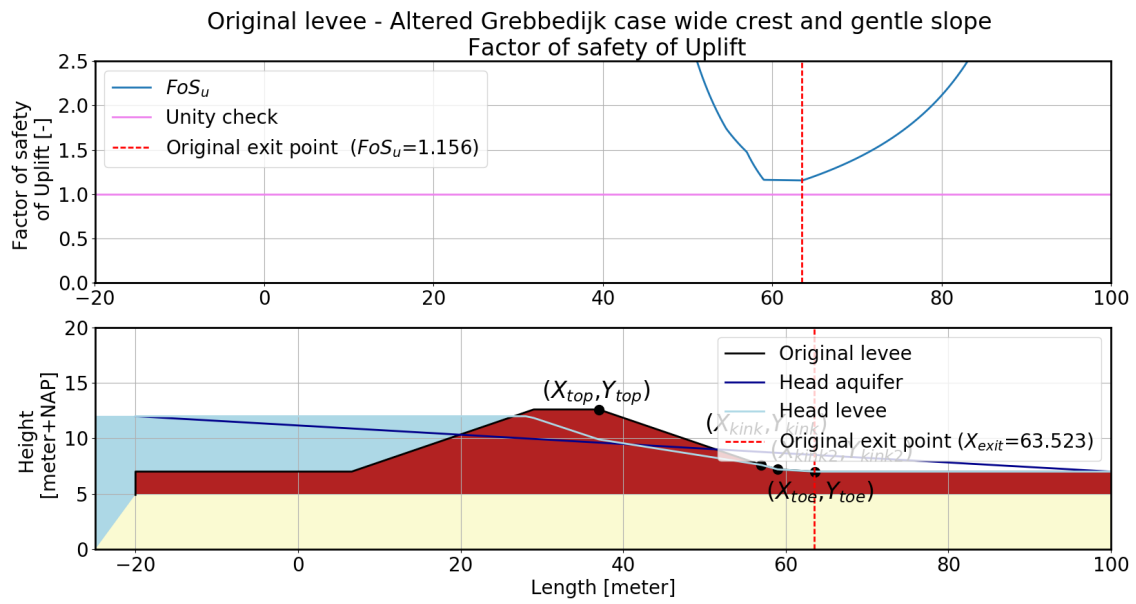

Figure F.29: Factor of safety of uplift of the original levee (Long foreshore case)

Table F.5: Results for thin blanket layer case (Original, remaining profile (assumption-scenario: 1C, 2B, 3B ,4B, 5B, 6B, 7A.))

Factor of safety	Original case	Value $[-]$	Remaining profile	Value $[-]$	Difference (Δ)	Value $[-]$
Uplift	$FoS_{u,original}(X_{exit})$	1.57	$FoS_u(X_{exit})$	1.56	ΔFoS_u	-0.01
Heave	$FoS_{h,original}(X_{exit})$	0.57	$FoS_h(X_{exit})$	0.57	ΔFoS_h	0.00
Piping	$FoS_{p,original}(X_{exit})$	1.40	$FoS_p(X_{exit})$	1.40	ΔFoS_p	0.00
BEP	$FoS_{BEP,original}(X_{exit})$	1.57	$FoS_{BEP}(X_{exit})$	1.56	ΔFoS_{BEP}	-0.01

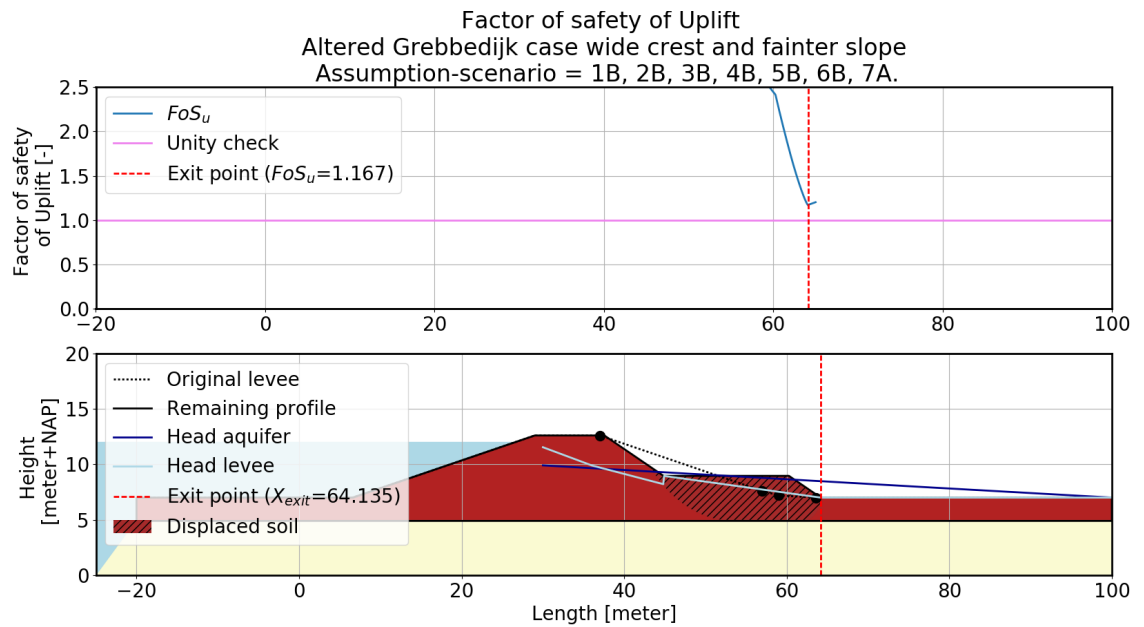Figure F.30: Factor of safety of uplift of the remaining profile, (Long foreshore case) base case (assumption-scenario = 1B, 2B, 3B, 4B, 5B, 6B, 7A.)
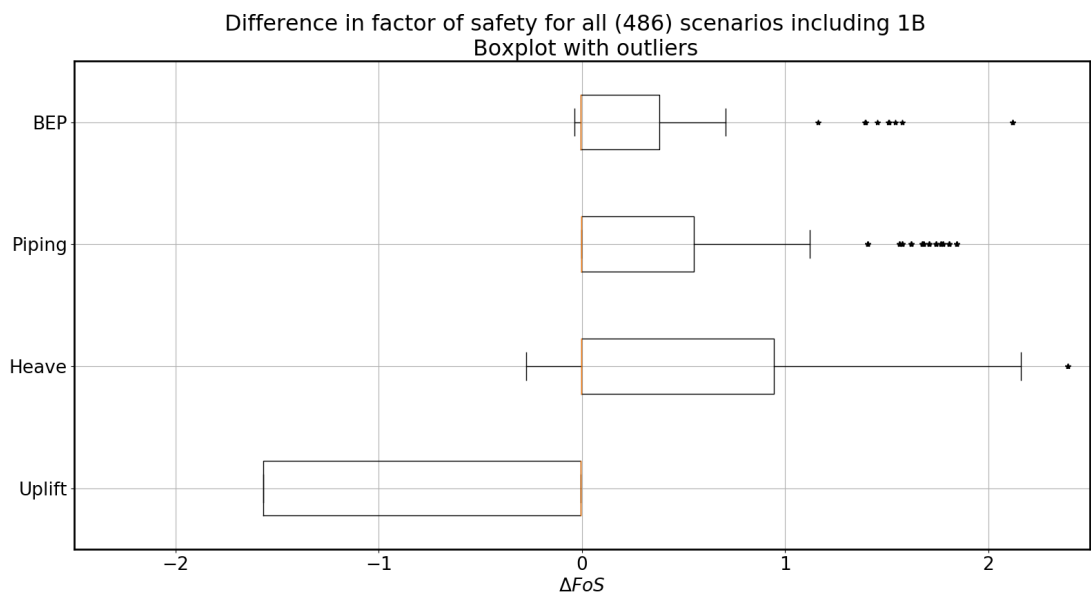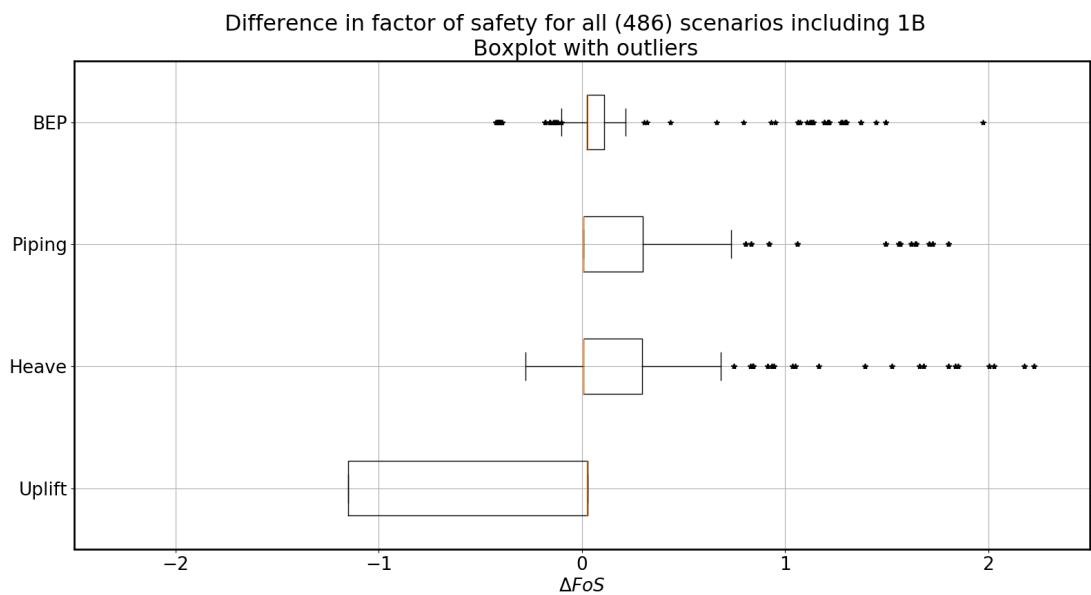

Figure F.31: The range in the differences between BEP, Uplift, Heave and Piping and the original situation for all 486 scenarios with the outliers (Long foreshore case)
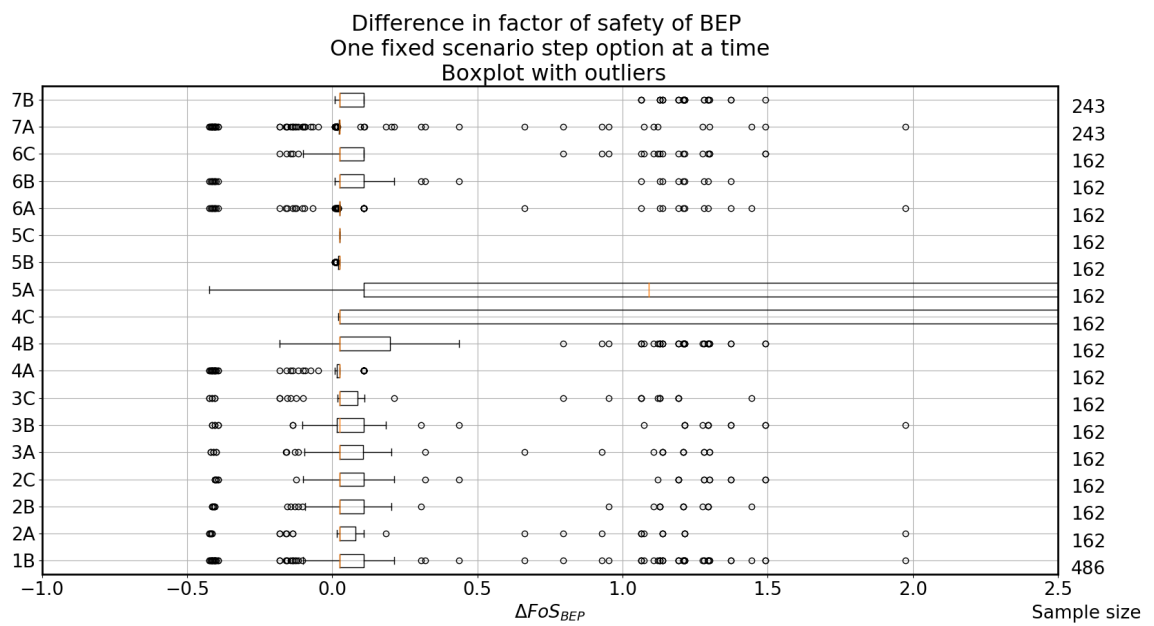
F.5.1. BEP

Figure F.32: The range in difference of BEP for fixed scenario options with outliers (Long foreshore case).
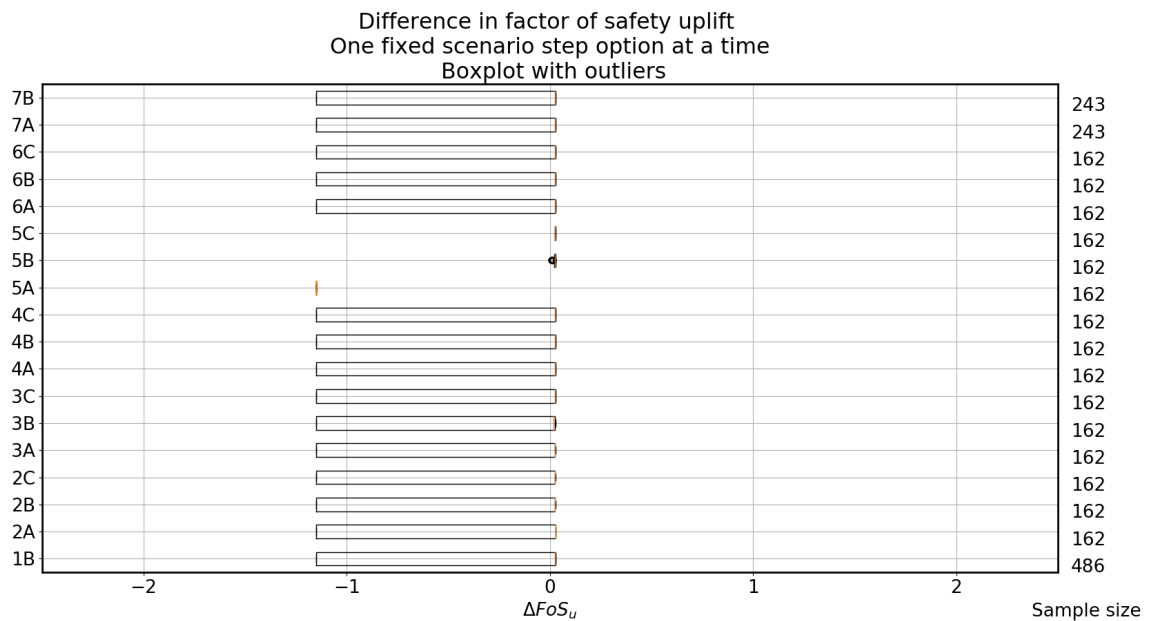
F.5.2. Uplift

Figure F.33: The range in difference of uplift for fixed scenario options with outliers (Long foreshore case).

F.5.3. Heave

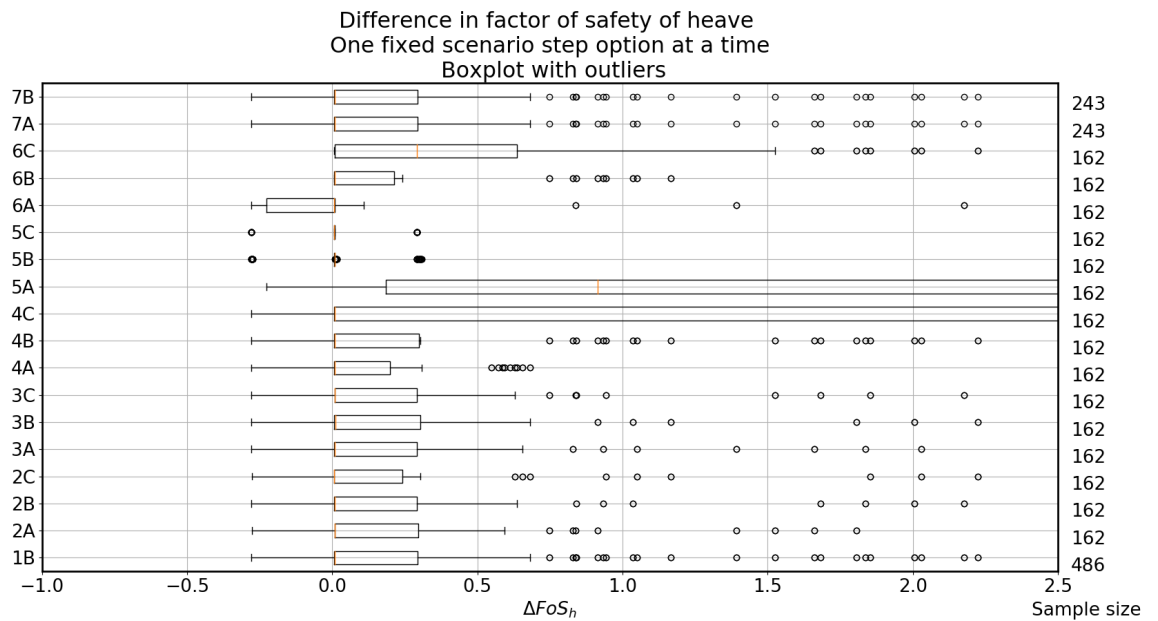Figure F.34: The range in difference of heave for fixed scenario options with outliers (Long foreshore case).

F.5.4. Piping

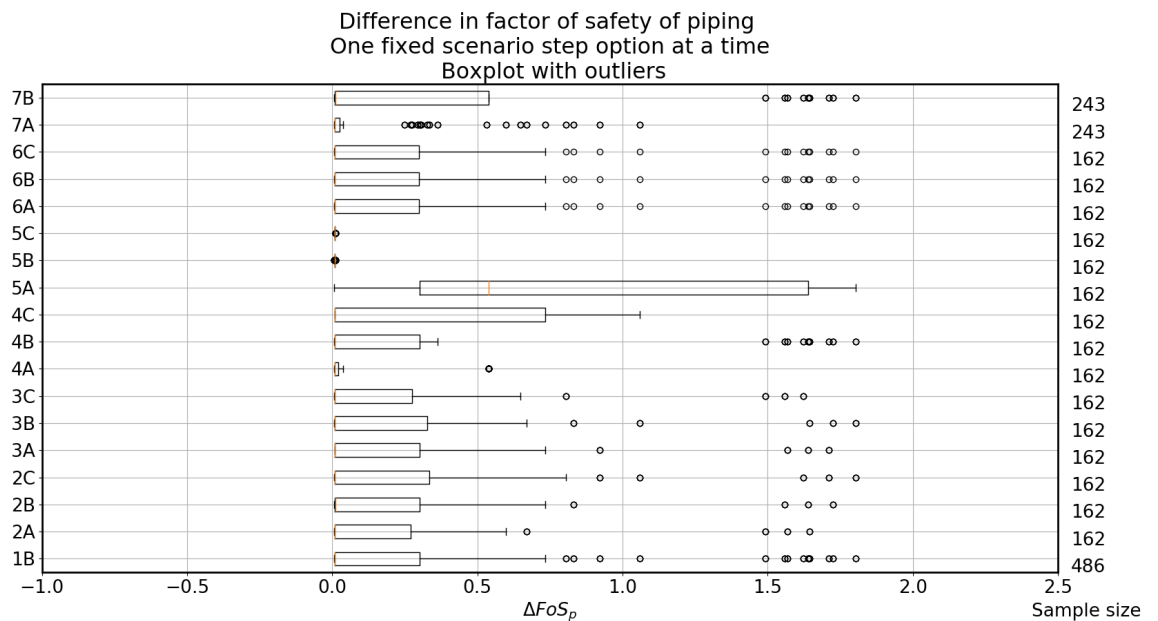Figure F.35: The range in difference of piping for fixed scenario options with outliers (Long foreshore case).

F.6. Wide crest and gentle slope

Figure F.36: Factor of safety of uplift of the original levee (Wide crest and gentle slope case)

Table F.6: Results for thin blanket layer case (Original, remaining profile (assumption-scenario: 1C, 2B, 3B ,4B, 5B, 6B, 7A.))

Factor of safety	Original case	Value $[-]$	Remaining profile	Value $[-]$	Difference (Δ)	Value $[-]$
Uplift	$FoS_{u,original}(X_{exit})$	1.15	$FoS_u(X_{exit})$	1.17	ΔFoS_u	0.24
Heave	$FoS_{h,original}(X_{exit})$	0.42	$FoS_h(X_{exit})$	0.43	ΔFoS_h	0.07
Piping	$FoS_{p,original}(X_{exit})$	0.72	$FoS_p(X_{exit})$	0.73	ΔFoS_p	0.08
BEP	$FoS_{BEP,original}(X_{exit})$	1.15	$FoS_{BEP}(X_{exit})$	1.17	ΔFoS_{BEP}	0.24

Figure F.37: Factor of safety of uplift of the remaining profile, (Wide crest and gentle slope case) base case (assumption-scenario = 1B, 2B, 3B, 4B, 5B, 6B, 7A.)

Figure F.38: The range in the differences between BEP, Uplift, Heave and Piping and the original situation for all 486 scenarios with the outliers (Wide crest and gentle slope case)

F.6.1. BEP

Figure F.39: The range in difference of BEP for fixed scenario options with outliers (Wide crest and gentle slope case).

F.6.2. Uplift

Figure F.40: The range in difference of uplift for fixed scenario options with outliers (Wide crest and gentle slope case).
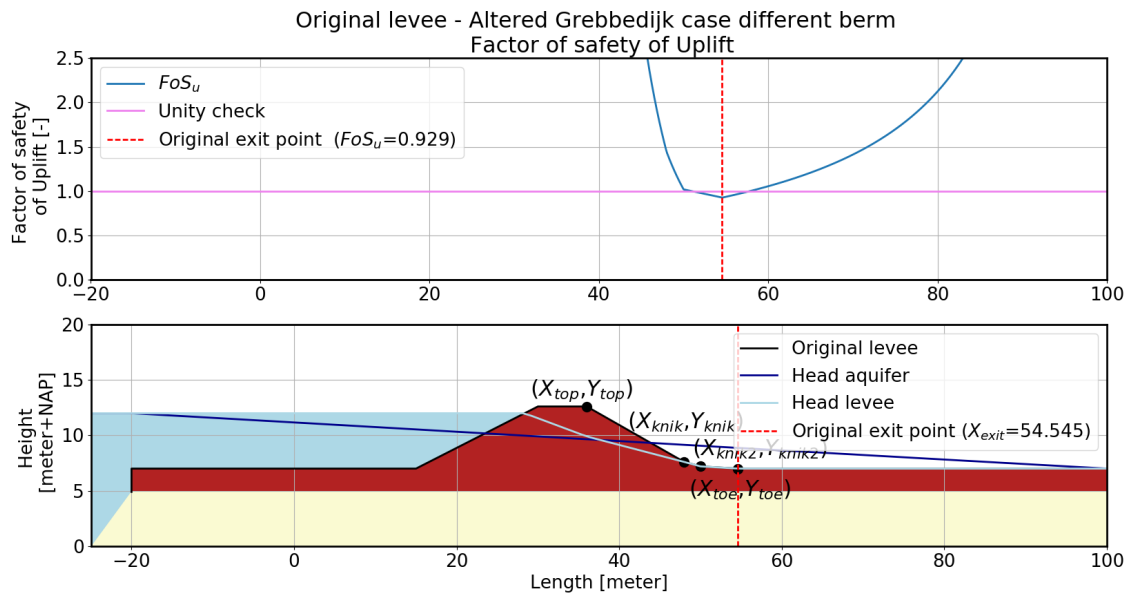
F.6.3. Heave

Figure F.41: The range in difference of heave for fixed scenario options with outliers (Wide crest and gentle slope case).

F.6.4. Piping

Figure F.42: The range in difference of piping for fixed scenario options with outliers (Wide crest and gentle slope case).

F.7. Triangular berm

Figure F.43: Factor of safety of uplift of the original levee (Triangular berm case)

Table F.7: Results for thin blanket layer case (Original, remaining profile (assumption-scenario: 1C, 2B, 3B ,4B, 5B, 6B, 7A.))

Factor of safety	Original case	Value $[-]$	Remaining profile	Value $[-]$	Difference (Δ)	Value $[-]$
Uplift	$FoS_{u,original}(X_{exit})$	0.93	$FoS_u(X_{exit})$	1.00	ΔFoS_u	0.07
Heave	$FoS_{h,original}(X_{exit})$	0.36	$FoS_h(X_{exit})$	0.36	ΔFoS_h	0.00
Piping	$FoS_{p,original}(X_{exit})$	0.65	$FoS_p(X_{exit})$	0.67	ΔFoS_p	0.02
BEP	$FoS_{BEP,original}(X_{exit})$	0.93	$FoS_{BEP}(X_{exit})$	1.00	ΔFoS_{BEP}	0.07

Figure F.44: Factor of safety of uplift of the remaining profile, (Triangular berm case) base case (assumption-scenario = 1B, 2B, 3B, 4B, 5B, 6B, 7A.)
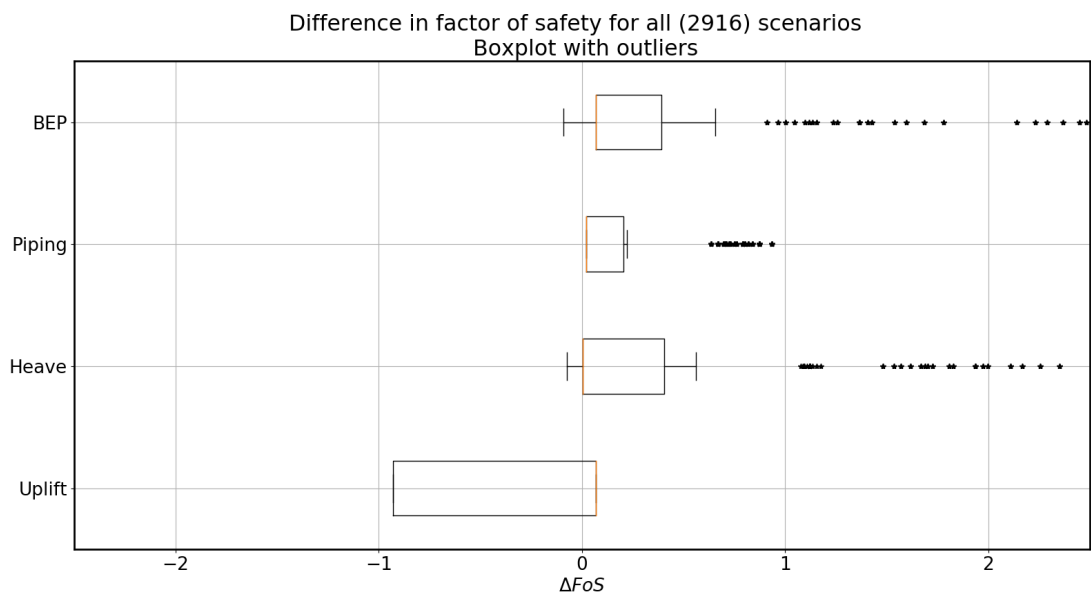

Figure F.45: The range in the differences between BEP, Uplift, Heave and Piping and the original situation for all 486 scenarios with the outliers (Triangular berm case)
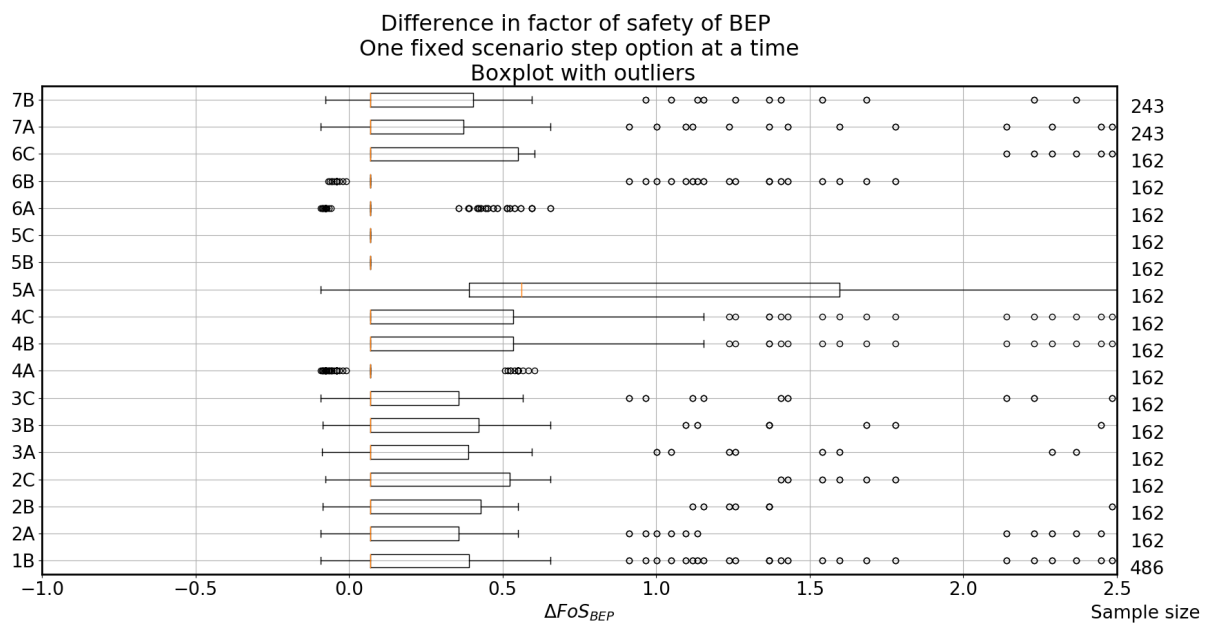
F.7.1. BEP

Figure F.46: The range in difference of BEP for fixed scenario options with outliers (Triangular berm case).
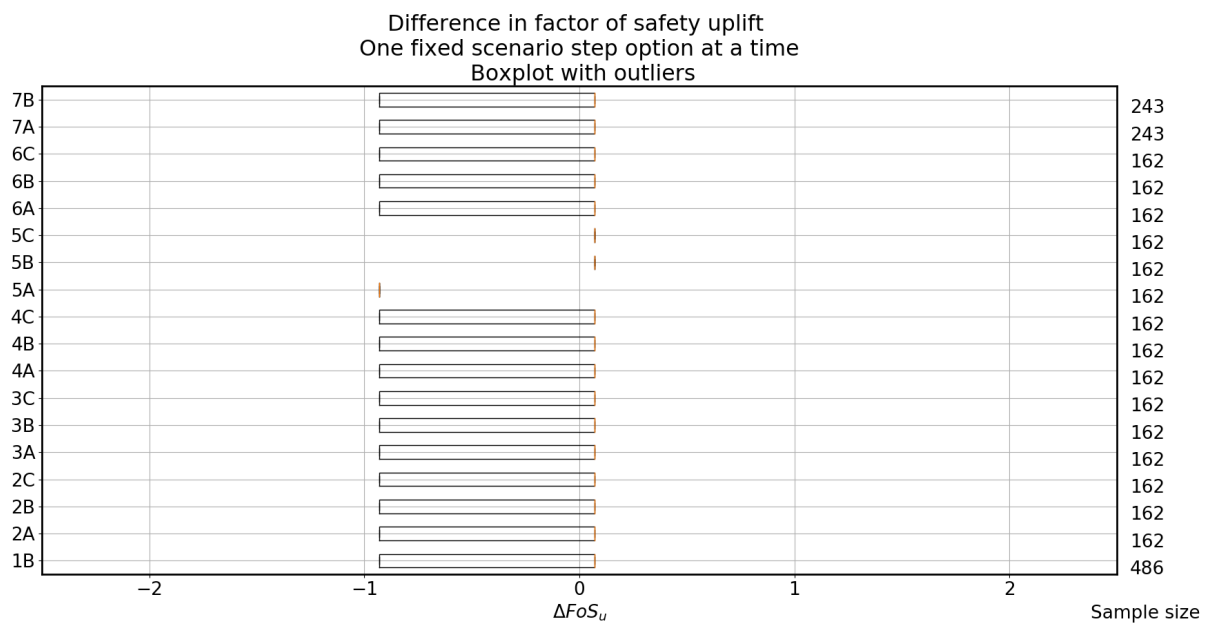
F.7.2. Uplift

Figure F.47: The range in difference of uplift for fixed scenario options with outliers (Triangular berm case).
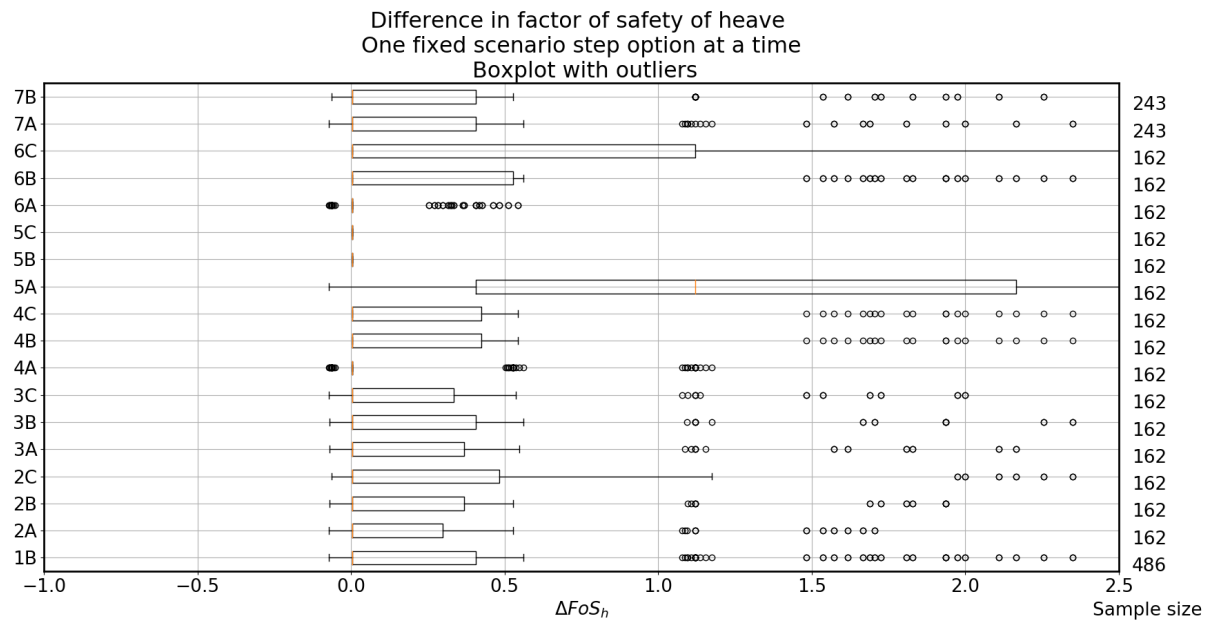
F.7.3. Heave

Figure F.48: The range in difference of heave for fixed scenario options with outliers (Triangular berm case).
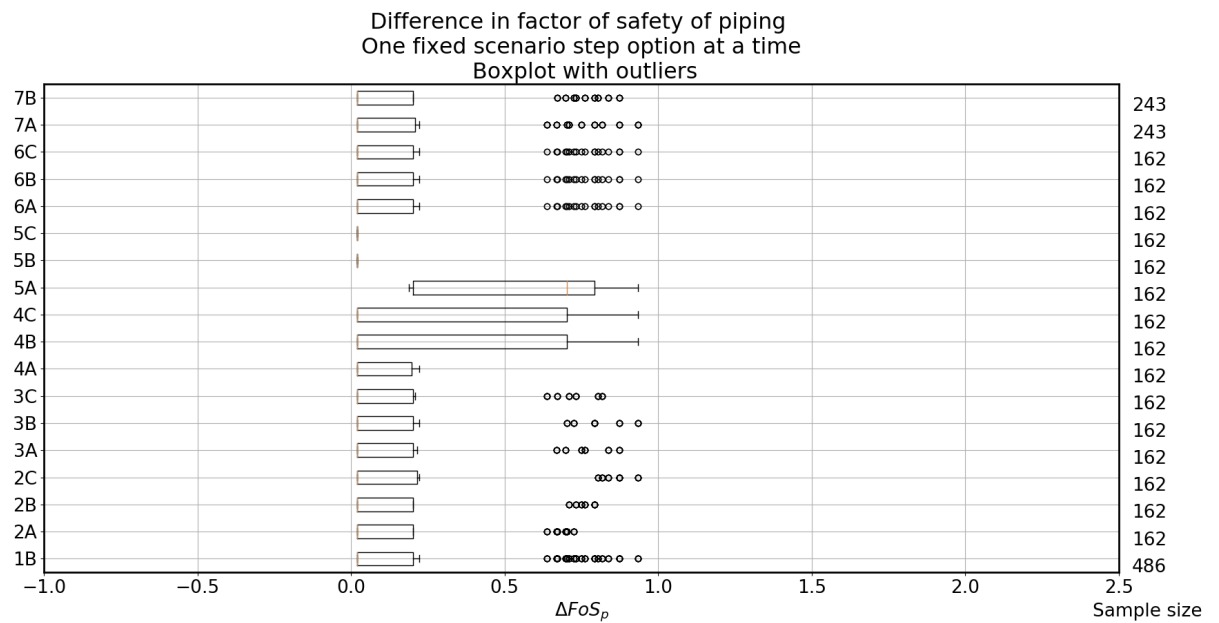
F.7.4. Piping

Figure F.49: The range in difference of piping for fixed scenario options with outliers (Triangular berm case).